AD_____

Award Number: W81XWH-06-1-0406

TITLE: New Advances in Molecular Therapy for Muscle Repair after Diseases and Injuries

PRINCIPAL INVESTIGATOR: Johnny Huard, Ph.D.
                           Yong Li, M.D., Ph.D.
                           Bruno Peault, Ph.D.
                           Bridget Deasy, Ph.D.
                           Xiao Xiao, Ph.D.
                           Paula Clemens, M.D.
                           Bing Wang, Ph.D.

CONTRACTING ORGANIZATION: Children's Hospital of Pittsburgh
                           Pittsburgh, PA 15213

REPORT DATE: April 2008

TYPE OF REPORT: Annual

PREPARED FOR: U.S. Army Medical Research and Materiel Command
                Fort Detrick, Maryland 21702-5012

DISTRIBUTION STATEMENT: Approved for Public Release;
                        Distribution Unlimited

The views, opinions and/or findings contained in this report are those of the author(s) and should not be construed as an official Department of the Army position, policy or decision unless so designated by other documentation.

REPORT DOCUMENTATION PAGE		*Form Approved* *OMB No. 0704-0188*

Public reporting burden for this collection of information is estimated to average 1 hour per response, including the time for reviewing instructions, searching existing data sources, gathering and maintaining the data needed, and completing and reviewing this collection of information. Send comments regarding this burden estimate or any other aspect of this collection of information, including suggestions for reducing this burden to Department of Defense, Washington Headquarters Services, Directorate for Information Operations and Reports (0704-0188), 1215 Jefferson Davis Highway, Suite 1204, Arlington, VA 22202-4302. Respondents should be aware that notwithstanding any other provision of law, no person shall be subject to any penalty for failing to comply with a collection of information if it does not display a currently valid OMB control number. **PLEASE DO NOT RETURN YOUR FORM TO THE ABOVE ADDRESS.**

1. REPORT DATE	2. REPORT TYPE	3. DATES COVERED
01-04-2008	Annual	3 Mar 2007 – 2 Mar 2008

4. TITLE AND SUBTITLE

New Advances in Molecular Therapy for Muscle Repair after Diseases and Injuries

5a. CONTRACT NUMBER

5b. GRANT NUMBER
W81XWH-06-1-0406

5c. PROGRAM ELEMENT NUMBER

6. AUTHOR(S)

Johnny Huard, Ph.D., Yong Li, M.D.,Ph.D., Bruno Peault, Ph.D.
 Bridget Deasy, Ph.D., Xiao Xiao, Ph.D., Paula Clemens, M.D., Bing Wang, M.D.,Ph.D.

Email: jhuard@pitt.edu

5d. PROJECT NUMBER

5e. TASK NUMBER

5f. WORK UNIT NUMBER

7. PERFORMING ORGANIZATION NAME(S) AND ADDRESS(ES)

Children's Hospital of Pittsburgh
Pittsburgh, PA 15213

8. PERFORMING ORGANIZATION REPORT NUMBER

9. SPONSORING / MONITORING AGENCY NAME(S) AND ADDRESS(ES)
U.S. Army Medical Research and Materiel Command
Fort Detrick, Maryland 21702-5012

10. SPONSOR/MONITOR'S ACRONYM(S)

11. SPONSOR/MONITOR'S REPORT NUMBER(S)

12. DISTRIBUTION / AVAILABILITY STATEMENT
Approved for Public Release; Distribution Unlimited

13. SUPPLEMENTARY NOTES

14. ABSTRACT

 Included on next page

15. SUBJECT TERMS
 Not provided

16. SECURITY CLASSIFICATION OF:			17. LIMITATION OF ABSTRACT	18. NUMBER OF PAGES	19a. NAME OF RESPONSIBLE PERSON USAMRMC
a. REPORT U	**b. ABSTRACT** U	**c. THIS PAGE** U	UU	142	**19b. TELEPHONE NUMBER** *(include area code)*

Standard Form 298 (Rev. 8-98)
Prescribed by ANSI Std. Z39.18

14. Abstract

Project #1
Background: Muscle injuries, especially pulls and strains, are among the most common and most frequently disabling injuries sustained by athletes and soldiers. Although injured muscles heal naturally, the regeneration is very slow and often yields incomplete functional recovery. In injured muscle, regeneration begins shortly after injury, but the healing process is rather inefficient and is hindered by fibrosis—that is, scar tissue formation. More importantly, the scar tissue that often replaces damaged myofibers may contribute to the tendency of strains to recur. We have observed that TGF-β1 plays a central role in skeletal muscle fibrosis and, more importantly, that the use of antifibrosis agents that inactivate this molecule, such as suramin (a Food and Drug Association [FDA]-approved drug that prevents fibrosis due to skin disorders), can reduce muscle fibrosis and consequently improve muscle healing, resulting in nearly complete recovery after laceration or strain injuries.

Objective/Hypothesis/Specific Aims/Study Design: We plan to develop biological approaches based on suramin to efficiently prevent the scarring process by blocking the action of TGF-β1; we will determine the appropriate time at which to administer suramin and the optimal suramin dosage after muscle contusion, a common military injury (**Technical Objective #1**). Because we have observed that suramin can both enhance muscle regeneration and neutralize the fibrotic effect of TGF-β1, we also propose experiments designed to further evaluate the beneficial effects of suramin on muscle regeneration (**Technical Objective #2A**). Finally, we will determine if this effect is mediated through suramin's interaction with muscle growth regulators, particularly its possible down-regulation of myostatin or up-regulation of follistatin (**Technical Objective #2B**).

Relevance: These studies should further our understanding of the muscle healing process, facilitate the identification of new techniques to promote efficient muscle healing, and contribute to the development of innovative therapies for various types of muscle injuries and diseases, such as muscular dystrophies.

Project #2
Background: Muscle injuries are very common musculoskeletal problems in traumatology that arise frequently in military training and combat. Injured skeletal muscle undergoes a natural process of regeneration; however, fibrosis—the formation of fibrous scar tissue—hinders this process and precludes the complete recovery of muscle function. Prevention of fibrosis could improve injured skeletal muscle healing; however, it often is not possible to treat muscle injuries before fibrosis occurs.

Objective/Hypothesis: We hypothesize that matrix metalloproteinase type 1 (MMP1), a collagen-digesting enzyme, can improve the microenvironment for muscle regeneration and accelerate healing by digesting existing scar tissue within recovering muscle.

Specific Aims/Study Design: First, we will culture muscle-derived fibroblasts and myogenic cells in vitro in the presence of MMP1 and assess its effects on fibroblast proliferation and collagen deposition (**Technical Objective #1A**) and myogenic cell migration and differentiation (**Technical Objective #1B**). We then will inject MMP1 directly into normal (noninjured) skeletal muscle to determine the safest and most effective dose of MMP1 in vivo (**Technical Objective #2A**). Next, we will evaluate the ability of MMP1 to digest fibrous scar tissue present within injured skeletal muscle and, by so doing, to enhance the regeneration and functional recovery of injured skeletal muscle (**Technical Objective #2B**). Finally, we will attempt to extend the effective half-life of MMP1 in fibrous scar tissue by genetically engineering myoblasts and muscle-derived stem cells (MDSCs) to express MMP1 (**Technical Objective #3**).

Relevance: The study results generated by the proposed project should shed further light on the effects of scar tissue on muscle healing after injury and could facilitate the development of methods by which to eliminate scar tissue and enhance the regeneration of muscle damaged by military- or sports-related injuries or diseases.

Project #3

Our preliminary studies point to a close developmental relationship between vascular endothelial cells and myogenic cells in the adult human muscle. We have, indeed, characterized two novel populations of muscle-derived, non-satellite cells that exhibit dramatic myogenic potential in culture and *in vivo:* genuine vascular endothelial cells and cells co-expressing markers of both myogenic and endothelial cell lineages, which we have named myo-endothelial progenitors. Both cell populations can be purified by flow cytometry as endothelial (CD56- CD 34+ CD144+) and myo-endothelial (CD56+ CD34+ CD144+), and cultured for several weeks without losing their myogenic potential. In our preliminary experiments, the myogenic potential in vivo of myo-endothelial progenitors is dramatically higher than that of endothelial cells, which are themselves much more efficient than regular myogenic cells. We propose experiments to further assess the respective myogenic potentials of human muscle-derived endothelial and myo-endothelial cells, whch will be compared qualitatively and quantitatively following injection into the injured SCID mouse muscle. Besides myogenesis, the development of other cell types, notably endothelial cells and pericytes, upon intramuscular injection will be examined. We hypothesize that upon myo-endothelial cell transplantation, high rates of donor cell survival and/or proliferation will promote skeletal muscle regeneration by generating more donor cells that can subsequently participate in the regeneration process. We propose a set of experiments to determine the rate at which these different populations of human muscle-derived cells survive and proliferate at different time points after injection, and to evaluate if such differences might affect the regeneration capacity of the cells after transplantation into the skeletal muscle. We will also perform experiments to investigate if these various human muscle-derived cell populations implanted in mice *via* intramuscular injection undergo self-renewal. We will also use a previously described protocol to determine if the donor-derived muscle precursor cells isolated from the skeletal muscle of primary recipient mice can be re-transplanted into the skeletal muscle of secondary recipients and improve skeletal muscle regeneration. To this aim, we will retrovirally modify human-derived myogenic, endothelial and myo-endothelial cells to express GFP. This will enable us to rapidly count the GFP-expressing cells isolated from primary recipients and sort them with high purity for re-transplantation into secondary recipients. Finally, we will also check if cell fusion between donor cells or between donor and host cells plays a significant role in muscle regeneration by these different subsets of human cells.

Project #4

Background: As progress toward understanding the basic biology of stem cells continues to grow, it is of vital importance that researchers maintain a focus on therapeutic applications of this technology by investigating preclinical models. Members of our laboratory have identified a mouse muscle-derived stem cell (MDSC) population that exhibits a highly enhanced ability to regenerate skeletal muscle in a muscular dystrophy model. Transplantation of this cell population results in significantly more efficient regeneration of skeletal muscle fibers and a significantly larger area of regeneration than does myoblast transplantation, a therapy that has already been tested in human clinical trials in both the United States and Canada. The isolation and transplantation of the human equivalent of these mouse MDSCs likely would improve the outcome of cell therapy for muscular disease and injury, including injuries frequently sustained by military personnel.

Objective/Hypothesis: The objectives of this project are 1) to identify the human stem cell populations that promote the most efficient skeletal muscle regeneration in a preclinical mouse model of muscle regeneration and Duchenne muscular dystrophy (DMD) and 2) to identify the optimal conditions under which to expand cell populations and obtain therapeutically relevant doses.

Study Design: We will screen human muscle-derived cells for a molecular and behavioral profile that correlates with efficient skeletal muscle regeneration in a preclinical model of DMD (Technical Objective #1). We also will identify the cell culturing conditions that best facilitate expansion of the potent populations (to therapeutically useful quantities) while maintaining the cells' phenotype and regeneration efficiency (Technical Objective #2).

Relevance: This project represents a critical step in cell therapy: Screening potential cell candidates and studying expansion kinetics and limits to generate stem cells for use in cell and gene therapy. This project is unique in that it takes the next step in moving muscle stem cells toward clinical application by investigating how to develop a safe and standardized approach by which to expand stem cell populations. The stem cell screening and expansion techniques that we plan to develop will facilitate the use of cell and gene therapy for myriad musculoskeletal injuries and diseases.

Project # 5

Congenital muscular dystrophy (CMD) is a group of severe forms of muscular dystrophy leading to early death in human patients. The majority of cases are caused by genetic mutations in the major laminin that contains the $\alpha 2$ chain (formerly named merosin) in the muscle basement membrane. The early morbidity/fatality and the lack of effective treatment require urgent search for novel therapeutics. Previously, we utilized mini-agrin, which has been proven to have a therapeutic effect in transgenic MCMD mice, to treat MCMD mice by AAV vector. Our preliminary studies showed that over-expression of mini-agrin protein by AAV vector greatly improved general health and muscle morphology in MCMD mice. However, the treated disease mice still developed gradual paralysis and displayed shorter life span than wild type mice. To further improve the current gene therapy paradigm, with the advanced AAV technology and muscle biology knowledge, we will vigorously test our hypothesis: whether muscle pathogenesis can be improved by inhibition apoptosis or promoting muscle growth. The specific aims are the following:

Aim1: To investigate whether muscle pathogenesis can be improved by delivery of BCL2, an anti-apoptotic gene, by AAV vector in MCMD mice. Mice that lack laminin $\alpha 2$ show severe muscle loss, poor regeneration, and a greatly shortened lifespan. A role for apoptosis in pathology of laminin $\alpha 2$-deficiency has been suggested by histological and in vitro studies, as well as transgenic studies. In this study, we will explore the potential therapeutic effect by delivering AAV-BCL2 vector into MCMD mice.

Aim2: To examine whether therapeutic effect can be obtained by delivery of insulin like growth factor 1 (IGF-1) gene, which can promote muscle growth, by AAV vector in MCMD mice. The MCMD mice show muscle atrophy and enhanced fibrosis as seen in human patients. Genes that promote muscle growth and inhibit fibrosis is theoretically beneficial for congenital muscular dystrophic muscle. Myostatin blockade, one of the strategies to promote muscle growth, has been shown to have a severe side effect of increasing postnatal lethality in MCMD transgenic studies. The reason for the side effect is due to significantly less brown and white fat in the absence of myostatin. In our preliminary studies, we observed that myostatin blockade significantly increased muscle weight, as well as decreased fat tissue in normal mice. However, over-expression of IGF-1 in normal mice only increased muscle weight without loosing fat. Considering less fat will result a severe side effect, we will deliver IGF1 gene to MCMD mice by AAV vector to study whether a therapeutic effect can be achieved in this proposal.

Upon completion, this project will establish complementary therapeutic strategies to combat the severe congenital muscular dystrophy in animal model, setting the base for the development of a clinically efficacious gene therapy strategy.

Project # 6

Background: Elegant studies show that certain cytokines trigger the activation of nuclear factor kappaB (NF-kB) mediated by phosphorylation and degradation of the NF-kB inhibitory protein, IkappaBalpha. Downstream effects of pathological NF-kB activation in skeletal muscle include the inhibition of new muscle formation and the degeneration of existing muscle. *In vitro* studies support the potential that the IkappaBalpha superrepressor (IKBSR), an IkappaBalpha genetically engineered to prevent its phosphorylation, can prevent the activation of NF-kB in skeletal muscle and could ameliorate or prevent muscle wasting. Our preliminary studies demonstrate the novel determination of inhibition of activation of NF-kB by cFLIP.

Objective/Hypothesis: The proposal will explore the mechanism of muscle wasting in an *in vitro* model and develop novel gene transfer vehicles testing the hypothesis that gene transfer strategies can promote muscle regeneration toward a goal of improving muscle bulk and strength in the setting of injuries or diseases that cause muscle atrophy.

Specific Aims:

Aim 1: To characterize an *in vitro* model of cancer-induced muscle wasting in primary muscle cells and in stable muscle cell lines expressing IKBSR or cFLIP.

Aim 2: To clone, rescue, and purify AAV serotype 1 vectors carrying IKBSR or cFLIP and characterize expression and function *in vitro* in anticipation of future use in an *in vivo* model of muscle wasting.

Study Design: We will characterize an *in vitro* model of muscle wasting studying NF-kB activation, the ubiquitin-proteasome system and caspase activation. We will test whether genetic modifications to muscle cells will confer a benefit by blocking pathways of muscle degeneration. We will develop gene transfer vectors designed to promote muscle regeneration.

Relevance: The ability to promote muscle regeneration in the setting of focal or generalized muscle loss could confer significant clinical benefit in the setting of focal neuropathic or other processes that cause muscle atrophy or chronic illnesses that cause cachexia.

Table of Contents

Project # 1
The use of suramin to improve muscle healing after military-related muscle injuries
(Johnny Huard)

Introduction

Muscle injuries, especially pulls and strains, are among the most common and most frequently disabling injuries sustained by athletes and soldiers. Although injured muscles heal naturally, the regeneration is very slow and often yields incomplete functional recovery. In injured muscle, regeneration begins shortly after injury, but the healing process is rather inefficient and is hindered by fibrosis—that is, scar tissue formation. More importantly, the scar tissue that often replaces damaged myofibers may contribute to the tendency of strains to recur. We have observed that TGF-β1 plays a central role in skeletal muscle fibrosis and, more importantly, that the use of antifibrosis agents that inactivate this molecule, such as suramin (a Food and Drug Association [FDA]-approved drug that prevents fibrosis due to skin disorders), can reduce muscle fibrosis and consequently improve muscle healing, resulting in nearly complete recovery after laceration or strain injuries.

Body

Original Proposal

Muscle injuries are very common musculoskeletal problems, and the experiments described in this application are highly relevant to currently unmet medical needs. Although we do not yet understand all the events required for efficient muscle healing, enough information exists for us to vigorously test the proposed research aims. Our extensive preliminary results, presented below, strongly suggest that researchers working to develop biological approaches to improve muscle healing after injury should focus on the elimination of fibrosis within injured muscle tissue. We have observed that TGF-β1 plays a central role in skeletal muscle fibrosis; the use of antifibrosis agents that inactivate this molecule can reduce muscle fibrosis and consequently improve muscle healing after injury. Although the effect of TGF-β1 can be blocked in various ways—including treatment with a neutralizing TGF-β1 antibody, the antisense and ribozyme to TGF-β1, decorin, IFN-γ and -α, or relaxin—the ability of suramin to neutralize the fibrotic effect of TGF-β1 and enhance muscle regeneration makes this molecule particularly well-suited for use in applications to improve muscle healing after injury. In addition, the fact that suramin is already approved by the FDA for use in humans makes this molecule an ideal candidate for use in clinical applications to improve muscle healing in soldiers. Using an animal model of muscle contusion, a common military injury, we will determine the appropriate dose and time of administration of suramin (**Technical Objective 1**). Better characterization of the mechanisms by which suramin enhances muscle regeneration is extremely important because an improved understanding of these mechanisms may reveal novel ways to promote muscle growth and regeneration (**Technical Objective 2A**). We also will investigate suramin's interaction with myostatin and follistatin, 2 important regulators of muscle growth (**Technical Objective 2B**). In summary, the studies proposed in this application will enable us to determine whether suramin, a drug already approved by the FDA, can improve muscle healing by preventing scar tissue formation after a common military injury (muscle contusion); we also will examine the mechanism(s) by which suramin promotes muscle regeneration. The results of these studies could aid in the development of innovative therapies to promote healing in muscles damaged by different types of injury or disease (e.g., muscular dystrophies), therapeutic approaches that could easily be translated from animal experiments to human clinical applications.

The overall goals of the proposed project are as follows: (i) demonstrate that suramin can improve muscle healing in a dose- and time-dependent manner by preventing scar tissue formation after muscle contusion (a common military injury); (ii) determine the mechanisms by which suramin enhances muscle healing after injury. We will investigate whether the enhanced muscle healing observed after suramin treatment is due solely to its inhibition of TGF-β1 activity (**Technical Objective 1)** or to suramin's promotion of muscle regeneration through potential interactions with muscle growth regulators, particularly its possible down-regulation of myostatin or up-regulation of follistatin (**Technical Objectives 2A and 2B**).

Continuation Proposal

New Technical Objective 1: To determine the pharmacokinetics of suramin delivery when administered via intramuscular injection in mice for the treatment of skeletal muscle injuries.

Our laboratory has shown that intramuscular (IM) injection of suramin after laceration and strain injuries decreases skeletal muscle fibrosis in mice and improves muscle healing, resulting in a near complete recovery of muscle function (Chan et al, 2002; Chan et al, 2003). The clinical availability of suramin makes this agent particularly appealing for its use in the treatment of muscle injuries in humans. However, to date, clinical investigations of the use of suramin have been primarily limited to intravenous administrations, which is complicated by a narrow therapeutic index, and dose-limiting toxicities. The dose-limiting toxicities are related to suramin plasma concentrations, of which acceptable levels and durations for humans have been previously reported (Eisenberger et al, 2005). With this in mind, we will perform pre-clinical pharmacokinetic studies in mice to evaluate the concentration/ time data of suramin when administered intramuscularly. Specifically, we will perform measures of therapeutic dosing, half-life and clearance calculations, which will then be used as a guide for the design of phase 1 clinical trials.

New technical objective 2: To evaluate the beneficial effect of decorin, another antifibrosis agent, on muscle regeneration and healing and its mechanism of action.

As mentioned above, various reports indicate that the overproduction of TGF-β1 in response to injury and disease is a major cause of tissue fibrosis in animals and humans. We have observed that TGF-β1 plays a central role in skeletal muscle fibrosis and that the use of antifibrosis agents to inactivate this molecule can reduce muscle fibrosis and consequently significantly improve muscle healing after injury. Although the effect of TGF-β1 can be blocked by various approaches—including treatment with a neutralizing TGF-β1 antibody, the antisense and ribozyme to TGF-β1, suramin [The focus of the last year research proposal], relaxin, and IFN-γ — the unique ability of decorin to neutralize the fibrotic effect of TGF-β1 and independently enhance muscle regeneration makes this molecule particularly well-suited for use in applications to improve muscle healing after injury. Our preliminary data demonstrate that the stimulation of myogenic cells (C2C12 cells) with decorin enhances myogenic differentiation in vitro. Similarly, C2C12 cells genetically engineered to express decorin display an enhanced ability to undergo myogenic differentiation in vitro and in vivo. We also have observed that direct gene transfer of decorin by injection into uninjured skeletal muscle can decrease the fibrosis and enhance the muscle regeneration observed after subsequent injury of that muscle. These results suggest that decorin may independently enhance muscle regeneration and impede fibrosis. On the basis of our prior and preliminary findings, we propose to validate the beneficial effect of decorin on muscle regeneration by conducting gain- and loss-of-function experiments.

Our previous work has shown that suramin can effectively prevent muscle fibrosis and enhance muscle regeneration in lacerated and strain-injured muscle (**Papers 1, 2**);

Paper 1: Chan YS, Li Y, Foster W, Horaguchi T, Somogyi G, Fu FH, Huard J. Antifibrotic effects of suramin in injured skeletal muscle after laceration. *J Appl Physiol* 2003;95:771–780 .

Paper 2: Chan YS, Li Y, Foster W, Fu FH, Huard J. The use of suramin, an antifibrotic agent, to improve muscle recovery after strain injury. *Am J Sports Med* 2004;33:43–51.

However, it is still not known whether suramin can improve muscle healing after contusion injury, the most commonly encountered muscle injury. It also remains unclear whether this enhanced muscle regeneration is a direct effect of suramin. We have performed studies during the first year of funding to examine whether suramin would promote differentiation of myogenic cells *in vitro* and improve injured muscle healing by enhancing regeneration and reducing fibrosis *in vivo*, by using an animal model of muscle contusion.

Original Technical Objective Results

Muscle-derived stem cell differentiation assay: Muscle-derived stem cells (MDSCs) were isolated from wild type mice (C57BL/6J) via the modified preplate technique. MDSCs (10^4 cells/well) were seeded into 12-well

plates and cultured in Dulbecco's modified Eagle's medium (DMEM) containing 10% fetal bovine serum, 10% horse serum, 0.5% chicken embryo extract, and 1% penicillin/streptomycin. After 24 hours, the medium was replaced with differentiation medium (DMEM containing 2% horse serum and 1% penicillin/streptomycin) containing different concentrations of suramin (0, 1, 10, and 100 L/mL). After another 24 hours, the medium was replaced with differentiation medium. All cells were grown at $37^{\circ}C$ in 5% CO_2. Three days after incubation, the fusion index was assessed by counting the number of nuclei in differentiated myotubes as a percentage of the total number of nuclei.

Immunocytochemistry in vitro: Immunocytochemistry was performed on the cells *in vitro* to examine their expression of fast myosin heavy chain (MyHC). Mouse anti-MyHC (1:250; Sigma) was used as the primary antibody, and biotinylated anti-mouse IgG (1:200; Vector) was used as the secondary antibody. Streptavidin 555 conjugate (1:500; Molecular Probes) was applied to detect the secondary antibody.

Animal model: The muscle contusion model was developed in normal wild-type mice (7 to10 weeks of age, with an average weight of 24.0g). A 17g stainless steel ball was dropped through an impactor from a height of 100 cm onto the animal's tibialis anterior (TA) muscle. Mice were divided into 4 groups (5 mice/group). Different concentrations of suramin (0, 2.5, 5, and 10 mg in 20 μL of phosphate-buffered saline [PBS]) were injected intramuscularly two weeks after injury. Cryostat sections of muscles (10 μm in thickness) were obtained and histologically stained (hematoxylin and eosin stain (H&E) and Masson's trichrome stain) four weeks after injury. Numbers of centronucleated regenerating myofibers from each group were counted to evaluate regeneration. Northern Eclipse software (Empix Image, Inc.) was used to quantify the total fibrotic area. Statistical analysis was performed with ANOVA.

Suramin stimulates MDSC differentiation: Suramin treatment promoted the differentiation of MDSCs *in vitro* in a dose-dependent manner. We observed a significantly higher fusion index in each of the two suramin treatment groups (10 and 100 μg/mL**)** than in the control group (0 μg/mL). Furthermore, 100 μg/mL of suramin treatment enhanced the differentiation significantly more than the other suramin treatments (1 and 10 μg/mL) (**Figs. 1, 2**).
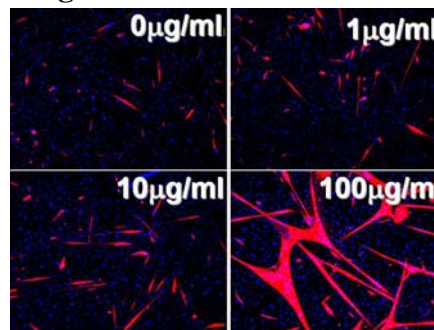
Figure 1

Figure 2

Figure 3

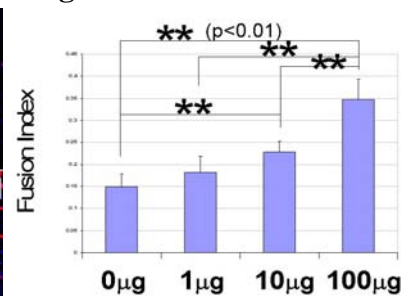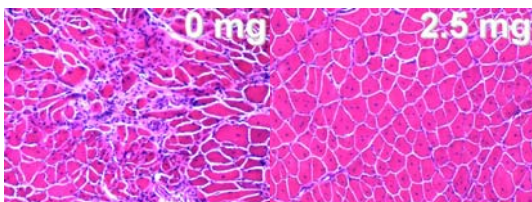**Figure 4**
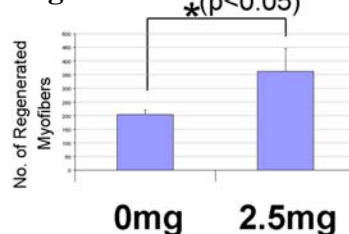
Suramin enhances muscle regeneration and decreases fibrosis after contusion injury: We observed a significant increase in the number of regenerating myofibers in all of suramin treated groups (2.5, 5, and 10 mg/20 μL PBS) when compared with the control group (0mg/20μL of PBS) (**Figs. 3, 4**).

Moreover, Masson's trichrome staining showed significantly less fibrotic area in all of suramin treated groups than in the control group (**Figs. 5, 6**). Although all three suramin treated groups showed significant improvement in healing by way of muscle

Figure 5

Figure 6

regeneration and fibrosis inhibition, there was no significant difference between the three suramin treatment groups (data not shown).

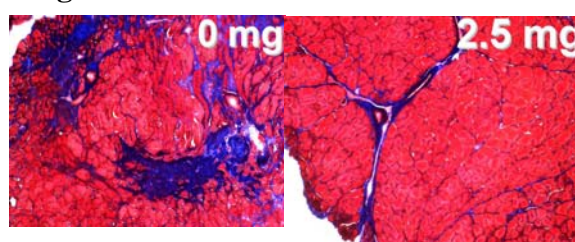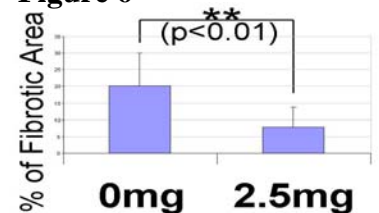These preliminary data indicate that the suramin-treated MDSC groups have higher fusion indices than the control group *in vitro* (**Paper 3**). This suggests that suramin can enhance the differentiation of MDSCs, and reveals a portion of the mechanism by which suramin enhances muscle regeneration following injury. This is the first study to show that suramin not only has antiproliferative effects on fibroblasts, it affects the differentiation of MDSCs directly. Our results clearly indicate that suramin can enhance muscle regeneration and prevent fibrosis after a contusion injury, the most common muscle injury (**Paper 3**). Our future study will investigate the mechanism(s) by which suramin enhances the differentiation of myogenic cells.

Paper 3: Nozaki M, Li Y, Zhu J, Ambrosio F, Fu FH and Huard J. The use of suramin to improve skeletal muscle healing after contusion injury. Presented at the Orthopaedic Research Society, Feb. 2007.

We have recently furthered these findings by performing a series of experiments to determine the mechanism (s) behind the beneficial effect of suramin on muscle healing after injury. Our hypothesis was that suramin enhances muscle healing by both stimulating muscle regeneration and preventing fibrosis in contused skeletal muscle. *In vitro*: Myoblasts (C2C12 cells) and muscle-derived stem cells (MDSCs) were cultured with suramin and the potential of suramin to induce their differentiation was evaluated. Furthermore, MDSCs were co-cultured with suramin and myostatin (MSTN) to monitor the capability of suramin to neutralize the effect of MSTN. *In vivo*: Varying concentrations of suramin were injected in the tibialis anterior muscle of mice two weeks after muscle contusion injury. Muscle regeneration and scar tissue formation were evaluated by histological analysis and functional recovery was measured by physiological testing Our results demonstrated that suramin stimulated the differentiation of myoblasts and MDSCs in a dose-dependent manner. Moreover, suramin neutralized the inhibitory effect of MSTN on MDSC differentiation. *In vivo*, suramin treatment significantly promoted muscle regeneration, decreased fibrosis formation, reduced myostatin expression in injured muscle, and increased muscle strength after contusion injury.

In conclusion our results indicate that intramuscular injection of suramin following a contusion injury improved overall skeletal muscle healing. Suramin enhanced myoblast and MDSC differentiation and neutralized MSTN's negative effect on myogenic differentiation *in vitro,* which suggests a possible mechanism for the beneficial effects that this pharmacological agent exhibits *in vivo*. We believe that these findings could contribute to the development of biological treatments to aid in muscle healing after experiencing a muscle injury.

These results were included in a manuscript entitled "***Improved muscle healing after contusion injury by the inhibitory effect of suramin on myostatin, a negative regulator of muscle growth by Masahiro Nozaki, MD, Yong Li, MD, PhD, Jinhong Zhu, MD, Fabrisia Ambrosio, PhD, MPT Kenji Uehara MD, PhD, Freddie H. Fu, MD, and Johnny Huard, PhD"*** that was recently submitted in the ***Am. Journal of Sports Medicine.***

In a final set of experiments, we have examined whether suramin treatment enhances muscle regeneration and reduce fibrosis by down-regulating myostatin expression *in vivo*. The muscle contusion was made on the tibialis anterior (TA) muscle of each mouse. Two weeks after injury, different concentrations of suramin (0 and 2.5 mg) were injected intramuscularly (n=20 mice/ group). At different time points (0.5, 1, 2, 10, and 14 days after injection), mice were sacrificed and cryosections of TA muscle were analyzed histologically. Suramin (2.5 mg) injection demonstrated a significant increase in the number of regenerating myofibers and reduction of fibrotic area when compared with the control group (0 mg). Furthermore, suramin injection effectively inhibited the expression of myostatin in the injured muscle. Our results suggest that suramin improved skeletal muscle healing by enhancing regeneration and reducing fibrosis after contusion injury through a potential decrease in myostatin expression in the injured skeletal muscle. Our findings may contribute to the development of progressive therapies for muscle injury.

The paper entitled "***Blocking Myostatin with Suramin Improves Skeletal Muscle Healing by Nozaki, M; [+]Li, Y; [+]Zhu, J; [+]***[*]Ambrosio, F; [+]*Uehara K; *Fu, F; and [+]*Huard, J*** has been accepted for presentation at the upcoming Am. Society for Sports Medicine meeting in July 2008.

Continuation Proposal Results

We have shown that decorin, a small leucine-rich proteoglycan, can inhibit TGF- 1 to prevent fibrous scar formation and improve muscle healing after injury. In the decorin-treated muscle, an enhancement of muscle regeneration is observed through histological examination. We have recently determined whether decorin has a direct effect on myogenic cells' differentiation. Our results indicate that myoblasts genetically engineered to express decorin (CD cells) differentiated into myotubes at a significantly higher rate than did control myoblasts (C2C12). This enhanced differentiation led to the up-regulation of myogenic genes (*Myf5, Myf6, MyoD*, and *myogenin*) in CD cells *in vitro*. We speculate that the higher rate of differentiation exhibited by the CD cells is due to the up-regulation of follistatin, PGC-1α, p21, and the myogenic genes, and the down-regulation of TGF- 1 and myostatin. Decorin gene transfer *in vivo* promoted skeletal muscle regeneration and accelerated muscle healing after injury. These results suggest that decorin not only prevents fibrosis, but also improves muscle regeneration and repair.

Paper 4 : Li Y., Li J., Zhu J., Sun, B., Branca M., Tang Y., Foster W., Xiao X**., Huard, J.** Decorin gene transfer promotes muscle cell differentiation and muscle regeneration. **Mol. Therapy. Vol. 15 #9, 1616-1622, 2007.**

Recent studies have shown that myostatin (MSTN), first identified as a negative regulator of skeletal muscle growth, may also be involved in the formation of fibrosis within skeletal muscle. In a recent study, we further explored the potential fibrotic role of MSTN, as well as its interactions with both transforming growth factor-beta1 (TGF-β1) and decorin. We discovered that MSTN stimulated fibroblast proliferation in vitro, and induced its differentiation into myofibroblasts. We further found that, while TGF-β1 stimulated MSTN expression, MSTN stimulated TGF-β1 secretion in C2C12 myoblasts. Decorin, a small leucine-rich proteoglycan, was found to neutralize the effects of MSTN in both fibroblasts and myoblasts, and up-regulate follistatin (FSTN), an antagonist of MSTN. Moreover, FSTN, an antagonist of MSTN, was up-regulated by decorin. The results of in vivo experiments showed that MSTN-knockout mice developed significantly less fibrosis and displayed better skeletal muscle regeneration when compared to wild-type mice at 2 and 4 weeks following laceration injury. In wild-type mice, we found that MSTN stimulated myofibers to express TGF-β1 in skeletal muscles at early time points following injection. Both TGF-β1 and MSTN were additionally seen to co-localize in myofibers in the early stages of injury. In summary, these findings define a fibrogenic property of MSTN, and indicate a coregulatory relationship between TGF-β1, MSTN, and decorin.

These results have been included in a recent paper entitled "***RELATIONSHIPS BETWEEN TGF-β1, MYOSTATIN, AND DECORIN: IMPLICATIONS FOR SKELETAL MUSCLE FIBROSIS by Jinhong Zhu, Yong Li ; Wei Shen , Chunping Qiao , Fabrisia Ambrosio , Mitra Lavasani, Masahiro Nozaki, Maria F. Branca , Johnny Huard*** " that has recently been published in the ***Journal of Biological Chemistry. (JBC, vol 282, #35: 25852-25863, 2007).***

Key Research Accomplishment

- Determined that Suramin can stimulate MDSC myogenic differentiation *in vitro.*

- Determined that Suramin can enhance skeletal muscle regeneration and reduce fibrous scar formation following a contusion injury.

- Determined that Suramin's beneficial effects on muscle healing is related to it's ability to enhance the proliferation and differentiation of myoblasts and MDSC and it's ability to inhibit myostatin and up-regulate follistatin.

- Determined that the antifibrotic ability of decorin not only relates to it's ability to inhibit TGF-β1 but also myostatin. We further showed that the up or down regulation of TGF-β1 simultaneously had the same effect on myostatin and vice versa.

Reportable Outcomes

1) **Nozaki M, Li Y, Zhu J, Ambrosio F, Fu FH and Huard J.** The use of suramin to improve skeletal muscle healing after contusion injury. Presented as a poster at the Orthopaedic Research Society meeting, Feb. 2007.
2) ***Masahiro Nozaki, MD, Yong Li, MD, PhD, Jinhong Zhu, MD, Fabrisia Ambrosio, PhD/ MPT Kenji Uehara MD, PhD, Freddie H. Fu, MD, and Johnny Huard, PhD.*** *Improved muscle healing after contusion injury by the inhibitory effect of suramin on myostatin, a negative regulator of muscle growth Under Review at* the *Am. Journal of Sports Medicine.*
3) **Li Y., Li J., Zhu J., Sun, B., Branca M., Tang Y., Foster W., Xiao X., Huard, J.** Decorin gene transfer promotes muscle cell differentiation and muscle regeneration. Mol. Therapy. Vol. 15 #9, 1616-1622, 2007.
4) **Jinhong Zhu, Yong Li, Wei Shen, Chunping Qiao , Fabrisia Ambrosio, Mitra Lavasani, Masahiro Nozaki, Maria F. Branca**, **Johnny Huard**. *RELATIONSHIPS BETWEEN TGF-β1, MYOSTATIN, AND DECORIN: IMPLICATIONS FOR SKELETAL MUSCLE FIBROSIS. Journal of Biological Chemistry Vol 282(35): 25852-25863, 20.*

Conclusions

This line of work has enabled us to identify two potentially useful compounds that could be utilized to prevent fibrous scar formation and aid in the healing and regeneration of injured skeletal muscle. Suramin is a drug that has been used clinically to treat individuals infected with trypanosomes and worms and is currently being investigated for the treatment of prostate cancer; therefore it could potentially be applied clinically expeditiously. Decorin too has shown great promise; however, it is not currently FDA approved for clinical application and would require more time to apply clinically since it would need to undergo clinical trials. From a basic science standpoint these studies have demonstrated the mechanisms that these two drugs utilize for their beneficial effect on the healing and regeneration of skeletal muscle. They firstly act by inhibiting two components that are major initiators of the fibrosis cascade, TGF-B1 and myostatin. They have also been shown to facilitate regeneration and healing by promoting myoblast and MDSC proliferation and differentiation into myotubes in vitro and myofibers in vivo. One of the pathways that they seem to work on for this enhancement in regeneration appears to be the up-regulation of follistatin. Additional work is currently underway to determine the pharmokinetics of these two promising compounds.

Appendices

Appendix 1 (Paper3): Nozaki M, Li Y, Zhu J, Ambrosio F, Fu FH and Huard J. The use of suramin to improve skeletal muscle healing after contusion injury. Presented at the Orthopaedic Research Society, Feb. 2007.

Appendix 2*: Masahiro Nozaki, MD, Yong Li, MD, PhD, Jinhong Zhu, MD, Fabrisia Ambrosio, PhD, MPT Kenji Uehara MD, PhD, Freddie H. Fu, MD, and Johnny Huard, PhD. Improved muscle healing after contusion injury by the inhibitory effect of suramin on myostatin, a negative regulator of muscle growth. Under Review at the Am. Journal of Sports Medicine.*

Appendix 3 (Paper 4*): :* Li Y., Li J., Zhu J., Sun, B., Branca M., Tang Y., Foster W., Xiao X**., Huard, J.** Decorin gene transfer promotes muscle cell differentiation and muscle regeneration. **Mol. Therapy. Vol. 15 #9, 1616-1622, 2007.**

Appendix 4: Jinhong Zhu, Yong Li ; Wei Shen , Chunping Qiao , Fabrisia Ambrosio , Mitra Lavasani, Masahiro Nozaki, Maria F. Branca , Johnny Huard. *RELATIONSHIPS BETWEEN TGF-β1, MYOSTATIN, AND*

Investigator: Johnny Huard

DECORIN: IMPLICATIONS FOR SKELETAL MUSCLE FIBROSIS. Journal of Biological Chemistry Vol 282(35): 25852-25863, 2007.

Project # 2
Improving muscle healing through digestion of scar tissue via MMP-1
(Yong Li)

Introduction:

Muscle injuries, which occur most frequently as sports injuries, and during military training, and battle, present a challenging problem in traumatology. After injury, damaged muscle fibers undergo a natural process of necrosis and the resulting dead tissue is removed by infiltrating lymphocytes. Meanwhile, locally released growth factors stimulate muscle regeneration by activating satellite cells. Unfortunately, the process of muscle regeneration is often incomplete because overgrowth of the extracellular matrix (ECM) leads to significant local fibrosis (i.e., fibrous scar formation). This scar tissue impedes the formation of normal muscle fibers in the injured muscle, resulting in incomplete functional recovery and a propensity for re-injury. We have begun to study the mechanism behind the fibrosis that occurs in injured skeletal muscle. Our previous studies have demonstrated that myogenic cells (including muscle-derived stem cells [MDSCs]) and regenerating myofibers in lacerated muscle can differentiate into fibrotic cells, and that transforming growth factor (TGF)-beta1 is a major stimulator of this differentiation. Using different animal models of muscle injury, we have investigated biological approaches by which to prevent fibrosis and thereby improve muscle healing. However, it often is not possible to treat injured muscles before the initiation of fibrosis—most patients with muscle injuries seek treatment only after the onset of fibrous scar formation, and the concomitant pain and functional deficits it produces. Moreover, chronic diseases (e.g., Duchenne muscular dystrophy [DMD]) generally present with significant amounts of fibrous scar tissue already present within the patients' muscles. Because prevention of fibrosis is infeasible in many cases, the development of a novel therapeutic approach by which to digest existing fibrous scar tissue and improve muscle healing would be very significant.

Matrix metalloproteinase type-1 (MMP1), a naturally occurring collagen-digesting enzyme, has shown great capacity for digesting fibrous scar formations in various tissues. Additionally, MMP1 is also able to increase cell migration in many tissues. We believe that MMP1 is able to facilitate the healing of injured muscle by digesting fibrous scar tissue and improving the local environment in which muscle regeneration occurs. Results obtained from this project may lead to the development of gene therapy applications that eliminate scar tissue within skeletal muscle. Such applications could drastically improve the regeneration of muscles damaged by trauma or by chronic muscle diseases, such as Duchenne and Becker muscular dystrophies.

In the past year, we have finished most of the proposed experiments. Through our work on **Objective #1**, we have determined that MMP1 increased muscle cell migration and differentiation/fusion capacity in vitro. In vivo, we also determined that MMP1 could improve muscle healing through increasing muscle cell migration, differentiation and regeneration (**Objective #2**). Finally, we have begun to investigate the effects of using MMP1 gene transfer techniques on muscle cells in vitro (**Objective #3**).

Body:

Technical Objective #1: To assess the effect of MMP1 on muscle cells *in vitro*.

The primary objective of this proposal is aim to investigate the effect(s) of MMP1 on various muscle cells *in vitro*. With respect to the approved statement of this objective, we have discovered that MMP1 does indeed affect muscle cells by inhibiting fibroblasts growth and collagens deposition as well as by enhancing myoblasts migration and fusion/differentiation of these cells *in vitro*.

We have previously observed MMP1 could slow fibroblast's growth and collagens deposition. To investigate the potential effects of MMP1 on muscle cell differentiation and migration, we have selected C2C12, a myoblast cell line as target cells. We designed a wound healing assay by using C2C12 that were cultured in 12-well plates in control medium until confluent. Cells were then treated with 0, 1.0, 10, or 100 ng/mL of MMP1 (M-1609, Sigma) in Dulbecco's Modified Eagle's Medium (DMEM, invitrogen). An artificial wound was created, at the same time, by denuding an area at the center of each well using a pipette tip to scrape off cells. Cells were incubated to different time-points (1, 4, 6, and 12 hours), and then fixed with cold methanol. Cells were stained with 4',6-Diamidino-2-phenylindole (DAPI, Sigma) to help visualize migration. This experiment has

been repeated 5 times for the statistic analysis, as shown in **Figure 1**, C2C12 display an enhanced ability to migrate into the wound area after 1, 4, and 6 hours of treatment with MMP-1 (10 ng/mL) compare to control non MMP1 treated C2C12.

Figure 1

Our Western Blot analysis further demonstrates that MMP-1 treatment enhances myoblast migration. It has been reported that PreMMP2 and TIMP are proteins that are upregulated with myoblast migration. We therefore observed any change on these proteins after MMP1 treatment. C2C12 cells were harvested after 48 hours incubation with or without MMP-1 (0, 1.0, 10, 100 ng/mL) in serum-free DMEM. After lysing, the samples were separated by 12% sodium dodecyl-sulfate-polyacrylamide electrophoresis gel and transferred to nitrocellulose membranes. Anti-PreMMP2 antibodies (Santa Cruz), and anti-TIMP (Santa Cruz) were used as primary antibodies. Mouse Glyceraldehyde 3-phosphate dehydrogenase (GAPDH, Sigma,) was used for protein quantification. Expression of PreMMP2 increased in a dose dependent manner when treated with 0.1, 1, 10, and 100 ng/mL of MMP-1 (**Fig. 2**). Expression of TIMP was also upregulated in a dose-dependent manner when treated with 0.1, 10, and 100 ng/mL of MMP-1 (**Fig. 2**).

Figure 2
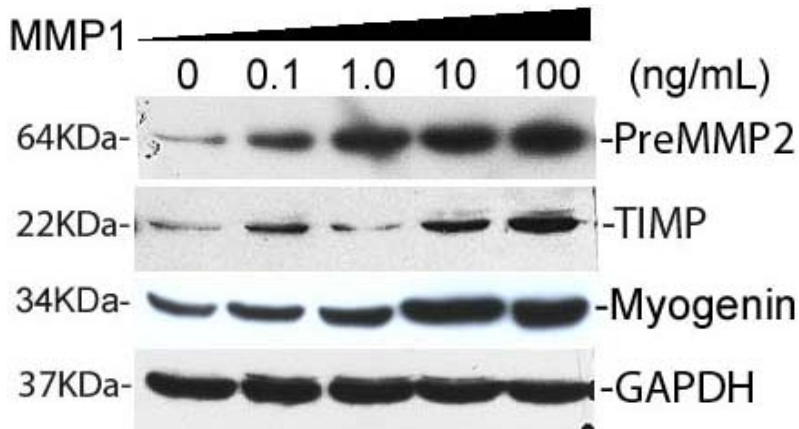
We also investigated if MMP1 could have any direct effect on muscle cell differentiation. C2C12 were cultured complete medium containing Dulbecco's Modified Eagle's Medium (DMEM; Invitrogen, Carlsbad, CA) supplemented with 10% fetal bovine serum, 10% horse serum, 0.5% chicken embryo extract, and 1% penicillin/streptomycin (P/S) at 37°C in a 5% CO_2 atmosphere in 12 well plates until 75% confluent. Cells were subsequently incubated in differentiation media containing

Figure 3

serum-free DMEM supplemented with 1% penicillin/streptomycin and treated with 0, 1.0, 10, or 100ng/mL of MMP-1 (Sigma, M1802) for 3, 5, and 7 days. Cells were fixed in cold methanol for 1 minute and washed with phosphate buffered saline (PBS). The fixed cells were immunostained for Myosin Heaven Chain (MyHC, Sigma) and 4',6-Diamidino-2-phenylindole (DAPI) to visualize mature myotubes. The differentiation was quantified by averaging the number of myotubes counted in 5 high power fields under a fluorescent microscope. With MMP-1 treatment, C2C12 cells displayed a dose-dependent increase in their ability to differentiate into myotubes at 3 and 5 days after incubation (**Fig. 3**) (*$P<0.05$). This points also was confirmed by western blot results that MMP1 increased myogenin expression on a dose dependent manner in vitro (see **Fig. 2**)
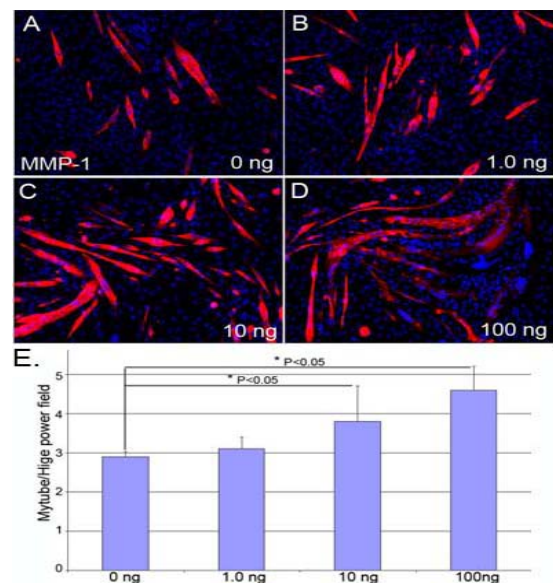
Technical Objective #2: To assess the effects of MMP1 on skeletal muscle *in vivo*.
What we proposed in this objective was to observe the effects of MMP1 on skeletal muscle healing in animal models *(in vivo)*. We have developed a reproducible muscle injury model in mice that induces significant fibrous scar formation and hindered myofiber regeneration during muscle healing. These injured muscles exhibit slower muscle healing that is incomplete due to the presence of scar tissue. Based on this model, we have determined that **MMP1 can digest the existing fibrous scar and enhance muscle healing in the injured skeletal muscles**. This proposed experiment has been done in past year, and this study has been published by the *Journal of Applied Physiology* 2007;102(6):2338-2345 (Please see attached copy of manuscript). In addition, to observe the effect of MMP1 on muscle cell migration and differentiation in vivo, we have selected MDX, a mouse model for Duchenne muscular dystrophy [DMD], to investigate if MMP1 could enhance muscle cell migration and differentiation in vivo. Our updated results have substantiated this point, means MMP1 can enhance muscle cell fusion as well as migration in dyatrophic muscle in deed. Results from this research have been organized into a manuscript entitle: '**MMP-1 enhances muscle cell migration and differentiation'** that has been send to publication on the Journal of *Cell Experimental Research*.

Technical Objective #3: To assess the use of MMP1–based gene therapy to digest fibrous scar tissue within injured skeletal muscle.
This proposal is planning to investigate whether MMP1 gene transduction in implantable myoblasts can extend MMP1 function as a means of digesting fibrous scar tissue and promoting muscle cell migration, fusion and regeneration within injured skeletal muscle. MMP1 can degrade collagens, but undergoes self–degradation, which results in a short biological half-life. As a result, the fibrous scar tissue has the potential to reform following MMP1 degradation. To extend the function of MMP1, we have constructed a retrovirus vector encoding the MMP1 gene.

We have investigated whether MMP1 gene transduction could have any effect on myogenic cell migration and differentiation. To investigate whether these MMP1-expressing cells are able to produce a better muscle graft in the skeletal muscle of *MDX* mice, we used a retrovirus vector to transfer the *LacZ* marker gene into genetically altered C2C12 cells that expressed MMP1 as wall as control C2C12 cells that did not express MMP1. These cells were then separately transplanted into the skeletal muscle of *MDX*/SCID (C57BL/10ScSn-Dmd^mdx crossed with C57BL/6J-Prkdc^scid/SzJ mice. Histological analysis was performed after cell transplantation, whereupon we detected both LacZ-positive (blue; see arrows in **Fig. 4A-D**) and dystrophin-positive (brown; see asterisks; **Fig. 4A-D**) myofibers in the host muscle at 2 weeks (**Fig. 4A & B**) and 4 weeks (**Fig. 4C & D**) after cell transplantation. However, we discovered that the MMP1-expressing C2C12 fuse/differentiate into better muscle grafts (**Fig. 4B & D**) after transplantation into the skeletal muscle of *MDX* mice than the control C2C12-transplanted groups (**Fig. 4A & C**) at both 2 and 4 weeks after cell transplantation. In future studies, we will measure the number and the diameter of LacZ-positive and dystrophin-positive myofibers from the skeletal muscle of control and MMP1-expressing cell therapy groups.

Figure 4
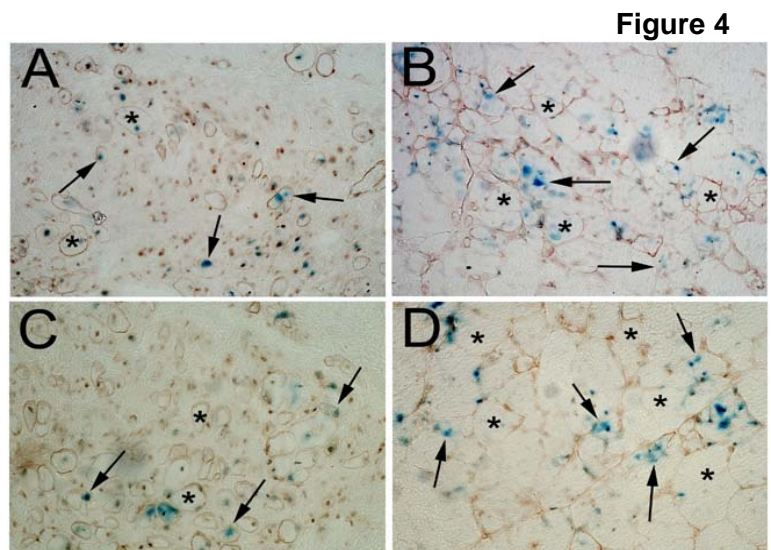
<u>The coming year's plans:</u> We have successfully completed **Objective #1 & #2**. For **Objective #3**, we will focus on investigating the use of MMP1 gene therapy in an animal model of injury to determine the effect of MMP1 gene therapy on the enhancement of regeneration, migration and reduction of scarring in the skeletal muscle of both trauma and diseased mice models.

Key Research Accomplishments:
1. Discovery of the effect of MMP1 on muscle cells, resulting in increased migration and differentiation of myogenic cells *in vitro*.
2. Discovery of the effect of MMP1 on scarring skeletal muscle, namely, the digestion of fibrous scar tissue, and improved muscle healing *in vivo*.
3. Discovery of the effect of MMP1 on muscle cell migrations and fusion in skeletal muscle of mice *in vivo*.

Reportable outcomes:
One of our manuscript entitled "Matrix Metalloproteinase Therapy Improves Muscle Healing" has been published in *Journal of Applied Physiology* . We have another manuscript entitled, "MMP1 enhances muscle cell migration and differentiation" that has been submitted to the Journal of *Cell Experiment Research.* We have prepared another manuscript to summarize our results from **Objective #3** to be entitled, "MMP1 gene therapy to enhance muscle cell migration and differentiation".

One abstract (attached) has been presented at four different national and international conferences and have won two awards in past two years: The Award for Outstanding Research in Biochemistry/Cell Biology and the prestigious Award for Overall Excellence in Research at the 2006 AMA-MSS National Research Poster Competition.

Conclusion:
In vitro, we have seen that MMP1 can enhance muscle cell migration and differentiation. The migration–related proteins are also up–regulated within MMP1–treated muscle cells. *In vivo*, the fibrous scar tissues that form within traumatically injured skeletal muscle could limit transplanted myogenic cell migration, fusion, and regeneration, and slow the overall muscle healing process. However, muscle healing was greatly improved following MMP1 treatment within these scarring skeletal muscles. We also discovered that the use of MMP1 gene–transferred myoblasts resulted in an increased differentiation capacity *in vitro* and enhanced muscle cell migration *in vivo*.

Appendices:

Appendix 5: "Matrix Metalloproteinase Therapy Improves Muscle Healing" has been published on the *Journal of Applied Physiology* 2007;102(6):2338-2345 resulted from **Objective #2**

Appendix 6: "MMP1 enhances muscle cell migration and differentiation" (sent for publication by the Journal of *Cell Experiment Research*) resulted from **Objective #1 & #2**.

Appendix 7: "Matrix Metalloproteinase-1 enhances muscle cell migration and dedifferentiation" (Poster Presentation at the ORS annual meeting, 2008)

References
The majority of relevant references may also be found in these manuscripts.

Project # 3
Repairing injured skeletal muscle through myogenic endothelial cells
(Bruno Peault)

INTRODUCTION

Multi-lineage developmental potential of human vascular pericytes
Pericytes, a.k.a. Rouget cells or mural cells, also named mesangial cells in the kidney and Ito cells in the liver, closely encircle, within long cytoplasmic extensions, endothelial cells in capillaries and microvessels. These cells contain α-smooth-muscle actin (α-SMA) and regulate microvessel contractility. Pericytes can also inhibit, *via* TGFβ secretion, the division of endothelial cells. Besides, pericytes are suspected to be, or include, progenitors of different cell types, although this assumption relies mostly on indirect evidence, obtained on unsorted cells, and on a limited range of cell lineages (principally, bone and cartilage), excluding notably skeletal myogenic cells.

Some of us have previously discovered, in primary cultures of skeletal muscle, a population of muscle-derived multipotent stem cells (MDSC), of yet unknown identity, that regenerate myofibers more efficiently than committed satellite cells. In the present project, we have focused on the role of human muscle-derived pericytes in muscle regeneration, following the hypothesis that pericytes represent the source of MDSC. Our results show that pericytes are indeed endowed with robust myogenic potential and represent a promising source of therapeutic progenitors for muscle regeneration.

Our recent results, reported in 2007 to the DOD, demonstrated that pericytes isolated prospectively from skeletal muscle and non-muscle human tissues are myogenic when placed in appropriate experimental conditions. We could rule out that the myogenic potential we had documented in pericytes sorted from skeletal muscle was due to contamination by regular myogenic cells since i- no Pax7 or CD56 mRNA was ever detected by RT-PCR analysis within extracts of sorted pericytes, ii- the average muscle regeneration index of pericytes was higher than that of CD56+ myogenic cells purified from the same muscles and iii- the same myogenic potential was detected in pericytes sorted from non-muscle tissues such as the pancreas and adipose tissue. In agreement with our results, multi-lineage progenitors have been previously identified in multiple adult human and rodent tissues. In this category enter the bone marrow-derived MSC (mesenchymal stem cell, or marrow stromal cell), which can differentiate into mesoderm lineage cells, including myoblasts, the muscle-derived stem cells (MDSC) some of us have previously characterized and the bone marrow derived MAPC (multipotent adult progenitor cells), that can contribute to mesodermal, endodermal and ectodermal cell lineages and which have equivalents in mouse brain, pancreas and skin dermis as well as in human skin and white adipose tissue. The existence of these adult multipotent progenitors has been, however, revealed only retrospectively in long-term cultures of the source tissues, and therefore their identity and anatomic distribution in native organs could not be determined. Our data supported the hypothesis that these progenitors are natively associated with blood vessel walls and, more precisely, are derived from pericytes. The omnipresence of pericytes in the organism explains why such multi-lineage progenitors have been found in a multitude of organs. **The recent results reported below further support the existence in the adult body of ubiquitous perivascular multi-lineage progenitors endowed notably with robust myogenic potential.**

BODY

Methods

Human tissues
Human fetal tissues were obtained following spontaneous, voluntary or therapeutic pregnancy interruptions performed at Magee Womens Hospital (University of Pittsburgh), in compliance with Institutional Review Board protocol number 0506176. Developmental age (16 to 24 weeks of gestation) was estimated by measuring foot length. Informed consent for the use of fetal tissues was obtained from patients in all instances. Adult human pancreas and muscle were procured by CORE (Center for Organ Recovery and Education, Pittsburgh) from multi-organ donors. Abdominal subcutaneous fat was obtained anonymously from female patients (mean age

of 51 years) undergoing abdominoplasty at the Department of Surgery of the University of Pittsburgh Medical Center.

Immunohistochemistry and cytochemistry
Fresh fetal and adult tissues were gradually frozen by immersion in isopentane (Merck) cooled in liquid nitrogen and embedded in tissue freezing medium (Triangle Biomedical Sciences). WAT was impregnated in gelatin/sucrose and frozen in the same conditions. Five- to 9-µm sections were cut on a cryostat (Microm) and fixed for 5 min with 50% acetone (VWR International) and 50% methanol (Fischer Chemical), or for 10 min in 4% paraformaldehyde (PFA, Sigma). Sections were then dried for 5 min at room temperature (RT) and washed 3 times for 5 min in PBS. Non-specific binding sites were blocked with 5% goat serum (Gibco) in PBS for 1 hour at RT. Sections were incubated with uncoupled primary antibodies overnight at 4ºC, or 2 hours at RT in the case of directly coupled antibodies. After rinsing, sections were incubated for 1 hour at RT with a biotinylated secondary antibody, then with fluorochrome-coupled streptavidin, both diluted in 5% goat serum in PBS. For intracellular stainings, cells were first permeabilized with PBS 0.1% Triton X-100 (Sigma). Cultured cells were fixed inside wells as described above, then washed 3 times in PBS 0.1% Triton X-100 and incubated for 1 hour in PBS, 5% goat serum. Cultured cells were then stained as described above. 0.1% Triton X-100 (Sigma) was added at all steps for intracellular antigen staining.

The following anti-human primary antibodies were used: uncoupled anti-CD140b (PDGF-Rβ; clone 28D4; Monoclonal Antibody Facility of the University Clinic of Tübingen, undiluted), uncoupled anti-CD146 (BD Pharmingen, 1:100), anti-CD31 (DAKO, 1:100), anti-CD34 (Serotec, 1:50), anti-CD44, anti-CD90 (both from Becton-Dickinson (BD), 1:20), anti-NG2 (BD Pharmingen, 1:300) and anti-lamin A/C (Novo Castra, 1:100). Coupled antibodies used included the following: anti-CD146-Alexa 488 (Chemicon, 1:200), anti-α-SMA-FITC (Chemicon, 1:100), anti-CD34-FITC (DAKO, 1:50 or Miltenyi, 1:20), anti-vWF-FITC (US Biological, 1:100), and biotinylated anti-CD144 (BD, 1:100). Skeletal muscle proteins were detected with anti-skeletal myosin heavy chain (fast) (Sigma 1:100), anti-skeletal myosin heavy chain (slow) (Sigma 1:100), anti-spectrin and anti-dystrophin (Novocastra, 1:20) and anti-desmin (1:50, Sigma). Rabbit anti-mouse dystrophin (Abcam, 1:100) was used to detect dystrophin positive myofibers in SCID/mdx mice. Directly biotinylated *Ulex europaeus* lectin (UEA-1) was also used as an endothelial cell marker (Vector, 1:200). Secondary goat anti-mouse antibodies were biotinylated (DAKO and Immunotech, 1:1000) or coupled to Alexa 488 (Molecular Probes, 1:500). Streptavidin-Cy3 (Sigma, 1:1000) was used. Nuclei were stained with DAPI (4', 6-diamino-2-phenylindole dihydrochloride, Molecular Probes, 1:2000) for 5 min at RT. An isotype-matched negative control was performed with each immunostaining. Slides were mounted in glycerol-PBS (1:1, Sigma) and observed on an epifluorescence microscope (Nikon Eclipse TE 2000-U).

Fluorescent in situ hybridization
Frozen tissue sections were fixed and stained with anti-human spectrin as described above. Slides were dehydrated in 100% ethanol (Pharmco Products Inc.) and air dried. Target DNA was denatured by incubation in 70% formamide (Roche) in saline-sodium citrate (SSC, 2X, Sigma Chemical Company) at $75^{O}C$ for 15 min, followed by dehydration in 100% ethanol. Simultaneously, a directly labeled fluorescent All-Human Centromere Satellite Probe (undiluted, Molecular Cytogenetics, Q-Biogene) was denatured at $75^{O}C$ for 10 min. Slides were incubated with 20uL of probe and sealed with rubber cement (Elmer's) overnight in a humidified $37^{O}C$ incubator. Post-hybridization washes were performed at $45^{O}C$ in 50% formamide in 2X SSC for 15 min, followed by 2X SSC and 4X SSC with Tween (Bio-Rad), each for 20 min. Nuclei were counterstained with DAPI (1:2000, Molecular Probes).

Flow cytometry
Perivascular cells present in skeletal muscle, myocardium, pancreas, placental chorionic villi, brain, skin, bone marrow and adult skeletal muscle, adipose tissue and pancreas were analyzed and sorted by flow cytometry. Fresh pancreas, skin, brain, bone marrow or muscle were cut into small pieces with a scalpel in Dulbecco's modified Eagle medium (DMEM, Gibco) containing 20% fetal calf serum (FCS, Gibco), 1 % penicillin-streptomycin (PS, Gibco) and collagenases I, II and IV (1mg/mL, Sigma), then incubated at 37ºC for 1 hour on a shaker. Final cell dissociation was achieved by gently pressing the tissue between ground glass slides. Cells were washed with PBS without calcium and magnesium (Gibco) and centrifuged at 1200 rpm for 5 min at 4ºC. Cell pellets were resuspended in DMEM, 20% FCS, 1% PS and filtered at 100 µm (Cell Strainer, BD Falcon) in

the same medium. Adult adipose tissues were finely minced, then digested in DMEM containing 3.5% bovine serum albumin (Sigma) and collagenase II (1mg/ml, Sigma) for 70 min under agitation at 37°C. Mature adipocytes were separated from pellets by centrifugation (2000 rpm, 10 min). Pellets were resuspended in erythrocyte lysis buffer (155 mM NH_4Cl, 10mM $KHCO_3$, 0,1mM EDTA) and incubated for 10 min at RT. Cells were washed; pellets were resuspended in DMEM, 20% FCS, 1% PS and passed through a 70-µm cell filter (BD Falcon). Vasculature from the mid-gestation placenta was minced and agitated in DMEM, 1% PS, 1mg/ml collagenases I, II and IV (1g tissue/1ml solution) for 30 min at 37°C, 120 rpm (MaxQMini 4000, Barnstead). 0.05% trypsin (Gibco) was added and the suspension was agitated for 10 more min. Enzymes were removed by centrifugation and cells were resuspended in DMEM, 1% PS. Cells were passed through a 70-µm cell strainer and centrifuged cells were resuspended in erythrocyte lysis buffer and incubated for 15 min at RT.

Cells from all tissues were counted following dead cell exclusion with Trypan blue (Sigma). Cells (10^5 for analysis and around 30.10^6 for sorting) were incubated with a combination of the following directly coupled mouse anti-human antibodies: anti-CD34-PE (DAKO, 1:100), anti-CD45-APC-Cy7 (Santa Cruz Biotechnologies, 1:200) or anti-CD45-APC (BD, 1:100), anti-CD56-PE-Cy7 and anti-CD146-FITC (Serotec, 1:100) in 1ml DMEM, 20% FCS, 1% PS at 4°C for 15 min in the dark.

For 6-color analysis of MSC marker expression by pericytes, cells were first incubated with uncoupled mouse anti-CD90 (BD, 1:20) and, after washing, with biotinylated goat anti-mouse (Dako, 1:250). Next, washed cells were incubated with a mixture of streptavidin-PB (pacific blue) (Molecular Probes, 1:500) and the 5 other directly conjugated antibodies: CD44-PECy5 (eBioscience, 1:20), CD34-PE (Dako, 1:50), CD146-FITC (Chemicon, 1:100), CD45-APC (BD, 1:100) and CD56-PECy7 (BD, 1:100). As negative controls, cell aliquots were incubated with isotype-matched mouse IgGs conjugated to PE (Chemicon, 1:100), APC (BD, 1:100), PECy5 (eBioscience, 1:20), PECy7 and FITC (US Biological or Chemicon, 1:100), under the same conditions. After washing and centrifugation, all labelled cells (except those labelled with PECy5) were incubated for 15 to 30 min with 7-amino-actinomycin D (7-AAD, 1:100, BD) for dead cell exclusion, passed through a 70-µm cell filter and then run on a FACSAria flow cytometer (BD).

Cultured cells were labeled, at different passages, with the following commercial antibodies: anti-CD13-PE (BD), anti-CD34-PE (BD), anti-CD44-FITC (BD), anti-CD45-PE-Cy7 (Beckman Coulter), anti-CD56-PE (Chemicon), anti-CD73-PE (BD), anti-CD90-PE (Chemicon), anti-CD105 FITC (ImmunoTools), anti-CD133-2-APC (Miltenyi Biotec), anti-CD146-PE (BioCytex), anti-alpha-SMA-FITC (Sigma), anti-HLA-ABC-FITC (Immunotech), anti-HLA-DR-PE (Becton Dickinson), anti-CXCR4 (BD), anti-NGF-R (BD) and anti-BB9 (BD), the latter being revealed with anti-mouse IgG1-FITC (Exalpha). Moreover, the following reagents from the monoclonal antibody facility of the University Clinic of Tübingen were used for flow cytometry analysis on cultured cells: anti-CD10 (CALLA; clone 97C5), anti-CD34 (clone 43A1), anti-CD56 (N-CAM; clone 39D5), anti-CD105 (endoglin; clone 1G2C2), anti-CD109 (clone W7C5), anti-CD133 (clone W6B1C3), anti-CD140b (PDGF-RB; clone 28D4), anti-CD164 (clone 67D2), anti-CD318 (CDCP1; clone CUB1), anti-CD324 (E-cadherin; clone 67A4), anti-CD326 (Ep-CAM; clone 9C4),), anti-CD340 (HER-2; clone 24D2), anti-CD344 (frizzled-4; clone CH3A4) and anti-CD349 (frizzled-9; clone W3C4E11). Anti-CD166 was purchased from BD-Pharmingen and the PE-conjugates against CD31, CD106 and CD108 were a kind gift from Dr. Gene Lay (BioLegend, San Diego, CA). Full information on the human cell markers used in this study can also been found at: http://www.hcdm.org . Isotype control immunoglobulins used were IgG1-PE, IgG1-FITC (both from Chemicon), IgG1-PE-Cy7) (Beckman Coulter) and IgG1-APC (BD). Resuspended cultured cells were stained as follows. Cells were permeabilized with 0.1% Triton X-100 (Sigma) when necessary. After washing the cells twice with PBS containing 1% FCS and 0.01% NaN_3 (FACS buffer), cells were incubated with polyglobin to block non-specific binding. Cells were then incubated with the indicated primary antibodies for 15 min on ice. After washing in FACS buffer, cells were incubated with a F(ab)$_2$ fragment of goat anti-mouse secondary antibody conjugated with R-phycoerythrin (PE; Dako Cytomation) for 15 min. Finally, cells were washed twice and at least 50,000 events were acquired on a FACSCanto II cytometer (BD), using FCS express software for analysis.

RT-PCR analysis

Total RNA was extracted from 10^4 freshly sorted or cultured perivascular cells or unfractionated cells using the Absolutely RNA nanoprep kit (Stratagene). cDNA was synthesized with SuperScript^{TM} II reverse transcriptase (Invitrogen). PCR was performed for 30 cycles at 58°C annealing temperature with Taq polymerase (Invitrogen), and PCR products were electrophoresed on 1% agarose gels. The primers used for PCR are

listed in Table 1. Each set of oligonucleotides was designed to span two different exons so that genomic DNA contamination is of no concern.

Long-term culture and genetic modification of perivascular cells

Sorted perivascular cells were seeded at 2 x 10^4 cells per cm^2 in endothelial cell growth medium 2 (EGM-2^{TM} ,Cambrex BioScience) and cultured at 37ºC for 2 weeks in plates coated with 0.2% gelatin (Calbiochem). Confluent cells were then detached by treatment with trypsin-EDTA (Gibco) for 10 min at 37ºC, then split 1:3 in uncoated plates in DMEM high glucose (Gibco), 20% FCS, 1% PS (Gibco). After the fifth passage, cells were then passaged 1:6 in the same conditions, and culture medium was changed every 4 days. We calculated the population doubling time (PDT) as previously described (Deasy et al., 2003, 2005). For gene transfer, cultured perivascular cells at passage 12 were detached with 0.25% trypsin/EDTA when the culture was near confluency and seeded at a density of 100,000 cells /cm^2. After 16 hours, medium was replaced with transduction medium (DMEM high glucose, 20% FCS, 1% P/S, 8 µg/mL polybrene) and an EIAV-based CMV-driven eGFP expression vector (Endo et al., 2007) was added at an MOI of 100. After 3 days, nearly 100% of cells expressed GFP and medium was returned to culture medium.

Myogenesis in culture

Freshly sorted or cultured perivascular cells (2x10^3 cells per cm^2) were cultured for 7 days in proliferation medium: DMEM high-glucose, 10% FCS, 10% horse serum (HS, Gibco), 1 % CEE (chicken embryo extract, Accurate), 1% PS, and then for 7 to 10 days in fusion medium: DMEM high-glucose, 1% FCS, 1% HS, 0.5% CEE, 1% PS (Gibco). Half of the medium was renewed every 4 days. Myogenesis was induced by lowering serum concentration to 2% and medium was changed every 4 days until elongated, multinucleated myofibers appeared.

Muscle regeneration in vivo

Eight- to 12-week old SCID-NOD mice were used for *in vivo* experiments. All animal subjects were anaesthetized by inhalation of isofluorane/O$_2$. Cardiotoxin (15 µg; CTX, Molecular Probes) was injected into the gastrocnemius muscle three hours prior to cell transplantation. Mice were anaesthetized a second time and freshly sorted or cultured perivascular cells suspended in 35 µL PBS, or the same volume of PBS as a control, were then slowly injected into the injured muscle. Care was taken that no cell suspension leaked out of the injection site. Mice were sacrificed 3 weeks after transplantation and muscle was harvested for immunohistochemistry analysis.

Alternatively, 8- to 12-week old dystrophic SCID-mdx mice conditioned or not by cardiotoxin injection were used as recipients of human perivascular cells isolated from placenta and muscle. Chimerism was analyzed as described above, by immunohistochemistry and *in situ* hybridization.

Muscles that had received GFP+ cultured perivascular cells were fixed in 1.5% paraformaldehyde, mounted in embedding medium (Tissue-Tek, Sakura), and sectioned as 10-µm thick transverse sections. After three 15-min washes in PBS, slides were mounted with 50% glycerol/DAPI solution. GFP was directly visualized by fluorescence microscopy using both standard bandpass as well as ratiometric techniques to eliminate background autofluoresence (Leica DMRBE).

Adipo-, osteo- and chondrogenesis in culture

Perivascular cells isolated from various tissues and cultured as described above were tested for multi-lineage differentiation potential. For adipogenic differentiation, cells at 70% confluence were cultured in DMEM, 10% FCS, 1µM dexamethasone, 0.5 µM isobutylmethylxanthine, 60µM indomethacine and 170 µM insulin (all from Sigma-Aldrich). After 14 days, cells were fixed in 2% paraformaldehyde at RT, washed in 60% isopropanol and incubated with Oil red O for 10 min at RT for the detection of lipid accumulation. Confluent cells not cultivated in adipogenic differentiation medium were fixed and stained as described and used as a negative control.

For chondrogenesis, high-density pellets were prepared by spinning down 3x10^5 cultured cells and grown in serum-free DMEM containing an insulin-transferrin-selenious acid mix (ITS) (BD Biosciences), 50µg/ml L-ascorbic acid 2-phosphate (WAKO), 100µg/ml sodium pyruvate, 40µg/ml L-proline (both from Invitrogen), 0.1µM dexamethasone (Sigma-Aldrich) and 10ng/ml transforming growth factor β1 (TGF-β1; Peprotech). Pellets cultured in the absence of TGF-β1 were considered as untreated and used as negative controls. After 21 days, pellets were fixed in 10% formalin, dehydrated using a graded series of ethanol washes and

embedded in paraffin after which 5-μm thick sections were rehydrated and stained with Alcian blue and nuclear fast red for the detection of sulfated glycosaminoglycans (s-GAG) and nuclei, respectively.

For *in vitro* bone formation, cells at 70% confluence were cultivated in osteogenic medium, consisting of DMEM, 10% FCS, 0,1 μM dexamethasone, 50 μg/mL L-ascorbic acid and 10 mM beta-glycerophosphate. After 21 days cells were fixed in 4% formaldehyde for 2 min and incubated for 10 min with alizarin red, pH 4.2 for the detection of calcium deposits. The osteogenic potential was further confirmed by alkaline phosphatase and von Kossa staining. Briefly, for alkaline phosphatase activity, fixed cells were incubated for 45 min in a mixture of naphtol AS-BI alkaline solution with fast blue BB according to manufacturer's protocols. Cells were then rinsed with deionized water and incubated in a 2.5% silver nitrate solution for 30 min in order to detect mineral deposition (all reagents from Sigma-Aldrich). Cells cultivated in DMEM, 20% FCS were used as a negative control.

An *in vivo* assay was also used to measure osteogenesis. A total of 5×10^5 cells in 100 μl was seeded on the surface of a 6x6-mm piece of sterile gelatin sponge (Gelfoam®), which was then placed in a 24-well plate. After the cell suspension was absorbed, 3 ml of DMEM supplemented with 10% FCS was added to the well and the implant was incubated overnight. The following day, the seeded gelfoam scaffold was implanted into a skeletal muscle pocket in the gluteofemoral muscle of a SCID-NOD mouse. X-ray analysis was performed 30 days after implantation to evaluate bone formation

KEY RESEARCH ACCOMPLISHMENTS
Since 2007 (see previous report), the following results have been obtained:
1. Immunodetection of vascular pericytes in human tissues
To the markers we have previously identified on human pericytes, we have added several other antigens. First, all pericytes were observed to express PDGF-Rβ, aka CD140, and α-SMA was reproducibly detected in pericytes surrounding venules and arterioles, but not around most capillaries. We also observed that a subset of pericytes in human fetal and adult muscle express CD133, aka prominin, an epithelial cell antigen also expressed on diverse tissue-specific stem cells.

Furthermore, Having shown that perivascular cells sorted to homogeneity from diverse human organs yield in culture a progeny of MSC (see below), we wished to determine whether this affiliation can be further supported on molecular grounds by showing that pericytes, in their native perivascular arrangement within intact tissues, already express MSC markers. To this end, antibodies to CD44 and CD90 were added, in a 6-color FACS analysis, to those used to typify pericytes as described before. One fetal (23 weeks) and 4 adult muscles (56-86 years), 3 mid-gestation and 2 term placentas and 2 adult white adipose tissue samples (27 and 42 years) were analyzed along this strategy. In this setting, CD146^high CD34- CD45- CD56- pericytes were found to express CD44 and CD90. This observation was confirmed by immunohistochemical staining of tissue sections (Fig. 7d,e). The pericyte identity of the cells expressing CD44 and CD90 was confirmed by double-staining with antibodies to smooth muscle actin and CD146.

In summary, human vascular pericytes can be characterized by expression of CD146, NG2, PDGF-Rβ, CD44, CD90 and αSMA, and absence of the endothelial cell antigens CD34, VE-cadherin, vWF and UEA-1 ligand. In addition, a subset of these cells in skeletal muscle express CD133.
2. Cultured perivascular cells give rise to mesenchymal stem cells
We have pursued the characterization of human pericytes sorted from multiple organs (muscle, pancreas, placenta, bone marrow, adipose tissue…) and cultured in vitro over the long term. We assessed, by flow cytometry and RT-PCR, antigens expressed by long-term cultured human perivascular cells. All pericytes still display, over extended culture, the markers their ancestors natively expressed in the tissue of origin (CD146, aSMA) and no cells in these cultures express markers of endothelial cells (CD34, CD144, CD31 and vWF), hematopoietic cells (CD45) or myogenic cells (MyoD, myogenin, m-cadherin, myf-5 and Pax7). We also investigated the expression by cultured pericytes of antigens that typify mesenchymal stem cells (MSC) derived from adult human bone marrow. Intriguingly, cultured human perivascular cells from either skeletal muscle, pancreas, adipose tissue, placenta or other organs expressed all recognized markers of MSC derived from bone marrow, including CD10, CD13, CD44, CD73, CD90, CD105, CD108 (Sema L), CD109 (platelet activation factor), CD140b (PDGF-RB), CD164 (MGC 24), CD166 (ALCAM), CD318 (CDCP1), CD340 (HER-2), CD349 (frizzled-9), SSEA-4 and HLA-Cl1. In contrast, cultured perivascular cells, similar to MSC, do not express CD56, CD106, CD133, CD324 (E-cadherin), CD326 (Ep-CAM), CD344 (frizzled-4) and HLA-DR (Fig. 6 and not shown). These results further suggested that the elusive MSC are derived from perivascular cells. To

further document this possible affiliation, we explored whether the developmental potential of cultured perivascular cells reflects that of MSC. Indeed, when cultured in respective inductive conditions, perivascular cells could differentiate into cartilage tissue and multilocular adipocytes. Cultured perivascular cells also gave rise to osteocytes *in vitro* and developed into ossified nodules when transplanted into a skeletal muscle pocket in an immunodeficient mouse.

We have, therefore, further demonstrated that the elusive mesenchymal stem cells (MSC), discovered in primary cultures of multiple adult organs, are derived from perivascular cells.

3. Transplanted pericytes improve cardiac function after infarction

A NOD/SCID mouse model of acute myocardial infarction (AMI) was created to assess the therapeutic capacity of pericytes *in vivo*. Immediately after ligation of the left anterior descending coronary artery, 3×10^5 muscle-derived pericytes cultured for 12 passages were injected into the right and left lateral borders and center of the infarct. The control group was injected with a saline solution, and the sham group received no injection. Echocardiography showed that two and eight weeks after AMI, mice in both pericyte-injected groups (n=8/group) had significant improved LV contractility, measured by percent fractional shortening (FS) and percent fractional area change (FAC), over the control group (n=5) and the sham group (n=3) ($P<0.05$). Pericyte-injected hearts also exhibited ameliorated LV chamber dilation, estimated by end systolic area (ESA) and end diastolic area (EDA), when compared to the control group ($P<0.05$). Histology at 2 weeks revealed a 38% reduction in scar area in pericyte-injected hearts as compared to the control group. CD31+ endothelial cells were also significantly more numerous in the peri-infarct areas in pericyte-injected hearts ($P<0.05$). The transplantation of skeletal muscle-derived pericytes can therefore improve the cardiac function in the post-infarct myocardium, possibly through reduction of myocardial fibrosis and elevation of angiogenesis.

REPORTABLE OUTCOMES

This ongoing project, and closely related works, have been the object in 2007-2008 of the following

reports and published abstracts:

Reports

Péault, B., Rudnicki, M., Torrente, Y., Cossu, G., Tremblay, J., Partridge, T., Gussoni, E., Kunkel, L., Huard, J. (2007). Stem and progenitor cells in skeletal muscle development, maintenance, and therapy. Molecular Therapy, 15(5), 867-877.

Zheng, B., Cao, B., Crisan, M., Sun, B., Li, G.H., Logar, A., Yap, S., Pollett, J.B., Drowley, L., Cassino, T., Gharaibeh, B., Deasy, B., Huard, J., Péault, B. (2007). Prospective identification of myogenic endothelial cells in human skeletal muscle. Nature Biotechnology, 25(9):1025-1034.

Crisan, M., Deasy, B., Gavina, M., Zheng, Bo., Huard, J., Lazzari, L., Péault, B. **(**2007) Purification and long-term culture of multipotent progenitor cells affiliated with the walls of human blood vessel: myoendothelial cells and pericytes. Methods In Cell Biology. In Press.

Crisan, M., Zheng, B., Sun, B., Yap, S., Logar, A., Huard, J., Giacobino, J.P., Casteilla, L., Péault, B. (2008). Purification and culture of human blood vessel-associated progenitor cells. Current Protocols in Stem Cell Biology. In Press.

Gharaibeh, B., Lu, A., Tebbets, J., Zheng, B., Feduska, J., Crisan, M., Péault, B. , Cummins, J., Huard, J. (2008). Isolation of murine muscle derived stem cells by differential adherence characteristics. Nature Protocols. In Press.

Project # 4
Cell therapy for muscle regeneration advances via
interdisciplinary-driven regenerative medicine (iDREAM)
(Bridget Deasy)

Introduction

1. **Technical Objective #1:** Use preplate isolation technique and a bioinformatic cell culture system to screen adult human stem cell candidates for their muscle regeneration potential.

> **Progress:** We have completed the experiments for this aim and we are currently preparing a manuscript which we be submitted in April 2008. To summarize,
>
> obtained human muscle-derived cells which were isolated by the preplate technique and we have characterized these cell populations using the bioinformatic system and in vivo regeneration model. These populations demonstrate variability in their in vitro characterization; however they do not demonstrate the same variability in their in vivo performance. We found that human muscle-derived cells were capable of participating in skeletal muscle regeneration in the mdx/SCID animal, but there was less variability as compared to the reported variability with mouse MDSC.

2. **Technical Objective #2:** Test culture conditions for extensive and long-term expansion of human myogenic cells to preserve the cells' phenotype and regeneration efficiency.

> **Progress:** Human myogenic cells can be expanded in culture to at least 10 population doublings. In earlier, preliminary experiments we observed one population that expanded to more than 95 population doublings. We have also observed that the molecular marker expression changes during this expansion.

Body and Key Accomplishments:

1. Technical Objective #1: Use preplate isolation technique and a bioinformatic cell culture system to screen adult human stem cell candidates for their muscle regeneration potential.

In the progress report of March 2007, we reported the examination of 8 populations of human muscle-derived cells which were isolated by Cook Myosite (Pittsburgh , PA). We examined those cells both in vitro and in vivo (n=5 injections) to determine their characteristics and in vivo regeneration potential. In those studies we did not identify significant differences among the cell populations. We have now received 4 additional populations (12 total) and we have grouped these populations into 3 categories according to their isolation characteristics related to the preplate technique. It has been previously shown that the preplate isolation technique can be used to isolate stem cells from the skeletal muscle of mouse [19] and rat [42], while direct defined FACS-sorting has been performed using tissue from mouse [19], rat [42] and human sources[43]. We have recently utilized the established preplate technique to obtain mouse and human muscle-derived cells from a skeletal muscle biopsy. This technique isolates muscle-derived stem cells (MDSCs) from a skeletal muscle biopsy by serial preplating of low-adherence cells[1, 19, 38-41]. Usually, myogenic precursors with characteristics of myoblasts or satellite cells are found within the early preplates (PP1–3), whereas cells isolated from the later preplates (PP5-6) have stem cell characteristics[1]. Briefly, tissues are enzymatically and mechanically digested and cultures are initiated on either collagen-coated or non-coated tissue culture plastic. For human preplate cells, we use non-coated flasks and culture the cells at a plating density of 600 cells/cm^2 and passage every 72-96 hours before confluence. Through a collaboration with Cook MyoSite Inc (Pittsburgh, PA), we now receive samples of human muscle cells that are derived using a preplate technique in a clinical cell processing facility. In fact, autologous cells isolated this way are currently being used by Cook MyoSite in clinical trials for urinary incontinence[114]. The cells which we propose to use in this study will be obtained from through our existing MTA or through purchase from Cook MyoSite (see collaboration letter). These cells are isolated based on their variable adherence, using a method similar to the preplate technique which was performed with mouse myogenic cells. We term the cells PP2, PP4 and PP6-- PP2 adhere prior to PP4 which adhere prior to PP6.

Characterization of myoblasts and muscle-derived cells In Vitro, by Live cell imaging + flow cytometry, and in terms of In Vivo Regeneration. Human MDCs were analyzed for the presence of the cell surface cluster of differentiation markers CD34, CD56, CD144, and CD146 by flow cytometry. For live cell imaging analysis 3 separate hMDCs preplate populations were examined – PP2, PP4, and PP6. By the preplate method, PP2 corresponds to myoblasts and PP6 corresponds to the muscle-derived stem cell candidate[1, 38, 40]. The cells were imaged using the automated cell imaging system[106]. Three separate visible

image sequences (20x) were captured at 10 minute intervals for each well over a culture time of 3 days. Image sequences were imported to ImageJ for user interactive analysis. Measurements included 17 parameters including area, centroid, center of mass, perimeter, circularity, skewness, and best fit ellipse. Sequences were divided into 18 hour increments with 10 separate cells outlined and measured over 30 minutes at each time point. Results from ImageJ measurement were imported into a predesigned worksheet for calculation and analysis. Cell motility was described as centroid velocity, dividing the change in centroid position by the scan time interval. Single cell measurements were averaged over each time point and image sequence yielding a morphological description of each well for the culture period. The mean area for PP2 (792 ± 151 um^2) was significantly smaller (P=0.022, type-2, 2-tailed) than PP6 (1248 ± 327 um^2). Furthermore, PP2 velocity (0.395 ± 0.056 um/min) was significantly greater (P=0.031) than PP6 (0.312 ± 0.044 um/min). Finally, examination of circularity (a measure of cell roundness) showed PP2 (0.517 ± 0.028) and PP4 (0.487 ± 0.058) were significantly different from PP6 (0.307 ± 0.052, P<0.01). Flow cytometry showed all PPs were negative for CD34 & CD144, with decreasing expression for CD146 & CD56 over time in culture. In sum, the results show that PP2 cells
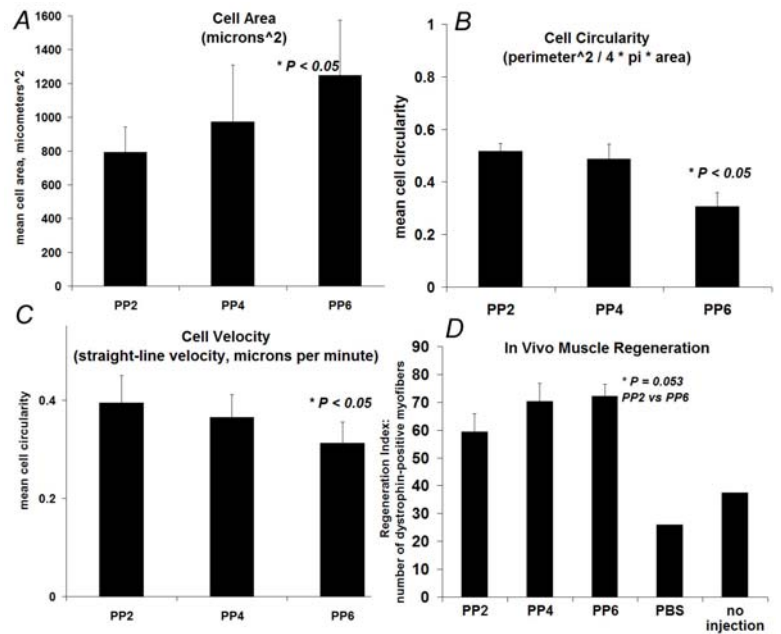

Figure 1. **Live Cell Imaging can detect significant differences in behavioral characteristics among muscle cell populations.** These same cells also differ in terms of in vivo performance. **(A-C)** In this analysis, 3 parameters – cell area, circularity and velocity—were significantly different in myoblasts (PP2) vs muscle-derived stem cells (PP6, p<0.05). **(D)** Further we detected a significant difference in the regeneration efficiency after in vivo transplantation of myoblasts (PP2) versus muscle-derived stem cells (PP6).
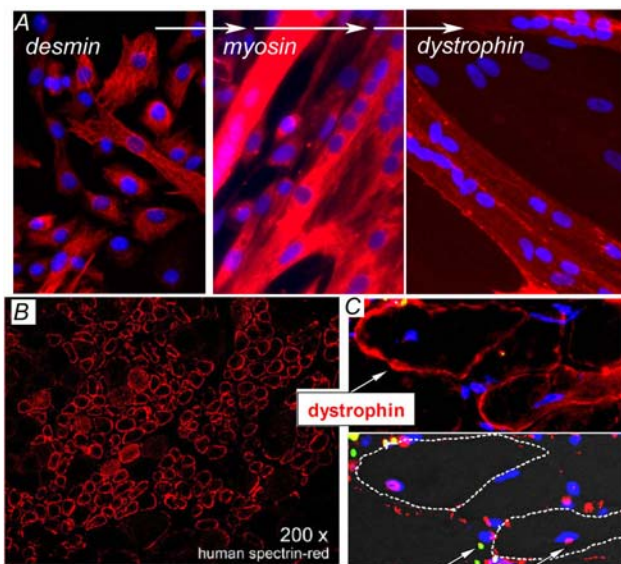
are significantly smaller and more motile with greater circularity than PP6, two populations previously resolved only by adherence rates. The LCI approach shows the ability to resolve differences in cell populations based on a number of behavioral measures only a few of which are presented here. Moreover subsequent in vivo experiments showed that this in vitro difference correlates with an in vivo difference in performance (**Fig 1D** and text below).

We have also examined the cells myogenic capability both in vitro and in vivo. **Figure 2A** illustrates the progression of differentiation in human MDCs as cells express desmin, myosin heavy chain and even dystrophin in vitro. We also show that we can transplant human myogenic cells into the skeletal muscle of *mdx*/SCID mice and detect both human spectrin and dystrophin. We used the murine disease model marked by progressive muscle weakness due to the lack of dystrophin expression at the sarcolemma of muscle fibers [31, 98-100]. (The level of in vivo regeneration was quantified in **Fig 1D**). Fluorescent staining of human

Figure 2. **(A)** In vitro myogenic differentiation. **(B)** Human muscle stem cells participate in skeletal muscle regeneration. **(C)** Donor cells fuse with mouse muscle fibers. Human specific dystrophin co-localize with mouse specific Y-chromosome

spectrin in the fibers of mice 1 month after cell transplantation (myoendothelial cells[43]) into the gastrocnemius muscle demonstrates the feasibility of cell transplantation in the mice and the specificity of the antibodies (**Fig 2B**). After transplantation of PP2, PP4 and PP6 (**Fig 1D and Fig 2C**) we observed significantly more regeneration using PP6 (72± 4.4 dystrophin-positive fibers) as compared to PP2 (59± 6.5 P=0.053, n=13-25 muscles, **manuscript in preparation**). Further, we can identify the donor cells by using a number of markers, including human laminA/C or human chromosomal markers. Human MDCs also show evidence of multi-potentiality.

2. **Technical Objective #2: Test culture conditions for extensive and long-term expansion of human myogenic cells to preserve the cells' phenotype and regeneration efficiency.**

In regards to cell expansion, we show that if we start with 100,000 cells on average for each sample, which are passage 5, we are able to attain more than 10^8 cells, or 674 million cells per sample, after 3.5 weeks of cell culture (n=3 human samples, **Fig 3**). These numbers would increase exponentially if we 1) use cells of an earlier passage or 2) obtain larger muscle biopsies. Numerically, these numbers will be sufficient for laboratory studies and transplantation to mice, but they may not be sufficient for regeneration of large human muscles, and stimulated expansion methods will

still be explored for clinical approaches. The goal of this objective is to determine the quality of the cells after they have been expanded, using parameters specific phenotypic parameters.
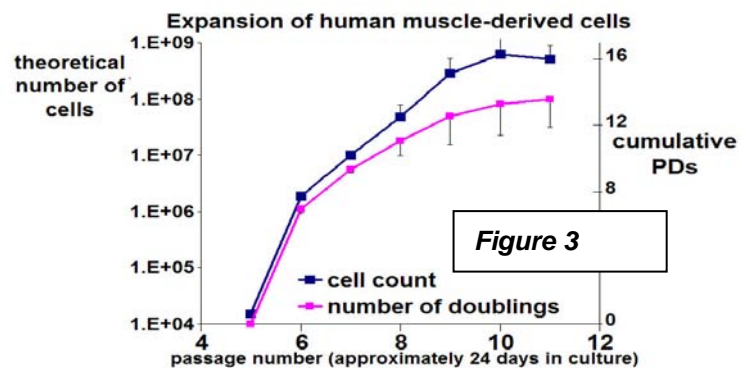
We are examining the effect of in vitro expansion on the human muscle derived cells isolated using a preplate method which was previously used to obtain mouse MDSCs. The murine counterparts have been observed to participate in skeletal and cardiac muscle regeneration and bone healing. However, it is estimated that the ratio of murine MDSCs to all other myogenic cells within a muscle biopsy is $1:10^5$. In vitro expansion is necessary, yet this process results inevitably in cell aging. Here we describe the phenotypic changes associated with cell aging due to culture expansion of hMDCs.

Muscle stem cell candidates were obtained by serial replating of single cell isolation from a skeletal muscle biopsy using a modified method of a previously described technique. Culture and expansion: Cells were plated at 600 cells/cm^2 and routinely passaged and characterized every 3-5 days. This continued for >13 population doublings. Cells were routinely examined for expression of CD34, CD144, CD56 and CD146. Using previously described methods, we obtained time-lapsed video records of cell growth and data related to cell size, cell migration and cell proliferation. We compared these characteristics throughout the expansion. Low and high passage cells were transplanted to the skeletal muscle of a murine model of muscular dystrophy (mdx/SCID) in order to assess the function after aging induced by culture expansion. Fourteen days after transplantation, we measured the number of dystrophin-positive myofibers in the host skeletal muscle which normally lacks dystrophin expression.

Human muscle stem cell candidate could be expanded for more than 13 population doublings. Low passage cells expressed the surface markers CD56 (or NCAM) and CD146 (one marker of perivascular cells); however the cells were negative for the stem and endothelial progenitor cell markers CD34 and CD144. As cells were expanded in culture, in the presence of EGM2 media, we observed a consistent and significant decrease in expression of both CD56 and CD146 (P < 0.05). Population expression of CD34 and CD144 remained low throughout the expansion. We also quantified changes in imaging parameters such as an increase in cell size associated with aging of the cell population. For example, the mean area of cells in the older population was 4500±600 pixels^2 while, young cells had a mean area of only 2030± 217 pixels^2 (P <0.05). Finally, we observed a reduction in the level of cell participation in muscle regeneration after intramuscular transplantation to the skeletal muscle of low passage versus high passage cells (64 ± 7 dystrophin fibers for low passage hMDCs, 73 ± 5 dystrophin fibers for high passage hMDCs, P =0.076).

Conclusions: Among the 12 populations, we observed that the significant differences both in vitro and in vivo are related to the preplate fraction of the isolation procedure. Hence, the established preplate technique can be used to obtain a fraction with measurable differences in cell characteristics (such as cell size, cell shape and cell velocity) and these characteristics correlate with in vivo performance. Studies are continuing to examine how the molecular and behavioral phenotype changes with in vitro expansion, and we will test how the in vivo outcome may be affected by in vitro expansion.

Recommended changes: We will continue to examine the other preplates in the human muscle cell isolates including preplates 1-3, pp4/5 and pp6. We will continue to examine the comprehensive behavioral profile by use of the bioinformatic approach. Finally we will continue with the studies to examine the effects of cryopreservation and other cell processing methods on the phenotype of the human muscle cells.

Reportable Outcomes:
Refer to Appendices and References section.

Appendices and References:

PUBLICATIONS,

1. **Deasy, B.M.** Asymmetric Behavior of Stem Cells. 2008. Regulatory Networks in Stem Cells. Humana /Springer Press. In press.
2. Schmidt, B.T., Feduska, J.M., Witt, A.M., and **B.M. Deasy.** 2008 Robotic cell culture system for stem cell assays. *Industrial Robot. 35 (2):116-124.*
3. Schugar, R.C., Robbins, P.D., and **B.M. Deasy.** 2007. Small molecules in stem cell self-renewal and differentiation. *Gene Therapy.* Published online Nov 8, 2007. doi:10.1038/sj.gt.3303062

ABSTRACTS

1. S.M. Chirieleison, J.M. Feduska, R.C. Schugar, S.L. Sanford, J. Huard, and **B.M. Deasy**. 2008. Identifying Regenerative Populations of Human Muscle-Derived Cells and Tracking Phenotypic Changes in Culture. MidWest Tissue Engineering Consortium. Cincinnati, OH, USA
2. S.M. Chirieleison, J.M. Feduska, R.C. Schugar, S.L. Sanford, J. Huard, and **B.M. Deasy**. 2008. Identifying Populations Of Human Muscle Derived Stem Cells To Participate In Skeletal Muscle Regeneration Based On Phenotypic Differences. Orthopaedic Research Society; San Francisco, CA.
3. Sanford, S. L., Schugar, R. C., and **B.M. Deasy**. 2008. Myogenic Potential of Human Umbilical Cord Cells in a Cell Therapy Model for Duchenne Muscular Dystrophy. Orthopaedic Research Society; San Francisco, CA.
4. Schugar, R.C. and **B.M. Deasy**. 2007. The Isolation and Characterization of Stem Cells from the Wharton's Jelly. American Society for Cell Biology; Washington, D.C.
5. Sanford, S.L., **B.M. Deasy**. 2007. User-Friendly Calculator to Obtain Cell Growth Parameters. American Society for Cell Biology; Washington, D.C.
6. Schugar, R.C. and **B.M. Deasy**. 2007. The Isolation and Characterization of Wharton's Jelly-Derived Stem Cells. Mid-West Tissue Engineering Consortium, Ann Arbor, Michigan. *PODIUM.*
7. Sanford, S; Feduska, J; Schugar, R; Athanassiou, H; and **B.M. Deasy.** 2007. User-friendly Tools to Measure Cell Growth Parameters: Measuring Growth Characteristics of Human Muscle Derived Cells Mid-West Tissue Engineering Consortium, Ann Arbor, Michigan.
8. Feduska, J.M. Schugar, R.C. Sanford S.L., J.Huard, and **B.M. Deasy**. 2007. Human Muscle-Derived Cells Isolated By the Preplate Method Participate in Skeletal Muscle Regeneration in Mdx/SCID Model. International Society for Stem Cell research ISSCR, Cairns, Australia.
9. Ambrosio, F., Ferrari, R., Fitzgerald, G.K., **Deasy, B.M**., O'Day, T., Boniger, M.L. Huard, J., 2007. Muscle Loading Enhances Stem Cell Contribution To Mdx Mouse Skeletal Muscle Contractile Function. International Society Of Stem Cell Research (ISSCR). Cairns, Australia.

10. Cassino TR, Okada M, Drowley L, Feduska J, **Deasy BM**, Huard J, LeDuc PR. Using mechanical stimulation to control the response of muscle-derived stem cell transplantation. The Biomedical Engineering Society (BMES) Annual Meeting; 2007 Sep 26-30; Los Angeles, CA.

Project # 5
Inhibiting cell death and promoting muscle growth for congenital muscular dystrophy
(Xiao Xiao)

Introduction:

Congenital muscular dystrophy (CMD) is a group of severe forms of muscular dystrophy leading to early death in human patients. The majority of cases are caused by genetic mutations in the major laminin that contains the $\alpha2$ chain (formerly named merosin) in the muscle basement membrane. The early morbidity/fatality and the lack of effective treatment require urgent search for novel therapeutics. Previously, we utilized mini-agrin, which has been proven to have a therapeutic effect in transgenic MCMD mice, to treat MCMD mice by AAV vector. Our preliminary studies showed that over-expression of mini-agrin protein by AAV vector greatly improved general health and muscle morphology in MCMD mice. However, the treated disease mice still developed gradual paralysis and displayed shorter life span than wild type mice. To further improve the current gene therapy paradigm, with the advanced AAV technology and muscle biology knowledge, we will vigorously test our hypothesis: whether muscle pathogenesis can be improved by inhibition apoptosis or promoting muscle growth. The specific aims are the following:

Body

Aim1: To investigate whether muscle pathogenesis can be improved by delivery of BCL2, an anti-apoptotic gene, by AAV vector in MCMD mice. Mice that lack laminin $\alpha2$ show severe muscle loss, poor regeneration, and a greatly shortened lifespan. A role for apoptosis in pathology of laminin $\alpha2$-deficiency has been suggested by histological and in vitro studies, as well as transgenic studies. In this study, we will explore the potential therapeutic effect by delivering AAV-BCL2 vector into MCMD mice.

Aim2: To examine whether therapeutic effect can be obtained by delivery of insulin like growth factor 1 (IGF-1) gene, which can promote muscle growth, by AAV vector in MCMD mice. The MCMD mice show muscle atrophy and enhanced fibrosis as seen in human patients. Genes that promote muscle growth and inhibit fibrosis is theoretically beneficial for congenital muscular dystrophic muscle. Myostatin blockade, one of the strategies to promote muscle growth, has been shown to have a severe side effect of increasing postnatal lethality in MCMD transgenic studies. The reason for the side effect is due to significantly less brown and white fat in the absence of myostatin. In our preliminary studies, we observed that myostatin blockade significantly increased muscle weight, as well as decreased fat tissue in normal mice. However, over-expression of IGF-1 in normal mice only increased muscle weight without loosing fat. Considering less fat will result a severe side effect, we will deliver IGF1 gene to MCMD mice by AAV vector to study whether a therapeutic effect can be achieved in this proposal.

Upon completion, this project will establish complementary therapeutic strategies to combat the severe congenital muscular dystrophy in animal model, setting the base for the development of a clinically efficacious gene therapy strategy.

Key Research Accomplishments:

1. Insulin-like growth factor 1 (IGF-1) gene transfer into normal mice can increase muscle mass.
2. Single IGF-1 gene delivery did not render therapeutic effect in laminin alpha 2 deficient congenital muscular dystrophic mice

Reportable Outcomes:

One of our specific aims is to examine whether therapeutic effect can be obtained by delivery of insulin like growth factor 1 (IGF-1) gene, which can promote muscle growth, by AAV vector in MCMD mice. With respect to the approved statement of this specific aim, we have achieved that AAV-mediated IGF-1 gene delivery results in growth and hypertrophy of skeletal muscle mass. We have also delivered IGF-1 gene into congenital muscular dystrophy mice, and we did not observe any significant therapeutic effect.

Insulin-like growth factor I (IGF-1), a peptide growth factor that is structurally related to proinsulin, has a primary role in promoting the differentiation and growth of skeletal muscle (2, 3). Numerous studies have

implicated IGF-1 as an important mediator of anabolic pathways in skeletal muscle cells (4, 6). Overexpression of IGF-I transgene can counter a decline in muscle mass and functional performance of aged animals (5). In addition, Barton et al. showed that moderate overexpression of IGF-I in mdx muscle resulted in decreased necrosis and fibrosis and increased muscle mass and strength (1). Those studies suggest that overexpression of IGF-I gene can be a therapeutic intervention for the treatment of age- or disease-related muscle frailty.

To investigate the possible beneficial outcome of IGF-1 on laminin $\alpha2$–deficient dystrophic mice, we cloned a paracrine form of the IGF-1 gene into rAAV vector driven by strong non-specific CMV promoter. *In vitro* transfection study demonstrated that this plasmid is functional (Fig. 1 a). We then injected AAV-IGF1 vector into neonates of BL/10 mice. Five months after vector injection, the mice were sacrificed. Individual muscles were dissected and subjected to weight analysis and cryosection. The majority of the skeletal muscle mass was increased. As shown in Figure 1b, the fiber diameter was significantly increased compare with the control one. Noteworthy, overexpression of IGF-1 did not decrease fat tissue on treated normal mice (data not shown). Considering decreasing yellow and white fat tissue are serious side effects of myostatin propeptide overexpression in MCMD mice, IGF-1 delivery may offer therapeutic potential in MCMD mice.
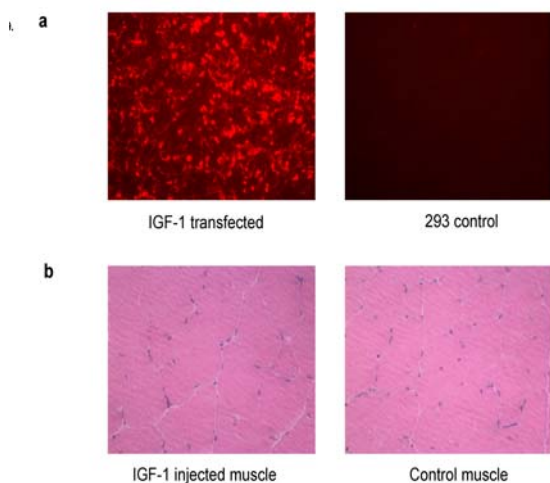

Fig1 A. In vitro immunoflurescent staining displayed that AAV-IGF1 plasmid is functional. B. Systemic AAV-IGF1 injection increased muscle fiber diameter. AAV-IGF1 vector was injected on neonates of BL10 mice. Five months after vector injection, the mice were sacrificed and muscles were subjected to cryosection. H & E staining displayed injected muscle size was bigger.

In addition, we injected AAV8-IGF1 vector into five neonates of homozygous dy^w/dy^w mice. Unfortunately, we did not see any significant therapeutic effect. The average life span of dy^w/dy^w mouse is 40 days, and most of the treated mouse died around 40 days.

The Coming year plans: We will inject AAV-Bcl-XL vector into homozygous dy^w/dy^w mice to see is there any therapeutic effect can be achieved.

Conclusions: AAV-IGF1 gene delivery can increase normal muscle mass. Single AAV-IGF1 gene delivery can not offer therapeutic benefit for laminin alpha 2 deficient dy^w/dy^w mice.

Recommend changes:
None.

Appendixes and References:

1. **Barton, E. R., L. Morris, A. Musaro, N. Rosenthal, and H. L. Sweeney.** 2002. Muscle-specific expression of insulin-like growth factor I counters muscle decline in mdx mice. J Cell Biol **157:**137-48.
2. **Coleman, M. E., F. DeMayo, K. C. Yin, H. M. Lee, R. Geske, C. Montgomery, and R. J. Schwartz.** 1995. Myogenic vector expression of insulin-like growth factor I stimulates muscle cell differentiation and myofiber hypertrophy in transgenic mice. J Biol Chem **270:**12109-16.
3. **Daughaday, W. H., and P. Rotwein.** 1989. Insulin-like growth factors I and II. Peptide, messenger ribonucleic acid and gene structures, serum, and tissue concentrations. Endocr Rev **10:**68-91.

4.   **Florini, J. R., D. Z. Ewton, and S. A. Coolican.** 1996. Growth hormone and the insulin-like growth factor system in myogenesis. Endocr Rev **17:**481-517.
5.   **Musaro, A., K. McCullagh, A. Paul, L. Houghton, G. Dobrowolny, M. Molinaro, E. R. Barton, H. L. Sweeney, and N. Rosenthal.** 2001. Localized Igf-1 transgene expression sustains hypertrophy and regeneration in senescent skeletal muscle. Nat Genet **27:**195-200.
6.   **Stewart, C. E., and P. Rotwein.** 1996. Growth, differentiation, and survival: multiple physiological functions for insulin-like growth factors. Physiol Rev **76:**1005-26.

Project # 6
Treatment for Muscle Wasting
(Paula Clemens)

Introduction:
The ability to promote muscle regeneration in the setting of focal or generalized muscle loss could confer significant clinical benefit in the setting of focal neuropathic or other processes that cause muscle atrophy or chronic illnesses that cause cachexia. We hypothesize that gene transfer strategies can promote muscle regeneration toward a goal of improving muscle bulk and strength in the setting of injuries or diseases that cause muscle atrophy.

Extensive evidence has shown that higher levels of some pro-inflammatory cytokines contribute to the development of cachexia. For example, serum tumor necrosis factor α (TNFα) and IL-1α levels are markedly increased in patients with rheumatoid arthritis and cancer. Other cytokines, such as IL-6, IL-1β and proteolysis-inducing factor (PIF) have been reported to contribute to the development of muscle wasting.

Elegant studies show that TNFα binds to its receptor on skeletal muscle resulting in the activation of nuclear factor κB (NF-κB) mediated by phosphorylation and degradation of the NF-κB inhibitory protein, IκBα. Downstream effects of pathological NF-κB activation in skeletal muscle include the inhibition of new muscle formation and the degeneration of existing muscle. *In vitro* studies support the potential that the IκBα superrepressor (IκBSR), an IκBα genetically engineered to prevent its phosphorylation, can prevent the activation of NF-κB in skeletal muscle and could ameliorate or prevent muscle wasting. Our preliminary studies demonstrate the novel determination of inhibition of activation of NF-κB by cellular FLIP (cFLIP).

Our hypothesis is that the inhibition of the downstream pathways of TNFα causing muscle atrophy and failure of muscle regeneration should be <u>effected intracellularly</u> in muscle fibers. A gene therapy strategy is ideal for the purpose of achieving an ongoing effect that is cell-type restricted. We anticipate that inhibition of NF-κB activation restricted to muscle fibers will provide a therapeutic effect on muscle while avoiding potential toxic effects of inhibiting NF-κB activation in other tissues.

Body:
To characterize an *in vitro* model of cancer-induced muscle wasting in primary muscle cells and in stable muscle cell lines expressing IκBSR or cFLIP.
We developed a new *in vitro* cell culture assay to study the effects of cancer cell cytokines on muscle cell differentiation and use this assay to test novel gene transfer approaches for the treatment of cancer cachexia. Exposure to conditioned media from selected human cancer cell lines resulted in failure of muscle cell differentiation. A known intracellular mechanism of NF-κB activation as a cause of cancer cachexia was recapitulated in this *in vitro* system. Consistent with previous reports *in vivo*, we demonstrated that human prostate cancer PC-3 cells express PIF as well as TNF-α and IL-1β transcripts. We observed a direct correlation between the inhibition of myogenic differentiation in the *in vitro* assay and the expression of IL-1β transcripts by specific human cancer cell lines tested. Furthermore, we observed a direct correlation between NF-κB activation and inhibition of myogenic differentiation in the *in vitro* assay. Exposure to inflammatory cytokines and to conditioned media from human cancer cells each resulted in NF-κB activation within primary muscle cells. Failure of myogenic differentiation and the associated activation of NF-κB were prevented by stable expression of either IKBSR or cFLIP, but not by Bcl-xL.

Previous studies demonstrate that activation of NF-κB plays a key role in cancer-induced cachexia. Consistent with previous studies, in this study we found that exposure to secreted factors from PC-3 and Mel cancer cell lines resulted in activation of NF-κB in treated myoblast cells, as demonstrated by higher binding activity of nuclear NF-κB to consensus NF-κB oligonucleotides and higher levels of NF-κB transcriptional activity.

cFLIP and Bcl-xL are both important anti-apoptotic molecules. In this study we investigated whether cFLIP and Bcl-xL influenced NF-κB activity and myogenic differentiation in primary cells derived from skeletal muscle. Interestingly, we observed that cFLIP over-expression inhibited IL-1β or PC-3 or Mel media-induced NF-κB activation in myoblast cells, thus promoting myogenic differentiation of treated myoblast cells, as demonstrated by enhanced myotube formation and muscle-specific protein expression. Stable expression of cFLIP yielded similar results to stable expression of IKBSR. Both IKBSR and cFLIP inhibited NF-κB activation, as determined by the levels of nuclear NF-κB binding activity and nuclear NF-κB-mediated transcription. In contrast, over-expression of Bcl-xL enhanced NF-κB activation in myoblast cells, with further increases upon exposure to conditioned media from PC-3 cells. The contrasting results with cFLIP and Bcl-xL were interesting and further studies will be required to understand the intricacies of signaling cascades that underpin this result.

Taken together, this study provides an *in vitro* assay that demonstrates secretion of cachexia-inducing factors by certain cancer cell lines that result in the inhibition of myogenic differentiation by activation of NF-κB. Over-expression of cFLIP in muscle cells inhibits both NF-κB-mediated and apoptotic pathways, thereby preventing tumor media-induced inhibition of myogenic differentiation and cytotoxicity. These findings point toward the potential to design novel molecular therapeutics for the treatment of cancer-induced muscle wasting.

To clone, rescue, and purify adeno-associated viral (AAV) vectors carrying IκBSR or cFLIP.
We are generating vectors with either ubiquitous or muscle-specific promoter control of expression. There are now AAV vectors with the potential for systemic delivery to skeletal muscle (eg. AAV8 and AAV9). Although widespread gene delivery to skeletal muscle is a significant advantage of systemic administration, a limitation is transduction of other undesired tissues. For this reason, we will employ vector design that confers muscle-specific control of expression for vectors that will be delivered systemically. Self-complimentary AAV vectors result in higher levels of transgene expression and decreased latency to onset of expression. Therefore, self-complimentary vectors are desirable for our studies, and the genes that we plan to express are sufficiently small to be accommodated by self-complimentary vectors.
We have rescued the following vectors as high-titer, purified AAV8 vectors: Conventional single strand AAV8 vectors were rescued with the following expression cassettes: CMV-GFP and CMV-cFLIP. Self-complimentary (double strand) AAV8 vectors were rescued with the following expression cassettes: CMV-IκBSR and MCK-GFP. The double strand MCK-GFP vector has been tested by direct intramuscular injection showing high levels of transgene expression. We will be testing expression of the other rescued vectors. The MCK-IκBSR double strand vector plasmid has been cloned. We will clone the MCK-cFLIP double strand vector plasmid and rescue both MCK-IκBSR and MCK-cFLIP as AAV8 vectors.

To apply AAV8 vector and NEMO-binding domain (NBD) peptide strategies to ameliorate cancer cachexia.
We have refined our model of muscle cachexia in mice in order to test molecular therapeutics *in vivo*. Using established procedures, we subcutaneously injected either PC-3 human prostate cancer cells into nude mice or MCA-26 murine cancer cells into immunocompetent mice. As shown in the figures below, we have demonstrated cachexia in both models, with a more rapid onset with MCA-26 tumors and a less rapid onset with PC-3 tumors. Furthermore, we have made the novel observation that atrophy of individual muscle fibers occurs in the PC-3 model, but not in the MCA-26 model.

In mice injected with MCA-26 cells, there is a significant reduction in the weight of 3 tested hind limb muscles; tibialis anterior (TA), quadriceps (quad) and gastrocnemius (gastroc) that parallels the total body weight loss observed. However, we do not observe atrophy of individual muscle fibers in this model (Fig. 1). Mice injected with PC-3 cells also had significant weight loss although the weight loss was less rapid (Fig. 2). Since the last submission, we completed the PC-3 experiment. We observed muscle atrophy in the PC-3 model as assessed by both muscle weights and by analysis of muscle fiber diameters (Fig. 3). This demonstrates an important difference between the 2 models of cachexia. It suggests different physiological responses to different tumors that could be important in the analysis of muscle wasting responses to cancer and have implications for treatment.
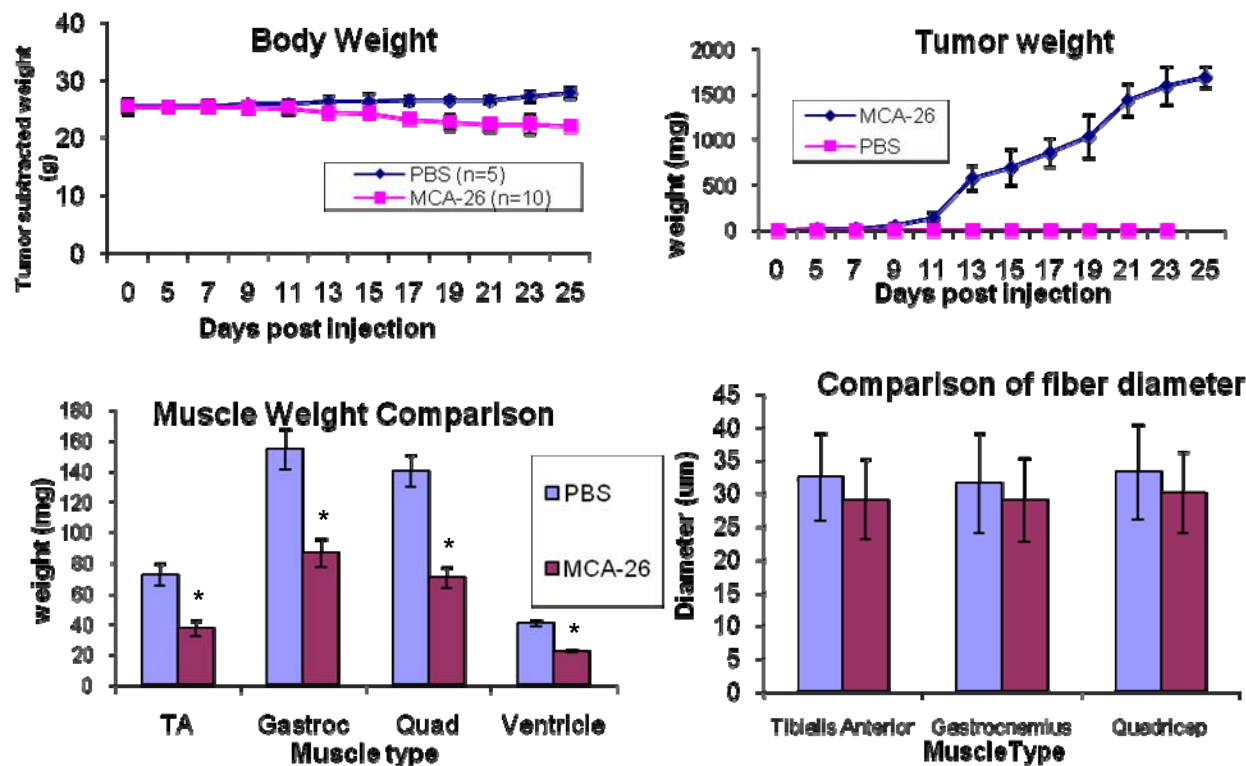
Figure 1. MCA-26 Tumors cause muscle cachexia. Mice ere injected subcutaneously with 1×10^{6} MCA-26 cells and followed for 25 days, serially determining body weight and tumor weigth. At collection, individual hind limb muscles were weighted. Muscle diameter were measured from cryostat sections. (Differences from PBS control are shown as * = p <0.05)
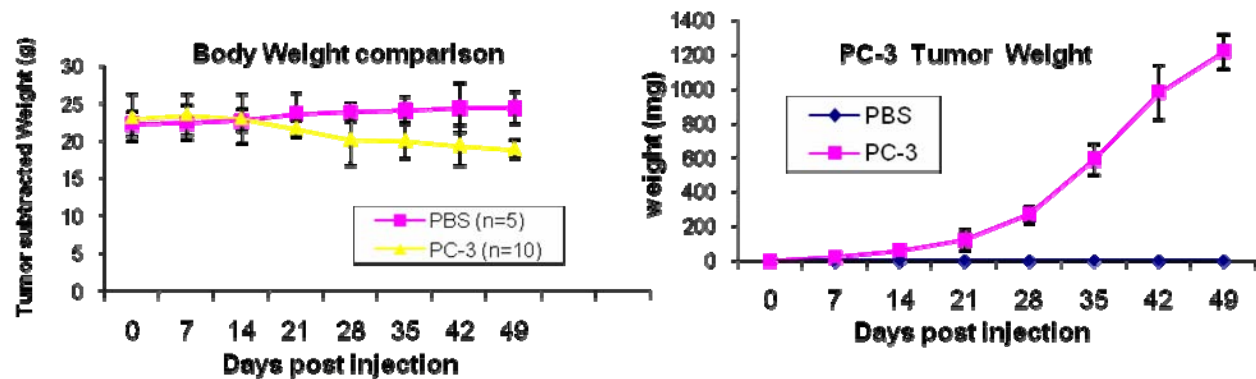

Figure 2. PC-3 tumors cause muscle cachexia. Nude mice were injected with 2×10^{7} PC-3 cells. Mice were serially followed measuring body and tumor weight.
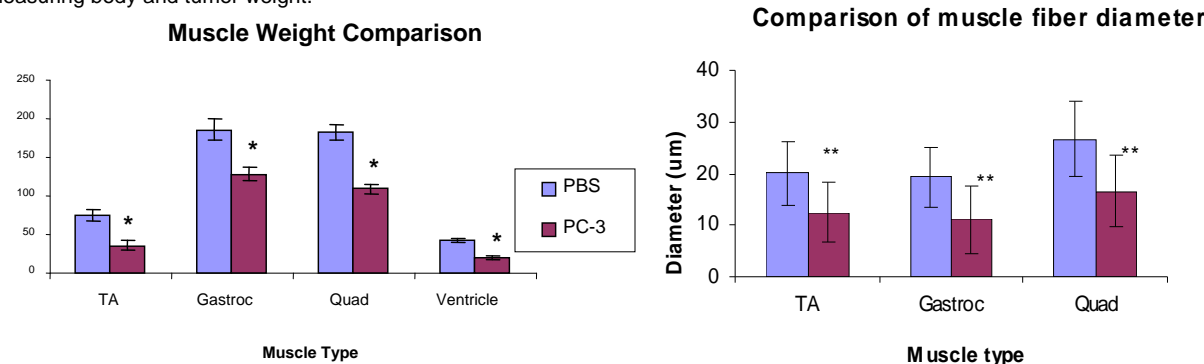

Figure 3. PC-3 tumors cause muscle cachexia as evidenced by decreased muscle weight and muscle fiber diameters. Hind limb muscles were collected at 49 days, weighted and snap frozen. Muscle fiber diameters were measured from cryostat sections. (Differences from PBS control are shown as * = p<0.05, ** = p<0.001)

Key Research Accomplishments:
- Development of an *in vitro* assay of muscle wasting induced by cancer cytokines
- Demonstration of importance of NF- B activation as a molecular mechanism for cancer-induced muscle wasting in the *in vitro* assay
- Use of the *in vitro* assay to identify cFLIP as a novel potential therapeutic agent for the treatment of cancer-induced muscle wasting
- Generation of single strand and double strand AAV8 vectors
- Refinement of 2 cancer cachexia models in mice

Reportable Outcomes:
Jiang Z, **Clemens PR.** Cellular caspase-8-like inhibitory protein (cFLIP) prevents inhibition of muscle cell differentiation induced by cancer cells. FASEB J 2006 Dec;20:E1979-E1989 (pdf attached).

Conclusions:
Our studies to date identify an *in vitro* assay that allows us to test molecular therapies that have the potential to treat muscle wasting induced by cancer. We anticipate that these results can be generalized to the treatment of other genetic and acquired causes of muscle wasting. We are generating AAV8 vectors with expression cassettes designed to inhibit activation of NF-κB and ameliorate cancer cachexia. We will apply the AAV8 vectors that we develop and NBD peptides in the cancer cachexia model in mice.

Appendix:
Appendix 8: Jiang Z, **Clemens PR.** Cellular caspase-8-like inhibitory protein (cFLIP) prevents inhibition of muscle cell differentiation induced by cancer cells. FASEB J 2006 Dec;20:E1979-E1989

Investigator: Johnny Huard

Vector Core
(Bing Wang)

Sub-title: The structure, production and purification of adeno-associated viral, adenoviral and retroviral vectors"

Introduction

rAAV-based gene therapy represents one of the most promising approaches to aid in the repair and regeneration of muscles. The benefits of utilizing rAAV include superior long-term gene transfer efficiency, the absence of an immune response to the virus, and the lack of toxicity, which is often associated with other viral vectors such as retrovirus and the adenovirus. The efficiency, safety and convenience associated with rAAV mediated gene therapy have led to the initiation of clinical trials for muscular dystrophies. In the last year, the Molecular Therapy Laboratory (MTL) has been working as a Vector Core of the DOD project (W81XWH-06-1-0406) for the production of a series of rAAV vectors for the PIs involved in this grant. The vectors have been used for: 1) *in vivo* therapy (direct rAAV injection into the injury site); 2) *ex vivo* therapy (indirect, *in vitro* infection of cells which will later be introduced to the site of injury). It is particularly important to identify the appropriate AAV serotype because the transduction efficiency of AAV vectors in different cell and tissue types varies widely, as a result of the unique tropism of each AAV vector. Accordingly, for the rAAV vector delivery method, either intramuscular or intravenous administration, the different serotypes of rAAV vectors were made and tittered by Dot blot assay. Also, the different promoters have been designed in rAAV vectors for enhancing gene expression or specific gene expression in muscle tissues (**Aim 1**).

In addition, we have developed new rAAV and lenti-viral vectors for the investigation of muscle repair after diseases and injuries. As described in **Figure 1**, this newly designed self-complimentary AAV vector packages two cassettes, one is human U6 promoter and multiple-linker for siRNA, the other is CMV promoter and GFP reporter. Unlike the common self-complimentary AAV vectors for delivery of therapeutic genes, this construct is used for insertion of small interfering RNA (siRNA) driven by the human U6 promoter, while GFP is a marker to evaluate the efficiency of gene transfer. siRNA gene silencers targeted to specific genes is a novel strategy to inhibit or decrease gene expression. Such as, siRNA targeting myostatin could locally increase muscle mass, and it targeting the orphan nuclear receptor (NOR-1), a target of β-adrenergic signaling in skeletal muscle, could enhance the repair of regenerating rat skeletal muscle after injury. However, the siRNA is very unstable during *in vivo* experiment, especially in systemic administration. Recently, viral-based siRNA delivery has been developed for muscle repair. rAAV-based siRNA has been proven to be one of the most promising approaches to promote muscle regeneration, to increase muscle mass and blood vessel counts, and to decrease myofibers apoptosis. In stem cell *ex vivo* gene therapy, another viral vector such as lenti-viral vector has developed in our Vector Core besides the AAV vector (**Figure 2**). Because of its long-term transduction in stem cells from different sources, the Lenti-viral vector has been used for genetic modified stem cell therapy, although it has a potential risk of insertional mutagenesis *in vivo* study (**Aim 2**).
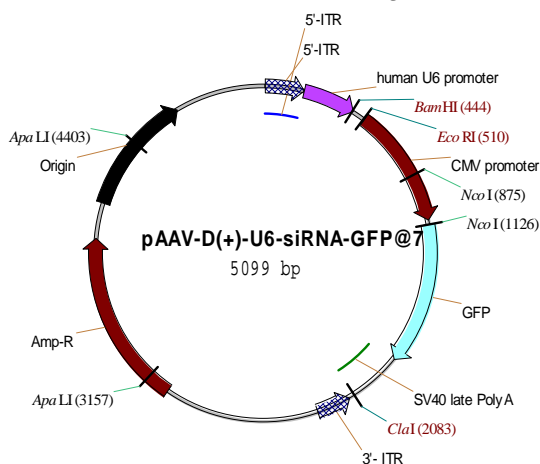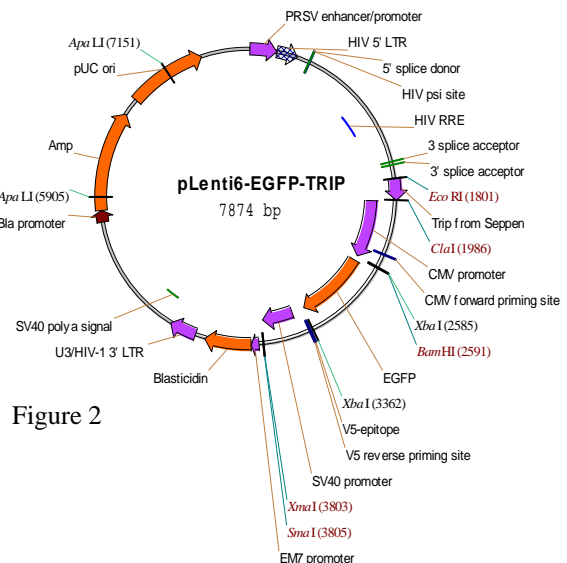

Figure 1

Figure 2

Besides the production and development of viral vectors for this proposal, we have been also engaging in a series of projects related to muscle wasting, and tendon and skin wound repair, by using a limited funding from the DOD and the Department of Orthopeadic Surgery, University of Pittsburgh. We are currently working on: 1) establishing a rAAV-based NF-κB blocking procedure which would aid in the treatment of inflammatory muscle wasting in *mdx* mice; 2) the enhancement of tendon and skin wound repair utilizing rAAV vectors such as TGF-β1 and VEGF; and, 3) the delivery of rAAV to stem cells (myo-endo) for *ex vivo* gene therapy approaches to muscle tissue regeneration and repair (**Aim 3**).

Based on our knowledge and experience with rAAV vectors and gene therapy, we are currently cooperating with other laboratories in the University of Pittsburgh, including Orthopaedic Surgery (Dr. Wang, Dr. Chu and Dr. Kang), Neurology (Dr. Clemens and Dr. Graham), Microbiology and Molecular Genetics (Dr. Glorioso and Dr. Robbins), Transplant Surgery (Dr. Dai), Cell Biology & Physiology (Dr. Zhao). In addition, we also have collaborations with Dr. Jay Liberman (the chairman of the Department of Orhtopaedic Surgery, University of Connecticut) for bone regeneration, and Dr. Denis Guttridge (Division of Human Cancer Genetics, The Ohio State University) for NF-κB blocking gene therapy of chronic joint inflammation in muscle.

Body
Aim 1. Production of rAAV vectors
1. AAV2-D(+)-CMV-eGFP
2. AAV6-D(+)-CMV-eGFP
3. AAV8-D(+)-CMV-eGFP
4. AAV9-D(+)-CMV-eGFP
5. AAV8-D(+)-CMV-eGFP
6. AAV8-D(+)-tMCK-eGFP
7. AAV2-D(+)-CB-eGFP
8. AAV2-1060-hrGFP
9. AAV2-1070-hrGFP
10. AAV2-1060—Gluciferase
11. AAV2-1070-GLuciferase
12. AAV2-CMV-sflt1
13. AAV2-D(+)-BMP2-spA
14. AAV2-D(+)-BMP2-SV40
15. AAV2-D(+)-CMV-TGFβ1
16. AAV2-CMV-minidystrophin (3858)
17. AAV2-dMCK-minidystrophin (3858)
18. AAV6-D(+)-CMV-BMP4
19. AAV2-D(+)-CMV-VEGF
20. AAV1-CMV-Decorin

Aim 2. Development of new novel rAAV and lenti-viral vectors
1. pAAV-D(+)-U6-siRNA-CMV-GFP
2. pAAV-D(+)-U6.3-siRNA
3. lenti-CMV-GFP

Aim 3. Viral based therapy for musculoskeletal degenerative diseases
1. AAV-based blocking of NF-IK for the treatment of chronic inflammation in muscle in mdx mice
2. Combined therapeutic strategy for muscle wasting in dystrophic mice
3. Molecular therapy for tendon and skin wound repair

Publication and abstracts in 2007 and 2008

1. **Bing Wang**, Juan Li, Freddie H. Fu, Chunlian Chen, Xiaodong Zhu, Liqiao Zhou, Xiancheng Jiang, and Xiao Xiao. Construction and analysis of compact muscle-specific promoters for AAV Vectors. (Accepted by Gene Therapy, Mar., 2008, **Corresponding Author**)
2. **Bing Wang**, Juan Li, Chunping Qiao, Chunlian Chen, Peiqi Hu, Xiaodong Zhu, Liqiao Zhou, Janet Bogan, Joseph Kornegay & Xiao Xiao. A canine mini-dystrophin is functional and therapeutic in *mdx* mice. (Accepted by Gene Therapy, Feb., 2008)
3. Chunping Qiao, Jianbin Li, Jiangang Jiang, Xiaodong Zhu, **Bing Wang**, Juan Li & Xiao Xiao. Myostatin propeptide gene delivery by AAV8 vectors enhances muscle growth and ameliorates dystrophic phenotypes in *mdx* mice. (Accepted by Human Gene Therapy, Jan., 2008)
4. Chunping Qiao, Jianbin Li, **Bing Wang**, Juan Li and Xiao Xiao. Ameliorating dystrophic pathology via AAV-mediated gene delivery of myostatin propeptide. *Molecular Therapy, 2007, vol.15, suppl 1, S139*
5. Chunping Qiao, Jianbin Li, **Bing Wang**, Juan Li and Xiao Xiao. Splieosome-mediated RNA trans-spcing for muscular dytrophies. *Molecular Therapy, 2007, vol.15, suppl 1, S142*
6. Michael Y. Mi, Ying Tang, Bo Zheng, Johnny Huard, **Bing Wang**. Stable transduction of rAAV-GFP in cultured dividing myo-endo cells. 11th Annual Meeting of the American Society of gene therapy in Boston, May 28 – June 1, 2008.
7. Ying Tang; Bin Li, James H-C Wang, Johnny Huard, Melessa Salay, **Bing Wang**. *In vitro* AAV-mediated gene transfer in human fibroblasts. 54th Annual Meeting of Orthopaedic Research Society, March 1st – March 6th, 2008
8. Bin Li, Micheal Lin, Ying Tang, **Bing Wang**, James H-C Wang. Micropatterned C2C12 cells exhibit enhanced differentiation into myotubes – a novel study using cell traction force microscopy. 54th Annual Meeting of Orthopaedic Research Society, March 1st – March 6th, 2008
9. Guangheng Li, Bo Zheng, Andres J. Quintero, Arvydas Usas, **Bing Wang**, Laura B. Meszaros, Karin A. Corsi, Johnny Huard. Therapeutic Utility of Heterotopic Ossification Induced by AAV-BMP4 in Skeletal Muscle. 54th Annual Meeting of Orthopaedic Research Society, March 1st – March 6th, 2008

Administrative Core
(Johnny Huard, James Cummins and Matthew Bosco)

INTRODUCTION:

The Administrative Core of the Stem Cell Research Center (SCRC) is directly responsible for ensuring the proper function and integration of the Research Laboratories (comprising the Core Research Laboratories, Affiliated Laboratories, and Research Core Facilities), the Clinical Trials Unit, and the Educational Programs that constitute the SCRC. The Administrative Core provides administrative services to all SCRC personnel, supports the ongoing activities of the SCRC, and provides a mechanism for regular evaluation of the SCRC. The Administrative Core also is responsible for fulfilling the secretarial, budgetary, and grant application and manuscript preparation needs of SCRC personnel. In addition, this Core also facilitates collaboration between SCRC researchers and scientists working in designated Collaborative Institutes or other, non- affiliated laboratories.

BODY:

The Administrative Core has provided managerial and financial oversight for the entire Department of Defense Program. The center administrator, Matthew Bosco, and Senior Scientist, James Cummins have played key roles in facilitating and administering all of the various projects within the Program. Mr. Bosco and Mr. Cummins help ensure that each project functions smoothly and efficiently while maintaining continuous communication between the various investigators and institutions.

The SCRC sponsored a Winter Retreat in December of 2007 which was organized by the Administrative Core as an additional method by which to foster collaboration and education of SCRC researchers and other interested scientists. The "research retreat" was a 1-day scientific meeting featuring formal oral presentations by SCRC senior faculty. Members of the Administrative Core attended this meeting and also presented material related to SCRC. Attached is an agenda from our the 2007 Winter Retreat. In addition, we are planning another retreat for the Fall 2008.

The Administrative Core also organizes a weekly/biweekly seminar series for SCRC researchers, affiliates, collaborators, and other interested scientists. The goal of each of these events was to bring in highly regarded scientists who are performing cutting edge research in cellular therapeutics. In addition to serving as a forum in which SCRC scientists can interact with other researchers who share similar interests, this series has helped to introduce the invited speakers to the SCRC and has also helped to promote the development of ongoing collaborations with these well-regarded research scientists. The goal of these meetings is to help SCRC researchers hone their scientific critical analysis skills and, by so doing, improve their own research and writing abilities. Starting on the next page is a list of the SCRC seminar series topics and the presenters:

Investigator: Johnny Huard

Date	Topic	Speaker, Title, Affiliation
January 17, 2007	*The Influence of Local Niche on Differentiation and Transformation of Stem Cells*	Jonathan Pollet, PhD, Postdoctoral Fellow
January 24, 2007	*Decorin Interacts with myostatin activities – implications for skeletal muscle healing*	Jenny Zhu, PhD Candidate
January 31,	*In vivo ratio between BMP4 and VEGF determines VEGF's role in ectopic bone formation*	G.H. Li, PhD, Postdoctoral Fellow
February 7, 2007	*ORS Practice A novel CD146+CD133+CD56+ cell population in human skeletal muscle and during ontogeny*	Mihaela Crisan, PhD Candidate
February 23, 2007	*PhD Dissertation Defense: The Effect of BMP4 and Mechanical Stimulation on Muscle-Derived Stem Cells: Implications for Bone and Articular Cartilage Regeneration.*	Karin Corsi, PhD Candidate
February 28, 2007	*Cellcelector TM automated stem cell harvesting applications*	Ralph Weber, B.Sc. Rochester, New York
March 14, 2007	*Calcineurin and CaMK signaling pathways in fast-to-slow fiber type transformation of cultured mouse skeletal muscle fibers*	Xiaodong Mu, PhD The John Hopkins School of Medicine
March 28, 2007	*Q-dots and fluorescence-based detection systems for biology and biotechnology*	Alan Waggoner, PhD Director, Molecular Biosensor and Imaging Center and NSF Science and Technology Center, Carngie Mellon University
April 4, 2007	*Orthopaedic research perspectives: informal discussion with the graduate students*	Scott Rodeo, MD Orthopaedic Biomechanics Lab, University of Iowa.
April 18, 2007	*Stem cells as novel models to study EWS-FLI1 mediated tumorigenesis*	Srinivas Somanchi, PhD Division of Hematology-Oncology at Childrens Hospital Los Angeles, California
May 16, 2007	*Regenerate Toronto practice Follistatin knock out, Myostatin knock out and muscle regeneration*	Jenny Zhu, Graduate Student, SCRC
June 6, 2007	*MDSCs and Myoendothelial cells uses in cardiac research at SCRC ISSCR, Sydney, Australia Practice Talk*	Masaho Okada, MD Medical Fellow, SCRC

Investigator: Johnny Huard

June 20	*Student Rotation Seminar*	Joe Marhefka Graduate Student, McGowan Institute for Regenerative Medicine (MIRM).
June 22	*Wnt 3, 11, and 16 signaling pathways.*	Guosheng Xiang PhD Columbia University Postdoctoral candidate
June 15	*Research update of ongoing projects at SCRC*	Karin Corsi and Laurie Meszaros PhD Candidate, and Graduate Students
June 22	*Update of ongoing research projects*	Theresa Cassino, PhD, PTEI postdoctoral fellow and Lauren Drowley, Graduate Student, SCRC
June 29	*Update of ongoing research projects*	Manuela Gavina, PhD, Melano, Italy and Masaho Okada, MD Postdoctoral Fellow, and Medical Fellow, SCRC
July 11	*Imaging in scientific publications—what is allowed and what is fraud.*	Burhan Gharaibeh, PhD Research Assistant Professor, SCRC And David Humiston, Science Editor, SCRC
July 18	*Update of ongoing research projects*	Masa Nozaki, MD Medical Fellow, Japan And Jenny Zhu, PhD Candidate, SCRC
July 25	*NIH Grant proposal review of Aims and criticque by SCRC personnel*	Fabrisia Ambrosio, PhD Research Assistant Professor, Rehabilitation Sciences Department, Research Faculty, SCRC

Investigator: Johnny Huard

Bioreactor Core Progress Report March 2008
(Johnny Huard and Bridget Deasy)

The Bioreactor Core continues to provide an innovative approach to cell and molecular biology studies. We utilize unique technology which enables a novel bioimaging approach. Our goal is to generate functional knowledge on cell behavior based on macromolecular changes and cell-cell interactions within the population niche. The core currently consists of 2 microscope systems; Nikon Eclipse TE 2000 U systems with customized robotic stages (Automated Cell, Inc, PA). Photo-metric ES Cool Snap cameras are capable of acquiring up to 30 frames per second. For fluorescent live cell microscopy in 6 colors, we use X-Cite 120 EXFO Fluorescence Illuminator. Users from several different departments at the University of Pittsburgh, and the core have collaborations and a research student from Carnegie Mellon University.

We recently described the benefits of the bioreactor core technology for stem cell assays(*1*). Automated high-throughput time lapsed imaging of stem cell cultures enhances the ability of biological researchers to conduct multivariate experiments with time dependent parameters. Time-lapsed microscopic imaging of cells has been in use for more than 50 years (*2-6*), though only recently have software advances allowed for expanded experimental capabilities in which image processing routines have been developed for the quantitative analysis of viable, growing cells (*7-11*). Previously, time lapsed imaging techniques required significant time allotments and were error prone due to less than ideal circumstances in which cells were monitored and tracked *in vitro* by hand. Also, multivariate experiments were scaled versions of typical experiments and were thus limited by the effort required to maintain them. With robotic control, high-throughput time lapsed imaging has become an ideal platform for stem cell experiments with multiple variables and measurements on time dependent parameters such as cell growth and cell velocity.

Our recent report described the robotic systems for microscopic imaging, LACI, (live automated cell imager) which is programmed by the user to observe a large number of regions of interest (ROIs) that are imaged in visible and/or epifluorescent light. The automated stage and focus are controlled by custom software. Each ROI may have its own variable condition and the imaging is repeated at user-defined time intervals. The output data are stacks of images for each ROI with the time-interval between consecutive images. A small, but growing number of investigators are developing custom time-lapsed imaging systems (*12-15*) to better study cell behavior. However, the details of such instrumentation to date has been brief and limited to short descriptions in the methods section, while focusing on assay endpoints and the challenge of image analysis (*16, 17*). In our study, we presented a full description of the LACI instrument. In addition to showing the design and features of LACI, we also focused on the design considerations that relate to the study of stem cells. We presented the results in which human stem cells of different ages were examined for cell proliferation rates, velocity and cell size in order to determine how each parameter relates to cell age, as cell age has been shown to be related to a decline in stem cell function. Each of these parameters could play a role in how stem cells perform in therapeutic treatment for disease or injuries. The advantages of a robotic time-lapsed microscopic imaging system for characterizing stem cells during *in vitro* biological assays were shown.

1.   B. T. Schmidt, J. Feduska, A. Witt, B. Deasy, *Industrial Robot* **35**, 116 (2008).
2.   R. Schrek, J. N. Ott, Jr., *AMA Arch Pathol* **53**, 363 (Apr, 1952).
3.   R. R. Klevecz, *Proc Natl Acad Sci U S A* **73**, 4012 (Nov, 1976).
4.   K. Norrby, *Cell Tissue Kinet* **10**, 89 (Jan, 1977).
5.   P. O. Montgomery, W. A. Bonner, *Exp Cell Res* **17**, 378 (Jun, 1959).
6.   J. Fear, *J Anat* **124**, 437 (Nov, 1977).
7.   H. Satoh, L. M. Delbridge, L. A. Blatter, D. M. Bers, *Biophys J* **70**, 1494 (Mar, 1996).
8.   P. J. Harris, J. Y. Chatton, P. H. Tran, P. M. Bungay, K. R. Spring, *Am J Physiol* **266**, C73 (Jan, 1994).
9.   C. L. Curl *et al.*, *Pflugers Arch* (Feb 17, 2004).
10.   I. Spadinger, S. S. Poon, B. Palcic, *Cytometry* **10**, 375 (Jul, 1989).
11.   W. Y. Xu-van Opstal *et al.*, *Microsc Res Tech* **28**, 440 (Aug 1, 1994).
12.   U. Liebel *et al.*, *FEBS Lett* **554**, 394 (Nov 20, 2003).
13.   B. Neumann *et al.*, *Nat Methods* **3**, 385 (May, 2006).
14.   E. D. Miller, G. W. Fisher, L. E. Weiss, L. M. Walker, P. G. Campbell, *Biomaterials* **27**, 2213 (Apr, 2006).
15.   A. Bahnson *et al.*, *BMC Cell Biol* **6**, 19 (2005).
16.   Y. L. Wang, K. M. Hahn, R. F. Murphy, A. F. Horwitz, *J Cell Biol* **174**, 481 (Aug 14, 2006).
17.   J. R. Swedlow, M. Platani, *Cell Struct Funct* **27**, 335 (Oct, 2002).

2007-2008 JOURNAL and ABSTRACT PUBLICATIONS which include Bioreactor Core Technology

JOURNAL PUBLICATIONS

11. Schmidt, B.T., Feduska, J.M., Witt, A.M., and B.M. Deasy. 2008. **Robotic cell culture system for stem cell assays**. Industrial Robot. 35 (2):116-124.

12. Zheng B, Cao B, Crisan M, Sun B, Li GH, Logar A, Yap S, Pollet J, Drowley L, Cassino T, Gharaibeh B, Deasy BM, Huard J, Peault B. 2007 **Prospective identification of myogenic endothelial cells in human skeletal muscle. Nature Biotechnology**. Sep;25 (9):1025-34.

ABSTRACT PUBLICATIONS

13. Kim, Joo Han. Sowa, G., Deasy, B., Nam, Vo., Studer, R., Kang, J. **Time Lapse Live Cell Imaging Of Notochordal Cells Demonstrating Differentiation To Chondrocytic Cells.** NASS 23rd Annual Meeting

14. Wescoe, Kristin E., Schugar, R.C. and B. M. Deasy. 2008. **Examination of the Behavior of Umbilical Cord (UC)-Derived Stem Cells on 3D Tissue-Engineered Scaffolds.** MidWest Tissue Engineering Consortium. Cincinnati, OH, USA

15. Schugar, R.C. and B. M. Deasy. 2008. **The effects of growth surface on phenotype and proliferation of Wharton's Jelly-derived mesenchymal stem cells.** MidWest Tissue Engineering Consortium. Cincinnati, OH, USA

16. S.M. Chirieleison, J.M. Feduska, R.C. Schugar, S.L. Sanford, J. Huard, and B.M. Deasy. 2008. **Identifying Regenerative Populations of Human Muscle-Derived Cells and Tracking Phenotypic Changes in Culture.** MidWest Tissue Engineering Consortium. Cincinnati, OH, USA

17. Plassmeyer, J., Wright, V., Weiss, C., Deasy BM., Huard, J., Sowa, G., Ambrosio, F. **Mechanical stretching enhances muscle derived stem cell resistance to inflammatory stress.** International Society for Stem Cell Research ISSCR, Philadelphia, PA, USA. *Pending*

18. S.M. Chirieleison, J.M. Feduska, R.C. Schugar, S.L. Sanford, J. Huard, and B.M. Deasy. 2008. **Identifying Populations Of Human Muscle Derived Stem Cells To Participate In Skeletal Muscle Regeneration Based On Phenotypic Differences. Orthopaedic Research Society**. San Francisco, CA.

19. Schugar, R.C., Schmidt, B., and B.M. Deasy. 2008. **A Novel Use of Wharton's Jelly-Derived Cells Provides Potential Benefits To Overcome Immunorejection In Stem Cell-Mediated Cartilage Repair**. Orthopaedic Research Society; San Francisco, CA . PODIUM

20. Kim, Joo Han. Sowa, G., Deasy, B., Nam, Vo., Studer, R., Kang, J., Georgescu, H. 2008 **Live Cell Imaging Of Notochordal Cells From The Rabbit Nucleus Pulposus Demonstrating Differentiation And Interaction With Chondrocytic Cells.** *Spine* 2008.

21. Wescoe, Kristin E., R.C. Schugar, D.W. Wilkinson, and B.M. Deasy. 2007. **Comparison of Potential 3D Organic Gels for Cartilage Tissue Engineering to Support Growth of Novel Human Umbilical Cord Cells**. American Society for Cell Biology; Washington, D.C.

22. Schugar, R.C., Schmidt, B., and B.M. Deasy. 2007. **Chondrogenic Potential of Wharton's Jelly-derived Stem Cells through Growth Factor Induction.** American Society for Cell Biology; Washington, D.C

23. Schugar, R.C. and B.M. Deasy. 2007. **The Isolation and Characterization of Stem Cells from the Wharton's Jelly.** American Society for Cell Biology; Washington, D.C.

24. Sanford, S.L., B.M. Deasy. 2007. **User-Friendly Calculator to Obtain Cell Growth Parameters**. American Society for Cell Biology; Washington, D.C.

25. Schmidt, B, Schugar, R.C., Crisan, M., Teng, B, Peault, B, B.M. Deasy. 2007. **Human Umbilical Cord Stem Cells from Wharton's Jelly: Potential for Cartilage Tissue Engineering.** International Society for Stem Cell Research ISSCR, Cairns, Australia.

On-going Collaborative Projects (a sample of several core collaborations)

1. *Effect of mechanical stress on substrate surfaces and cell growth.* Dr. James Wang, Assistant Professor of Orthopedic Surgery. University of Pittsburgh.

2. *Invesitgation of the Inhibition of OsteoSarcoma Metastatic potential with Noggin and s-Flt.* Dr. Kurt Weiss, Department of Orthopedic Surgery, University of Pittsburgh Medical Center.

Micro-CT Core
(Johnny Huard and Arvydas Usas)

We continue to use Scanco vivaCT 40 imaging system for noninvasive detection of calcified matrix deposition in vitro and in vivo. The system comes equipped with the computer software that enables nondestructive two-dimensional and three-dimensional visualization and quantitative evaluation of bone volume, density and architecture.

Recently we developed technique that allows continuous in vitro evaluation of cell's osteogenic potential after stimulation and enables to screen for the best cellular candidates for bone tissue engineering.

We also initiated imaging studies of skeletal muscle vascularity that involve transcardiac perfusion of vascular system and injection with Microfil® silicone rubber compound that after polymerization opacifies microvascular network and other spaces in post-mortem tissues of non-surviving animals.

Research accomplishments to date:

1. Osteogenic capacity of muscle-derived stem cells under BMP4 stimulation in pellet culture (Corsi KA et al. Journal of Bone and Mineral Research 22(10); 1592-602, 2007).
2. Inhibition of bone formation by using ex vivo Noggin gene therapy in animal model of craniosynostosis (Cooper G et al. Manuscript in revision in "Plastic and Reconstructive Surgery").
3. Ectopic bone formation in fast and slow skeletal muscle (Meszaros L., "Influence of vascularity on muscle regeneration, fibrosis and heterotopic ossification". Poster at the ORS 2008).
4. Influence of the host gender and resident osteoprogenitor cells on bone formation (Meszaros L., "Effect of host animal sex on ectopic bone formation by MDSCs". Poster at the ORS 2008).
5. Osteogenic potential of human meniscus-derived stem cells (Osawa A., "Isolation and characterization of human meniscus-derived vascular stem cells". Poster at the ORS 2008).
6. Osteogenic potential of human muscle-derived stem cells (Zheng B., "Multipotency of adult human myoendothelial cells demonstrated by single-cell-derived clonal populations". Poster and short talk at the ORS 2008).
7. The effect of mechanical stimulation on osteogenic differentiation of BMP-4-expressing MDSCs (Liu J. Poster at the ORS 2008).
8. Therapeutic utility of heterotopic ossification induced by AAV-BMP4 in skeletal muscle (Li G., Poster at the ORS 2008).
9. MicroCT analysis of vertebral bony microstructure (Vo N., "A novel accelerated aging murine model exhibiting severe proteoglycan deficiency in disc nucleus pulposus". Poster at the University of Pittsburgh Conference on Aging, 2008).

Following is the list of current projects:

1. Evaluation of skeletal muscle vascularity after injury (laceration, contusion), electrical stimulation and physical exercise in mice. (In progress).
2. Relationship between angiogenesis and fibrosis formation after skeletal muscle injury. (In progress).
3. Control of bone regeneration and bone defect healing using spatial BMP4 protein distribution on prefabricated fibrin and collagen scaffolds using 3D printing technology. (In progress).
4. Osteogenic potential of human muscle-derived cells after transplantation into critical-size calvarial defect (In progress).
5. Role of PI3K, ERK1/2, and p38 MAPK pathways in BMP4-induced matrix mineralization by MDSCs. (In progress).

Suramin can enhance the skeletal muscle healing by blocking myostation

*Nozaki M, *Li Y, *Zhu J, *Kenji Uehara, *Ambrosio F, **Fu FH, +*Huard J
*Stem Cell Research Center, Children's Hospital of Pittsburgh and **Department of Orthopaedic Surgery, University of Pittsburgh, Pittsburgh, PA
jhuard@pitt.edu

INTRODUCTION:
Muscle injuries are very common musculoskeletal problems encountered in sports medicine. Although this type of injury is capable of healing, complete functional recovery is hindered by the development of scar tissue formation triggered by TGF-β1 [1]. We already reported suramin can effectively prevent the formation of fibrotic scar and block the proliferative effect of TGF-β1 on fibroblasts and can stimulate the differentiation on myogenic cells *in vitro* (unpublished data). Thus suramin can enhance muscle regeneration in the lacerated and strain-injured muscle [2, 3]. Furthermore we also reported blockade of myostatin (MSTN), a member of TGF-β super family, by decorin, other anti-fibrotic agent, showed enhancement of the fusion on myoblasts and inhibitory effect of fibroblast proliferation *in vitro* [4]. This finding brought us more interest to investigate another pathway of suramin to regulate fibroblasts and myoblasts by blocking the effect of MSTN. We performed this study to examine whether suramin would block MSTN's proliferative effect on fibroblasts and inhibitory effect of myoblasts differentiation *in vitro* and reduce the expression of MSTN in injured muscle to improve muscle healing *in vivo*, using an animal model of muscle contusion.

MATERIALS AND METHODS:
3T3 cell proliferation assay: 3T3 fibroblasts were cultured in 96 well plates (n=5) with DMEM containing 2% serum replacement (Sigma, St Louis, MO) and different concentration of MSTN (0 and 1 μg/ml) and suramin (0 and 50 μg/ml). Three days after incubation CellTiter Cell Proliferation Assay kit (Promega, Madison, WI) was used to measure cell proliferation.

C2C12 cell differentiation assay: C2C12 myoblasts were cultured in 24 well plates (n=4) with differentiation medium (DMEM containing 2% horse serum and 1% penicillin/streptomycin) containing different concentration of MSTN (0 and 1 μg/ml) and suramin (0, 1,and 25 μg/ml). Three days after incubation immunocytochemistry of myosin heavy chain was done and the fusion index was assessed by counting the number of nuclei in differentiated myotubes as a percentage of the total number of nuclei.

Animal model: The muscle contusion model was developed in tibialis anterior muscle of normal wild-type mice. Different concentrations of suramin (0 and 2.5 mg in 20μl of Phosphate-buffered solution [PBS]) were injected intramuscularly two weeks after injury (five mice in each group). Cryostat sections of muscles were obtained and histologically stained (hematoxlin and eosin stain (H&E) and Masson's Trichrome stain) to evaluate the regeneration by counting the number of centronucleated regenerating myofibers and measuring fibrosis four weeks after injury. Specific peak force and specific tetanic force were mesured as physiological tests to evaluate functional recovery after muscle injury using same protocol as above (five mice in each group). Furthermore immunohistochemistry of MSTN was performed at different time point (0.5, 1, 2, 10 days after suramin (0 and 2.5 mg) injection) to evaluate the expression of MSTN (five mice in each group at each time point). Northern Eclipse software (Empix Image, Inc.) was used to quantify the total fibrotic area and expression of MSTN. Statistical analysis was performed with student's t-test or ANOVA. Statistical significance was defined as $P < .05$ (*: $P<.05$, **: $P<.01$).

RESULTS:
Suramin blocked the proliferative effect of MSTN on fibroblasts and the inhibitory effect of MSDN of myoblast differentiation: MSTN treatment significantly promoted the proliferation on fibroblasts and the differentiation on myoblasts. However, suramin treatment significantly blocked both of those MSTN's effects and moreover suramin treatment stimulated the fusion on myoblasts in a dose-dependent manner in the presence of MSTN (Fig. 1A, B).

Suramin inhibits the myostatin expression in injured skeletal muscle: Suramin (2.5 mg) injection 2 weeks after contusion injury effectively inhibited the expression of MSTN when compared with the control group (0 mg) at different time points (0.5, 1, 2, 10 days after suramin injection) (Fig. 2A, B).

Suramin enhances muscle regeneration and decreases fibrosis and improves functional recovery after contusion injury: We observed a significant increase in the number and in the diameter of regenerating myofibers in the suramin treated group (2.5 mg) when compared with the control group (0mg) (Fig. 3A, B,). Moreover suramin treated group showed significantly less fibrotic area than control group (Fig. 3C). Furthermore the suramin treatment showed significant advantage in physiological evaluation (specific peak force and specific tetanic force) compared to control group.
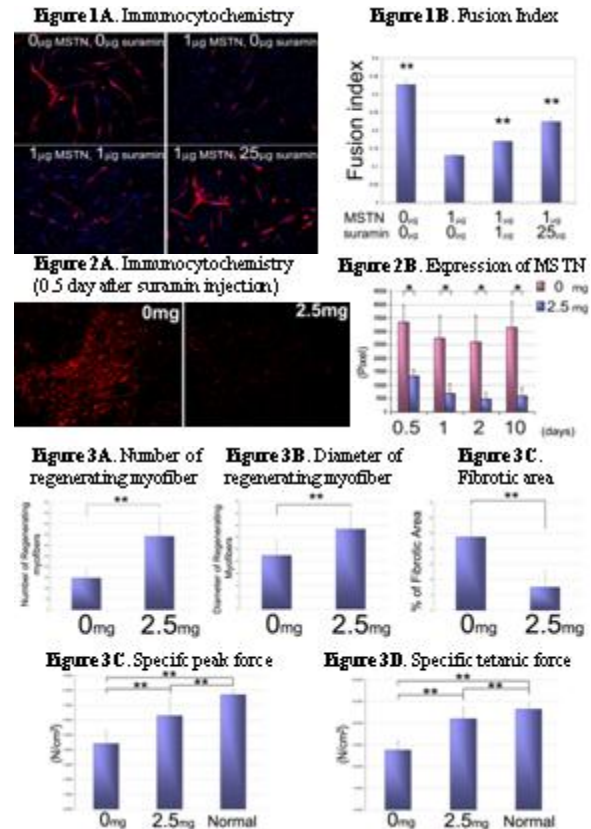
DISCUSSION:
We have reported that suramin can effectively prevent muscle fibrosis and enhance muscle regeneration by blocking TGF-β1 after laceration and strain injury [2, 3]. Nevertheless, whether suramin would regulate the effect of MSTN, negative regulator of muscle growth, to improve muscle healing was still unknown. This is the first study to show that suramin down-regulates the proliferation on fibroblasts and up-regulates the differentiation on myoblasts by neutralizing MSTN. Moreover suramin injection in injured skeletal muscle effectively inhibited the expression of MSTN and enhanced the muscle regeneration and reduced the fibrosis *in vivo*. These results may reveal the hidden mechanism by which suramin improve the muscle healing after injuries. We have reported important anti-fibrotic molecules such as Decorin to improve injured skeletal muscles. However suramin has been already approved by FDA and this makes suramin more suitable agent for the therapy of muscle injury. Our findings may contribute to the development of biological therapies for muscle injury.

REFERENCES:
1. Li Y, Foster W *et al.*, *Am J Pathol* 2004;164: 1007-19.
2. Chan Y, Li Y *et al.*, *J Appl Physiol* 2003;95:771-80.
3. Chan Y, Li Y *et al.*, *Am J Sports Med* 2005; 33:43-51.
4. Zhu J, , Li Y *et al.*, *J Biol Chem* 2007, in print

Improved muscle healing after contusion injury by the inhibitory effect of suramin on myostatin, a negative regulator of muscle growth

[+][*]Masahiro Nozaki, MD, [+][‡]Yong Li, MD, PhD, [+][§]Jinhong Zhu, MD,

[**]Fabrisia Ambrosio, PhD, MPT [+][*]Kenji Uehara MD, PhD,

[*]Freddie H. Fu, MD, and [+][*]Johnny Huard, PhD

+Stem Cell Research Center, Children's Hospital of Pittsburgh, PA

*Department of Orthopaedic Surgery, University of Pittsburgh, Pittsburgh, PA

§Department of Bioengineering, University of Pittsburgh, Pittsburgh, PA,

‡Department of Pathology, University of Pittsburgh School of Medicine, Pittsburgh, PA

** Department of Physical Medicine and Rehabilitation, University of Pittsburgh,

Pittsburgh, PA

Corresponding Author: Johnny Huard, PhD
4100 Rangos Research Center, 3469 Fifth Avenue
Pittsburgh, PA, 15213-2582
E-mail: jhuard@pitt.edu

1

Abstract

Background:

Muscle contusions are the most common muscle injuries in sports medicine. Although these injuries are capable of healing, incomplete functional recovery often occurs.

Hypothesis:

Suramin enhances muscle healing by both stimulating muscle regeneration and preventing fibrosis in contused skeletal muscle.

Study Design:

Controlled laboratory study

Methods:

In vitro: Myoblasts (C2C12 cells) and muscle-derived stem cells (MDSCs) were cultured with suramin and the potential of suramin to induce their differentiation was evaluated. Furthermore, MDSCs were co-cultured with suramin and myostatin (MSTN) to monitor the capability of suramin to neutralize the effect of MSTN. *In vivo*: Varying concentrations of suramin were injected in the tibialis anterior muscle of mice two weeks after muscle contusion injury. Muscle regeneration and scar tissue formation were evaluated by histological analysis and functional recovery was measured by physiological testing

Results:

In vitro: Suramin stimulated the differentiation of myoblasts and MDSCs in a dose-dependent manner. Moreover, suramin neutralized the inhibitory effect of MSTN on MDSC differentiation. *In vivo*, suramin treatment significantly promoted muscle regeneration, decreased fibrosis formation, reduced myostatin expression in injured muscle, and increased muscle strength after contusion injury.

Conclusion:

Intramuscular injection of suramin following a contusion injury improved overall skeletal muscle healing. Suramin enhanced myoblast and MDSC differentiation and neutralized MSTN's negative effect on myogenic differentiation *in vitro,* which suggests a possible mechanism for the beneficial effects that this pharmacological agent exhibits *in vivo*.

Clinical Relevance:

These findings could contribute to the development of biological treatments to aid in muscle healing after experiencing a muscle injury.

Keywords:

Muscle contusion injury; suramin; myostatin; muscle regeneration; fibrosis

Muscle injuries are common musculoskeletal problems encountered in sports medicine clinics. Muscle contusion, produced by the impact of a nonpenetrating object[8] is one of the most common of muscle injuries.[3] Current therapies including RICE (rest, ice, compression, and elevation), immobilization, as well as active and passive range of motion exercise are the norm for treatment; however, complications such as muscle atrophy, contracture formation, and pain leading to functional and structural deficits, often occur following severe muscle injury.[8, 23, 24, 36] Optimal treatment strategies have not yet been clearly defined.

We have observed that the healing process of injured skeletal muscle in animal models consists of three phases: degeneration and inflammation, regeneration, and fibrosis.[19]

The first phase, which occurs in the first few days post-injury, is characterized by local swelling at the injury site, the formation of a hematoma, necrosis of muscle tissue[18, 22], degeneration, and an inflammatory response, which consists of the infiltration of activated macrophages and T-lymphocytes into the injured tissue. The next phase, regeneration, usually occurs five to ten days after injury and includes phagocytosis of the damaged tissue, and regeneration of the injured muscle. This phase is promoted by released growth factors such as insulin-like growth factor-1 (IGF-1), hepatocyte growth factor (HGF), epidermal growth factor (EGF), transforming growth factors (TGF-β1 and TGF-β2), and platelet-derived growth factors (PDGF-A and PDGF-B), which regulate myoblast proliferation and differentiation, produce connective-tissue scar, and induce capillary in-growth at the injury site.[1, 4, 14]

The final phase, the formation of scar tissue (fibrosis), usually begins between the second and third weeks post-injury. The formation of scar appears to be the end product of the muscle repair process, and hinders full muscle regeneration. We have previously reported that TGF-β1 is a major factor in triggering the fibrotic cascade within injured skeletal muscle.[29]   TGF-β1 also plays a role in the differentiation of muscle-derived stem cells (MDSCs) towards a myofibroblastic lineage.[30] With this in mind, we have focused on the use of antifibrotic agents (such as decorin and γ-interferon) that inhibit TGF-β1 expression, reduce scar tissue formation, and consequently improve muscle healing after injury.[10, 11] Administration of decorin after muscle injury showed improvement of muscle healing both histologically and physiologically.[11] The injection of γ-interferon into injured skeletal muscle also showed similar effects.[10] Despite these compelling findings, which were derived from various murine injury models, the fact that decorin is not clinically available limits it's translation to human subjects and γ-interferon demonstrates serious side effects in spite of FDA approval. A recently published study has shown that myostatin (MSTN), a member of the TGF-β1 superfamily and a negative regulator of muscle growth, simulates scar tissue formation after skeletal muscle injury *in vivo*.[46] It was also shown in this study that decorin could inhibit MSTN's activity *in vitro*.[46] We therefore hypothesized that suramin may also possess a similar anti-MSTN activity as decorin.

Suramin, an antiparastic and antineoplastic agent, can inhibit TGF-β1's ability to bind to its receptors and has been shown to enhance muscle regeneration following strain and laceration injuries.[5, 6] Furthermore, suramin has a long history of clinical use as an anti-parasitic drug. During the past few decades, suramin's use for the treatment for prostate

cancer has also been of interest. Therefore, one of the biggest advantages of using this drug instead of the other antifibrotic agents is that it has already been approved by Food and Drug Administration (FDA). We therefore focused on the use of suramin in the current study by examining ~~in vitro~~ whether suramin would promote differentiation of myoblasts and MDSCs and neutralize the effect of MSTN *in vitro*. We also investigated if suramin could improve muscle healing after muscle contusion, a common muscle injury, by enhancing regeneration and reducing fibrosis *in vivo*.

MATERIALS AND METHODS

In Vitro Potential of Suramin to Induce Myogenic Differentiation

Effect of suramin on C2C12 myoblasts

C2C12 cells, a well-known myoblast cell line, were cultured with Dulbecco's modified Eagle's medium (DMEM) (Invitrogen, Carlsbad, CA) containing 10% fetal bovine serum (FBS) (Invitrogen), and 1% penicillin/streptomycin (P/S) (Invitrogen). Cells were plated at a density of 10,000 cells/well into 12-well plates. After a 24-h incubation period, the medium was completely removed and low serum-containing medium (DMEM, 2% horse serum (HS) (Invitrogen), and 1% P/S) was added with varying concentrations of suramin (0, 0.25, 2.5, 25 µg/ml) (Sigma, St. Louis, MO). Medium was replaced with fresh medium (containing the same concentrations of

6

suramin) every 2 days. All of the cells were grown at 37°C in 5% CO_2 for a total of 4 days.

The effect of suramin on MDSCs isolated from skeletal muscle

MDSCs were isolated from 3-week-old male mice (C57BL10J+/+) via the previously described modified preplate technique.[30, 34, 35] MDSCs were cultured in proliferation medium (PM) containing DMEM, 10% FBS, 10% HS, 1% P/S, and 0.5% chick embryo extract (CEE) (Sera Laboratories International, West Sussex, UK). Cells were plated at a density of 10,000 cells/well into 12-well plates. After a 24-h incubation period, the medium was completely removed and low serum medium was added with different concentrations of suramin (0, 1, 10, 100 µg/ml) for the next 24 hrs. Medium was replaced with fresh low serum medium for 1 more day. All of the cells were grown at 37°C in 5% CO_2 for a total of 3 days.

The ability of suramin to neutralize MSTN's inhibition of MDSCs differentiation

MDSCs were cultured in PM and plated at a density of 5,000 cells/well into 24-well plates. After a 24-h incubation period, the medium was removed and low serum containing medium was added with varying concentrations of suramin (0, 1, 10, 100 µg/ml) and MSTN (0 and 100 ng/ml) for the next 24 hrs. Medium was replaced with fresh low serum medium containing the same concentrations of MSTN for 1 additional day. All of the cells were grown at 37°C in 5% CO_2 for a total of 3 days.

Immunocytochemistry

To quantify the differentiation of the C2C12 cells and MDSCs, cells were fixed in cold methanol for 2 min and washed in Dulbecco's phosphate buffered saline (PBS) for 10 min at room temperature (RT). Samples were washed three times in PBS, then incubated in blocking buffer (10% HS) for 30 min at RT. Cells were incubated overnight at 4°C with primary antibodies (monoclonal anti-skeletal myosin (fast) clone MY-32 (Sigma)) in 2% HS. After washing in PBS, samples were incubated with the secondary antibody (goat anti-mouse IgG conjugated with Cy3 (Sigma)) in 2% HS for 1 h at RT. The cell nuclei were stained with a Hoechst 33258 dye for 10 min at room temperature. Fusion index (ratio of nuclei in myotubes to all nuclei) was calculated to evaluate the myogenic differentiation capacity of cells.

Evaluation of the Histological and Physiological Effects of Suramin on Muscle Healing After Contusion Injury In Vivo

Animal model

The policies and procedures followed for the animal experimentation performed in these studies are in accordance with those detailed by the US Department of Health and Human Services and the National Institutes of Health *Guide for the Care and Use of Laboratory Animals*. The authors' Institutional Animal Care and Use Committee

approved the research protocol used for these experiments (protocol No. 19/05). An animal model of muscle contusion was developed in normal mice (C57BL6J+/+; Jackson Laboratory, Bar Harbor, ME) based on previously described studies.[8, 25] Thirty three mice, with an age of 8 - 10 wk old and weight of 21.0 - 26.3g, were used in this experiment.

The mice were anesthetized with 1.0–1.5% isoflurane (Abbott Laboratories, North Chicago, IL, USA) in 100% O_2 gas. The mouse's hindlimb was positioned by extending the knee and plantarflexing the ankle 90 degree. A 16.2 g, 1.6 cm stainless steel ball (Small Parts Inc., Miami Lakes, FL) was dropped from a height of 100 cm onto the impactor which hit the mouse's tibialis anterior (TA) muscle. The mice were divided into four groups (6 mice / group) on the basis of the different concentrations of suramin to be injected (0, 2.5, 5, and 10 mg in 20 µl of PBS) after contusion injury. Suramin was injected 2 wks post-injury. All animals were sacrificed to evaluate the healing histologically and physiologically at 4 wks post-injury. Three mice (6 muscles) per group were assessed histologically, three mice (6 muscles) per group were assessed physiologically, and three mice were used as normal control in the physiological tests.

Furthermore, two concentrations of suramin (0 and 2.5 mg in 20 µl of PBS) were injected 2 wk post-injury (3 mice/group). The mice of both groups were sacrificed 2 days post-injection for histological analysis of MSTN expression.

Evaluation of muscle regeneration after suramin therapy

TA muscles that were used for histological evaluation were isolated and frozen in 2-methylbutane pre-cooled in liquid nitrogen and subsequently cryosectioned. Hematoxylin

& Eosin (HE) staining was done to monitor the number of regenerating myofibers within the injury sites treated with suramin (0, 2.5, 5, or 10 mg in 20 µl of PBS), and the results were compared among the different groups. Centronucleated myofibers were considered to be regenerating myofibers.[21] Analysis of regenerating myofibers was performed using Northern Eclipse software (Empix Imaging Inc., Cheektawaga, NY). The total number of regenerating myofibers within the injury site was quantitated by using ten random fields selected from each sample in accordance with a previously described protocols.[10, 11, 25, 32]

Evaluation of fibrosis after suramin therapy

To measure areas of fibrotic tissue in the injury sites, Masson's trichrome staining (IMEB Inc., Chicago, IL) was performed. After Masson's trichrome staining, the ratio of the fibrotic area to the total cross-sectional area was calculated to estimate the fibrosis formation by using Northern Eclipse software (Empix Imaging Inc.). The ratio of the fibrotic area within the injury sites was quantitated using a previously described protocol.[10, 11, 25, 32]

Evaluation of MSTN expression after suramin therapy

To measure the MSTN expression in injured muscle, cryosectioned tissue was fixed in 4% formalin for 5 min followed by two 10-min washes with PBS. The sections were then blocked with 10% HS for 1 h at RT. Sections were incubated overnight at 4°C with primary antibodies (Goat anti GDF-8 AF-788 (R&D Systems Inc., Minneapolis, MN)) in

2% HS. After washing in PBS, samples were incubated with the secondary antibody (donkey anti-goat IgG conjugated with Alexa Fluor 555 (Invitrogen)) in 2% HS for 1 h at RT.

The total MSTN positive area was calculated using Northern Eclipse software (Empix Imaging Inc.) The total positive area within the injury site was quantitated using a previously described protocol.[10, 11, 25, 32]

Physiological evaluation of muscle contractile properties after suramin therapy

Contusion injuries were made on TA muscles of both legs of normal mice and treated as described above. Four weeks after injury, muscles from both legs were tested to evaluate peak twitch and tetanic force. TA muscles were harvested bilaterally placed in a vertical chamber that was constantly perfused with mammalian Ringer solution aerated with 95% O_2–5% CO_2 and maintained at 25°C. The distal attachment of the muscle was mounted to a glass tissue support rod, and the proximal end of muscle on tibia was connected to a force transducer and length servo system (Aurora Scientific, Ontario, Canada). The muscles were stimulated by monophasic rectangular pulses of current (1 millisecond in duration) delivered through platinum electrodes placed 1 cm apart. The current was increased by 50% more than the current necessary to obtain peak force (250-300 mA) to ensure maximal stimulation. Using a micropositioner, muscles were first adjusted to their optimum length (Lo), defined as the length at which maximum isometric twitch tension was produced. Maximal tetanic force was assessed via a stimulation

frequency of 75 Hz delivered in a 500-millisecond train. After the procedure, each

muscle was weighed, and specific peak twitch force and specific peak tetanic force were

calculated and expressed in force per unit cross-sectional area (N/cm^2).

Statistical analysis

All of the results from this study were expressed as the mean ± S.D. The result of

MSTN expression *in vivo* was analyzed using *t*-test and all the other results were

statistically analyzed using ANOVA. Differences among the groups were analyzed by

using Scheffe multiple comparisons (post hoc test). Statistical significance was defined as

$P < 0.05$.

RESULTS

In Vitro Potential of Suramin to Induce Myogenic Differentiation

The effect of suramin on myoblasts

The effect of suramin on the differentiation of C2C12 cells is shown in Fig.1. The

fusion index of C2C12 cells in the group treated with suramin (25 μg / ml) (0.162 ±

0.018) was significantly higher at 4 days of incubation as compared to the fusion index in

the control group (0 μg / ml) (0.953 ± 0.015). Moreover, the high dose suramin treated group (25 μg / ml) displayed a significantly higher fusion index when compared with the low dose suramin treatment group (0.25 μg / ml). The effect of suramin to induce the differentiation of C2C12 appeared to be dose-dependent.

The effect of suramin on MDSCs

Suramin also stimulated MDSC differentiation in a dose-dependent manner (Fig. 2E). Suramin treated MDSCs enhanced the differentiation of MDSCs after 3 days of incubation. Suramin treated groups (10 and 100 μg / ml) (Fig. 2C and 2D) showed significantly higher fusion indexes (0.228 ± 0.025, 0.347 ± 0.0456) than the control group (0 μg / ml) (Fig. 2A) (0.149 ± 0.030). Among the suramin treated groups, the high dose suramin treatment group (100 μg / ml) (Fig. 2D) displayed a significantly higher fusion index when compared with the two lower dose treatment groups (1 and 10 μg / ml) (Fig. 2B and 2C).

The ability of suramin to neutralize MSTN's inhibition of MDSCs differentiation

The group containing only MSTN (0 μg/ml suramin and 100 ng/ml MSTN) (Fig. 3B) showed a significantly lower fusion index (0.091 ± 0.020) than the control group (0 μg/ml suramin and 0 ng/ml MSTN) (Fig. 3A) (0.152 ± 0.035). All groups containing both suramin and MSTN (1, 10 and 100 μg/ml suramin and 100 ng/ml MSTN) (Fig. 3C, 3D, and 3E) demonstrated significantly higher fusion indexes (0.153 ± 0.035, 0.162 ± 0.048,

0.279 ± 0.041) when compared with the group containing only MSTN (Fig. 3B). Suramin appeared to neutralize MSTN's inhibitory effect on MDSC differentiation and, moreover, appeared to stimulate the fusion of MDSCs in a dose-dependent manner (Fig. 3F).

The Histological and Physiological Effects of Suramin on Muscle Healing

After Contusion Injury In Vivo

The effect of suramin treatment on muscle regeneration after contusion injury

All the centronucleated regenerating myofibers present in the injured muscle were counted and compared among the groups (Fig. 4E). The suramin treated muscles displayed numerous regenerating myofibers at the contusion site. All the suramin treated groups (2.5, 5, and 10 mg) (Fig. 4B, 4C, and 4D) showed significantly higher numbers of regenerating myofibers (361.6 ± 84.39, 341.1 ± 57.21, 308.5 ± 84.33) compared with the control group (0 mg of suramin) (Fig. 4A) (204.6 ± 15.27).

The effect of suramin therapy on muscle fibrosis after contusion injury

After Masson's trichrome staining, the area of fibrotic scar tissue was evaluated and compared among the groups (Fig. 5E). All the suramin treatment groups (2.5, 5, and 10 mg) (Fig. 5B, 5C, and 5D) showed significantly less fibrotic area (6.856 ± 2.588, 7.677 ± 2.897, 8.993 ± 2.980) compared with the untreated control group (0 mg of suramin) (Fig. 5A) (19.109 ± 3.215).

Suramin injection down-regulated MSTN expression in injured muscle

Immunohistochemical staining was performed to detect MSTN expression in the contusion injured TA muscles. The MSTN positive areas were measured and compared between the various treatment groups (Fig 6C). The muscle treated with 2.5 mg suramin injection 2 wk post-injury showed significantly less MSTN expression (4466.7 ± 7306.1) when compared with the untreated control (0 mg suramin) (27830.2 ± 23206.3) (Fig 6A and B).

Suramin injection improved muscle strength after contusion injury

The results of the physiological evaluations are shown in Table 1. The control group (0mg of suramin) and all the suramin treated groups, with the exception of the 2.5 mg suramin treatment group, showed significantly less specific peak force (twitch and tetanic) when compared with the normal non-injured group. On the other hand, the muscles treated with 2.5mg suramin showed significantly greater specific peak force (twitch and tetanic) than the untreated control group. There was no significant difference between injured muscle that had been treated with 2.5 mg suramin and normal non-injured muscle. In addition, the muscles injected with 2.5mg suramin also showed significantly greater specific peak tetanic force than the other suramin treated groups (5 and 10mg) and the control group (0 mg of suramin).

DISCUSSION

The aim of this study was to evaluate the effect of suramin on myogenic cell differentiation and muscle healing after contusion injury. We hypothesized that suramin treatment would lead to better biological healing by both stimulating muscle regeneration and preventing fibrosis in contused muscle. Histologically, the muscle treated with suramin 2 weeks after injury showed more regenerating myofibers and less fibrotic scar formation when compared with the control group (0 mg of suramin) at 4 weeks after contusion injury. Furthermore, suramin treatment also showed an increase in muscle strength compared to the untreated control group.

The muscle contusion injuries we modeled in this study are among the most common muscle injuries encountered in contact sports and by military personnel. More than 90% of muscle injuries are caused either by contusion or by excessive strain of the muscle. [3, 12] Although contusion injury is capable of healing, an incomplete functional recovery often occurs, depending on the severity of the initial trauma. Skeletal muscle has a great regenerative potential,[4, 12, 13, 20, 25, 27, 32, 43] largely attributed to the activation of muscle progenitor cells and their fusion into mature multinucleated myofibers[21, 38, 39] ;however, scar tissue formation occurs simultaneously and likely competes with muscle regeneration during the muscle healing process.[10, 25, 31]

We have investigated the effect of some treatments, such as suture or immobilization, which are normally used in the clinic for the muscle injury, by using animal models. One study showed that immobilization after muscle laceration had no significant effect on fibrosis reduction. Suture repair promoted better healing of the injured muscle and

prevented the development of fibrosis at the deep tissue level, but not ~~at the~~ superficially.[32]

Suramin, which is a polysulphonated naphthylurea, was designed as an antiparastic drug [16] and is used for the treatment of human sleeping sickness, onchocerciasis and other diseases caused by trypanosomes and other worms. In addition, it is under investigation as a treatment for some malignancies such as prostate, adrenal cortex, lymphoma, breast, and colon cancer [47] and HIV-1.[28] The major systemic side effects of suramin are malaise, neuropathy [2, 7] mineral corticoid insufficiency [26] and corneal deposits [17] and occasionally neutropenia [9] thrombocytopenia [45] and renal failure [40] have also been observed. The toxicity of suramin when it is injected intramuscularly, which we used in our animal model, has not yet been determined. Although we observed no adverse effects in the mice injected with up to 10 mg of suramin in this study, we did not specifically test to evaluate side effects. Suramin is known as a heparin analog which can bind to heparin–binding proteins and inhibit the effect of growth factors by competitively binding to growth factor receptors.[41, 47] TGF-β1, -2, and -3, platelet-derived growth factor (PDGF) A and B; and Epidermal Growth Factor (EGF) are growth factors that are known to be inhibited by suramin. Among them, TGF-β1 and -2 and PDGF A and B are known to have the potential to promote fibroblast proliferation.[42, 44]

In our *in vivo* study using the muscle contusion model direct injection of suramin at 2 weeks after muscle injury demonstrated a significant reduction of fibrous tissue formation when compared with the untreated control (0 mg of suramin). We found that suramin treatment led to a beneficial effect in contused muscle, as was previously seen in suramin treated lacerations and strains[5, 6] as well as when using other anti-fibrotic agents

such as decorin and γ-INF [10, 11]. Moreover, our results indicate that 2.5 mg suramin treatment group was the optimal dose for the treatment of muscle contusions. Higher doses of suramin (5 and 10 mg) did not show significant differences to the 2.5 mg suramin treatment group.

This study also showed that suramin enhanced muscle regeneration when it was injected directly into the muscle 2 weeks after receiving a contusion injury. We found many regenerating myofibers at the injury site usually sequestered by a large amount of fibrotic tissue. All of the suramin treated groups showed a significant increase in the number of regenerating myofiber at 4 weeks after receiving the injury.

Functional recovery after muscle injury is the most important variable determining the likelihood for clinical translation of this therapy in the treatment of skeletal muscle injury. As was observed with other antifibrotic agents (decorin and γ-INF) [10, 11] suramin also appears to have a beneficial effect on the physiological recovery of skeletal muscle. Our results showed that there was no significant difference in the specific peak twitch and tetanic forces between normal non-injured muscle and 2.5 mg suramin-treated contused muscle. These results strongly indicate that the injection of 2.5 mg of suramin at 2 weeks after contusion injury can improve muscle strength and promote functional recovery after muscle injury.

Taken together, our *in vitro* study about the effect of suramin on myogenic cell differentiation provides insight as to the underlying mechanism by which suramin enhances muscle regeneration *in vivo*. Our *in vitro* results showed 25 μg/ml of suramin can significantly enhance C2C12 differentiation at 4 days after incubation and, in addition, suramin treatment leads to significant increases in the fusion index in a dose-

18

dependent manner. Further, we observed an even more prominent dose-dependent effect on MDSC differentiation 3 days after initiating the incubation with suramin. Moreover, suramin also showed a neutralizing effect on MSTN which inhibits differentiation of MDSCs in a dose-dependent manner.

We found that suramin stimulates myogenic differentiation *in vitro*. It is consistent with our *in vivo* results showing that suramin is capable of enhancing muscle regeneration and improving muscle healing after muscle injury. Furthermore, as expected, we observed that MSTN significantly inhibits the myogenic differentiation of MDSCs; however, in the presence of suramin, the inhibitory effect of MSTN on myogenic differentiation was attenuated in a dose-dependent manner. These results suggest that suramin can neutralize MSTN activity. Therefore, we hypothesize that when myoblasts and MDSCs are treated with suramin, suramin stimulates myogenic differentiation by neutralizing the effect of endogenous MSTN. A similar neutralizing effect on MSTN has been seen when cells were treated with decorin, a TGF-β1 blocker .[46]

Based on these results, we further investigated whether suramin exerts a beneficial effect in the injured muscle through regulating MSTN expression. Not surprisingly, it was revealed that treatment with suramin significantly decreased MSTN expression in the injured muscle. Our previous study showed that MSTN can act with TGF-β1 to magnify fibrosis cascades in injured muscles.[46] Taken together, it may suggest that suramin administration effectively leads to enhanced muscle regeneration and reduced fibrosis after muscle injury via down-regulation of endogenous MSTN.

This is the first study which showed suramin can enhance myogenic cell differentiation and neutralize the effect of MSTN that down regulates MDSC

differentiation. Moreover, these *in vitro* results may reveal a possible mechanism by which suramin directly enhances muscle regeneration after muscle injury. Future studies should investigate further the mechanism by which suramin appears to stimulate myogenic differentiation and promote muscle healing via MSTN regulation. The current findings also have implications in athletics. Given inhibition of the human myostatin gene is likely to result in increased muscle mass and muscle strength,[15] intramuscular treatment with suramin could potentially provide an unfair advantage to athletes. With this in mind, novel testing tools may need to be developed to screen for "doping" through suramin administration as well as decorin. It may be needed to investigate further the mechanism in which suramin interacts with MSTN, in order to develop possible ways to identify potential molecules for anti-doping strategies.

In summary, we demonstrated that the direct injection of suramin at 2 weeks after contusion injury effectively reduces fibrotic scar formation and enhances muscle regeneration 4 weeks after injury. Physiological evaluation also showed that suramin can enhance muscle functional recovery after contusion injury. Our *in vitro* study demonstrated that culture of either C2C12 myoblasts or MDSCs with suramin led to a significant increase in the fusion index. Moreover, with the addition of both suramin and MSTN in cell culture, suramin was able to counteract MSTN's biological activity, thereby rescuing MSTN-inhibited myogenic differentiation of MDSCs.

The biggest advantage of using suramin is that this drug has already been approved by the FDA.[33, 37] Future studies should consider the use of this agent for off-label use in the treatment of skeletal muscle injuries. Our findings could contribute to the development of progressive therapies for muscle injury.

ACKNOWLEDGEMENTS

Figure 1.

Fusion index was measured to evaluate C2C12 myoblast differentiation stimulated by different concentration of suramin (0, 0.25, 2.5, and 25 µg / ml). **, $P < .01$.

Figure 2.

Immunocytochemical staining of MDSCs for fast myosin heavy chain at three days after incubation with different dose of suramin (A: 0 µg / ml suramin, B: 1 µg / ml suramin, C: 10 µg / ml suramin, and D: 100 µg / ml suramin). Myotubes are shown in red and nucleus are in blue (original magnification, × 200). E: Comparison of fusion index of MDSCs differentiation. **, $P < .01$.

Figure 3.

Immunocytochemical staining of MDSCs for fast myosin heavy chain at three days after incubation in 2% DMEM with different dose of suramin and MSTN (A: 0 µg / ml suramin and 0 ng / ml MSTN, B: 0 µg / ml suramin and 100 ng /ml MSTN, C: 1µg / ml suramin and 100 ng /ml MSTN, D: 10 µg / ml suramin and 100 ng /ml MSTN, and E: 100 µg / ml suramin and 100 ng /ml MSTN). Myotubes are shown in red and nucleus are in blue (original magnification, × 200). F: Comparison of fusion index of MDSCs differentiation. *, $P < .05$, **, $P<.01$.

Figure 4.

Histological evaluation of muscle regeneration at four weeks after contusion injury by hematoxylin and eosin staining of TA muscle treated with different concentrations of

suramin (A: 0 mg / 20 μl PBS, B: 2.5 mg / 20 μl PBS, C: 5 mg / 20 μl PBS, D: 10 mg / 20 μl PBS) injected at two weeks after injury. Regenerating myofibers were defined by centronucleated myofibers (original magnification, ×100). E: Quantification of the number of regenerating myofibers treated with various concentrations of suramin. *, P < .05, **, P < .01.

Figure 5.

Histological evaluation of the formation of scar tissue at four weeks after contusion injury by Masson trichrome staining of TA muscle treated with different concentrations of suramin (A: 0 mg / 20 μl PBS, B: 2.5 mg / 20 μl PBS, C: 5 mg / 20 μl PBS, D: 10 mg / 20 μl PBS) injected at two weeks after injury. Scar tissues are shown in blue and muscles are in red (original magnification, ×100). E: Quantification of the scar tissue area in TA muscle treated with various concentrations of suramin. **, P < .01.

Figure 6.

Immunohistochemical staining for MSTN at two days after suramin injection 2wk post-injury (A: 0 mg suramin / 20μl PBS, B: 2.5 mg suramin / 20 μl PBS). C: Quantification of the total MSTN positive area treated with suramin. *, P < .05.

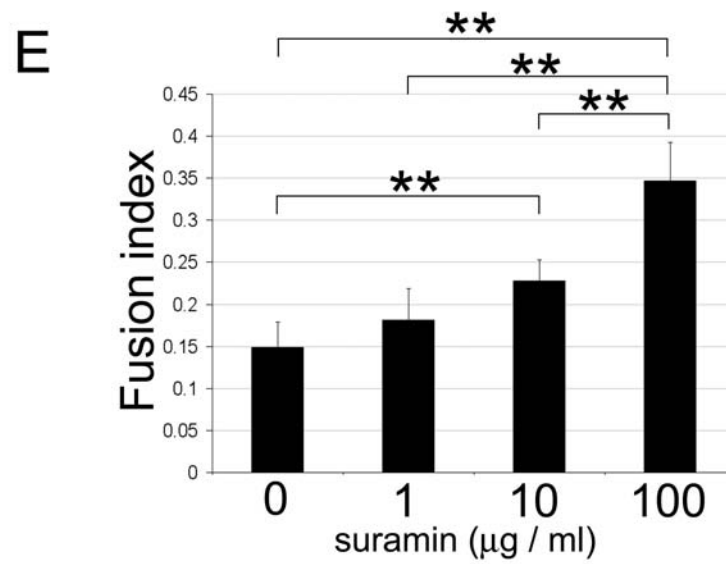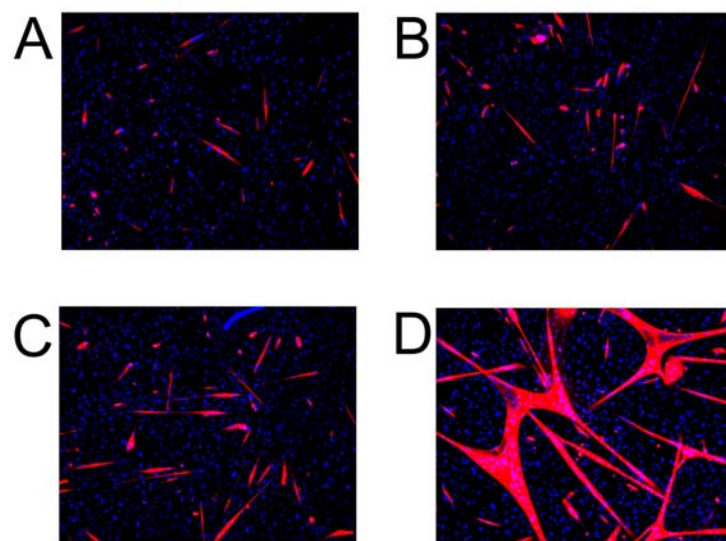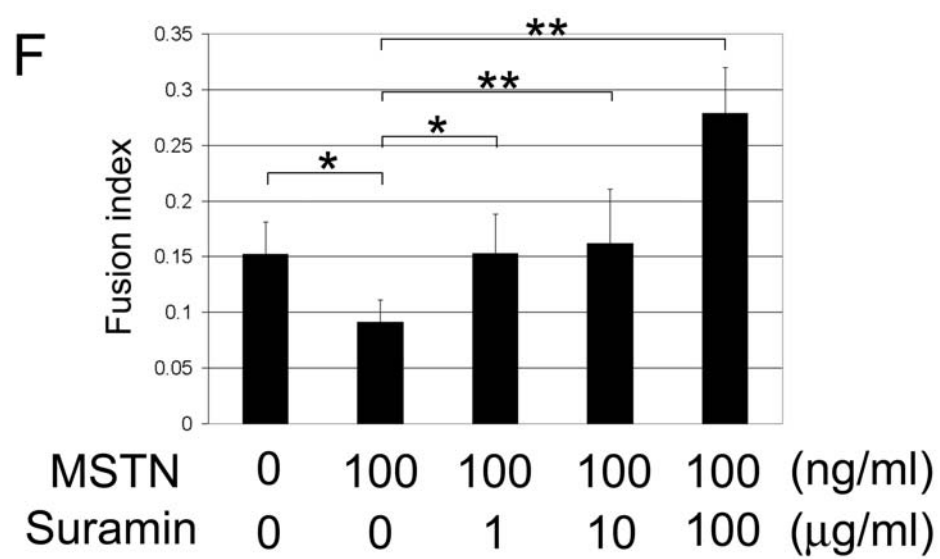Figure 1.
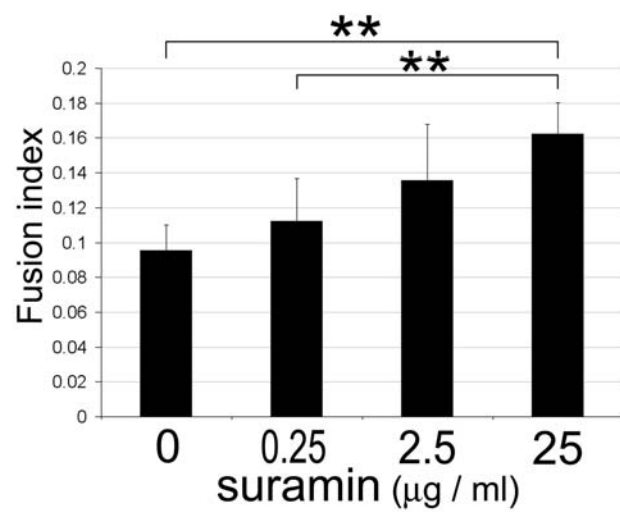
Figure 2.

Figure 3.
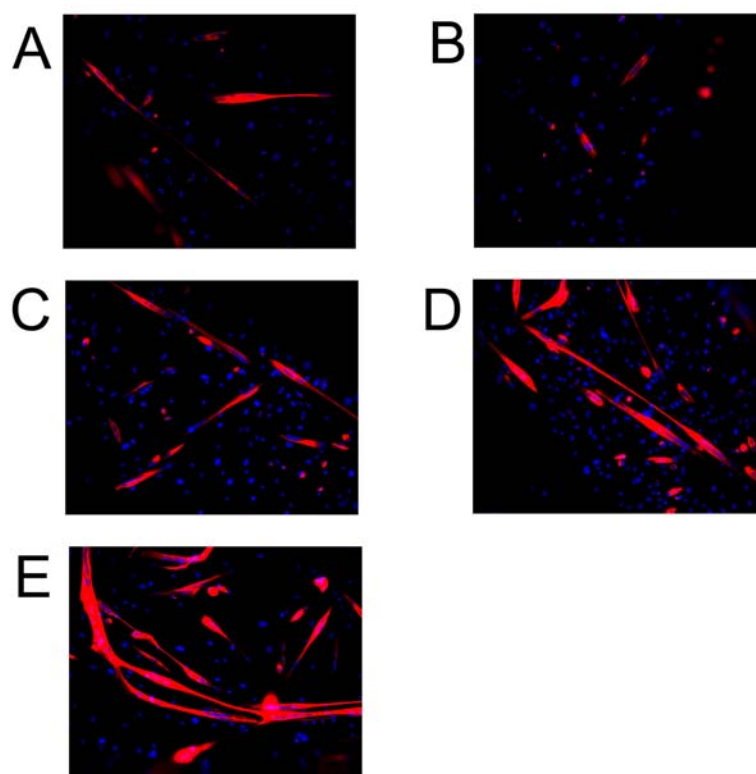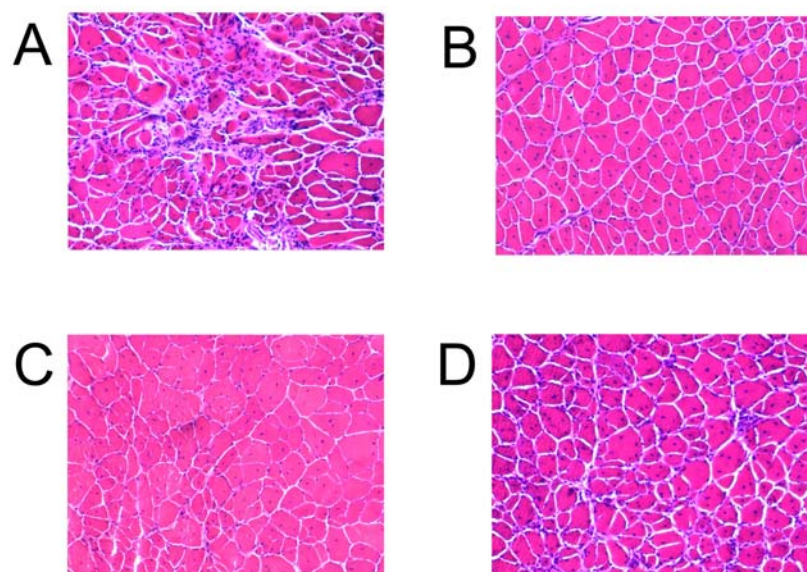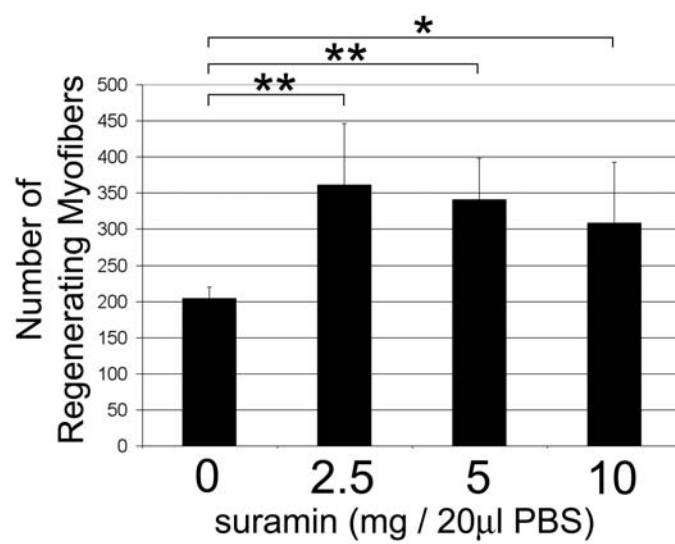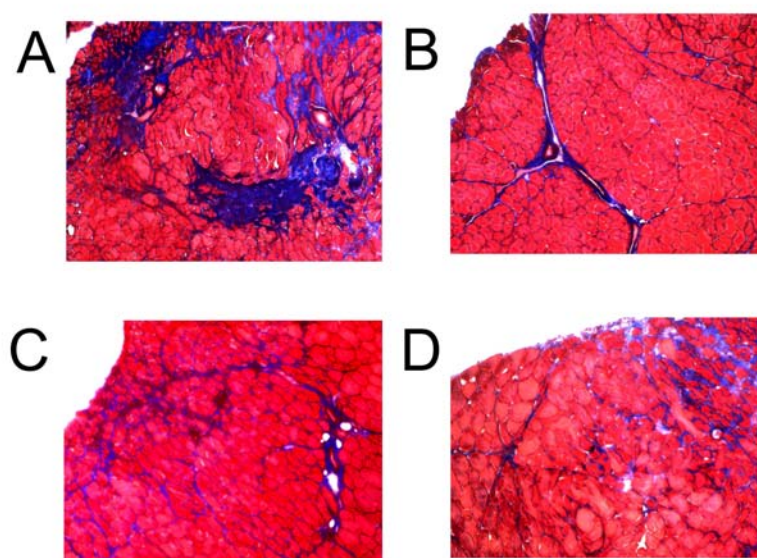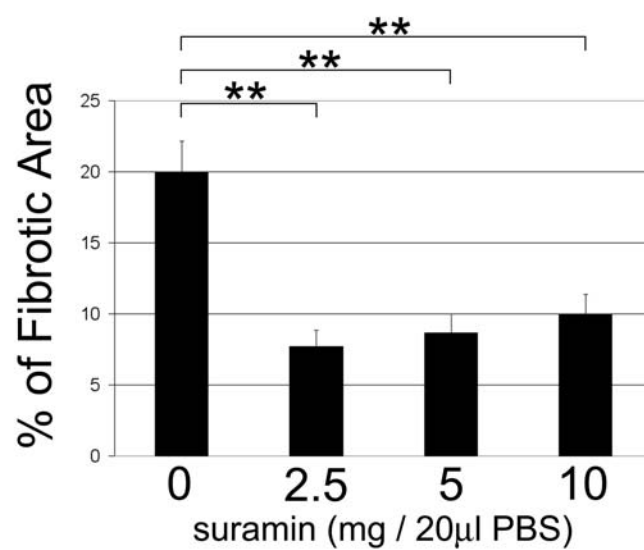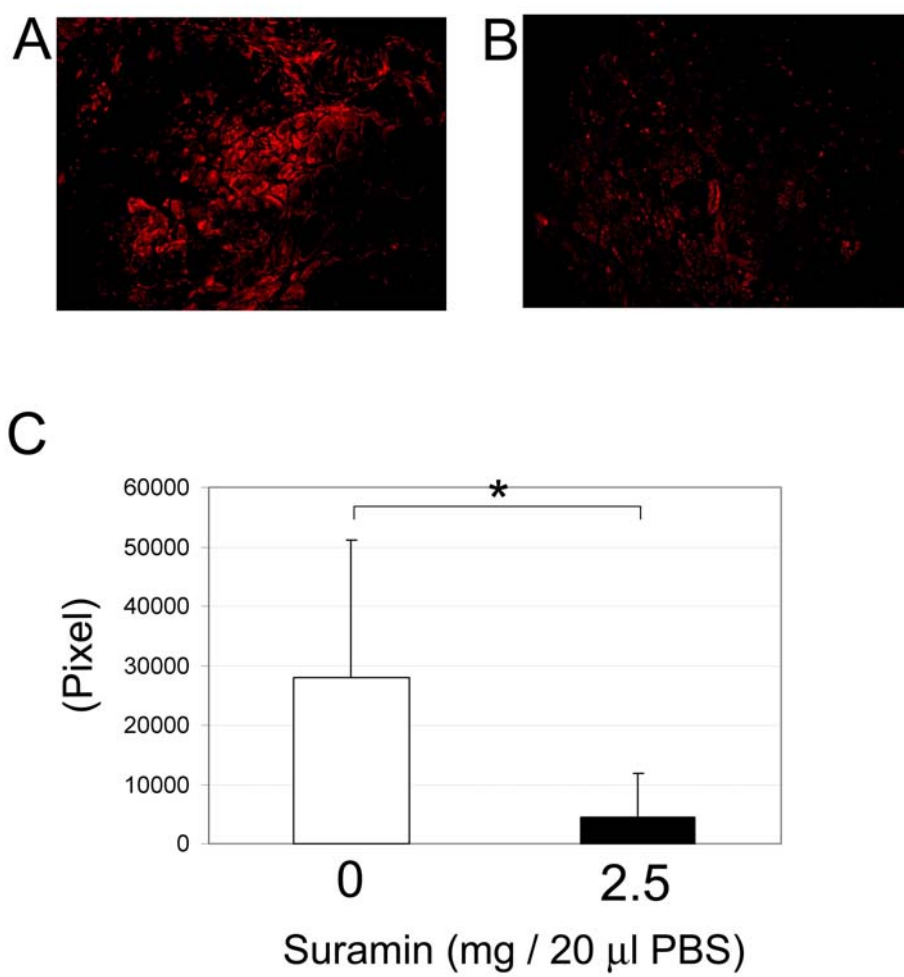
Figure 4.

Figure 5.

Figure 6.

Table 1

Results of specific peak twitch and tetanic force

Group	Specific Peak Twitch Force (N / cm^2)	Specific Peak Tetanic Force (N / cm^2)
Normal (non-injured)	7.728 ± 0.312 [a]	23.272 ± 1.334 [b]
0mg Suramin	4.431 ± 0.903	13.797 ± 2.136
2.5mg Suramin	6.305 ± 1.239 [c]	21.055 ± 2.662 [d]
5mg Suramin	5.014 ± 0.337	15.131 ± 0.830
10mg Suramin	4.993 ± 1.074	15.085 ± 2.792

Mean ± SD
a : $P < .01$ compared with 0, 5, and 10 mg suramin groups
b : $P < .01$ compared with 0, 5, and 10 mg suramin groups
c : $P < .05$ compared with 0 mg suramin group
d : $P < .01$ compared with 0, 5, and 10 mg suramin groups

Reference

1.   Alameddine HS, Dehaupas M, Fardeau M. Regeneration of skeletal muscle fibers from autologous satellite cells multiplied in vitro. An experimental model for testing cultured cell myogenicity. *Muscle Nerve.* Jul 1989;12(7):544-555. PMID: 2674704

2.   Bitton RJ FW, Venzon DJ, Dalakas MC, Bowden C, Headlee D, Reed E, Myers CE, Cooper MR Pharmacologic variables associated with the development of neurologic toxicity in patients treated with suramin. *J Clin Oncol* 1995;13:2223. PMID: 7666080

3.   Canale ST, Cantler ED, Jr., Sisk TD, et al. A chronicle of injuries of an American intercollegiate football team. *Am J Sports Med.* Nov-Dec 1981;9(6):384-389. PMID: 7316020

4.   Carlson BM, Faulkner JA. The regeneration of skeletal muscle fibers following injury: a review. *Med Sci Sports Exerc.* 1983;15(3):187-198. PMID: 6353126

5.   Chan YS, Li Y, Foster W, et al. The use of suramin, an antifibrotic agent, to improve muscle recovery after strain injury. *Am J Sports Med.* Jan 2005;33(1):43-51.

6.   Chan YS, Li Y, Foster W, et al. Antifibrotic effects of suramin in injured skeletal muscle after laceration. *J Appl Physiol.* Aug 2003;95(2):771-780.

7.   Chaudry VEM, Sinibaldi VJ, Sheikh H, Griffin JW, Cornblath DR A prospective study of suramin induced peripheral neuropathy. *Brain* 1996;119:2039.

8.   Crisco JJ, Jokl P, Heinen GT, et al. A muscle contusion injury model. Biomechanics, physiology, and histology. *Am J Sports Med.* Sep-Oct 1994;22(5):702-710. PMID: 15610998

9.   Dawson NA, Lush RM, Steinberg SM, et al. Suramin-induced neutropenia. *Eur J Cancer.* Aug 1996;32A(9):1534-1539. PMID: 8911114

10.   Foster W, Li Y, Usas A, et al. Gamma interferon as an antifibrosis agent in skeletal muscle. *J Orthop Res.* Sep 2003;21(5):798-804. PMID: 12919866

11.   Fukushima K, Badlani N, Usas A, et al. The use of an antifibrosis agent to improve muscle recovery after laceration. *Am J Sports Med.* Jul-Aug 2001;29(4):394-402. PMID: 11476375

12.   Garrett WE, Jr. Muscle strain injuries: clinical and basic aspects. *Med Sci Sports Exerc.* Aug 1990;22(4):436-443. PMID: 2205779

13.   Garrett WE, Jr., Seaber AV, Boswick J, et al. Recovery of skeletal muscle after laceration and repair. *J Hand Surg [Am].* Sep 1984;9(5):683-692. PMID: 6491212

14.   Grounds MD. Towards understanding skeletal muscle regeneration. *Pathol Res Pract.* Jan 1991;187(1):1-22. PMID: 2027816

15.   Haisma HJ, de Hon O. Gene doping. *Int J Sports Med.* Apr 2006;27(4):257-266. PMID: 16572366

16.   Hawking F. Suramin: with special reference to onchocerciasis. *Adv Pharmacol Chemother.* 1978;15:289-322. PMID: 358805

17. Hemady RK, Sinibaldi VJ, Eisenberger MA. Ocular symptoms and signs associated with suramin sodium treatment for metastatic cancer of the prostate. *Am J Ophthalmol.* Mar 1996;121(3):291-296. PMID: 8597272

18. Honda H, Kimura H, Rostami A. Demonstration and phenotypic characterization of resident macrophages in rat skeletal muscle. *Immunology.* Jun 1990;70(2):272-277. PMID: 2197218

19. Huard J, Li Y, Fu FH. Muscle injuries and repair: current trends in research. *J Bone Joint Surg Am.* May 2002;84-A(5):822-832. PMID: 12004029

20. Hughes Ct, Hasselman CT, Best TM, et al. Incomplete, intrasubstance strain injuries of the rectus femoris muscle. *Am J Sports Med.* Jul-Aug 1995;23(4):500-506. PMID: 7573664

21. Hurme T, Kalimo H. Activation of myogenic precursor cells after muscle injury. *Med Sci Sports Exerc.* Feb 1992;24(2):197-205. PMID: 1549008

22. Hurme T, Kalimo H, Lehto M, et al. Healing of skeletal muscle injury: an ultrastructural and immunohistochemical study. *Med Sci Sports Exerc.* Jul 1991;23(7):801-810. PMID: 1921672

23. Jackson DW, Feagin JA. Quadriceps contusions in young athletes. Relation of severity of injury to treatment and prognosis. *J Bone Joint Surg Am.* Jan 1973;55(1):95-105. PMID: 4691666

24. Jarvinen MJ, Lehto MU. The effects of early mobilisation and immobilisation on the healing process following muscle injuries. *Sports Med.* Feb 1993;15(2):78-89. PMID: 8446826

25. Kasemkijwattana C, Menetrey J, Somogyl G, et al. Development of approaches to improve the healing following muscle contusion. *Cell Transplant.* Nov-Dec 1998;7(6):585-598. PMID: 9853587

26. Kobayashi K, Weiss RE, Vogelzang NJ, et al. Mineralocorticoid insufficiency due to suramin therapy. *Cancer.* Dec 1 1996;78(11):2411-2420. PMID: 8941013

27. Lefaucheur JP, Sebille A. Muscle regeneration following injury can be modified in vivo by immune neutralization of basic fibroblast growth factor, transforming growth factor beta 1 or insulin-like growth factor I. *J Neuroimmunol.* Mar 1995;57(1-2):85-91. PMID: 7706442

28. Levine AM, Gill PS, Cohen J, et al. Suramin antiviral therapy in the acquired immunodeficiency syndrome. Clinical, immunological, and virologic results. *Ann Intern Med.* Jul 1986;105(1):32-37. PMID: 2424353

29. Li Y, Foster W, Deasy BM, et al. Transforming growth factor-beta1 induces the differentiation of myogenic cells into fibrotic cells in injured skeletal muscle: a key event in muscle fibrogenesis. *Am J Pathol.* Mar 2004;164(3):1007-1019. PMID: 14982854

30. Li Y, Huard J. Differentiation of muscle-derived cells into myofibroblasts in injured skeletal muscle. *Am J Pathol.* Sep 2002;161(3):895-907. PMID: 12213718

31. Menetrey J, Kasemkijwattana C, Day CS, et al. Growth factors improve muscle healing in vivo. *J Bone Joint Surg Br.* Jan 2000;82(1):131-137. PMID: 10697329

32. Menetrey J, Kasemkijwattana C, Fu FH, et al. Suturing versus immobilization of a muscle laceration. A morphological and functional study in a mouse model. *Am J Sports Med.* Mar-Apr 1999;27(2):222-229. PMID: 10102105

33. Mietz H, Chevez-Barrios P, Feldman RM, et al. Suramin inhibits wound healing following filtering procedures for glaucoma. *Br J Ophthalmol.* Jul 1998;82(7):816-820. PMID: 9924379

34. Qu Z, Balkir L, van Deutekom JC, et al. Development of approaches to improve cell survival in myoblast transfer therapy. *J Cell Biol.* Sep 7 1998;142(5):1257-1267. PMID: 9732286

35. Rando TA, Blau HM. Primary mouse myoblast purification, characterization, and transplantation for cell-mediated gene therapy. *J Cell Biol.* Jun 1994;125(6):1275-1287. PMID: 8207057

36. Ryan JB, Wheeler JH, Hopkinson WJ, et al. Quadriceps contusions. West Point update. *Am J Sports Med.* May-Jun 1991;19(3):299-304. PMID: 1867338

37. Schrell UM, Gauer S, Kiesewetter F, et al. Inhibition of proliferation of human cerebral meningioma cells by suramin: effects on cell growth, cell cycle phases, extracellular growth factors, and PDGF-BB autocrine growth loop. *J Neurosurg.* Apr 1995;82(4):600-607. PMID: 7897522

38. Schultz E. Satellite cell behavior during skeletal muscle growth and regeneration. *Med Sci Sports Exerc.* Oct 1989;21(5 Suppl):S181-186. PMID: 2691829

39. Schultz E, Jaryszak DL, Valliere CR. Response of satellite cells to focal skeletal muscle injury. *Muscle Nerve.* Mar-Apr 1985;8(3):217-222. PMID: 4058466

40. Smith A, Harbour D, Liebmann J. Acute renal failure in a patient receiving treatment with suramin. *Am J Clin Oncol.* Aug 1997;20(4):433-434. PMID: 9256906

41. Stein CA. Suramin: a novel antineoplastic agent with multiple potential mechanisms of action. *Cancer Res.* May 15 1993;53(10 Suppl):2239-2248. PMID: 8485709

42. Sullivan KM, Lorenz HP, Meuli M, et al. A model of scarless human fetal wound repair is deficient in transforming growth factor beta. *J Pediatr Surg.* Feb 1995;30(2):198-202; discussion 202-193. PMID: 7738738

43. Taylor DC, Dalton JD, Jr., Seaber AV, et al. Experimental muscle strain injury. Early functional and structural deficits and the increased risk for reinjury. *Am J Sports Med.* Mar-Apr 1993;21(2):190-194. PMID: 8465911

44. Thomas DW, O'Neill ID, Harding KG, et al. Cutaneous wound healing: a current perspective. *J Oral Maxillofac Surg.* Apr 1995;53(4):442-447. PMID: 769950

45. Tisdale JF, Figg WD, Reed E, et al. Severe thrombocytopenia in patients treated with suramin: evidence for an immune mechanism in one. *Am J Hematol.* Feb 1996;51(2):152-157. PMID: 8579057

46. Zhu J, Li Y, Shen W, et al. Relationships between transforming growth factor-beta1, myostatin, and decorin: implications for skeletal muscle fibrosis. *J Biol Chem.* Aug 31 2007;282(35):25852-25863. 17597062

47. Zumkeller W, Schofield PN. Growth factors, cytokines and soluble forms of receptor molecules in cancer patients. *Anticancer Res.* Mar-Apr 1995;15(2):343-348. PMID: 7763004

Decorin Gene Transfer Promotes Muscle Cell Differentiation and Muscle Regeneration

Yong Li[1,2,3], Juan Li[2], Jinghong Zhu[1], Bin Sun[1], Maria Branca[1], Ying Tang[1], William Foster[1], Xiao Xiao[2] and Johnny Huard[1,2,4]

[1]Stem Cell Research Center, Children's Hospital of Pittsburgh, Pittsburgh, Pennsylvania, USA; [2]Department of Orthopaedic Surgery, University of Pittsburgh, Pittsburgh, Pennsylvania, USA; [3]Department of Pathology, University of Pittsburgh, Pittsburgh, Pennsylvania, USA; [4]Department of Molecular Genetics and Biochemistry, University of Pittsburgh, Pittsburgh, Pennsylvania, USA

We have shown that decorin, a small leucine-rich proteo-glycan, can inhibit transforming growth factor (TGF)-β1 to prevent fibrous scar formation and improve muscle healing after injury. In the decorin-treated muscle, an enhancement of muscle regeneration is observed through histological examination. In this article, we report our determination of whether decorin has a direct effect on myogenic cells' differentiation. Our results indicate that myoblasts genetically engineered to express deco-rin (CD cells) differentiated into myotubes at a significantly higher rate than did control myoblasts (C2C12). This enhanced differentiation led to the up-regulation of myogenic genes (*Myf5*, *Myf6*, *MyoD*, and myogenin) in CD cells in vitro. We speculate that the higher rate of differentiation exhibited by the CD cells is due to the up-regulation of follistatin, peroxisome-proliferator-activated receptor-gamma co-activator-1α (PGC-1α), p21, and the myogenic genes, and the down-regulation of TGF-β1 and myostatin. Decorin gene transfer *in vivo* promoted skeletal muscle regeneration and accelerated muscle healing after injury. These results suggest that decorin not only prevents fibrosis but also improves muscle regeneration and repair.

INTRODUCTION

Decorin, a small leucine-rich proteoglycan, is a component of the extracellular matrix of all collagen-containing tissues.[1] Decorin is pivotal in regulating the proper assembly of collagenous matrices and in controlling cell proliferation under various conditions.[2] On the basis of its ability to bind fibrillar collagen and delay *in vitro* fibrillogenesis, decorin is regarded as a key modulator of matrix assembly.[3,4] This proteoglycan can modulate the bioactivity of growth factors and act as a direct signaling molecule to different cells.[5] Decorin, which is expressed at high levels in skeletal muscle during early development,[6] also interferes with muscle cell differentiation and migration and regulates connective tissue formation in skeletal muscle.[7–9]

Because terminal differentiation is critical for initial skeletal muscle development and regeneration after injury and disease,[10] we examined decorin's role in remodeling healing skeletal muscle. We have shown that the direct injection of bovine decorin decreased muscle fibrosis and provided nearly complete functional recovery.[11] Decorin blocks fibrosis (mostly by inhibiting transforming growth factor (TGF)-β activity), which improves muscle healing. However, the role of decorin in muscle cell differentiation and regeneration is still unknown. Although we hypothesize that decorin's effect on muscle fibrosis may indirectly impact regeneration, we were unable to exclude the possibility that decorin promotes regeneration independent of its effects on fibrosis formation.

Many studies have investigated the mechanism behind the antifibrotic effect of decorin.[3,12–14] Others have shown that hepatocyte growth factor increases decorin production by fibroblasts through the extracellular signal–regulated kinase 1/2, and p38 mitogen-activated protein kinase–mediated pathways.[14] Decorin stimulates the growth of smooth muscle cells under specific conditions and influences the growth of epidermal cells by interacting with epidermal growth factor and its receptors.[15,16] Recent research has shown that decorin can bind both insulin-like growth factor-I and its receptor; this interaction leads to the phosphorylation of protein kinase B (Akt) and p21 expression in endothelial cells.[17]

Decorin also influences muscle cell behavior by interacting with p21, an important cyclin-dependent kinase inhibitor.[18,19] Follistatin and myostatin are involved in the control of muscle mass during development. These two proteins have opposite effects on muscle growth, as documented by genetic models.[21,22] Recent studies have shown that myostatin action is inhibited by decorin,[23] resulting in enhanced healing and reduced fibrosis within myostatin-null mice compared with wild-type mice.[24] A recent study indicates that peroxisome-proliferator-activated receptor-gamma co-activator-1α (PGC-1α), is also involved in the muscle healing process and influences muscle fiber–type determination.[25,26] Decorin may also interact with PGC-1α expression in skeletal muscle after injury.

In this study, we investigated the *in vitro* effect of decorin on the differentiation of myoblasts (C2C12) and characterized the *in vitro* and *in vivo* behavior of myoblasts transfected with the

Correspondence: *Johnny Huard, Stem Cell Research Center (SCRC), 4100 Rangos Research Center, 3460 Fifth Avenue, Pittsburgh, Pennsylvania 15213-2583, USA. E-mail: jhuard@pitt.edu*

decorin gene (CD cells). We also studied the influence that decorin over-expression had on myostatin, follistatin, PGC-1α, and p21 expression. Using an adeno-associated virus (AAV) vector, we transduced the decorin gene into injured skeletal muscle to further investigate its function on muscle healing. Our overall goal in this study was to determine whether decorin could improve skeletal muscle healing by enhancing muscle regeneration independently of its antifibrotic action.

RESULTS

Genetic engineering of myogenic cells to over-express decorin

We used lipofectin to transfect a pAAV-CMV-decorin plasmid (**Figure 1a**) into both 293 cells (packaging cell line) and C2C12 cells (myoblast cell line). The results of western blot analysis (**Figure 1b**) showed decorin in both the supernatant (culture media) and the lysate of the 293 cells 48 hours after transfection. The transfected C2C12 cells (CD clone cells) expressed decorin (**Figure 1c**: lane 2, 24 hours; lane 4, 48 hours; lane 5, decorin-positive control), whereas non-transfected C2C12 cells did not (**Figure 1c**: lane 1, 24 hours; lane 3, 48 hours). We also detected decorin in both myoblasts (C2C12) and muscle-derived stem cells after mDecorin-AAV (mDec-AAV) gene transfer *in vitro* (**Figure 1d** and **e**).

Decorin stimulates myoblast differentiation *in vitro*

To investigate myoblast differentiation, we compared decorin-co-cultured C2C12 cells with non-treated C2C12 cells *in vitro*. C2C12 cells cultured with decorin (10 μg/mL) and grown in differentiation/fusion medium exhibited significantly enhanced differentiation and fusion *in vitro*. After 3 and 4 days of stimulating C2C12 cells with decorin, we observed a significant increase in the number of myotubes when compared with un-stimulated C2C12 (control) cells ($P < 0.01$ at 3 days and $P < 0.05$ at 4 days, respectively). However, the numbers of myotubes 5 days after treatment were not significantly different (**Figure 2a**). We then evaluated whether CD cells exhibited a greater propensity to undergo myogenic differentiation than did non-transfected C2C12 cells. As shown in **Figure 2b** (myotubes stained in mouse anti-myosin heavy chain are red) and **Figure 2c**, CD cells generated significantly more myotubes overall and created significantly larger myotubes than did non-transfected C2C12 cells.

Decorin increases myoblast differentiation and induces myogenic gene expression *in vitro*

We investigated whether the CD cells expressed higher levels of myogenic genes than did non-transfected C2C12 (control) cells. Our results, shown in **Figure 3a**, demonstrate that decorin gene transfer led to higher expression of the myogenic genes *Myf5*, *Myf6*, *MyoD*, and *myogenin*. Desmin expression levels in CD and C2C12 cells remained similar.

Decorin up-regulates p21, follistatin, and PGC-1α, but down-regulates TGF-β1 and myostatin in C2C12

We also performed experiments designed to investigate the mechanism by which decorin influences the differentiation of muscle cells. We found that CD cells exhibited increased p21
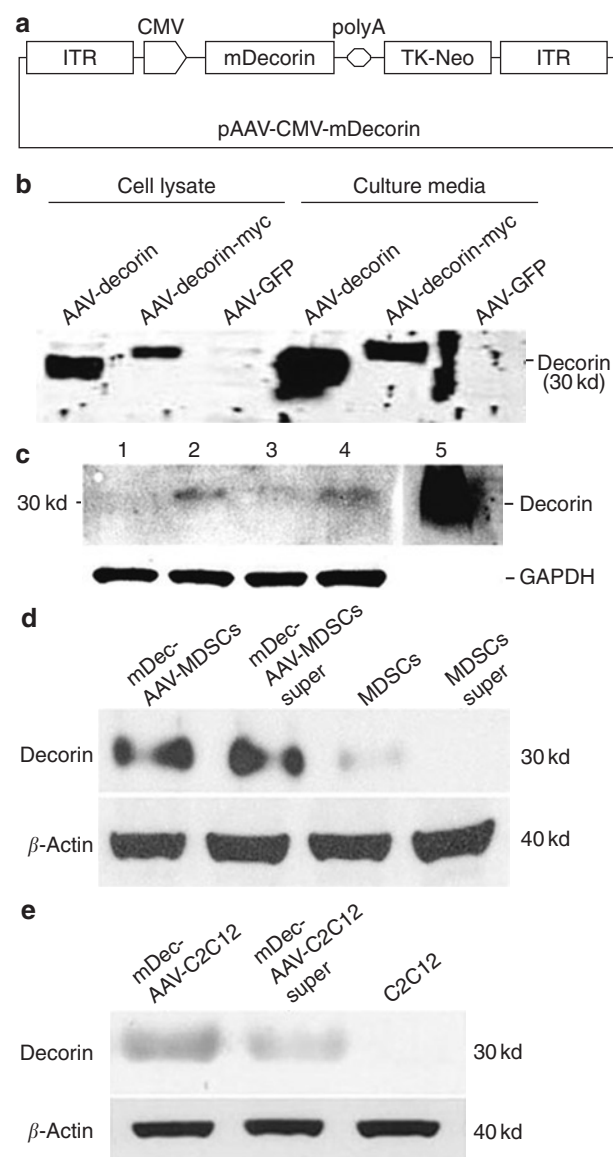

Figure 1 Decorin plasmid construction and initial transfection *in vitro.* (**a**) The decorin plasmid used for the study contained the full sequence of a mouse decorin gene inserted at the *Not*I site, which placed it under the control of a cytomegalovirus (CMV) promoter. (**b**) We transfected the plasmid into 293 cells. We observed decorin expression in both the 293 cells and their supernatant, but not in the control adeno-associated virus (AAV)–transfected (green fluorescent protein, GFP) cells. (**c**) Western blot analysis also revealed decorin expression in CD clone cells within different time period cultures (lane 2, 24 hours; lane 4, 48 hours), but not in C2C12 (lane 1, 24 hours; lane 3, 48 hours). We used 5 μg of decorin as a positive control (lane 5). GAPDH, glyceraldehyde-3-phosphate dehydrogenase is used as a control. (**d**) Decorin expression in muscle-derived stem cells (MDSCs) in pellet form was low, but this was not the case in the supernatant. Both MDSCs and their cultured supernatant strongly expressed decorin after mDec-AAV gene transfer. β-actin is used as a control. (**e**) We did not detect decorin in normal C2C12 cells, but C2C12 cells and their cultured supernatant both expressed decorin after mDec-AAV gene transfer.

expression and decreased myostatin expression (**Figure 3b**). The C2C12 cells can be induced to express TGF-β1 in an autocrine manner, as we have previously determined;[27] however, the CD cells do not show any detectable expression of TGF-β1 after

a The effect of decorin on myoblast differentiation

b

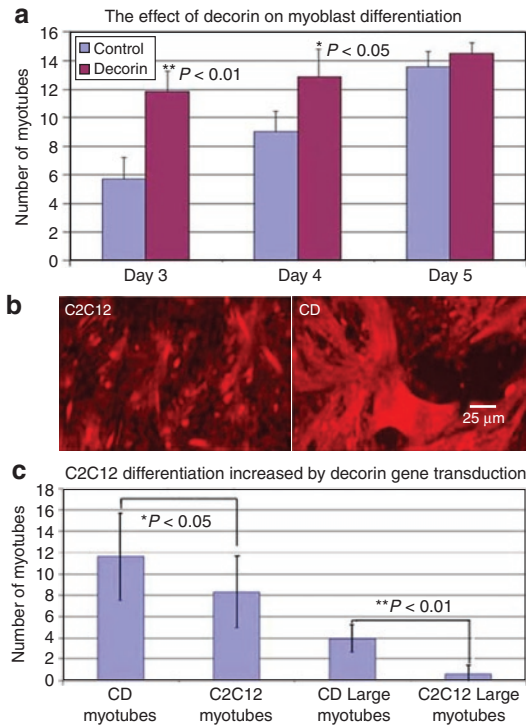**c** C2C12 differentiation increased by decorin gene transduction

Figure 2 Decorin stimulates C2C12 differentiation *in vitro*. (a) Decorin treatment accelerated the differentiation and fusion of myoblasts (C2C12 cells) compared with non-treated myoblasts (C2C12 cells). **(a)** The cultures of decorin-treated C2C12 cells contained more myotubes at the 3- and 4-day time points than control cells. **(b, c)** Similarly, decorin-transfected C2C12 clone cells (CD cells) produced more myotubes than did C2C12 cells, including larger myotubes (containing more than three nuclei) *in vitro*. Red staining shows myosin heavy chain fluorescence after immunostaining **(b)**.

TGF-β1 stimulation. More importantly, we detected that both follistatin and PGC-1α (**Figure 3b**) had been up-regulated when compared with C2C12 cells. We also discovered that follistatin and PGC-1α messenger RNA were altered in C2C12 cells after decorin stimulation, as determined by real-time polymerase chain reaction. Specifically, we found that PGC-1α and follistatin increased in a dose-dependent manner after 18 hours of stimulation with decorin, and that myostatin was decreased in a dose-dependent manner after 24 hours of stimulation with decorin (**Figure 3c**). In CD cells, we also observed increased amounts of all three genes (*p21*, *follistatin*, and *PGC-1α*), but a decrease in myostatin was observed (**Figure 3c**).

The up-regulation of *follistatin*, *PGC-1α*, *p21*, and myogenic genes, including *MyoD* (**Figure 3a**), in CD cells could at least partially explain how decorin promotes muscle cell differentiation. Alternatively, the down-regulation of myostatin, a well-known negative regulator of muscle growth during muscle regeneration, could also benefit muscle cell differentiation.

The implantation of CD cells in skeletal muscle results in improved muscle regeneration

The implantation of CD cells within skeletal muscle resulted in significantly better muscle regeneration than that observed for control C2C12 cells, as determined 4 weeks after injection of the cells into *MDX*/SCID mice. Although the number of LacZ-positive
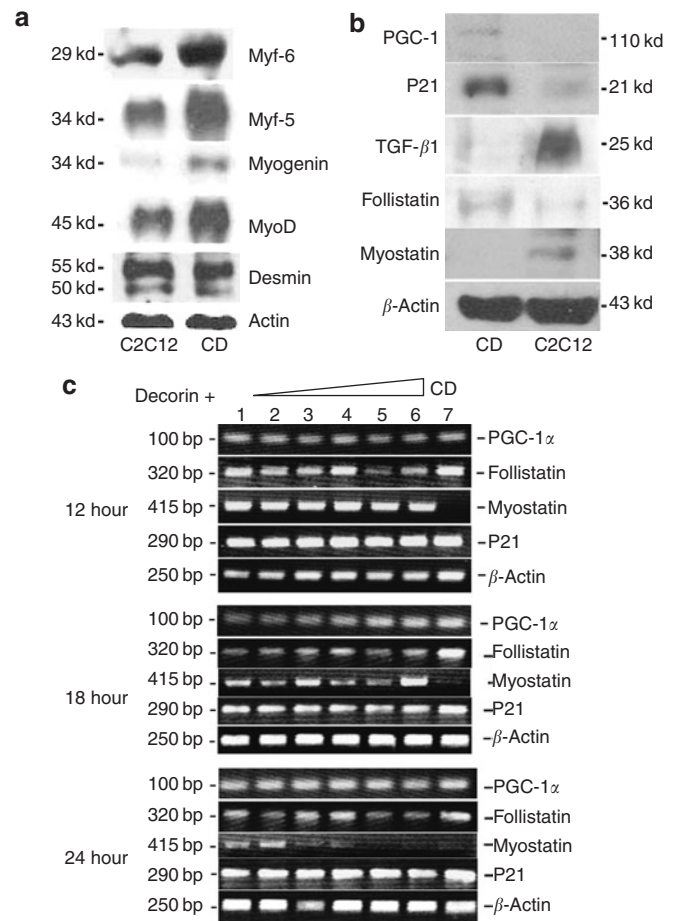
a

b

c

Figure 3 Decorin gene transfer up-regulates myogenic proteins and p21 and down-regulates myostatin during muscle cell differentiation. (a) Genetic engineering of myoblasts to express decorin influenced the expression of myogenic proteins (including Myf5/6, Myogenin, and MyoD), as shown by western blot results. However, C2C12 cells and CD clone cells expressed comparable levels of desmin. **(b)** We detected the presence of p21 expressed in CD clone cells. We also detected peroxisome-proliferator-activated receptor-gamma co-activator-1α (PGC-1α) and follistatin expressed in CD, but not C2C12, cells. In addition, CD cells exhibited lower levels of myostatin, a negative regulator of muscle mass. The induction of tumor growth factor (TGF)-β1 auto-expression was also inhibited by decorin over-expression in CD cells. **(c)** Similar results were obtained by real-time polymerase chain reaction. Lanes 1–6 show results for C2C12 cells exposed to different concentrations of decorin (0, 0.001, 0.01, 0.1, 1.0, and 5.0 ng/ml, respectively). Lane 7 displays the test results for CD cells, which served as the positive control. We did not detect a visible change in the expression of PGC-1α, follistatin, myostatin, or p21 after 12 hours of stimulation with different concentrations of decorin. PGC-1α and follistatin were up-regulated in C2C12 cells in a dose-dependent manner after 18 hours of stimulation with decorin. Myostatin was down-regulated in C2C12 cells in a dose-dependent manner after 24 hours of decorin stimulation. The concentration of p21 did not visibly change after cell stimulation with any experimental concentration of decorin over all time points. With decorin gene transfer, we found that CD cells consistently expressed follistatin, p21, and PGC-1α but were negative for myostatin. Note that β-actin was selected as a positive gene control.

muscle fibers (*i.e.*, regenerating muscle fibers) did not differ between the groups (**Figure 4a, c,** and **d**), the diameters of the regenerating muscle fibers (*e.g.*, dystrophin-positive myofibers) in the muscles injected with CD cells were significantly larger than those of the regenerating muscle fibers in the control muscles
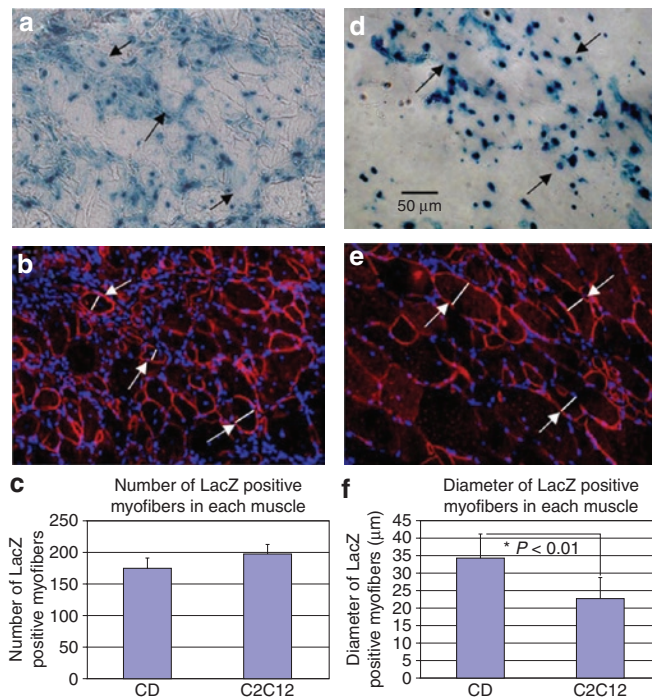
Figure 4 Decorin gene transfer stimulates muscle regeneration *in vivo*. C2C12 cells regenerated muscle fibers after transplantation into skeletal muscle of *MDX*/SCID mice, as shown on both (**a**) LacZ- and (**b**) dystrophin-expressing myofibers. However, transplantation of CD clone cells, rather than C2C12 cells, resulted in larger muscle fibers in *MDX*/SCID mice, as shown in some of the (**d**) LacZ- and (**e**) dystrophin-positive myofibers. (**c**) Although there was no significant difference between the number of LacZ-labeled muscle fibers that formed in muscles transplanted with C2C12 or CD cells, (**f**) the transplantation of CD cells resulted in the regeneration of larger-diameter myofibers (*P* < 0.01).

(**Figure 4b**, **e**, and **f**; dystrophin is red). The larger diameters of the dystrophin-positive muscle fibers generated by CD cells could indicate that implantation of CD cells accelerated muscle regeneration; however, we were unable to exclude the possibility that the CD cells may have a greater propensity to fuse in host myofibers than C2C12 control cells.

mDec-AAV gene transfer promotes muscle regeneration and reduces fibrosis

Better muscle regeneration was observed within mDec-AAV-treated muscle (**Figure 5a** and **b**) than within non-mDec-AAV-treated muscle at 2 weeks after injury (**Figure 5c** and **d**). Histological analysis of total collagen deposition 4 weeks after injury revealed that mDec-AAV-injected muscles contained less fibrous scar tissue in the injured area than did non-treated control muscles (**Figure 5f**, **h**, and **j**; collagen deposition areas are blue). We also observed that decorin stimulated skeletal muscle regeneration 4 weeks after laceration injury. We found that mDec-AAV-injected muscles contained more centronucleated (regenerating) myofibers and less scar tissue 4 weeks after injury than did control muscles (**Figure 5e**, **g**, and **i**).

DISCUSSION

Results from these experiments show that decorin is able to activate the differentiation of skeletal muscle cells (C2C12) *in vitro*
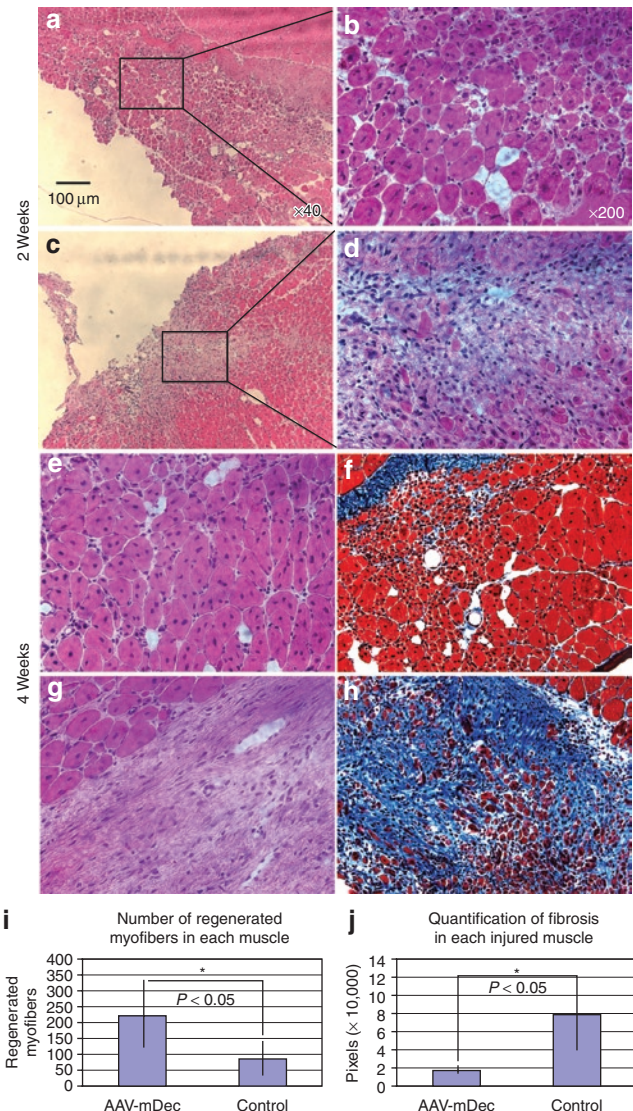

Figure 5 mDec-AAV vector gene therapy in injured muscle prevents fibrosis and promotes muscle regeneration. Decorin-treated muscle exhibits a greater number of regenerating myofibers than the control muscle at all time points (**a–d** 2 weeks; **e–h** 4 weeks). (**i**) The mDec-AAV-injected muscle contained significantly higher numbers of centronucleated (regenerated) myofibers than did control (sham-injected) muscle at 4 weeks after therapy. We also found that decorin gene therapy minimized fibrosis in injured skeletal muscle. We used Masson's trichrome staining to reveal collagen in injured skeletal muscle, the results of which show that (**f**) mDec-AAV-injected muscle contained significantly less fibrosis in the injured area than did the (**h**) control muscle at (**j**) 4 weeks after injury.

and enhances muscle regeneration in two mouse models *in vivo*. The mechanism behind decorin's accelerated muscle healing is not yet known; however, our results demonstrate that decorin up-regulates the expression of PGC-1α, follistatin, p21, and a variety of myogenic proteins (including MyoD) but down-regulates myostatin expression. These results, in addition to decorin's ability to neutralize the effects of TGF-β1, likely explain the beneficial action that decorin has on muscle cell differentiation and muscle regeneration.

Our previous studies have demonstrated that myogenic cells (including muscle-derived stem cells) in injured muscle can
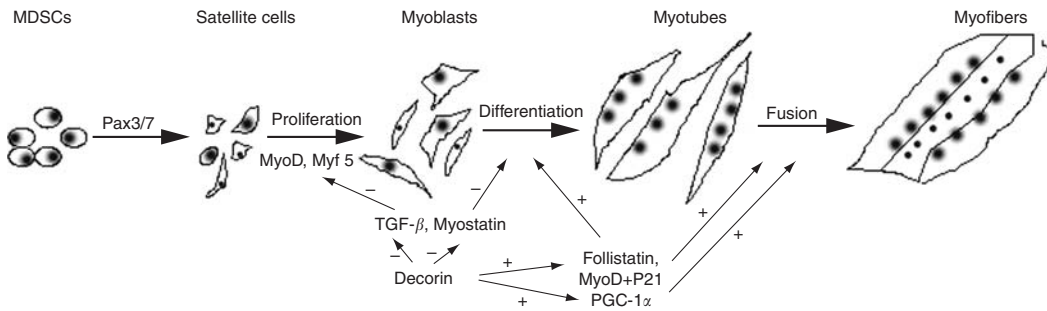
Figure 6 Schematic of the potential effect of decorin on muscle healing. Decorin may improve muscle healing through various pathways: inhibition of tumor growth factor (TGF)-β1, up-regulation of follistatin, peroxisome-proliferator-activated receptor-gamma co-activator-1α (PGC-1α), p21, and myogenic genes (such as *MyoD*), and down-regulation of myostatin expression. MDSCs, muscle-derived stem cells.

differentiate into fibrotic cells and that TGF-β1 is a major stimulator of this differentiation.[27,28] Using different animal models of muscle injury, we have investigated biological approaches to prevent fibrosis and thereby improve muscle healing.[11,27,29–31] We have used various molecules, such as decorin, that impede fibrosis by blocking TGF-β1 to facilitate the near-complete recovery of injured skeletal muscle.[11] The ability of decorin to inhibit TGF-β1 activity is the likely mechanism by which this molecule blocks fibrosis formation. However, our results indicate that the improved muscle healing observed after decorin treatment is due to both its inhibiting effect on fibrosis and its stimulating effect on muscle regeneration. **Figure 6** summarizes the potential effect of decorin on muscle healing.

The repair of injured skeletal muscle occurs through the activation of muscle precursor cells located between the basal lamina and the sarcolemma, including satellite cells and stem cells.[32] The activation and growth of these cells are regulated by various growth factors released by infiltrating lymphocytes, injured myofibers, and the extracellular matrix.[10,32] Some growth factors, such as insulin-like growth factor-1 and hepatocyte growth factor, can stimulate precursor cell proliferation and differentiation by increasing the transcriptional activity of the muscle basic helix–loop–helix.[33–36] Healing and organizational processes are dependent upon the extra- and intracellular signaling that induces the expression of myogenic genes, including *MyoD*, *Myf5*, and *myosin*.[37,38] When properly stimulated, precursor cells fuse with one another or with local myofibers to repair the damaged muscle.[39]

Muscle regeneration, the key event in muscle healing, is often incomplete, particularly in severely injured muscle.[10,11,27,28,32,40] The overgrowth of the extracellular matrix leads to significant local fibrosis (*i.e.*, fibrous scar formation) in the injured area, which can impede the formation of normal muscle fibers. The presence of fibrous scar tissue in injured muscle results in incomplete functional recovery and a propensity for re-injury.[41] Muscle regeneration and fibrosis in injured muscle often occur simultaneously and thus compete with one another during the muscle healing process.[32,36,40] A persistent imbalance between collagen biosynthesis and degradation contributes to hypertrophic scar formation and fibrosis in many tissues.[42,43] Several studies have revealed high levels of collagen in injured regions of skeletal muscle, and shown that inhibition of collagen deposition reduced the formation of scar tissue in injured skeletal muscle.[27,28,30,31]

Interactions between decorin and TGF-β1 have been observed in many tissues, and researchers have used various animal models to study the antifibrotic effect of decorin.[3,11,13,44] Researchers have also shown that hepatocyte growth factor can increase the level of decorin expression in fibroblasts, perhaps by activating the extracellular signal–regulated kinase 1/2 and p38 mitogen-activated protein kinase–mediated pathways.[14] Such findings could explain the antifibrotic effect of hepatocyte growth factor in a variety of tissues.[14,45–47] In endothelial cells, decorin binds with both insulin-like growth factor-I and its receptor to influence cell behavior.[17] Decorin can also control and suppress cancer growth and invasion, presumably by influencing the biological activity of growth factors such as TGF-β1, platelet-derived growth factor, vascular endothelial growth factor, and epidermal growth factor, all of which are released by cancer cells.[5,15] These decorin-induced effects appear to be mediated, at least in part, by a specific interaction between the decorin protein core and the epidermal growth factor receptor.[15,16] This interaction triggers a signal cascade that results in activation of mitogen-activated protein kinase, mobilization of intracellular calcium, up-regulation of p21, and, ultimately, the suppression of tumor growth.[18,19]

Cell cycle exit and the differentiation of muscle cells are coordinated by p21, which is essential for normal myogenic progenitor cell differentiation and skeletal muscle regeneration. Studies have indicated that p21 is necessary for MyoD-induced activity in cells, allowing them to enter into and be stabilized in a postmitotic state. Since MyoD plays a central role in the differentiation of muscle cells, TGF-β1 controls myostatin-related regulation of myogenesis in muscle cells by down-regulating both p21 and MyoD. In this study, we determined that the treatment of myoblasts with decorin down-regulated the expression of myostatin, which might influence p21 and myogenic protein expression. In addition, myostatin and follistatin interact directly in the skeletal muscle system. Follistatin can inhibit myostatin, leading to muscle differentiation in a concentration-dependent manner.[21] PGC-1α, which is expressed in several tissues, including brown fat and the skeletal muscle of mammals, activates mitochondrial biogenesis and oxidative metabolism.[26] PGC-1α is a principal factor involved in determining muscle fiber type in injured skeletal muscle and is involved in exercise-induced mitochondrial biogenesis.[48] In this experiment, we observed that decorin treatment increased PGC-1α expression in skeletal muscle cells. Combined with our previous research results, our current findings suggest that decorin not

only acts as an antifibrotic agent but also enhances muscle regeneration in skeletal muscle.

Successful muscle differentiation during limb development requires decorin expression.[6] Previous findings have shown that decorin can improve muscle healing by inhibiting fibrosis and that myoblasts and muscle satellite cells expressing decorin in an injured site regenerated damaged myofibers faster than the controls.[11,27] The results of this study demonstrate that decorin is also a potent stimulator of skeletal muscle regeneration. Myoblasts expressing decorin differentiated and fused to form myotubes and myofibers at a significantly higher rate than did normal myoblasts *in vitro* and *in vivo*. We attribute this enhanced differentiation to the up-regulation of p21, follistatin, PGC-1α, and myogenic gene expression and the down-regulation of TGF-β1 and myostatin. These results provide at least a partial explanation of the way in which decorin promotes muscle regeneration and may explain why there is such a high level of decorin expression in developing skeletal muscle. It is possible that decorin increases muscle fiber growth and limits the overgrowth of connective tissues. These findings indicate that decorin could be very useful in promoting the healing of muscles damaged by injury or disease.

MATERIALS AND METHODS

Gene transfection and transfer. An AAV-mDecorin plasmid, which encodes for a mouse decorin sequence under the control of the cytomegalovirus promoter (**Figure 1**), was used for gene transfection. This plasmid also contains a neomycin resistance gene to enable G418 selection. The AAV-mDecorin plasmid was transfected into 293 packaging cells and C2C12 cells with lipofectin; clone cells were selected for treatment of the cells with G418 (500 µg/mL) (Gibco BRL, Grand Island, NY) for 2 weeks. The selected decorin-transfected C2C12 clone cells (CD cells) were cultured in Dulbecco's modified Eagle's medium (Gibco BRL, Grand Island, NY) containing the same concentration of G418 for the remainder of the project.

The mDec-AAV vector was produced by co-transfection methods described previously by Dr. Xiao.[49] Muscle-derived stem cells and myoblasts (C2C12 cells) were each grown to 50–60% confluency. Fresh Dulbecco's modified Eagle's medium (without fetal bovine serum or penicillin/streptomycin) containing the mDec-AAV vector (5×10^4 particles/cell) was then added directly to the cells. The cultures were incubated at 37 °C in a 5% CO$_2$ incubator for 1 hour. Normal culture medium (Dulbecco's modified Eagle's medium supplemented with 10% fetal bovine serum and 1% Abs) was then added for another 24 hours, at which point the cells were collected for analysis of decorin expression by western blotting.

Differentiation of myoblasts and immunocytochemistry. Three different groups of cells (C2C12 cells, C2C12 cells cultured with decorin, and CD cells) were seeded into 12-well plates containing proliferation medium.[28] All cells were transferred into serum-free medium 12 hours later to induce differentiation. The myotubes that formed in the cultures were counted daily for 5 days, and the numbers were compared among the groups. We considered myotubes containing three or more nuclei to be large myotubes *in vitro*. At different time points, the cells were fixed with cold acetone (3 minutes) for immunostaining. Mouse anti-myosin heavy chain antibody (Novocastra Lab) at a 1:200 dilution was applied for 1 hour at room temperature (RT). The primary antibody was detected using anti-mouse-Cy3, 1:250 for 45 minutes at RT. Results were analyzed by fluorescent microscopy (Nikon microscope, Nikon, Melville, New York).

Real-time polymerase chain reaction. Total RNA was extracted from the treated and non-treated C2C12 cells using a Nucleospin column (Clontech, Mountan View, CA), and the complementary DNA was synthesized with SuperScript II reverse transcriptase (Invitrogen, Carlsbad, CA), both according to manufacturer's instructions. Primers specific for *myostatin*, *follistatin*, *p21*, and *PGC-1α* were designed using Oligo software (OligoPerfect Designer; Invitrogen, Carlsbad, CA). The protocol for amplification was as follows: 94 °C for 30 seconds, 58 °C for 30 seconds, and 72 °C for 30 seconds for 30 cycles. Polymerase chain reaction products were separated by size in a 1.5% agarose gel.

Western blot analysis. C2C12 and CD cells were lysed when cell density reached 70% confluency. The samples were separated on a 12% sodium dodecyl sulfate–polyacrylamide electrophoresis gel and transferred to nitrocellulose membranes used to perform immunostaining. The primary antibodies were anti-decorin (a gift from Dr. Fisher of the National Institutes of Health), anti-TGF-β1 (4 µg/mL; BD Pharmingen, San Diego, CA), anti-p21 (BD Pharmingen, San Diego, CA), anti-myf5, anti-myf6, anti-MyoD, and anti-myogenin (Santa Cruz Bio, Santa Cruz, CA), all at concentrations of 1:1,000, and anti-myostatin, anti-follistatin (Chemicon, Temecula, CA), and anti-desmin (Sigma, St. Louis, MO), all at concentrations of 1:2,000 for 1 hour at RT. Mouse anti-β-actin and anti-glyceraldehyde-3-phosphate dehydrogenase (Sigma, St. Louis, MO) were used for protein quantification and were diluted to 1:8,000. The secondary anti-rat horseradish peroxidase or anti-rabbit horseradish peroxidase (Pierce, Rockford, IL) was used at a concentration of 1:5,000 for 1 hour. Peroxidase activity was determined by enhanced chemiluminescence (Amersham Pharmacia Biotech, Piscataway, NJ), and the positive bands were detected on X-ray film. Northern Eclipse software v.6.0 (Empix Imaging, Mississauga, Canada) was used to evaluate all results.

Animal experiments. All animal experiments were approved by the Children's Hospital of Pittsburgh. The Animal Research Committee at the authors' institution approved all experimental protocols (No. 15/03).

Group 1: C2C12 and CD cell transplantation. Twenty-four female *MDX*/SCID mice (C57BL/10ScSn-*Dmd^mdx^* crossed with C57BL/6J-*Prkdc^scid^*/SzJ, 6–8 weeks of age) were used for the C2C12 and CD cell transplantation. C2C12 and CD clone cells were transduced with a retrovirus vector encoding for LacZ.[27] LacZ-positive CD cells (1×10^6) were injected into the left gastrocnemius muscles (GMs); the same quantity of LacZ-positive C2C12 cells were injected into the right GMs as a control. At various times after injection, mice were killed, and the GMs were collected for histological analysis by LacZ staining and immunohistochemistry to stain for dystrophin-positive myofibers.

Group 2: mDec-AAV gene therapy administered to injured skeletal muscle. Twenty mice (C57BL6J$^{+/+}$, 6 weeks old; Jackson Laboratory, Bar Harbor, ME) were used for these experiments. The mDec-AAV vector (2×10^{11} particles in 20 µL of Dulbecco's modified Eagle's medium) was injected directly into the left GM of each mouse; the contralateral leg was injected with the same volume of phosphate-buffered saline (20 µL) as a control. One week after injection, both GMs were lacerated in accordance with our previously described muscle injury model.[11,27,28,40] Mice were killed at different time points (5 days and 1, 2, 3, and 4 weeks after injury), and the GMs were collected for histological analysis by either hematoxylin and eosin or Masson's trichrome staining. The regeneration and fibrous scar tissue formation in the two groups were compared.

Immunohistochemical analysis. Serial 10-µm cryostat sections were prepared using standard techniques.[27,28] For immunohistochemistry, the slides were fixed with formalin (4%) for 5 minutes after LacZ staining, and then blocked with donkey serum (10%) for 1 hour. Rabbit anti-dystrophin antibody (Abcam, Cambridge, MA) was applied to the slides at a 1:300 dilution for 60 minutes at RT. The second antibody, goat anti-rabbit IgG (Alexa Fluor® 488; Molecular Probes, Eugene, OR), was used at a concentration of 1:200 for 45 minutes at RT. Negative controls were performed concurrently with all immunohistochemical staining. The nuclei of the sections were revealed using 4′,6′-diamidino-2-phenylindole hydrochloride

staining (Sigma, St. Louis, MO), and fluorescent microscopy was used to visualize the results as described above.

Statistical analysis. LacZ-positive myofibers were counted in 10 representative sections. Both the diameter and number of LacZ- and dystrophin-positive myofibers were assessed at different time points in each group. The statistical significance of differences between the various groups was determined using a t-test or one-way or two-way analysis of variance.

ACKNOWLEDGMENTS

REFERENCES

1. Hocking, AM, Shinomura, T and McQuillan, DJ (1998). Leucine-rich repeat glycoproteins of the extracellular matrix. *Matrix Biol* **17**: 1–19.
2. Sottile, J, Hocking, DC and Swiatek, PJ (1998). Fibronectin matrix assembly enhances adhesion-dependent cell growth. *J Cell Sci* **111**: 2933–2943.
3. Giri, SN, Hyde, DM, Braun, RK, Gaarde, W, Harper, JR and Pierschbacher, MD (1997). Antifibrotic effect of decorin in a bleomycin hamster model of lung fibrosis. *Biochem Pharmacol* **54**: 1205–1216.
4. Noble, NA, Harper, JR and Border, WA (1992). *In vivo* interactions of TGF-beta and extracellular matrix. *Prog Growth Factor Res* **4**: 369–382.
5. Stander, M, Naumann, U, Dumitrescu, L, Heneka, M, Loschmann, P, Gulbins, E *et al.* (1998). Decorin gene transfer-mediated suppression of TGF-beta synthesis abrogates experimental malignant glioma growth *in vivo*. *Gene Ther* **5**: 1187–1194.
6. Nishimura, T, Futami, E, Taneichi, A, Mori, T and Hattori, A (2002). Decorin expression during development of bovine skeletal muscle and its role in morphogenesis of the intramuscular connective tissue. *Cells Tissues Organs* **171**: 199–214.
7. Brandan, E, Fuentes, ME and Andrade, W (1991). The proteoglycan decorin is synthesized and secreted by differentiated myotubes. *Eur J Cell Biol* **55**: 209–216.
8. Casar, JC, McKechnie, BA, Fallon, JR, Young, MF and Brandan, E (2004). Transient up-regulation of biglycan during skeletal muscle regeneration: delayed fiber growth along with decorin increase in biglycan-deficient mice. *Dev Biol* **268**: 358–371.
9. Yoshida, N, Yoshida, S, Koishi, K, Masuda, K and Nabeshima, Y (1998). Cell heterogeneity upon myogenic differentiation: down-regulation of MyoD and Myf-5 generates 'reserve cells'. *J Cell Sci* **111**: 769–779.
10. Li, Y, Cummins, J and Huard, J (2001). Muscle injury and repair. *Curr Opin Orthop* **12**: 409–415.
11. Fukushima, K, Badlani, N, Usas, A, Riano, F, Fu, F and Huard, J (2001). The use of an antifibrosis agent to improve muscle recovery after laceration. *Am J Sports Med* **29**: 394–402.
12. Harper, JR, Spiro, RC, Gaarde, WA, Tamura, RN, Pierschbacher, MD, Noble, NA *et al.* (1994). Role of transforming growth factor beta and decorin in controlling fibrosis. *Methods Enzymol* **245**: 241–254.
13. Isaka, Y, Brees, DK, Ikegaya, K, Kaneda, Y, Imai, E, Noble, NA *et al.* (1996). Gene therapy by skeletal muscle expression of decorin prevents fibrotic disease in rat kidney. *Nat Med* **2**: 418–423.
14. Kobayashi, E, Sasamura, H, Mifune, M, Shimizu-Hirota, R, Kuroda, M, Hayashi, M *et al.* (2003). Hepatocyte growth factor regulates proteoglycan synthesis in interstitial fibroblasts. *Kidney Int* **64**: 1179–1188.
15. Csordas, G, Santra, M, Reed, CC, Eichstetter, I, McQuillan, DJ, Gross, D *et al.* (2000). Sustained down-regulation of the epidermal growth factor receptor by decorin. A mechanism for controlling tumor growth *in vivo*. *J Biol Chem* **275**: 32879–32887.
16. Iozzo, RV, Moscatello, DK, McQuillan, DJ and Eichstetter, I (1999). Decorin is a biological ligand for the epidermal growth factor receptor. *J Biol Chem* **274**: 4489–4492.
17. Schonherr, E, Sunderkotter, C, Iozzo, RV and Schaefer, L (2005). Decorin, a novel player in the insulin-like growth factor system. *J Biol Chem* **280**: 15767–15772.
18. De Luca, A, Santra, M, Baldi, A, Giordano, A and Iozzo, RV (1996). Decorin-induced growth suppression is associated with up-regulation of p21, an inhibitor of cyclin-dependent kinases. *J Biol Chem* **271**: 18961–18965.
19. Schonherr, E, Levkau, B, Schaefer, L, Kresse, H and Walsh, K (2001). Decorin-mediated signal transduction in endothelial cells. Involvement of Akt/protein kinase B in up-regulation of p21(WAF1/CIP1) but not p27(KIP1). *J Biol Chem* **276**: 40687–40692.
20. Budasz-Rwiderska, M, Jank, M and Motyl, T (2005). Transforming growth factor-beta1 upregulates myostatin expression in mouse C2C12 myoblasts. *J Physiol Pharmacol* **56** (suppl. 3): 195–214.
21. Amthor, H, Nicholas, G, McKinnell, I, Kemp, CF, Sharma, M, Kambadur, R *et al.* (2004). Follistatin complexes Myostatin and antagonises Myostatin-mediated inhibition of myogenesis. *Dev Biol* **270**: 19–30.
22. Lee, SJ and McPherron, AC (2001). Regulation of myostatin activity and muscle growth. *Proc Natl Acad Sci USA* **98**: 9306–9311.
23. Miura, T, Kishioka, Y, Wakamatsu, J, Hattori, A, Hennebry, A, Berry, CJ *et al.* (2006). Decorin binds myostatin and modulates its activity to muscle cells. *Biochem Biophys Res Commun* **340**: 675–680.
24. McCroskery, S, Thomas, M, Platt, L, Hennebry, A, Nishimura, T, McLeay, L *et al.* (2005). Improved muscle healing through enhanced regeneration and reduced fibrosis in myostatin-null mice. *J Cell Sci* **118**: 3531–3541.
25. Duguez, S, Feasson, L, Denis, C and Freyssenet, D (2002). Mitochondrial biogenesis during skeletal muscle regeneration. *Am J Physiol Endocrinol Metab* **282**: E802–E809.
26. Lin, J, Wu, H, Tarr, PT, Zhang, CY, Wu, Z, Boss, O *et al.* (2002). Transcriptional co-activator PGC-1 alpha drives the formation of slow-twitch muscle fibres. *Nature* **418**: 797–801.
27. Li, Y, Foster, W, Deasy, BM, Chan, Y, Prisk, V, Tang, Y *et al.* (2004). Transforming Growth Factor-beta1 Induces the Differentiation of Myogenic Cells into Fibrotic Cells in Injured Skeletal Muscle: A Key Event in Muscle Fibrogenesis. *Am J Pathol* **164**: 1007–1019.
28. Li, Y and Huard, J (2002). Differentiation of muscle-derived cells into myofibroblasts in injured skeletal muscle. *Am J Pathol* **161**: 895–907.
29. Chan, YS, Li, Y, Foster, W, Fu, FH and Huard, J (2005). The use of suramin, an antifibrotic agent, to improve muscle recovery after strain injury. *Am J Sports Med* **33**: 43–51.
30. Chan, YS, Li, Y, Foster, W, Horaguchi, T, Somogyi, G, Fu, FH *et al.* (2003). Antifibrotic effects of suramin in injured skeletal muscle after laceration. *J Appl Physiol* **95**: 771–780.
31. Sato, K, Li, Y, Foster, W, Fukushima, K, Badlani, N, Adachi, N *et al.* (2003). Improvement of muscle healing through enhancement of muscle regeneration and prevention of fibrosis. *Muscle Nerve* **28**: 365–372.
32. Huard, J, Li, Y and Fu, FH (2002). Muscle injuries and repair: current trends in research. *J Bone Joint Surg Am* **84-A**: 822–832.
33. Engert, JC, Berglund, EB and Rosenthal, N (1996). Proliferation precedes differentiation in IGF-I-stimulated myogenesis. *J Cell Biol* **135**: 431–440.
34. McFarland, DC, Pesall, JE and Gilkerson, KK (1993). The influence of growth factors on turkey embryonic myoblasts and satellite cells *in vitro*. *Gen Comp Endocrinol* **89**: 415–424.
35. Sheehan, SM and Allen, RE (1999). Skeletal muscle satellite cell proliferation in response to members of the fibroblast growth factor family and hepatocyte growth factor. *J Cell Physiol* **181**: 499–506.
36. Tatsumi, R Anderson, JE, Nevoret, CJ, Halevy, O and Allen, RE (1998). HGF/SF is present in normal adult skeletal muscle and is capable of activating satellite cells. *Dev Biol* **194**: 114–128.
37. Beauchamp, JR, Heslop, L, Yu, DS, Tajbakhsh, S, Kelly, RG, Wernig, A *et al.* (2000). Expression of CD34 and Myf5 defines the majority of quiescent adult skeletal muscle satellite cells. *J Cell Biol* **151**: 1221–1234.
38. Chambers, RL and McDermott, JC (1996). Molecular basis of skeletal muscle regeneration. *Can J Appl Physiol* **21**: 155–184.
39. Bischoff, R (1994). The satellite cell and muscle regeneration. In Engel, AG and Franzini-Armstrong, C (eds). *Myology: Basic and Clinical*. McGraw-Hill, New York. pp. 97–118.
40. Shen, W, Li, Y, Tang, Y, Cummins, J and Huard, J (2005). NS-398, a cyclooxygenase-2-specific inhibitor, delays skeletal muscle healing by decreasing regeneration and promoting fibrosis. *Am J Pathol* **167**: 1105–1117.
41. Jarvinen, TA, Jarvinen, TL, Kaariainen, M, Kalimo, H and Jarvinen, M (2005). Muscle injuries: biology and treatment. *Am J Sports Med* **33**: 745–764.
42. Branton, MH and Kopp, JB (1999). TGF-β and fibrosis. *Microbes Infect* **1**: 1349–1365.
43. Franklin, TJ (1997). Therapeutic approaches to organ fibrosis. *Int J Biochem Cell Biol* **29**: 79–89.
44. Zhao, J, Sime, PJ, Bringas, P, Gauldie, J and Warburton, D (1999). Adenovirus-mediated decorin gene transfer prevents TGF-beta-induced inhibition of lung morphogenesis. *Am J Physiol* **277**: L412–L422.
45. Gong, R, Rifai, A, Tolbert, EM, Centracchio, JN and Dworkin, LD (2003). Hepatocyte growth factor modulates matrix metalloproteinases and plasminogen activator/plasmin proteolytic pathways in progressive renal interstitial fibrosis. *J Am Soc Nephrol* **14**: 3047–3060.
46. Taniyama, Y, Morishita, R, Nakagami, H, Moriguchi, A, Sakonjo, H, Shokei, K *et al.* (2000). Potential contribution of a novel antifibrotic factor, hepatocyte growth factor, to prevention of myocardial fibrosis by angiotensin II blockade in cardiomyopathic hamsters. *Circulation* **102**: 246–252.
47. Yang, J, Dai, C and Liu, Y (2002). Hepatocyte growth factor gene therapy and angiotensin II blockade synergistically attenuate renal interstitial fibrosis in mice. *J Am Soc Nephrol* **13**: 2464–2477.
48. Norrbom, J, Sundberg, CJ, Ameln, H, Kraus, WE, Jansson, E and Gustafsson, T (2004). PGC-1alpha mRNA expression is influenced by metabolic perturbation in exercising human skeletal muscle. *J Appl Physiol* **96**: 189–194.
49. Xiao, X, Li, J and Samulski, RJ (1998). Production of high-titer recombinant adeno-associated virus vectors in the absence of helper adenovirus. *J Virol* **72**: 2224–2232.

Relationships between Transforming Growth Factor-β1, Myostatin, and Decorin
IMPLICATIONS FOR SKELETAL MUSCLE FIBROSIS

Jinhong Zhu[‡§1], **Yong Li**[‡¶‖1], **Wei Shen**[‡§], **Chunping Qiao**[¶], **Fabrisia Ambrosio**[‡**], **Mitra Lavasani**[‡§],
Masahiro Nozaki[‡¶], **Maria F. Branca**[‡], and **Johnny Huard**[‡§¶2]

*From the ‡Stem Cell Research Center, Children's Hospital of Pittsburgh, Rangos Research Center, Pittsburgh, Pennsylvania 15213-2583,
the §Department of Bioengineering, University of Pittsburgh, Pittsburgh, Pennsylvania 15261, the ¶Department of Orthopaedic
Surgery, University of Pittsburgh School of Medicine, Pittsburgh, Pennsylvania 15213, the ‖Department of Pathology, University of
Pittsburgh School of Medicine, Pittsburgh, Pennsylvania 15261, and the **Department of Physical Medicine and Rehabilitation,
University of Pittsburgh School of Medicine, Pittsburgh, Pennsylvania 15213-200*

Recent studies have shown that myostatin, first identified as a negative regulator of skeletal muscle growth, may also be involved in the formation of fibrosis within skeletal muscle. In this study, we further explored the potential role of myostatin in skeletal muscle fibrosis, as well as its interaction with both transforming growth factor-β1 and decorin. We discovered that myostatin stimulated fibroblast proliferation *in vitro* and induced its differentiation into myofibroblasts. We further found that transforming growth factor-β1 stimulated myostatin expression, and conversely, myostatin stimulated transforming growth factor-β1 secretion in C2C12 myoblasts. Decorin, a small leucine-rich proteoglycan, was found to neutralize the effects of myostatin in both fibroblasts and myoblasts. Moreover, decorin up-regulated the expression of follistatin, an antagonist of myostatin. The results of *in vivo* experiments showed that myostatin knock-out mice developed significantly less fibrosis and displayed better skeletal muscle regeneration when compared with wild-type mice at 2 and 4 weeks following gastrocnemius muscle laceration injury. In wild-type mice, we found that transforming growth factor-β1 and myostatin co-localize in myofibers in the early stages of injury. Recombinant myostatin protein stimulated myofibers to express transforming growth factor-β1 in skeletal muscles at early time points following injection. In summary, these findings define a fibrogenic property of myostatin and suggest the existence of co-regulatory relationships between transforming growth factor-β1, myostatin, and decorin.

Skeletal muscle injuries are one of the most common injuries encountered in sports, accounting for 10–55% of all sports related injuries (1–3). Despite their clinical significance, current treatments remain conservative, such as the RICE principle (rest, ice, compression, and elevation) and non-steroidal anti-inflammatory drugs. However, increasing evidence shows that the administration of non-steroidal anti-inflammatory drugs decreases regeneration and increases fibrosis by inhibiting inflammation (4–8). Although injured skeletal muscle can spontaneously undergo regeneration, muscle regeneration must compete with the ensuing formation of fibrosis, especially in acute injuries (9–11). The resulting excessive fibrotic tissue might form a dense mechanical barrier that prevents the regenerating muscle fibers from maturing (12, 13), thereby resulting in incomplete skeletal muscle healing (14, 15). Researchers have widely accepted that transforming growth factor-β1 (TGF-β1)[3] is a potent stimulator of fibrosis in various tissues (16–19) and is closely associated with skeletal muscle fibrosis as well (20). TGF-β1 levels are elevated in both dystrophic muscles and injured muscles (21, 22). Researchers have also shown that TGF-β1 effectively induces myofibroblastic differentiation of fibroblasts both *in vitro* and *in vivo* (23, 24). The resulting overgrowth of myofibroblasts is responsible for the ensuing excessive accumulation of fibrotic tissue (23, 24). We have previously reported that TGF-β1 plays a significant role in both the initiation of fibrosis and the induction of myofibroblastic differentiation of myogenic cells in injured skeletal muscle (20, 25). Additionally, we have shown that antifibrosis therapies, such as interferon-gamma (INF-γ), suramin, relaxin, and decorin (DCN), improve the healing of injured muscle both histologically and physiologically by blocking the activity of TGF-β1 (26–32). However, it is unclear whether TGF-β1 acts alone or requires interaction with other molecules during the development of muscle fibrosis. Indeed, recent studies have shown that

[3] The abbreviations used are: TGF-β1, transforming growth factor-β1; MSTN, myostatin; INF, interferon; DCN, decorin; MSTN^{−/−}, myostatin knockout; MSTN^{−/−}/*mdx* mice, *mdx* mice with myostatin gene knockout; GM, gastrocnemius muscle; PM, proliferation medium; DM, differentiation medium; HS, horse serum; PP1 cells, a population of preplated cells; α-SMA, α-smooth muscle actin; FN, fibronectin; MTT, 3-(4,5-dimethylthiazol-2-yl)-2,5-diphenyltetrazolium bromide; ELISA, enzyme-linked immunosorbent assay; PBS, phosphate-buffered saline; WT, wide-type; M.O.M., Mouse on Mouse; ECM, extracellular matrix; MRF, muscle regulatory factor; LTP, long-term proliferating; FLST, follistatin; Q-RT-PCR, quantitative reverse transcription-PCR; TβRII, TGF-β1 receptor type II.

myostatin (MSTN), a member of the TGF-β superfamily, may also be involved in fibrosis formation within skeletal muscle (33), although a direct link between MSTN and fibrosis has yet to be identified.

MSTN was initially identified as a negative regulator of muscle development (34), but unlike the ubiquitous expression of TGF-β1, MSTN is predominantly expressed in skeletal muscle. MSTN knock-out (MSTN$^{-/-}$) mice, as well as cattle and humans with a naturally occurring MSTN gene mutation, are characterized by a dramatic and widespread increase in skeletal muscle mass (34–36). Interestingly, recent reports suggest that *mdx* mice (an animal model for Duchenne muscular dystrophy) in which expression of the MSTN gene has been ablated (MSTN$^{-/-}$/*mdx*) not only showed better skeletal muscle regeneration but also exhibited decreased fibrosis when compared with *mdx* mice (MSTN$^{+/+}$/*mdx*) (33). These results strongly suggest that MSTN plays an important role in muscle fibrosis. To investigate this possibility, we evaluated the effect of MSTN on fibrosis formation in injured skeletal muscle. Because TGF-β1 plays a major role in the formation of fibrosis, we hypothesized that a relationship between TGF-β1 and MSTN exists. Because DCN has been shown to strongly inhibit fibrosis formation in various tissues via blocking of TGF-β1 activity (26, 27, 37–40), we investigated the potential for DCN to inhibit the activity of MSTN as it does for TGF-β1. Our findings demonstrated that MSTN is involved with fibrosis formation and interacts with TGF-β1 and that DCN has the ability to counteract the action of MSTN. These results contribute to a better understanding of the mechanism of skeletal muscle healing and indicate that MSTN represents a potential pharmacological target for anti-fibrogenic therapy.

EXPERIMENTAL PROCEDURES

Isolation of Fibroblasts from Skeletal Muscle—The preplate technique was used to isolate fibroblasts from skeletal muscle (41). Collagen-coated flasks were used in the isolation process, because fibroblasts adhere more readily to collagen than myoblasts. After 6-week-old female C57BL/6J mice were sacrificed, their gastrocnemius muscles (GMs) were removed and minced into a coarse slurry. The muscle slurry was digested with 0.2% collagenase (type XI) for 1 h, followed by a dispase digestion (grade II, 240 ml) for 30 min, followed by a 0.1% trypsin digestion for a final 30 min at 37 °C. The extracted muscle cells were resuspended in proliferation medium (PM) consisting of Dulbecco's modified Eagle's medium (Invitrogen), 10% horse serum (HS, Invitrogen), 10% fetal bovine serum (Invitrogen), 1% penicillin/streptomycin (Invitrogen), and 0.5% chicken embryo extract (Accurate Chemical & Scientific Corp., Westbury, NY) and plated onto collagen-coated flasks. A population of preplated cells (PP1), consisting of mostly fibroblasts that attached within the first 2 h, was collected and used, in these experiments, as skeletal muscle-derived fibroblasts. This preplate technique was also used to isolate long-term proliferating (LTP) cells (muscle-derived stem cell-like cells) from WT and MSTN$^{-/-}$ muscle (41). Two hours after the initial plating, most of the rapidly adhering fibroblasts attached; the remaining non-adherent cells were transferred to a new collagen-coated flask every 24 h. As this process was repeated, the subsequent populations of late-adhering cells were identified as PP2, PP3, PP4, and PP5 in sequence. Following the collection of PP5, the rest of the cell suspension was incubated for an additional 72 h to allow the cells to attach in another collagen-coated flask. The final adherent cells are LTP cells (41).

Cell Culture—The NIH3T3 fibroblast cell line and the C2C12 myoblast cell line were purchased from the American Type Culture Collection (Manassas, VA). The cell lines or isolated PP1 fibroblasts were maintained in PM consisting of Dulbecco's modified Eagle's medium, 10% fetal bovine serum, and 1% penicillin/streptomycin until further needed. PP1 fibroblasts were plated onto collagen-coated 96-well plates for cell-proliferation analysis and onto 6-well plates for the evaluation of α-smooth muscle actin (α-SMA), fibronectin (FN), collagen (types Iα1, IIα2, and IIIα1), and MSTN expression. Following an overnight incubation, PM was replaced with serum-free medium supplemented with a serum replacement (Sigma) consisting of heat-treated bovine serum albumin, heat-treated bovine transferrin, and bovine insulin. This serum replacement does not contain growth factors, steroid hormones, glucocorticoids, or cell adhesion factors. We further supplemented this media with varying concentrations of recombinant human MSTN (Leinco Technologies, Inc., St. Louis, MO) for proliferation assays (0, 100, 500, or 1000 ng/ml) and for Western blot analysis (0, 100, or 500 ng/ml). After incubation for 48 h, an MTT (3-(4,5-dimethylthiazol-2-yl)-2,5-diphenyltetrazolium bromide) cell proliferation assay kit (Roche Diagnostics, Germany) was used to measure cell proliferation ($n = 6$) following the instructions from the manufacturer. Western blot analysis was used to examine α-SMA, FN, and MSTN expression. Some of the above procedures were repeated using NIH3T3 fibroblasts to confirm the effect of MSTN on fibroblasts.

C2C12 myoblasts, a widely used myogenic cell line (42–44), were used to examine whether DCN neutralized the inhibitory effect of MSTN on cell differentiation. We seeded C2C12 myoblasts in 12-well plates in PM at a density of 10,000 cells/well. Following an overnight incubation, PM was replaced with fresh differentiation medium (DM) containing Dulbecco's modified Eagle's medium, 2% HS, and 1% penicillin/streptomycin. We maintained a total of four sets of cultured cells. The control set received only DM, whereas the other sets received DCN alone or 1 μg/ml MSTN combined with 0–50 μg/ml DCN ($n = 3$). Cells were cultured for 5 more days during which DM, MSTN, and DCN were changed every other day. Following a similar procedure, we examined whether recombinant follistatin (FLST) protein stimulated myogenic differentiation of C2C12 myoblasts ($n = 3$), and whether soluble TGF-β1 receptor type II (TβRII, 100 and 1000 ng/ml, R&D Systems, Inc., Minneapolis, MN) was able to attenuate MSTN-inhibited myoblast differentiation ($n = 3$).

Western Blot Analysis—After culturing, the cells were lysed with T-PER® Tissue Protein Extraction Reagent with the addition of protease inhibitors (Pierce). Equal amounts of cellular protein were loaded into each well and separated by 10% SDS-PAGE. Nitrocellulose membrane blotting was performed under standard conditions. The following primary antibodies were used for immunoblotting: mouse anti-β-actin IgG (1:8000, Sigma), mouse anti-glyceraldehyde-3-phosphate dehydrogen-

Relationships between TGF-β1, Myostatin, and Decorin

TABLE 1
Sequence of primer set

Gene name (GenBank™ no.)	Primer pair (S: sense primer, A: anti-sense primer)	PCR products
		bp
Procollagen type Iα1 (BC050014)	S: 5′-GAAGAACTGGACTGTCCCAAC-3′	103
	A: 5′-CCTCGACTCCTACATCTTCTG-3′	
Procollagen type Iα2 (AK075707)	S: 5′-TCTGGTAAAGAAGGCCCTGTG-3′	106
	A: 5′-GTCCAGGGAATCCGATGTTG-3′	
Procollagen type IIIα1 (AK041115)	S: 5′-AGGCTGAAGGAAACAGCAAA-3′ (45)	116
	A: 5′-TAGTCTCATTGCCTTGCGTG-3′	
TGF-β1 (BC 013738)	S: 5′-CTAATGGTGGACCGCAACAAC-3′	99
	A: 5′-CACTGCTTCCCGAATGTCTGA-3′	
18 S rRNA (?)[a]		N/A

[a] Sequences of the primer pairs for 18 S rRNA not provided by Applied Biosystems Inc. for proprietary reasons.

ase IgG (1:5000, Abcam Inc., Cambridge, MA), rabbit anti-MSTN IgG (1:3000, Chemicon, Temecula, CA), mouse anti-α-SMA IgG (1:1000, Sigma), mouse anti-FN IgG (1:3000), and rat anti-TGF-β1 IgG (1:1000, BD Pharmingen, San Jose, CA).

Quantitative RT-RCR—Quantitative RT-PCR (Q-RT-PCR) was used to examine the mRNA expression levels of procollagen (types Iα1, Iα2, and IIIα1) in PP1 fibroblasts treated with MSTN (100, 200, and 500 ng/ml) for 12, 24, and 48 h. The mRNA was extracted using an RNeasy Plus kit (Qiagen). The cDNA templates for Q-RT-PCR were synthesized using a RETROscript® kit (Ambion Inc., Austin, TX). Q-RT-PCR was carried out in an ABI Prism 7000 sequence detector (Applied Biosystems Inc., Foster City, CA) with SYBR Green PCR Master Mix Reagent (Applied Biosystems) as a detector. All target gene expressions were normalized to 18 S rRNA levels. The primer pair of procollagen IIIα1 was from a previous study (45). The primer pairs are displayed in Table 1.

ELISA—Enzyme-linked immunosorbent assay (ELISA) was performed to determine whether recombinant MSTN protein stimulated TGF-β1 secretion in C2C12 myoblasts. C2C12 myoblasts were plated into a 48-well plate and exposed to a range of MSTN concentrations from 0 to 500 ng/ml. Fresh, recombinant MSTN protein was added every 2 days. Cell supernatants were collected at 2 and 4 days (*n* = 5). These supernatants were centrifuged to remove cell debris and stored at −80 °C until the ELISA was performed. The mouse/rat/porcine TGF-β1 immunoassay kit (R&D Systems, Inc.) was used to quantitatively measure the secreted TGF-β1 levels in cell culture supernatants, according to the manufacturer's protocol.

Immunocytochemistry—To monitor the differentiation capacity of the myogenic cells, they were fixed in cold methanol for 2 min after induction of differentiation in 12-well plates. Following a phosphate-buffered saline (PBS) wash, the cells were blocked with 10% HS (Vector Laboratories, Inc., Burlingame, CA) for 30 min, and then incubated with an anti-myosin heavy chain antibody (Sigma) in 2% HS overnight. A negative control was performed by omitting the primary antibody. The next day, after several PBS rinses, the cells were incubated with the secondary antibody goat anti-mouse IgG conjugated with Cy3 (Sigma) for 1 h. Hoechst 33258 dye was used in each experiment to stain cell nuclei. Fusion index (ratio of nuclei in myotubes to all nuclei) was calculated (%) to evaluate myogenic differentiation.

Animal Model—All experimental animal protocols were approved by the Animal Research and Care Committee at Children's Hospital of Pittsburgh (protocols 15-3 and 17-05).

C57BL/6 wild-type (WT) (Jackson Laboratories, Bar Harbor, ME) and MSTN^{−/−} mice (7–8 weeks of age) were used in this study. All MSTN^{−/−} mice used were offspring of MSTN^{−/−} homozygotes, and PCR was used to confirm the genotype of all MSTN^{−/−} mice. The RT-PCR test was randomly used to confirm the lack of MSTN gene transcription in MSTN^{−/−} mice throughout the experiments. The skeletal muscle mass of MSTN^{−/−} mice and WT mice were also compared to confirm the desired phenotype. The mice were anesthetized with isoflurane controlled under an IMPAC6 anesthetic delivery machine (VetEquip, Pleasanton, CA). Both GMs of each mouse were laterally lacerated to create an injury model as previously described (27–29). A surgical blade (no. 11) was used to make a lateral laceration through 50% of the muscle width and 100% of the muscle thickness in the area of the GM with the largest diameter. We harvested the mouse GMs at 2 and 4 weeks post-surgery. There were 6–8 mice (12–16 GMs) in the WT and MSTN^{−/−} mouse groups for both time points. The muscles were isolated, removed, and snap-frozen in 2-methylbutane pre-cooled in liquid nitrogen. After Masson's trichrome staining (IMEB Inc., Chicago, IL), Northern Eclipse software (Empix Imaging, Inc., Cheektawaga, NY) was used to measure areas of fibrotic tissue in the injured sites. In each sample, three representative non-adjacent sections were chosen. The ratio of the fibrotic area to the cross-sectional area was used to estimate the extent of fibrosis formation. To determine the skeletal muscle's regeneration efficiency, minor axis diameters (the smallest diameter) of regenerating muscle fibers were measured using Northern Eclipse software on cross-sections of GMs. The diameters of over 350 consecutively centro-nucleated myofibers were measured in each GM.

To analyze the expression of MSTN in the injured GM, 18 8-week-old female C57BL/6 WT mice underwent bilateral GM laceration. Mice were sacrificed at 1, 3, 5, 7, 10, 14, 21, and 30 days after injury (*n* = 3 for each time point), and GMs were harvested, frozen, and stored at −80 °C.

300,000 LTP cells obtained from MSTN^{−/−} mice were transplanted in the GMs of 3 8-week-old *mdx*/scid mice using a protocol previously described (41). The same amount of cells obtained from WT mice was injected into contralateral GMs of *mdx*/scid mice to serve as our control. Mice were sacrificed after 4 weeks, and GMs were frozen in liquid nitrogen. Immunostaining with anti-mouse dystrophin antibody (Abcam Inc.) was performed to detect dystrophin-positive myofibers that regenerated from transplanted cells.

To examine whether the injection of MSTN induced TGF-β1 expression, we injected MSTN (1000 ng in 10 μl of PBS) into the non-injured GM of WT mice. Contralateral GMs were injected with 10 μl of PBS and served as a control. Three WT mice were used at each time point. Mice injected with MSTN were sacrificed at 4, 10, 24, and 48 h after injection ($n = 3$ for each time point). Immunohistochemical staining was performed to detect MSTN and TGF-β1 expression in muscle fibers.

Immunohistochemistry—Frozen GMs were sectioned at 10-μm thickness, and immunohistochemical analysis was performed to detect MSTN and TGF-β1 expression. Tissue sections were fixed in 4% formalin for 5 min followed by two 10-min washes with PBS. The sections were then blocked with 10% HS for 1 h. The rabbit MSTN primary antibody was diluted 1:100 in 2% HS and incubated with sections overnight at 4 °C. The following day, the sections were washed three times with PBS and then incubated with the secondary antibody, goat anti-rabbit IgG conjugated with Cy3 (Sigma). The Mouse-on-Mouse immunodetection kit (M.O.M., Vector Laboratories, Inc.) was then used to stain for TGF-β1 following the manufacturer's protocol. The slides were incubated with M.O.M. blocking reagent for 1 h, washed with PBS, and then incubated with M.O.M. diluent for 5 min. TGF-β1-specific primary antibodies (Vector Laboratories, Inc.) were diluted 1:150 in the M.O.M. diluent and incubated with the slides for 30 min. After washing with PBS, the sections were incubated with anti-mouse IgG conjugated with fluorescein isothiocyanate (diluted 1:200 with M.O.M. diluent, Sigma) for 1 h. Hoechst 33258 dye was used to stain the nuclei. In a separate experiment following a similar procedure, polyclonal rabbit anti-DCN IgG (LF-113, National Institute of Dental Research, Bethesda, MD) was used to stain tissue sections of WT and MSTN$^{-/-}$ GMs 2 weeks after laceration.

Statistical Analysis—All of the results from this study are expressed as the mean $\pm$ S.D. The differences between means were considered statistically significant if $p < 0.05$. The Student's t test was used to compare the difference in skeletal muscle regeneration, fibrosis formation between MSTN$^{-/-}$ and WT mice, and the myogenic differentiation capacity between MSTN$^{-/-}$ and WT LTP cells. All other data were analyzed by analysis of variance followed by post hoc Tukey's multiple comparison test. *Error bars* on the figures represent the $\pm$S.D. (*, $p < 0.05$; **, $p < 0.01$).

RESULTS

Effects of MSTN on Fibroblasts—MTT proliferation tests showed that, after 48 h of incubation, MSTN significantly stimulated the proliferation of PP1 and NIH3T3 fibroblasts in a dose-dependent manner (Fig. 1*A*). α-SMA, the actin isoform originally found in contractile vascular smooth muscle cells, has been the most reliable marker of myofibroblasts to date (24). Western blot analysis indicated that MSTN (100 and 200 ng/ml) increased α-SMA expression in PP1 and NIH3T3 fibroblasts (Fig. 1*B*). Q-RT-PCR revealed that MSTN stimulated procollagen (type Iα1, Iα2, and IIIα1) mRNA expression at 48 h (Fig. 1*C*). Additionally, MSTN stimulated the expression of FN

protein, a component of the extracellular matrix (ECM), in PP1 fibroblasts (Fig. 1*D*).

MSTN Expression in Injured Skeletal Muscle—After laceration injury, different time points were selected to detect MSTN expression in GMs. The degenerative and repair remodeling phases were represented by post-injury time points of 1–3 and 5–30 days following injury, respectively. Immunostaining for MSTN indicated MSTN expression within degenerative myofibers at 1 and 3 days after the injury (data not shown). On day 5, by the time a majority of newly regenerating myofibers was seen, faint MSTN signals were detected in the cytoplasm of regenerating centro-nucleated myofibers (*red fluorescence* and *white arrowheads*), whereas green collagen IV immunostaining indicates basal lamina of myofibers (Fig. 2*A*). MSTN expression was also observed in the nuclei of both the mononuclear cells (*white arrows*) and the regenerating centro-nucleated myofibers (Fig. 2*A*), which is especially obvious in the enlarged image (*white arrowhead* Fig. 2*A*, *inset*). On day 7 (Fig. 2*B*), a decrease in MSTN expression within most of the regenerating myofiber cytoplasm was seen (*white arrowheads*), whereas some myotubes without intact basal lamina were strongly stained with MSTN antibody, which is increased 14 days post-injury (*white arrows*, Fig. 2*C*). The nuclei of myofibers remained MSTN-positive (*yellow arrowhead*, Fig. 2, *B* and *C*, *insets*). MSTN staining disappeared from most regenerated myofibers 30 days after laceration (*white arrowheads*, Fig. 2*D*). Fig. 2, *E*, *F*, *G*, and *H*, depict negative controls of injured muscle at 5, 7, 14, and 30 days after laceration, respectively, where the MSTN antibody was replaced by the non-immune rabbit IgG. Collagen type IV was also stained on these samples to visualize the basal lamina.

Reduced Fibrosis and Enhanced Skeletal Muscle Regeneration in MSTN$^{-/-}$ Mice after Laceration—At 2 weeks following injury, we observed extensive deposition of collagenous tissue in the WT and MSTN$^{-/-}$ mice (data not shown). After 4 weeks, the deepest area of the injured site was filled with regenerating myofibers of large diameter, and the fibrotic region was limited to the superficial zone of the laceration site (Fig. 3*A*). We observed fewer fibrotic connective tissue deposits between regenerating myofibers in the injured muscle of MSTN$^{-/-}$ mice compared with the prominent scar region in the injured WT mouse muscle (Fig. 3*A*). Quantification of fibrotic tissue (*i.e.* the ratio of the fibrotic area to the cross-sectional area) revealed that there was a significantly smaller fibrous area in MSTN$^{-/-}$ skeletal muscle as compared with WT skeletal muscle at 2 weeks (11.5 $\pm$ 3.5% *versus* 15.3 $\pm$ 3.1%; $p < 0.01$) and at 4 weeks (2.1 $\pm$ 0.4 *versus* 6.3 $\pm$ 2.1; $p < 0.01$) after injury (Fig. 3*B*).

We used the minor axis diameter (smallest diameter) of centro-nucleated regenerating myofibers to evaluate skeletal muscle regeneration after laceration injury. At 2 weeks after GM laceration, regenerating myofibers were relatively small (data not shown). At 4 weeks, some large, mature myofibers could be observed among the small, centro-nucleated, regenerating myofibers (Fig. 3*C*). Quantification showed that MSTN$^{-/-}$-regenerating myofibers had diameters 38.8% larger than WT myofibers (36.1 $\pm$ 2.5 μm *versus* 26.0 $\pm$ 2.2 μm, $p < 0.01$) at 2 weeks after laceration, and the mean diameter of regenerating myofibers in MSTN$^{-/-}$ mice remained 21.1% larger than the

A.
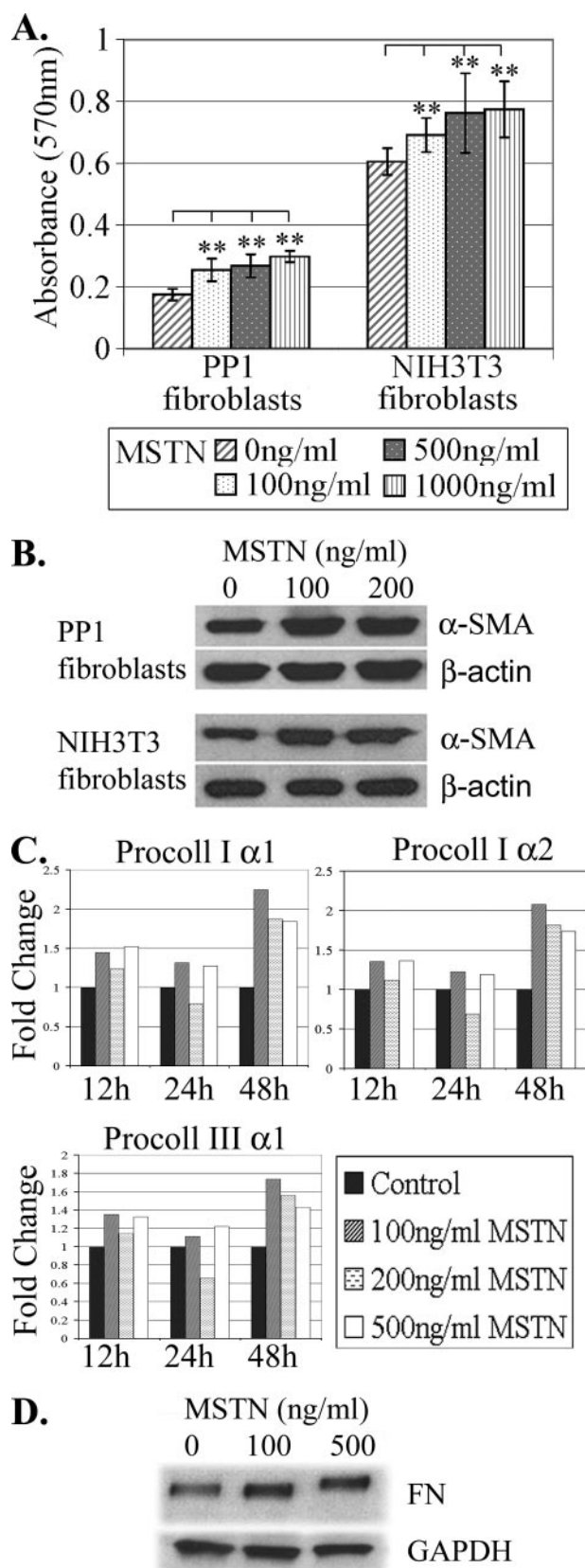

B.

C.

D.

FIGURE 1. **MSTN stimulated fibroblast proliferation and fibrotic protein expression in fibroblasts.** *A*, both muscle-derived fibroblasts (*PP1*) and NIH3T3 fibroblasts were cultured with MSTN, varying in concentration from 0 to 1000 ng/ml for 48 h. Cell proliferation was determined by MTT assay. These results are presented as absorbance values (*n* = 6) of purple formazan crystal at 570 nm, which directly correlates to the number of living cells. Fibroblasts
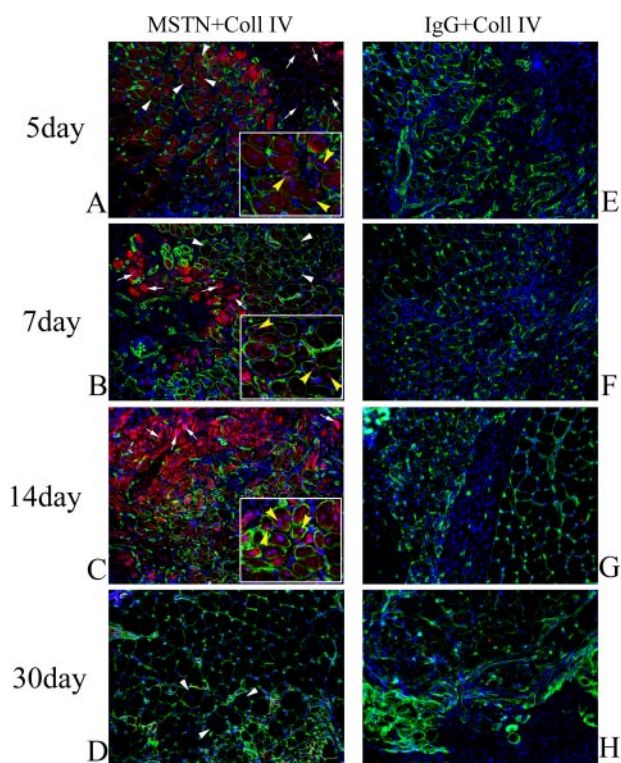

FIGURE 2. **MSTN localization in injured GMs.** *A–H*, GMs from WT mice were harvested at different time points after laceration injury, and frozen sections were immunostained with rabbit anti-MSTN and goat anti-collagen type IV antibodies. MSTN, collagen IV, and cell nuclei are *red*, *green*, and *blue*, respectively (*A–D*). Non-immune rabbit IgG was used as negative control for rabbit anti-MSTN antibody (*E–H*), but were stained with the collagen type IV antibody. *A*, at 5 days, faint MSTN signals could be detected in the cytoplasm of newly formed myofibers (*white arrowheads*) with basal lamina, and a relatively higher MSTN staining can be observed in the nuclei of regenerating myofiber (*yellow arrowhead*) and mononuclear cells (*white arrow*). *B*, at 7 days, MSTN staining is not evident in the cytoplasm of most regenerating myofibers (*white arrowhead*), whereas some of the regenerating small myotubes without basal lamina show intense MSTN staining in the cytoplasm (*white arrows*). *Yellow arrowheads* in the *inset* indicate positive signal in nuclei of regenerating myofibers. *C*, at 14 days, there were more MSTN-positive myotubes without basal lamina (*white arrow*). *Yellow arrowheads* in the *inset* indicate positive signal in nuclei of regenerating myofibers. *D*, at 30 days, most of regenerating myofibers were MSTN-negative (*arrowheads*). (Magnification, ×200; *inset* magnification, ×400.)

mean diameter of regenerating myofibers in the WT mice (37.7 ± 2.7 μm *versus* 31.1 ± 1.8 μm, *p* < 0.01) 4 weeks after injury (Fig. 3*D*). The distribution of the regenerating myofiber diameters showed that there was an increase in the percentage of larger regenerating myofibers in MSTN$^{-/-}$ mice compared with WT mice (*e.g.* ~7.38% of regenerating myofiber diameters in MSTN$^{-/-}$ mice fell into a range of 50–55 μm *versus* 1.92% of those in WT mice).

Improved Myogenic Potential with MSTN$^{-/-}$ LTP Cells— LTP cells were isolated from WT and MSTN$^{-/-}$ mice. When we cultivated these MSTN$^{-/-}$ LTP cells in low serum medium, they differentiated into myotubes that were significantly larger

were cultured in DM for 2 days with the addition of various concentrations of MSTN. Expressions of different proteins were analyzed by Western blot. *B*, the expression of α-SMA in PP1 fibroblasts or NIH3T3 fibroblast is shown. *C*, Q-RT-PCR analysis of procollagen (types Iα1, Iα2, and IIIα1) mRNA expression in PP1 fibroblasts treated with MSTN. Results are presented as the ratio against the gene expression in the control. *D*, expression of FN in PP1 fibroblasts after MSTN treatment (*, *p* < 0.05; **, *p* < 0.01).
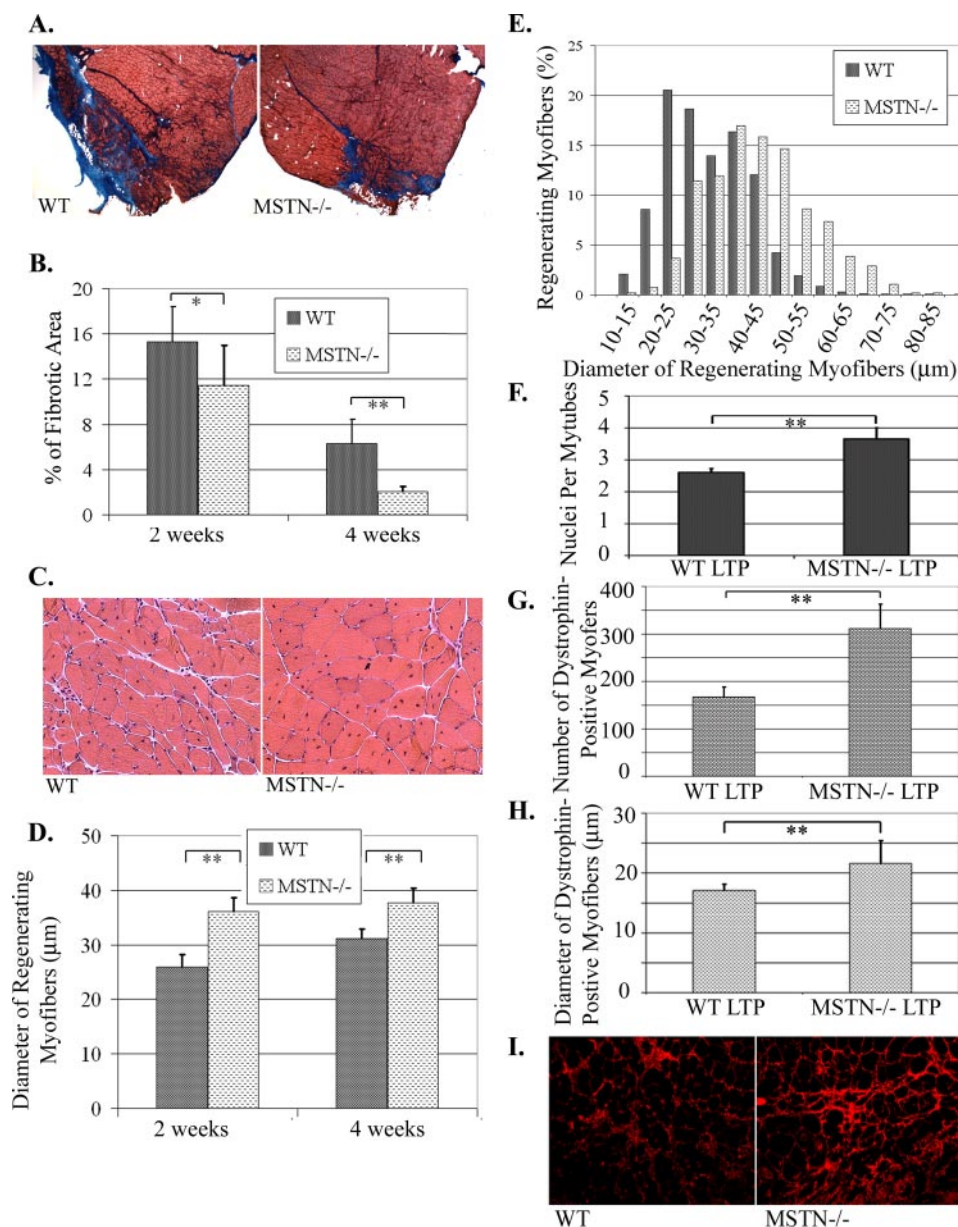
The Journal of Biological Chemistry

FIGURE 3. **Inhibition of MSTN favors skeletal muscle regeneration.** *A*, sections from injured WT and MSTN$^{-/-}$ GMs were stained with Masson's trichrome-staining protocol 4 weeks after laceration to determine fibrotic tissue levels. As a result, collagenous tissue is stained *blue*. *B*, quantification of fibrotic tissue of WT *versus* MSTN$^{-/-}$ GMs 2 and 4 weeks after laceration. *C*, myofibers in WT and MSTN$^{-/-}$ GMs were visualized by hematoxylin and eosin staining 4 weeks after laceration. Regenerating myofibers were distinguished by their centralized nuclei. *D*, quantification of the diameters of regenerating myofibers. *E*, the distribution of regenerating myofiber diameters at 4 weeks after laceration injury. *F*, myogenic differentiation capacity of WT and MSTN$^{-/-}$ LTP cell *in vitro*. *In vivo*, transplantation of MSTN$^{-/-}$ LTP into *mdx*/scid mice led to a high number of dystrophin-positive muscle fibers when compared with WT LTP. *G*, the number of dystrophin-positive myofibers was counted. *H*, the diameter of dystrophin-positive myofibers was measured. *I*, increased DCN immunostaining in injured skeletal muscle of MSTN$^{-/-}$ mice compared with WT mice 2 weeks after laceration. DCN (*red*) is detected in the ECM between myofibers. (Magnifications: in *C* and *I*, ×200; in *A*, ×100; *, $p < 0.05$; **, $p < 0.01$.)

(more nuclei per myotube, $n = 3$) than the myotubes formed by the fusion of WT LTP cells (Fig. 3*F*). When we injected the MSTN$^{-/-}$ LTP cells into the muscle of *mdx*/scid mice, they regenerated significantly more dystrophin-positive muscle fibers than did the WT LTP (Fig. 3*G*). These regenerating muscle fibers were also significantly larger in diameter (Fig. 3*H*).

Elevated DCN Expression in Injured MSTN$^{-/-}$ Mice—To investigate the underlying mechanism for improved muscle healing in MSTN$^{-/-}$ mice, we examined the expression of DCN, a molecule that has been shown to decrease fibrosis and enhance muscle regeneration (20, 27) in injured MSTN$^{-/-}$ skeletal muscle. Immunohistochemical staining revealed that there was more abundant DCN expression in the regenerating skeletal muscle of MSTN$^{-/-}$ mice than that of WT mice 2 weeks after injury (Fig. 3*I*). This higher level of DCN expression may be involved with the increased regeneration and decreased fibrosis observed in the injured muscle of MSTN$^{-/-}$ mice.

Relationship between TGF-β1 and MSTN$^{-/-}$—Western blot analysis showed that the levels of MSTN in C2C12 myoblasts treated with different concentrations of TGF-β1 were elevated in a dose-dependent manner when compared with non-treated controls, suggesting that TGF-β1 stimulates MSTN expression in C2C12 myoblasts (Fig. 4*A*). After incubation with increasing concentrations of recombinant MSTN protein, MSTN was shown to stimulate TGF-β1 expression in C2C12 myoblasts (especially with the highest dose) at 4 days post-stimulation (Fig. 4*B*). Furthermore, ELISA showed that MSTN significantly increased TGF-β1 secretion by C2C12 myoblasts in a dose-dependent manner at 2 and 4 days. After 4 days of stimulation with MSTN (500 ng/ml), C2C12 myoblasts secreted ~2-fold more TGF-β1 as compared with control cells (Fig. 4*C*). Q-RT-PCR revealed that MSTN (100, 200, and 500 ng/ml) also increased TGF-β1 mRNA expression 48 h post-stimulation (Fig. 4*D*).

PP1 fibroblasts did not express detectable MSTN protein. However, after treatment with MSTN (100 and 200 ng/ml) for 48 h, PP1 fibroblasts began to express MSTN as indicated by Western blot analysis (Fig. 4*E*). MSTN also stimulated MSTN expression in C2C12 myoblasts (Fig. 4*E*). MSTN-induced MSTN autocrine expression in PP1 fibroblasts is reduced by soluble TβRII, which blocks the TGF-β1 signaling pathway (Fig. 4*F*). Moreover, our results indicated that soluble TβRII was also able to restore MSTN-inhibited C2C12 myoblast differentiation (Fig. 4*G*). We also examined whether exogenous
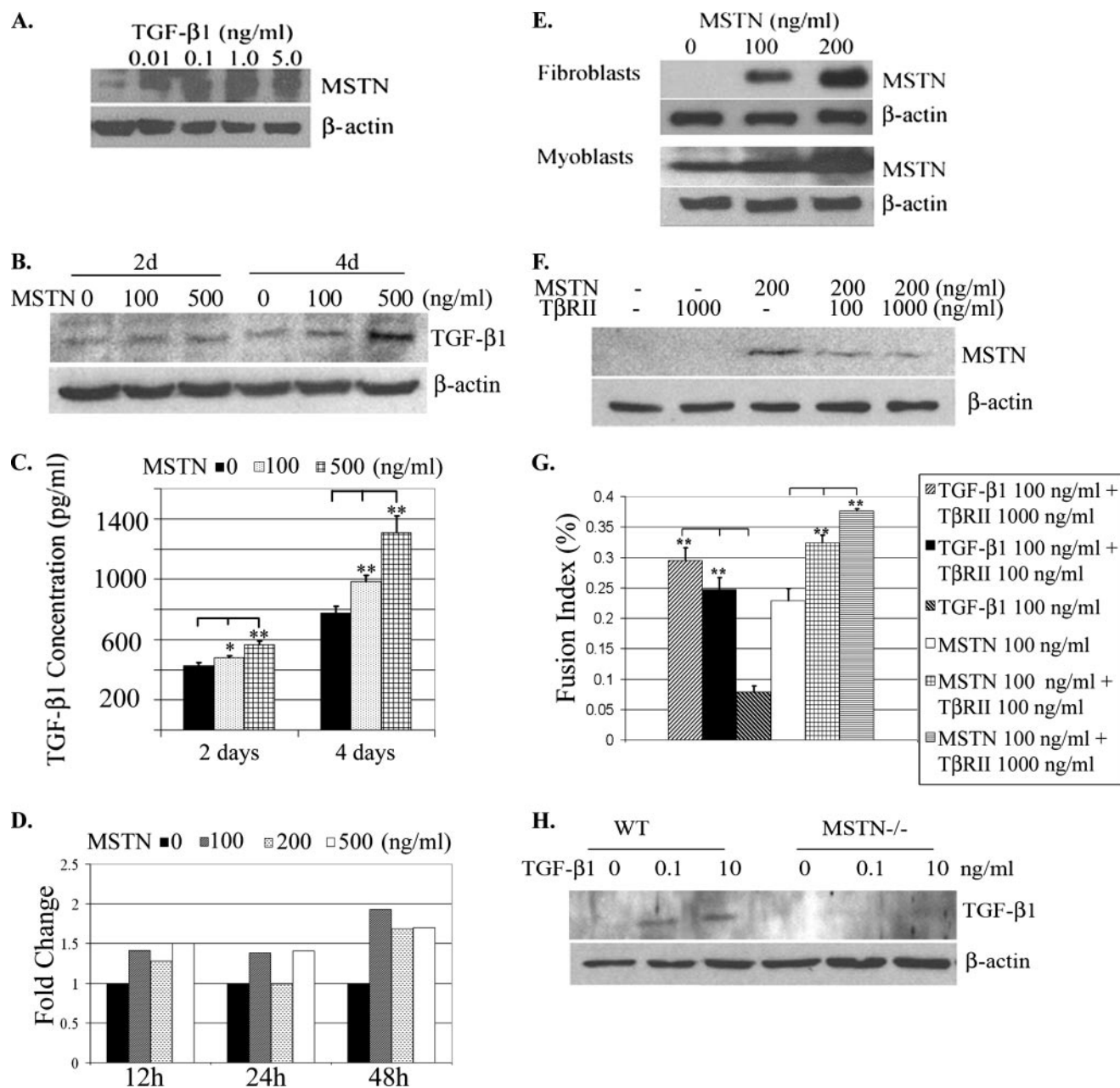
FIGURE 4. **The relationship between TGF-β1 and MSTN *in vitro*.** *A*, Western blot analysis of MSTN expression in C2C12 myoblasts treated with different concentrations of TGF-β1 ranging from 0 to 5.0 ng/ml for 48 h. *B*, C2C12 myoblasts were treated with different concentrations of MSTN in DM. Cell lysates were collected at 2 and 4 days to examine TGF-β1 expression by Western blot; *C*, while the conditioned medium was collected at the same time points, the levels of TGF-β1 in the medium were also analyzed by ELISA. *D*, Q-RT-PCR for TGF-β1 after MSTN treatment (100, 200, and 500 ng/ml) in PP1 fibroblasts. *E*, the level of MSTN expression in PP1 fibroblasts *and C2C12 myoblasts* treated with MSTN recombinant protein. *F*, Western blots were used to determine MSTN expression level in PP1 fibroblasts after cells were treated with either MSTN or both MSTN and soluble TβRII for 48 h. *G*, C2C12 myoblasts were cultured in DM with different treatments, TGF-β1, MSTN, TGF-β1 and TβRII, or MSTN and TβRII, for 4 days. Fusion indexes were used to access impacts of treatments on C2C12 myoblast differentiation. *H*, myoblasts isolated from WT, and MSTN$^{-/-}$ GMs were grown for 48 h under stimulation by TGF-β1. Western blot analysis was used to detect TGF-β1 expression in WT and MSTN $^{-/-}$ cells (*, $p < 0.05$; **, $p < 0.01$).

TGF-β1 recombinant protein was able to stimulate autocrine expression of TGF-β1 in MSTN$^{-/-}$ muscle cells as it does in C2C12 myoblasts (20). We observed that exogenous TGF-β1 could induce its autocrine expression in WT primary myoblasts but not on primary MSTN$^{-/-}$ myoblasts (Fig. 4*H*).

In vivo, We observed co-expression of TGF-β1 (*green*) and MSTN (*red*) in degenerative myofibers 1 and 3 days after laceration injury (*white arrow*, Fig. 5*A*). By day 5, MSTN was

detected mainly in the nuclei of the regenerating myofibers (*white arrowhead*) with the exception of a few MSTN-positive necrotic myofibers, whereas TGF-β1 was present in the surrounding ECM (*white arrow*). MSTN was still detected in the nuclei of regenerating myofibers 21 days after injury (*white arrow*, Fig. 5*A*). The injection of MSTN into non-injured GMs induced TGF-β1 expression in the myofibers at 4, 10, and 24 h after injection. As shown in Fig. 5*B*, MSTN (*red*) and TGF-β1 (*green*) were co-expressed in myofibers at
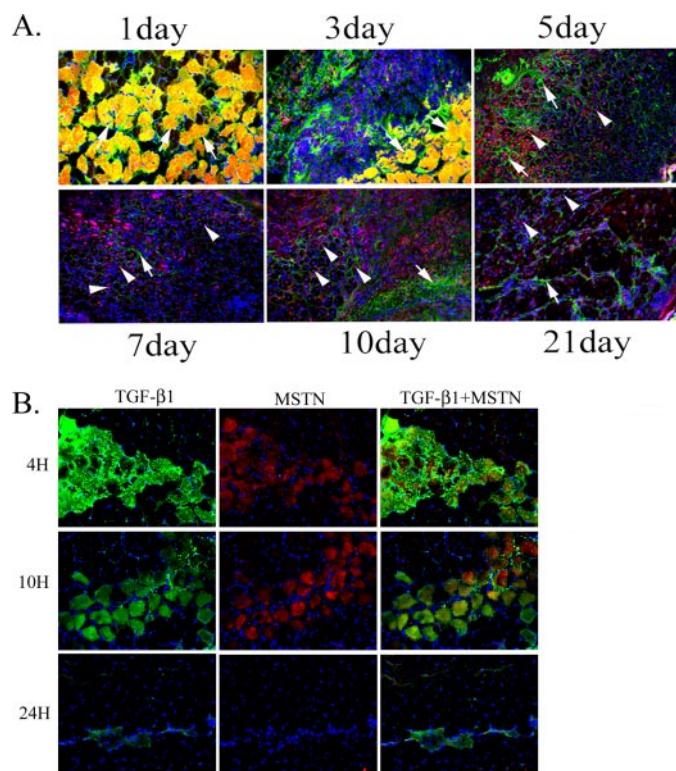
FIGURE 5. **The relationship between TGF-β1 and MSTN *in vivo.*** *A*, both GMs of each adult WT mouse underwent laceration injury. Mice GMs were harvested at the indicated times. Double staining of TGF-β1 (*green*) and MSTN (*red*) was performed. In the 1- and 3-day images, a *white arrow* indicates degenerative myofibers. At all other time points, the *white arrow* and *arrowhead* indicate ECM and nuclei of myofibers, respectively. *B*, co-localization of TGF-β1 and MSTN in myofibers after recombinant MSTN protein injection. We injected 1000 ng of MSTN protein in 10 μl of PBS into GMs of WT mice. Mice were sacrificed at different time points after injection. Frozen sections of GMs were double-stained with anti-TGF-β1 and anti-MSTN antibodies (magnification, ×200).

4 and 10 h. After 24 h, MSTN disappeared, and only a few TGF-β1-positive myofibers could be observed.

DCN Counteracts the Effect of MSTN—As previously shown in Fig. 1*A*, 0.1 μg/ml MSTN significantly stimulated PP1 fibroblast proliferation. This dosage was selected to examine whether DCN could reduce the proliferative influence of MSTN on PP1 fibroblasts. After PP1 fibroblasts were incubated with MSTN and exposed to varying concentrations of DCN for 48 h, MTT assay revealed that the addition of DCN significantly repressed the stimulatory effect of MSTN on PP1 proliferation in a dose-dependent manner as expected (Fig. 6*A*). These findings are comparable to a previous report showing that DCN blocked the stimulatory effect of TGF-β1 on PP1 fibroblasts (27).

Our earlier results indicated that MSTN induced its own expression, in an autocrine manner, in PP1 fibroblasts (Fig. 4*E*). Therefore, we examined the ability of DCN to block the MSTN autocrine expression in PP1 fibroblasts. As previously shown, PP1 fibroblasts that were not treated with MSTN failed to express detectable MSTN protein, whereas PP1 fibroblasts treated with MSTN showed a high level of MSTN expression in comparison to the control (Figs. 4*E* and 6*B*). However, DCN decreased MSTN autocrine expression by PP1 fibroblasts in a dose-dependent manner (Fig. 6*B*).

Our previous experiments showed that 1 μg/ml MSTN almost completely inhibited myoblast differentiation (data not shown). Therefore, we chose this dose to assess whether DCN treatment could reverse MSTN-inhibited myogenic differentiation in C2C12 cells. Except for the control cells, the cultures were treated with DCN alone or 1 μg/ml MSTN combined with increasing concentrations of DCN (0–50 μg/ml). Following a 5-day incubation, DCN-treated groups (data not shown) and controls showed widespread myosin heavy chain-positive myotubes, whereas cells treated with MSTN alone contained only a few myotubes (Fig. 6*C*). The addition of DCN reversed the inhibition of MSTN on myogenic differentiation, as indicated by the increase in the number and size of myotubes in comparison to the MSTN-treated group (Fig. 6*C*). Measurements showed that DCN treatment promoted C2C12 myoblast differentiation by significantly increasing fusion indexes in a dose-dependent manner (Fig. 6*D*), suggesting that DCN attenuated the inhibitory effect of MSTN and, thereby, stimulated myoblast fusion.

Inhibitory Effects of DCN on MSN May Be Mediated by FLST—To further explore whether DCN regulated MSTN activity via an intermediate molecule, we investigated the effect of DCN on the expression of FLST, which is able to bind to MSTN and suppress its activity (46). We found an up-regulation of FLST expression by C2C12 myoblasts 48 and 72 h after addition of 10 μg/ml DCN (Fig. 7*A*). Our results also revealed the ability of FLST to stimulate myogenic differentiation, which was demonstrated by the presence of larger myotubes containing more nuclei in comparison to the control group (Fig. 7*B*). In a dose-dependent manner, FLST treatment led to a significant increase in fusion index (Fig. 7*C*) compared with the control group, suggesting that FLST promotes myogenic differentiation and accelerates the maturation of myotubes.

DISCUSSION

MSTN has been drawing more and more attention due to mounting evidence indicating that inhibition of MSTN significantly improves skeletal muscle diseases such as muscle dystrophy. But, the role of MSTN in injured skeletal muscle and its relationships with other molecules such as TGF-β1 and DCN (important key factors in muscle healing) remain unknown. Recent studies reported by Yamanouchi *et al.* (47) highlight the expression of MSTN in fibroblasts in injured skeletal muscle, suggesting that fibroblasts may be a source of MSTN. Previously, we have shown that TGF-β1 significantly promotes proliferation of PP1 fibroblasts (27). Here, our *in vitro* study shows that MSTN activates fibroblasts by stimulating fibroblast proliferation and inducing their expression of α-SMA analogous to that of TGF-β1. Like TGF-β1 (48), MSTN may transiently attract fibroblasts into an injury site, further inducing them to express MSTN in an autocrine fashion; they then differentiate into myofibroblasts, thereby accelerating the deposition of the ECM. Researchers widely believe that prolonged presence and excessive activity of myofibroblasts is associated with the abnormal accumulation of ECM components in injured and diseased tissue (49, 50). Moreover, MSTN has been shown to induce procollagen (types Iα1, Iα2, and IIIα1), mRNA, and FN protein expression in PP1 fibroblasts. McCroskery *et al.* (51) recently confirmed the correlation of MSTN expression to the
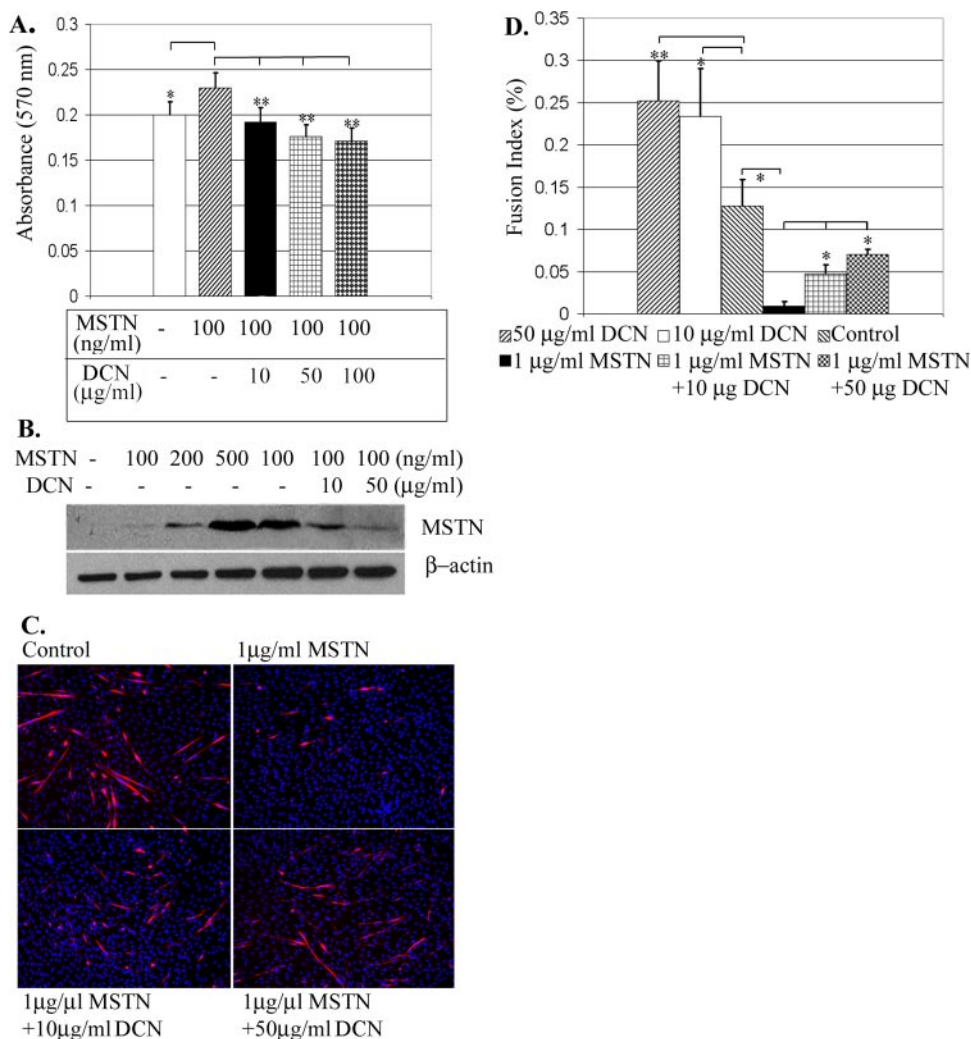
FIGURE 6. **DCN blocks the effects of MSTN on PP1 fibroblasts and C2C12 myoblasts.** *A*, PP1 fibroblasts were treated for 48 h with 100 ng/ml MSTN or combinations of MSTN and DCN. Non-treated cell cultures were used as a control. MTT assay was performed to assess cell proliferation. *B*, after incubation of PP1 fibroblasts with MSTN, or a combination of MSTN and DCN, Western blot analysis was performed to determine whether DCN reduced the autocrine expression of MSTN in PP1 fibroblasts stimulated with MSTN. *C*, C2C12 myoblasts were cultured without treatment, with 1 μg/ml MSTN alone, or co-incubated with 1 μg/ml MSTN and different concentrations of DCN for 5 days. Myotubes were monitored by anti-skeletal myosin heavy chain immunostaining; nuclei were stained by Hoechst 33258 (magnification, ×100). *D*, fusion indexes were determined to estimate the differentiation capacity of C2C12 myoblasts in response to different treatments.

muscle displays less fibrosis than WT muscle after injury, the expression levels of TGF-β1 in injured WT mice *versus* that expressed in injured MSTN$^{-/-}$ mice should be compared more closely.

As members of the TGF-β superfamily, TGF-β1 and MSTN share many similarities in structure, signaling pathway, and function (52, 53). It has also been shown that TGF-β1 plays a critical role in skeletal muscle fibrosis after injury (20, 26–32). Because both TGF-β1 and MSTN promote fibrosis, it is very important to understand the potential relationships between these two molecules. Recent reports demonstrated that exogenous TGF-β1 strongly stimulated the expression of MSTN in C2C12 myoblasts (44). In fact, our *in vitro* data show that TGF-β1 increases MSTN expression in C2C12 myoblasts (and *vice versa*), and TGF-β1 and MSTN are found to co-localize in the same myofibers shortly after MSTN injection or after injury.

We found that MSTN is able to induce its autocrine expression in both fibroblasts and myoblasts. In the presence of soluble TβRII, MSTN autocrine expression in fibroblasts is decreased. We have known that MSTN inhibits C2C12 myoblast differentiation. When TβRIIs are blocked by soluble TβRII, the ability of MSTN to inhibit C2C12 myoblast differentiation is reduced. Apart from that, Q-RT-PCR results show that MSTN also stimulates TGF-β1 mRNA expression in PP1 fibroblasts. Our previous study has shown that TGF-β1 is able to induce autocrine expression of TGF-β1 in C2C12 myoblasts (20), nevertheless, our present data revealed that TGF-β1 failed to induce its autocrine expression in MSTN$^{-/-}$ primary muscle cells. Although TGF-β1 and MSTN may target different cell membrane receptors (52), our results suggest that they may also bind to the same receptor, indicating that their signaling may be somehow related. It is likely, then, that the inducement of skeletal muscle fibrosis by TGF-β1 is partially mediated by its interaction with MSTN. However, the mechanism by which TGF-β1 interacts with MSTN to cause fibrosis warrants further investigation.

Satellite cells serve as a reservoir of myogenic progenitor cells for the repair and maintenance of skeletal muscle. MSTN negatively regulates self-renewal and differentiation of satellite
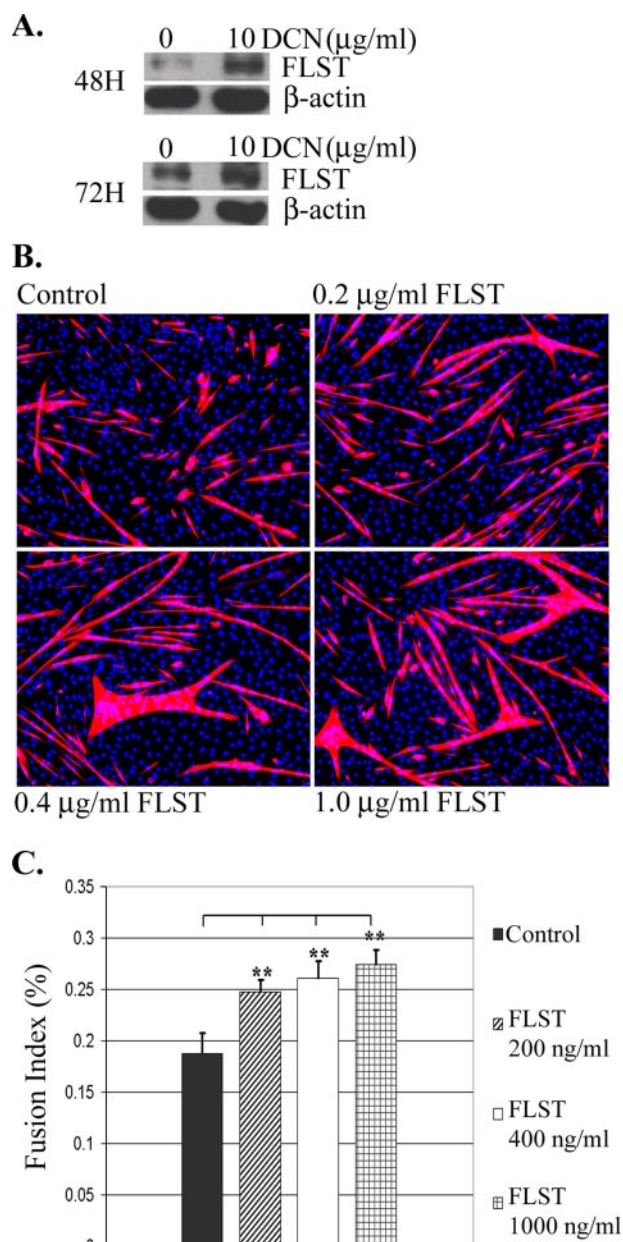
formation of fibrosis by showing less fibrosis formation in the notexin-damaged tibialis anterior muscle in MSTN$^{-/-}$ mice 4 weeks after injury as compared with WT mice. Given the results collected in our *in vitro* study, we hypothesized that a lack of MSTN in knock-out mice would decrease the proliferation of fibroblasts and reduce their production of collagenous tissue in injured skeletal muscle. This was made evident by a significant decrease in the formation of fibrosis in MSTN$^{-/-}$ mice at 2 and 4 weeks after injury when compared with WT mice. Moreover, we found an elevated expression level of DCN, an inhibitor of TGF-β1, in injured MSTN$^{-/-}$ skeletal muscles compared with injured WT muscles at 2 weeks after injury. In accordance with this result, increased DCN mRNA has been observed in regenerating MSTN$^{-/-}$ muscle (51). Increased DCN might inhibit the effect of TGF-β1, thereby partially explaining the reduced fibrosis and enhanced regeneration in injured MSTN$^{-/-}$ muscle. To understand the mechanism by which MSTN$^{-/-}$

FIGURE 7. **The elevated FLST expression by DCN and the capacity of FLST to enhance myogenic differentiation of C2C12 myoblasts.** *A*, DCN increased the expression of FLST in C2C12 myoblasts 48 and 72 h after treatment. *B*, immunofluorescence analysis of myotubes. C2C12 myoblasts were maintained in DM for 5 days in the presence of different concentrations of FLST. Myotubes were double-labeled with an antibody recognizing skeletal myosin heavy chain and with the fluorescent nuclear dye Hoechst 33258 (magnification, ×100). *C*, fusion indexes were calculated to evaluate the degree of C2C12 myoblast differentiation upon FLST stimulation.

cells (54) and decreases the expression of members of the basic helix-loop-helix muscle regulatory factors (MRF) (MyoD, Myf5, mrf4, and myogenin) (43, 55). MSTN$^{-/-}$ mice show an increased number of satellite cells activated and differentiated toward a myogenic lineage (54). In this study, our data demonstrate that MSTN$^{-/-}$ mice contain regenerating myofibers with significantly larger diameters than WT mice at 2 and 4 weeks after GM laceration. The increased number of satellite cells in MSTN$^{-/-}$ mice could, in part, explain the enhanced regeneration revealed by the larger diameter of regenerated

myofibers in MSTN$^{-/-}$ mice compared with WT mice. Indeed, it has been reported that blocking MSTN signals by isolating myoblasts from transgenic mice carrying the mutated MSTN receptor results in improved success of myoblast transplantation in *mdx* mice compared with normal myoblasts (56). Our results show that MSTN$^{-/-}$ LTP more readily undergo myogenic differentiation *in vitro* and regenerate skeletal muscle *in vivo* in a more effective manner than wild-type cells.

Furthermore, high levels of MSTN protein have been reported within necrotic fibers in the skeletal muscles of rats damaged by notexin (57), and Western blot analysis revealed the up-regulation of MSTN protein at early time points following notexin-induced injury in rat skeletal muscle (58). Interestingly, it has been shown that MSTN interferes with the chemotaxis of macrophages *in vitro* (51); recombinant MSTN protein significantly reduces the migration of macrophages and myoblasts toward chemoattractants *in vitro*, which likely promotes skeletal muscle regeneration (51). These results suggest that MSTN could impede recruitment of macrophages and myoblasts into the injured site *in vivo*. Macrophages infiltrate damaged tissue to remove debris that could hinder muscle regeneration. Macrophages also secrete a variety of growth factors and cytokines that have chemotactic and/or mitogenic effects on muscle precursor cells, thereby accelerating muscle regeneration (59–63). Compared with WT mice, MSTN$^{-/-}$ mice have shown elevated recruitment of macrophages and myoblasts and an accelerated inflammatory response after muscle injury (51). These results suggest that the earlier initiation of skeletal muscle regeneration in the injured skeletal muscle of MSTN$^{-/-}$ mice compared with the injured muscle of WT mice may be due, in part, to accelerated removal of muscle debris. When we monitored the expression of MSTN at the injured site for up to 30 days after injury, we observed an intense expression of MSTN in the cytoplasm of degenerative myofibers 1 and 3 days after laceration. On day 5 after injury, MSTN signal was detected in the cytoplasm of regenerating myofibers. Our results show that the MSTN signal decreases with maturation of regenerating myofibers. Interestingly, there is strong MSTN immunostaining in regenerating small myotubes lacking basal lamina 7 and 14 days post-injury. During skeletal muscle healing (following active muscle regeneration at early time points after injury) fibrosis initiates ~1 week post-injury, and peaks at 4 weeks (10, 15, 64). Li *et al.* (20) reported that some regenerating myofibers probably differentiate into myofibroblasts to contribute the formation of fibrosis. This correlation between fibrosis development and increased MSTN and TGF-β1 expression (20) in the early phase of healing may suggest the differentiation of regenerating myotubes/myofibers into myofibroblasts and a potential interaction between TGF-β1, MSTN, and DCN, as previously hypothesized (65).

MSTN-positive signals were also seen within the nuclei of the newly formed fibers at 5, 7, and 10 days post-injury. The nuclear localization of MSTN is supported by previous studies indicating that MSTN was detected in the nuclei of myoblasts and myotubes (66). Consequently, MSTN protein might modulate the muscle fiber regeneration process through the early events of phagocytosis and inflammation (57) and later control myofiber maturation. In this way, MSTN seems to act as a reg-

ulatory molecule that is produced by the tissue to specifically suppress and control the size of muscle growth and development (67).

DCN, a small chondroitin-dermatan sulfate leucine-rich proteoglycan, exists ubiquitously in the ECM. Due to its binding to and inhibition of TGF-β1, DCN has been used as a potent anti-fibrosis agent in various organs and tissues (26, 27, 37–40), including skeletal muscle (26, 27). However, the ability of DCN to regulate MSTN activity is still unknown. DCN, which is composed of a core protein and a single glycosaminoglycan chain (68, 69), has the ability to bind to TGF-β1 due to the fact that the core protein of DCN contains two binding sites for TGF-β1 (70). Similarly, Miura *et al.* (65) have shown that DCN, or the core protein of DCN, directly binds to active MSTN molecules to block MSTN-mediated inhibition of C2C12 myoblast proliferation. The actual location of the MSTN binding site in the DCN core protein and evidence that shows whether TGF-β1 and MSTN competitively bind to DCN are topics for further investigation. Of further interest is the possibility that DCN may regulate MSTN by influencing another intermediate molecule like FLST, an antagonist of MSTN (46). Our results not only show that DCN reduces the effects of MSTN on fibroblasts and myoblasts, but also indicates that it stimulates the expression of FLST in C2C12 myoblasts. Exogenous FLST then stimulates C2C12 myoblast differentiation, which is probably due to FLST's neutralization of endogenous MSTN. These results indicate that the effect of DCN on MSTN may be related to the up-regulation of FLST, which would consequently suppress MSTN activity. Nevertheless, more experiments that would, for example, examine the effect of DCN on FLST knock-out cells, need to be done to establish the role of FLST in DCN-inhibited MSTN activity. Furthermore, we have shown that TGF-β1 probably plays a role in the MSTN signaling pathway, because TGF-β1-soluble receptor antagonizes, at least in part, the effect of myostatin on muscle cells. Overall, DCN probably regulates MSTN activity via three ways: (i) directly binding MSTN, (ii) indirectly down-regulate MSTN by binding to TGF-β1, and (iii) indirectly down-regulating MSTN by stimulating FLST expression.

In summary, our results suggest the following: (i) MSTN stimulates the formation of fibrosis in skeletal muscle after injury, (ii) TGF-β1 and MSTN up-regulate the expression level of each other, and (iii) DCN is capable of inhibiting MSTN activity as it does for TGF-β1. These results, combined with the fact that TGF-β1 plays a key role in skeletal muscle fibrosis and that DCN reduces fibrosis in injured skeletal muscle, suggest that TGF-β1 and MSTN probably act together; they synergistically amplify the fibrotic process in injured or diseased skeletal muscles resulting in greater fibrosis than either could induce individually.

Our findings may help to further increase the understanding of the mechanism by which MSTN$^{-/-}$ mice show decreased fibrosis and enhanced regeneration after injury and suggest that the inhibition of MSTN might be a new therapeutic approach for improving skeletal muscle healing through enhancement of regeneration and reduction of fibrosis.

REFERENCES

1. Beiner, J. M., and Jokl, P. (2001) *J. Am. Acad. Orthop. Surg.* **9,** 227–237
2. Garrett, W. E., Jr. (1996) *Am. J. Sports Med.* **24,** Suppl. 6, S2–S8
3. Jarvinen, M. J., and Lehto, M. U. (1993) *Sports Med.* **15,** 78–89
4. McLennan, I. S. (1985) *Exp. Neurol* **89,** 616–621
5. McLennan, I. S. (1987) *Muscle Nerve* **10,** 801–809
6. Mishra, D. K., Friden, J., Schmitz, M. C., and Lieber, R. L. (1995) *J. Bone Joint Surg. Am.* **77,** 1510–1519
7. Obremsky, W. T., Seaber, A. V., Ribbeck, B. M., and Garrett, W. E., Jr. (1994) *Am J. Sports Med.* **22,** 558–561
8. Shen, W., Li, Y., Tang, Y., Cummins, J., and Huard, J. (2005) *Am J. Pathol.* **167,** 1105–1117
9. Schultz, E., Jaryszak, D. L., and Valliere, C. R. (1985) *Muscle Nerve* **8,** 217–222
10. Li, Y., Cummins, H. J., and Huard, J. (2001) *Curr. Opin. Orthop.* **12,** 409–415
11. Huard, J., Li, Y., and Fu, F. H. (2002) *J. Bone Joint Surg. Am.* **84-A,** 822–832
12. Jarvinen, M. (1975) *Acta Pathol. Microbiol. Scand. A* **83,** 269–282
13. Jarvinen, M. (1976) *Acta Chir. Scand.* **142,** 47–56
14. Jarvinen, M., and Sorvari, T. (1975) *Acta Pathol. Microbiol. Scand. A* **83,** 259–265
15. Lehto, M., Jarvinen, M., and Nelimarkka, O. (1986) *Arch. Orthop. Trauma Surg.* **104,** 366–370
16. Border, W. A., and Noble, N. A. (1994) *N. Engl. J. Med.* **331,** 1286–1292
17. Lijnen, P. J., Petrov, V. V., and Fagard, R. H. (2000) *Mol. Genet. Metab.* **71,** 418–435
18. Waltenberger, J., Lundin, L., Oberg, K., Wilander, E., Miyazono, K., Heldin, C. H., and Funa, K. (1993) *Am. J. Pathol.* **142,** 71–78
19. Yamamoto, T., Noble, N. A., Miller, D. E., and Border, W. A. (1994) *Kidney Int.* **45,** 916–927
20. Li, Y., Foster, W., Deasy, B. M., Chan, Y., Prisk, V., Tang, Y., Cummins, J., and Huard, J. (2004) *Am. J. Pathol.* **164,** 1007–1019
21. Bernasconi, P., Torchiana, E., Confalonieri, P., Brugnoni, R., Barresi, R., Mora, M., Cornelio, F., Morandi, L., and Mantegazza, R. (1995) *J. Clin. Invest.* **96,** 1137–1144
22. Gosselin, L. E., Williams, J. E., Deering, M., Brazeau, D., Koury, S., and Martinez, D. A. (2004) *Muscle Nerve* **30,** 645–653
23. Desmouliere, A., Geinoz, A., Gabbiani, F., and Gabbiani, G. (1993) *J. Cell Biol.* **122,** 103–111
24. Tomasek, J. J., Gabbiani, G., Hinz, B., Chaponnier, C., and Brown, R. A. (2002) *Nat. Rev. Mol. Cell. Biol.* **3,** 349–363
25. Li, Y., and Huard, J. (2002) *Am. J. Pathol.* **161,** 895–907
26. Sato, K., Li, Y., Foster, W., Fukushima, K., Badlani, N., Adachi, N., Usas, A., Fu, F. H., and Huard, J. (2003) *Muscle Nerve* **28,** 365–372
27. Fukushima, K., Badlani, N., Usas, A., Riano, F., Fu, F., and Huard, J. (2001) *Am. J. Sports Med.* **29,** 394–402
28. Foster, W., Li, Y., Usas, A., Somogyi, G., and Huard, J. (2003) *J. Orthop. Res.* **21,** 798–804
29. Chan, Y. S., Li, Y., Foster, W., Horaguchi, T., Somogyi, G., Fu, F. H., and Huard, J. (2003) *J. Appl. Physiol.* **95,** 771–780
30. Chan, Y. S., Li, Y., Foster, W., Fu, F. H., and Huard, J. (2005) *Am. J. Sports Med.* **33,** 43–51
31. Li, Y., Negishi, S., Sakamoto, M., Usas, A., and Huard, J. (2005) *Ann. N. Y. Acad. Sci.* **1041,** 395–397
32. Negishi, S., Li, Y., Usas, A., Fu, F. H., and Huard, J. (2005) *Am. J. Sports Med.* **33,** 1816–1824
33. Wagner, K. R., McPherron, A. C., Winik, N., and Lee, S. J. (2002) *Ann. Neurol.* **52,** 832–836
34. McPherron, A. C., Lawler, A. M., and Lee, S. J. (1997) *Nature* **387,** 83–90
35. McPherron, A. C., and Lee, S. J. (1997) *Proc. Natl. Acad. Sci. U. S. A.* **94,**

12457–12461

36. Williams, M. S. (2004) *N. Engl. J. Med.* **351,** 1030–1031; author reply 1030–1031

37. Giri, S. N., Hyde, D. M., Braun, R. K., Gaarde, W., Harper, J. R., and Pierschbacher, M. D. (1997) *Biochem. Pharmacol.* **54,** 1205–1216

38. Grisanti, S., Szurman, P., Warga, M., Kaczmarek, R., Ziemssen, F., Tatar, O., and Bartz-Schmidt, K. U. (2005) *Invest. Ophthalmol. Vis. Sci.* **46,** 191–196

39. Huijun, W., Long, C., Zhigang, Z., Feng, J., and Muyi, G. (2005) *Exp. Mol. Pathol.* **78,** 17–24

40. Shimizu, I. (2001) *Curr. Drug. Targets Infect. Disord.* **1,** 227–240

41. Qu-Petersen, Z., Deasy, B., Jankowski, R., Ikezawa, M., Cummins, J., Pruchnic, R., Mytinger, J., Cao, B., Gates, C., Wernig, A., and Huard, J. (2002) *J. Cell Biol.* **157,** 851–864

42. Thomas, M., Langley, B., Berry, C., Sharma, M., Kirk, S., Bass, J., and Kambadur, R. (2000) *J. Biol. Chem.* **275,** 40235–40243

43. Langley, B., Thomas, M., Bishop, A., Sharma, M., Gilmour, S., and Kambadur, R. (2002) *J. Biol. Chem.* **277,** 49831–49840

44. Budasz-Rwiderska, M., Jank, M., and Motyl, T. (2005) *J. Physiol. Pharmacol.* **56,** Suppl. 3, 195–214

45. Yamazaki, K., Fukata, H., Adachi, T., Tainaka, H., Kohda, M., Yamazaki, M., Kojima, K., Chiba, K., Mori, C., and Komiyama, M. (2005) *Mol. Reprod. Dev.* **72,** 291–298

46. Amthor, H., Nicholas, G., McKinnell, I., Kemp, C. F., Sharma, M., Kambadur, R., and Patel, K. (2004) *Dev. Biol.* **270,** 19–30

47. Yamanouchi, K., Soeta, C., Naito, K., and Tojo, H. (2000) *Biochem. Biophys. Res. Commun.* **270,** 510–516

48. Pierce, G. F., Mustoe, T. A., Lingelbach, J., Masakowski, V. R., Griffin, G. L., Senior, R. M., and Deuel, T. F. (1989) *J. Cell Biol.* **109,** 429–440

49. Phan, S. H. (2002) *Chest* **122,** Suppl. 6, 286S–289S

50. Thannickal, V. J., Toews, G. B., White, E. S., Lynch, J. P., 3rd, and Martinez, F. J. (2004) *Annu Rev. Med.* **55,** 395–417

51. McCroskery, S., Thomas, M., Platt, L., Hennebry, A., Nishimura, T., McLeay, L., Sharma, M., and Kambadur, R. (2005) *J. Cell Sci.* **118,** 3531–3541

52. Rebbapragada, A., Benchabane, H., Wrana, J. L., Celeste, A. J., and Attisano, L. (2003) *Mol. Cell. Biol.* **23,** 7230–7242

53. Zhu, X., Topouzis, S., Liang, L. F., and Stotish, R. L. (2004) *Cytokine* **26,** 262–272

54. McCroskery, S., Thomas, M., Maxwell, L., Sharma, M., and Kambadur, R. (2003) *J. Cell Biol.* **162,** 1135–1147

55. Joulia, D., Bernardi, H., Garandel, V., Rabenoelina, F., Vernus, B., and Cabello, G. (2003) *Exp. Cell Res.* **286,** 263–275

56. Benabdallah, B. F., Bouchentouf, M., and Tremblay, J. P. (2005) *Transplantation* **79,** 1696–1702

57. Kirk, S., Oldham, J., Kambadur, R., Sharma, M., Dobbie, P., and Bass, J. (2000) *J. Cell. Physiol.* **184,** 356–363

58. Mendler, L., Zador, E., Ver Heyen, M., Dux, L., and Wuytack, F. (2000) *J. Muscle Res. Cell Motil.* **21,** 551–563

59. Cantini, M., Massimino, M. L., Bruson, A., Catani, C., Dalla Libera, L., and Carraro, U. (1994) *Biochem. Biophys. Res. Commun.* **202,** 1688–1696

60. Chazaud, B., Sonnet, C., Lafuste, P., Bassez, G., Rimaniol, A. C., Poron, F., Authier, F. J., Dreyfus, P. A., and Gherardi, R. K. (2003) *J. Cell Biol.* **163,** 1133–1143

61. Lescaudron, L., Peltekian, E., Fontaine-Perus, J., Paulin, D., Zampieri, M., Garcia, L., and Parrish, E. (1999) *Neuromuscul. Disord.* **9,** 72–80

62. Merly, F., Lescaudron, L., Rouaud, T., Crossin, F., and Gardahaut, M. F. (1999) *Muscle Nerve* **22,** 724–732

63. Robertson, T. A., Maley, M. A., Grounds, M. D., and Papadimitriou, J. M. (1993) *Exp. Cell Res.* **207,** 321–331

64. Menetrey, J., Kasemkijwattana, C., Fu, F. H., Moreland, M. S., and Huard, J. (1999) *Am. J. Sports Med.* **27,** 222–229

65. Miura, T., Kishioka, Y., Wakamatsu, J., Hattori, A., Hennebry, A., Berry, C. J., Sharma, M., Kambadur, R., and Nishimura, T. (2006) *Biochem. Biophys. Res. Commun.* **340,** 675–680

66. Artaza, N. J., Bhasin, S., Mallidis, C., Taylor, W., Ma, K., and Gonzalez-Cadavid, F. N. (2002) *J. Cell. Physiol.* **190,** 170–179

67. Kocamis, H., and Killefer, J. (2002) *Domest. Anim. Endocrinol.* **23,** 447–454

68. Yamaguchi, Y., and Ruoslahti, E. (1988) *Nature* **336,** 244–246

69. Krusius, T., and Ruoslahti, E. (1986) *Proc. Natl. Acad. Sci. U. S. A.* **83,** 7683–7687

70. Schonherr, E., Broszat, M., Brandan, E., Bruckner, P., and Kresse, H. (1998) *Arch. Biochem. Biophys.* **355,** 241–248

The Journal of Biological Chemistry

Hany Bedair, T. Thomas Liu, Joel L. Kaar, Shawn Badlani, Alan J. Russell, Yong Li and Johnny Huard

You might find this additional information useful...

This article cites 27 articles, 9 of which you can access free at:
http://jap.physiology.org/cgi/content/full/102/6/2338#BIBL

Medline items on this article's topics can be found at http://highwire.stanford.edu/lists/artbytopic.dtl
on the following topics:
      Biochemistry .. Microbial Collagenase
      Physiology .. Muscle Regeneration
      Developmental Biology .. Regeneration
      Genetics .. Reporter Genes
      Medicine .. Fibrosis
      Physiology .. Mice

Updated information and services including high-resolution figures, can be found at:
http://jap.physiology.org/cgi/content/full/102/6/2338

Additional material and information about *Journal of Applied Physiology* can be found at:
http://www.the-aps.org/publications/jappl

This information is current as of March 31, 2008 .

Matrix metalloproteinase-1 therapy improves muscle healing

Hany Bedair,[1,2] T. Thomas Liu,[1,2] Joel L. Kaar,[3] Shawn Badlani,[1]
Alan J. Russell,[3] Yong Li,[1,2,3,4] and Johnny Huard[1,2,3,5]

[1]*Stem Cell Research Center, Children's Hospital of Pittsburgh;* [2]*Department of Orthopaedic Surgery,*
[3]*McGowan Institute for Regenerative Medicine, Department of Surgery,* [4]*Department of Pathology,*
[5]*Department of Molecular Genetics and Biochemistry, University of Pittsburgh, Pittsburgh, Pennsylvania*

**Bedair H, Liu TT, Kaar JL, Badlani S, Russell AJ, Li Y, Huard
J.** Matrix metalloproteinase-1 therapy improves muscle healing. *J Appl
Physiol* 102: 2338–2345, 2007; doi:10.1152/japplphysiol.00670.2006.—
Muscle undergoes time-dependent phases of healing after injury,
which ultimately results in residual fibrosis in the injured area. The
use of exogenous matrix metalloproteinases (MMPs) may improve
recovery after muscle injury by promoting the digestion of existing
fibrous tissue and releasing local growth factors. In the current
experiment, bilateral gastrocnemius (GM) lacerations were created in
severe combined immunodeficient mice. Twenty-five days after injury
(peak posttraumatic fibrosis), C2C12 cells (myoblasts) transduced
with the *LacZ* reporter gene were injected with exogenous MMP-1
into the right GMs at the site of injury; the cells were also injected
along with PBS (control) at the site of injury in the left GMs. The
muscle tissues were examined histologically via X-gal, hemotoxylin
and eosin, and Masson's trichrome staining. The MMP-treated limbs
contained more regenerating myofibers than did the control limbs
(MMP 170 ± 96 fibers, control 62 ± 51 fibers; $P < 0.001$). Less
fibrous tissue was observed within MMP-treated muscles (MMP:
24 ± 11%, control: 35 ± 15%; $P < 0.01$). These results suggest that
the direct injection of MMP-1 into the zone of injury during fibrosis
can enhance muscle regeneration by increasing the number of myo-
fibers and decreasing the amount of fibrous tissue.

muscle injury; fibrosis; regeneration

SKELETAL MUSCLE PAIN, the majority of which is related to
muscle strain injuries, is among the most common ailment
treated by physicians in a general medical practice according to
ICD-9 code billing data. (http://www.aafp.org/fpm/20050900/
49icd9.html). The natural process of muscle injury repair
follows a highly coordinated sequence of steps with the goal of
restoring normal tissue architecture and function. Unfortu-
nately, the regenerative capacity of injured skeletal muscle is
limited; the growth of fibrotic tissue commonly predisposes the
muscle to diminished function and possible reinjury (13).
Clinical experience reveals a high recurrence rate of skeletal
muscle strain injuries among athletes, approaching 12% in
professional soccer players and up to 30% in Australian foot-
ballers (20, 25). The majority of these recurrent injuries ap-
pears following early return to play. This vulnerable clinical
time period correlates histologically with the presence of en-
hanced type III collagen formation and decreased myofiber
regeneration (3). Experimental work has elucidated key events
in the formation of fibrous tissue following muscle injury and
the apparent central role of transforming growth factor-β1
(TGF-β1) in orchestrating this process (16, 17). Studies dem-

onstrated the successful use of TGF-β1 blockade in restoring
near normal architecture and function (5, 8, 9, 18). Although
known therapeutic interventions may prevent the onset of
fibrous changes after injury, a more likely clinical scenario
would be the presentation of a patient after the onset of fibrotic
remodeling with associated pain and dysfunction. This presents
a challenge to the treating physician as conventional therapies
of rest (12), ice (26), and anti-inflammatory medications (1) are
of limited efficacy in preventing reinjury.

A better approach for treating fibrosis following muscle
injury may rest with a family of proteolytic enzymes, the
matrix metalloproteinases (MMPs). MMPs are widely found in
plants and animals and are intimately involved in the mainte-
nance of the extracellular matrix (ECM) and cell migration;
each member of this proteolytic family has a specific affinity
toward certain elements of the ECM (4). MMP collagenases,
including MMP-1, -8, -13, and -18, have an ability to cleave
interstitial collagen types I, II, and III, whereas MMP gelati-
nases (MMP-2 and -9) degrade denatured collagen (24).

After an injury, satellite cells, muscle cell precursors known
to express MMP, become activated; an elevated level of MMP
production is thought to result in cell migration into injured
areas with subsequent differentiation and fusion of satellite
cells into myofibers (7, 14, 15). While this process of regen-
eration proceeds for 10–14 days after injury, its abrupt end is
heralded by the onset of fibrous changes within the muscle
(13). This dense organization of the ECM prohibits further cell
migration and regeneration, thus resulting in a terminal resid-
ual fibrotic state within the muscle.

We hypothesize that the introduction of exogenous MMP-1
into the zone of injury following skeletal muscle laceration will
decrease the amount of residual fibrosis and, in turn, result in
more regenerating myofibers in the area of injury.

MATERIALS AND METHODS

In Vitro

MMP-1 activity assay. To investigate the inherent activity of the
MMP-1 supplied by the manufacturer (M1802, Sigma, St. Louis, MO)
as a combination of active and proenzyme, an MMP activity assay
was performed. Initially, latent MMP-1 was activated via incubation
with trypsin (0–20 ng trypsin/ng proMMP-1) in buffer (50 mM
HEPES, 10 mM calcium chloride, pH 7.5) for 1 h at 37°C. The
activation reaction was terminated by the addition of soybean trypsin
inhibitor (Sigma) at a minimum of a 2:1 mass ratio of inhibitor to
trypsin and subsequent incubation of the enzyme solution for 10 min
at room temperature (RT). The activity of MMP-1 was assayed by

measuring the rate of hydrolysis of the peptide substrate acetyl-Pro-Leu-Gly-[2-mercapto-4-methyl-pentanoyl]-Leu-Gly-OC$_2$H$_5$ (P-125, BIOMOL, Plymouth, PA). Free sulfhydryls formed by cleavage of the peptide reacted with DTNB (5,5′-dithiobis 2-nitrobenzoic acid) to produce a colorimetric product. Trypsin-activated MMP-1 (0–0.35 ng/μl) was added to buffer (50 mM HEPES, 10 mM calcium chloride, pH 7.5) containing substrate (100 μM) and DTNB (1 mM) (Sigma) in 96-well polystyrene microplate. The total volume of the reaction solution was 100 μl. Enzyme activity expressed as change in (optical density) per second was measured by monitoring substrate hydrolysis at 412 nm for 5 min at 37°C using a SpectraMax 340PC^{384} microplate spectrophotometer (Sunnyvale, CA).

Matrix-assisted laser desorption/ionization mass spectrometry analysis of the MMP-1. Matrix-assisted laser description/ionization (MALDI) analysis of the untreated MMP-1 preparation was carried out using an Applied Biosystems PerSeptive STR Mass Spectrometer (Foster City, CA). A saturated sinapinic acid matrix solution (0.4 ml water, 0.3 ml acetonitrile, and 1 μl trifluoroacetic acid) was mixed with the enzyme in a 1:1 volumetric ratio. The mixture was spotted onto a MALDI sample plate and incubated at RT until dry. After evaporation of the solvent, the protein spectrum was recorded. The instrument was operated in a linear mode using a 2.5 kV accelerating voltage.

Cell culture and proliferation assays. National Institutes of Health (NIH) 3T3 cells (fibroblast cell line) and C2C12 myoblasts, purchased from American Type Culture Collection (ATCC, Rockville, MD) were chosen as a well established, standardized, purified, and homogenous cell line population that represents muscle fibroblast and myoblasts. These cells were cultured with DMEM (Invitrogen, Carlsbad, CA) containing 10% FBS, 10% horse serum, 0.5% chicken embryo extract, and 1% penicillin/streptomycin. All cells were cultured at 37°C in 5% CO$_2$. NIH 3T3 and C2C12 cells were separately seeded in different 96-well plates at a density of 313 cells/cm^2. Cells were cultured in medium (described above) and either 0, 0.1, 1.0, or 10 ng/ml of human MMP-1 (Sigma Chemical) to verify the safety of the MMP1 application in vivo. Cell proliferation assays were performed at 24, 48, 72, 96, and 120 h post seeding using the CellTiter 96 AQ 1 proliferation assay (Promega, Madison, WI) according to the manufacturer's specifications.

In Vivo

Safety testing. Seven mice (C57BL/6J Prkdc; Jackson Laboratory, Bar Harbor, ME) were allocated for safety dose testing of MMP-1. These 4- to 6-wk-old mice were injected with 10, 100, or 400 ng of MMP-1 in 10 μl volume PBS in the mid-gastrocnemius muscle. The solutions contained fluorescence beads (1 μg/ml, Molecular Probes, Eugene, OR) and were prepared by diluting stock with PBS. Control limbs were injected with 10 μl of PBS only. Three mice were killed 6 days after injection, and an additional four were killed 21 days after injection. The muscle was isolated and snap frozen as described below. Muscle sections were analyzed by both hematoxylin and eosin (H&E) staining as well as by immunofluorescence with anti-laminin (Chemicon, Temecula, CA) and anti-α-smooth muscle actin (SMA; Sigma) antibodies to assess the integrity of the basal lamina.

MMP in injured mouse skeletal muscle. Twenty-one SCID mice (C57BL/6J Prkdc; Jackson Laboratory) were used for histological analysis to prevent an immunogenic reaction following the intramuscular delivery of the localizing C2C12 (Lac-Z) cells. Seventeen immunocompetent mice (C57Bl/6J; Jackson Laboratory) were used for physiological testing in this experiment as no C2C12 cells were injected in this group. The histological testing group had an average age of 82 ± 33 days, average weight of 28 ± 6 g, and contained 8 females and 13 males. The physiological testing group had an average age of 48 ± 1 days, ranged in weight from 20.7–27.0 g, and consisted of males only to eliminate any variability in inherent strength due to differences in sex. The animals were housed in cages and fed with commercial pellets and water ad libitum. The policies and procedures

of the animal laboratory are in accordance with those detailed by the US Department of Health and Human Services, and the Animal Research Care Committee (ARCC) of the authors' institution approved the research protocols for these experiments (ARCC protocol #25-03). A previously reported muscle laceration injury model was employed for these experiments. However, the differences in the laceration protocol between the histological group [50% width and 100% thickness of gastrocnemius muscle (GM)] and the physiological testing group [100% width and 100% thickness of the tibialis anterior (TA) muscle] were due to constraints of the experimental apparatus and the fact that preliminary experiments had been performed with 50% width injury in the TA muscle with the healing process being significantly faster than the healing process for similarly injured GM muscle. Specifically, the healing time for 100% injured TA muscle most closely corresponded with 50% width injury (histological group) healing time for the GM muscle. Therefore, we performed a 100% width injury in the TA muscle to mimic the healing process in the 50% width injured GM.

The healing process for this model is histologically similar to strain injury models, an injury type that accounts for the most common clinically reported pattern of injury (5, 9, 10, 13, 17). The mice were anesthetized with 0.016 ml of ketamine and 0.008 ml of xyaline in 0.025 ml of PBS by intraperitoneal injection. For the histological analysis group (the SCID group of mice), lacerations were performed bilaterally on the GM through 50% of its width and 100% of its thickness at 60% of its length from its insertion. In the physiological testing group, lacerations were performed bilaterally through 100% of the width and thickness of the TA at 60% of its length from insertion to ensure a detectable difference. We used the group of 17 immunocompetent mice in accordance with prior physiological testing protocols. All laceration sites were tagged with a single 4-0 silk suture, and the skin was then closed with a 4-0 silk suture. After an average time period of 21 ± 3 days (range 21–28 days), to allow for the formation of muscle fibrosis, 100 ng of human MMP-1 (Sigma) in 10 μl PBS was injected at the tagged laceration sites of the right GMs of the SCID mice; 10 μl PBS was injected at the tagged laceration sites of the left GMs of the SCID mice. C2C12 myoblasts (5 × 10^6 cells) transduced with the Lac-Z reporter gene were injected at each site to serve as confirmation of delivery of the MMP-1 solution into the appropriate site following subsequent histological evaluation. Immunocompetent mice had the same MMP-1 therapy delivered into the TAs (without including the injection of transduced C2C12 cells). Fourteen days later, all the SCID mice were killed. The injured muscles (GMs) were isolated, mounted, and snap frozen in liquid-nitrogen-cooled 2-methylbutane. Samples were serially sectioned at 10 μm with a cryostat for histological analysis; the entire area of injury identified by the suture tag was sectioned. Immunocompetent mice were killed at 6 days (7 mice) and 21 days (10 mice), and the isolated muscles (TAs) were prepared for physiological testing.

Evaluation of MMP-1 delivery. Muscle sections from all SCID mice were fixed in 2% glutaraldehyde for 1 min and rinsed with PBS. Sections were then stained with X-gal for sufficient time to identify Lac-Z-expressing cells (13, 14); all sections were then counterstained with eosin to confirm delivery of the therapeutic intervention to the appropriate site. Only those animals with Lac-Z-positive cells in the area of injury were included for additional histological analysis.

Muscle fibrosis. Sections from each limb of each animal were washed in deionized water and stained with a modified Masson's trichrome staining kit (IMEB, San Marcos, CA) according to the manufacturer's specifications. This particular technique stains nuclei black, muscle red, and collagen blue (3, 14) and was previously validated through immunohistochemisty as an accurate technique for evaluating fibrous tissue within skeletal muscle (8). Five randomly selected high-powered image fields within the injured area for each limb were obtained using a Nikon Eclipse 800 fitted with a Spot camera (Diagnostic Instruments). Images were analyzed using the Northern Eclipse image analysis software (Empix, Ontario, Canada)

to measure the percent area of collagen (blue staining tissue) within the injury zone. Color threshold levels within the software program were set to isolate the blue staining regions and calculate the area of that region within the zone of injury, corresponding to the area of fibrosis. This value was expressed as a percentage of the entire cross-sectional area of the muscle. A blinded observer performed all analyses.

Muscle regeneration. Muscle sections were stained with hematoxylin and eosin. Muscle regeneration was assessed by counting the number of centronucleated myofibers (3, 6, 7, and 15). Five high-powered fields from the injury zone were analyzed for each muscle, and the average number of regenerating myofibers per field was compared with other groups. A blinded observer performed all analyses.

Physiology testing. Technical and financial constraints excluded the use of immunodeficient animals for physiological testing. Therefore, 17 immunocompetent mice were used for muscle strength testing; 7 mice were tested 6 days after MMP-1 treatment, and 10 mice were tested 21 days after MMP-1 treatment. The mice were anesthetized by using 70 mg/kg of pentobarbital sodium via intraperitoneal injection. After the mice were killed, TA muscles were removed with their bony origins and insertions intact and mounted in a vertical chamber that was constantly perfused with mammalian Ringer solution aerated with 95% O_2-5% CO_2 and maintained at 25°C. The origin was mounted to a glass tissue support rod, and the insertion was connected to a force transducer and length servo system (Aurora Scientific, ON, Canada). The length at which the peak force (single burst stimulation) for each muscle was generated determined the optimal testing length of each muscle. The muscle was allowed to rest and reach an equilibrium state for 5 min after the determination of the optimal testing length to reduce the effects of fatigue. The tetanic force for each muscle was then measured by stimulating the tissue with monophasic rectangular pulses of current (1 ms in duration) delivered through a platinum plate electrode 1 cm apart. Current was increased to 50% over the necessary current to obtain the peak twitch force (250–300 mA) so as to ensure the greatest stimulation. Maximal tetanic force was assessed with a stimulation frequency of 75 Hz delivered in a 500-ms-duration train. Each muscle was then weighed after tendon and bone attachments were removed. The Close formula was used to correct force values for cross-sectional area to normalize for variability in muscle size, which are expressed as specific peak force and specific tetanic force in Newtons per cross-sectional area.

Statistical analysis. Comparisons in cell proliferation between 3T3 and C2C12 cells, muscle fibrotic area, number of regenerating myofibers, and physiological testing were compared with ANOVA and two-tailed Student's *t*-tests.

RESULTS

Intrinsic Activity of MMP-1 Preparation

MMP-1, like all MMPs, is expressed as a zymogen (proMMP-1) and must, therefore, be activated by disrupting the interaction between a cysteine (Cys92) molecule in the enzyme's pro-peptide domain and a zinc molecule situated in the active site. Latent MMP-1 can be activated in vitro by incubation with organomercurial compounds and other chemical agents that modify sulfhydryl groups. Nonspecific proteases such as trypsin, which cleave the pro-peptide domain, can also be used to activate latent MMP-1 (6, 24). In vivo, latent MMPs are activated by the proteolytic activity of plasmin as well as other MMPs (4).

As a first approximation to in vivo systems, the MMP-1 was not activated prior to use in all experiments described in this paper. According to the supplier, the protein preparation consisted of a mixture of zymogen and active forms of the enzyme.

The level of enzymatic activity in the preparation was assayed using a colorimetric peptide substrate. Results indicated that the activity of the enzyme relative to the enzyme that had been activated with 20 ng trypsin/ng latent MMP-1 (considered to be fully active) was 12.5% (Fig. 1*A*).

The fraction of active enzyme in the MMP-1 preparation was also approximated by MALDI mass analysis (Fig. 1*B*). In the MALDI spectra of the protein, peaks at 44,451 and 51,939 Da are consistent with the molecular weights of active and latent MMP-1, respectively (6, 19, 23, 27). Results of the MALDI analysis confirm, based on quantification of the relative ratio of peak heights corresponding to active and latent MMP-1, that <26% of the protein preparation was active.

Influence of MMP-1 on Cell Proliferation

To determine the effect of MMP-1 on cell proliferation, fibroblasts (NIH 3T3 cell line) and myoblasts (C2C12 cell line) were cultured with varied concentrations of MMP-1 for a period of 1–5 days. MMP-1 appeared to have no deleterious effect on NIH 3T3 or C2C12 proliferation in vitro compared
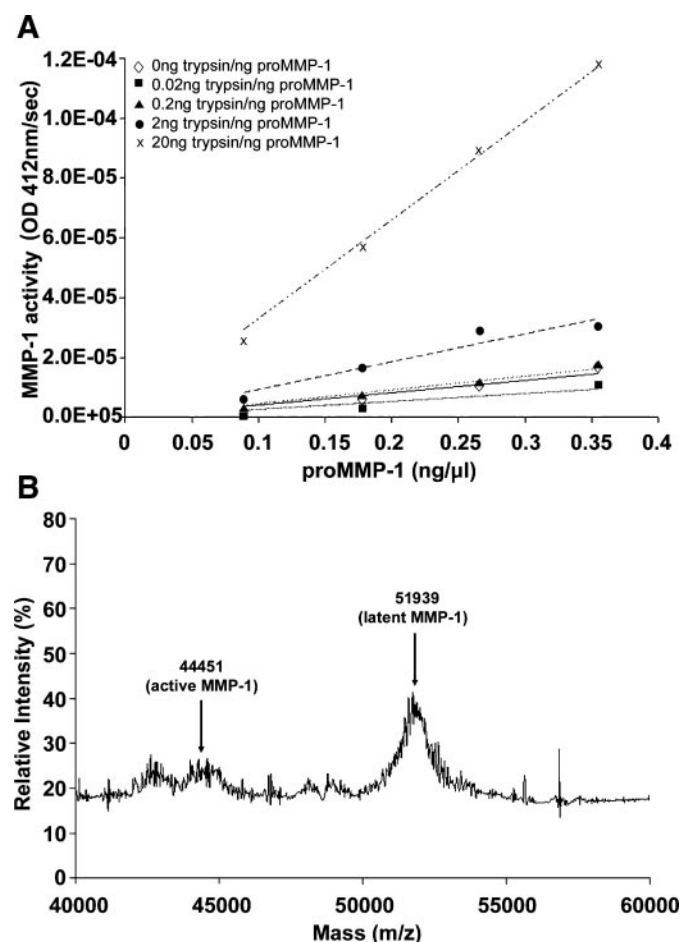

Fig. 1. Enzymatic activity of matrix metalloproteinases (MMP)-1 preparation. MMP-1 preparation was activated via proteolytic digestion using a range of trypsin to proMMP-1 mass ratios. The relative activity of nonactivated MMP-1 (0 ng trypsin/ng proMMP-1), which was employed in all experiments, to that of the fully active enzyme (20 ng trypsin/ng proMMP-1) was 12.5% (*A*). MALDI spectra of MMP-1 preparation. Peaks representing latent and active MMP-1 are labeled are shown in *B*. OD, optical density; *m/z*, mass-to-charge ratio.

with controls (see supplementary data Figs. S1 and S2 in the online version of this manuscript).

MMP-1 Use is Safe in Normal Muscle in Vivo

A large dose range of MMP-1 was injected into the GM of otherwise healthy mice with the highest dose being near the stock concentration of the MMP-1 enzyme. When the muscles were isolated 6 or 21 days after injection, the muscles showed no signs of injury or increased fibrosis at the site of MMP-1 injection as determined by the location of fluorescence beads and compared with control limbs on H&E sections. Immunofluorescent anti-laminin staining was also used to assess the integrity of the basal lamina (Fig. 2). There were no defects observed in any of the sections.

Evaluation of MMP-1 Delivery

Twenty-one mice had bilateral GMs injected with MMP-1/C2C12-Lac-Z cells (right side) and PBS/C2C12-Lac-Z cells (left side). Lac-Z-positive staining cells were recovered from 16 right GMs (MMP-1 therapy group) and 17 left GMs (control group). Fourteen animals had Lac-Z-positive cells within GMs injected bilaterally. The percutaneous injection of the MMP-1 into the desired target was observed >75% of the time. Three weeks after cell transplantation, the injured muscles demonstrated more regenerating myofibers in the MMP-1-treated fibrotic areas than in the control fibrotic areas (Fig. 3, *A–C*, $P < 0.01$). The transplanted Lac-Z-positive myoblasts were unable to fuse and form myofibers in the control fibrotic areas (Fig. 3*A*, arrowheads), whereas transplanted Lac-Z-positive myoblasts in the MMP1-treated fibrotic areas did fuse and form myofibers (Fig. 3*B*, arrows). Furthermore, more Lac-Z-positive myofibers were observed in the treated group than in the control group (Fig. 3*C*).

Effect of MMP-1 on Skeletal Muscle Fibrosis After Injury

Sixteen GM sections were analyzed from the MMP-1 group and 17 GM sections from the control group to determine the percent area of fibrosis within the zone of injury. The MMP-1 therapy group had significantly less fibrosis ($24 \pm 11\%$ fibrosis) compared with the control group ($35 \pm 15\%$ fibrosis; $P < 0.01$) as demonstrated in Fig. 4.

Muscle Regeneration with MMP-1 Therapy

Sixteen MMP-1-treated muscles and 17 control muscles were examined for the number of centronucleated myofibers within the zone of injury that represented the number of regenerating myofibers. The MMP-1 therapy group demonstrated enhanced numbers of regenerating (centronucleated) myofibers per high-powered field after injury; the MMP-1 therapy group had 170 ± 96 myofibers whereas the control groups ($P < 0.01$) had 62 ± 51 myofibers as demonstrated in Fig. 5.

Muscle Physiology

The cross-sectional area specific peak force for MMP-1 and the control groups were 5.2 ± 1.7 and 5.4 ± 0.7 N/cm^2, respectively, at 6 days after MMP-1 therapy and 5.8 ± 0.8 and 6.0 ± 0.8 N/cm^2 at 21 days after therapy. The cross-sectional area specific tetanic force for the MMP-1-treated group and the control group were 16 ± 4 and 18 ± 2 N/cm^2 at 6 days and 19 ± 4 and 19 ± 4 N/cm^2 at 21 days, respectively (Fig. 6).

DISCUSSION

The role of MMP-1 in the treatment of fibrotic diseases has shown much success in other organ systems, most notably experimentally induced hepatic fibrosis, where MMP-1 has been shown to reverse fibrosis and begin the restoration of
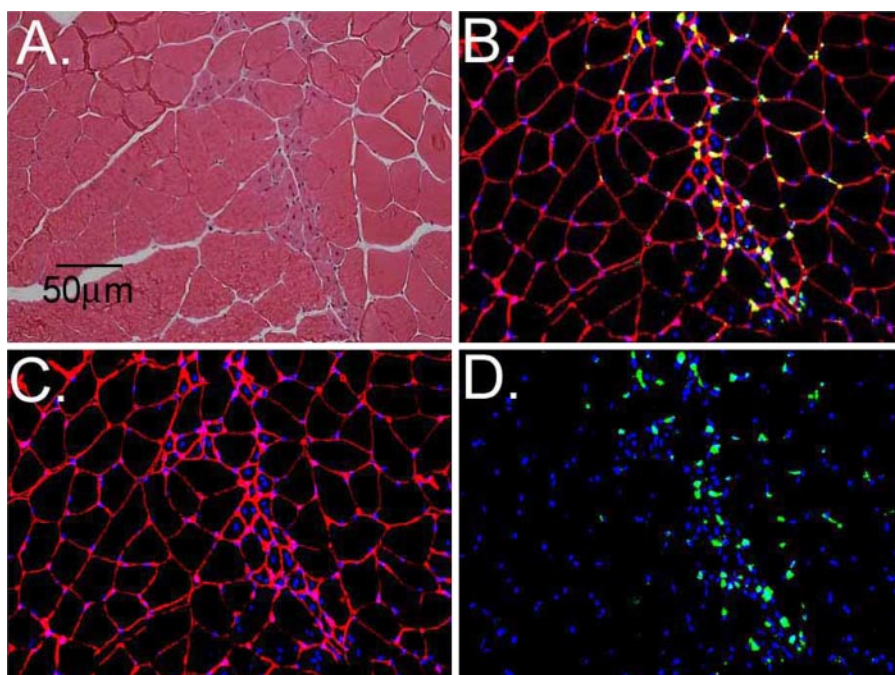

Fig. 2. The safety test of MMP-1 in normal muscle in vivo. We detected no damage in the skeletal muscle tissues of mice at the area of MMP-1 injection. No detectable damage was seen up to 21 days with hemotoxylin and eosin (*A*), immunofluorescence (*B–D*), and anti-laminin (*B, C*) staining: neither the basal lamina nor the muscle fiber was destroyed in the injection zone.

Fig. 3. Evaluation of MMP-1 delivery. Our preliminary results showed that the transplanted Lac-Z-positive myoblasts were unable to fuse and form myofibers in the control scarred areas (*A*, arrowheads). Whereas, the transplanted Lac-Z-positive myoblasts in the MMP-1-treated scarred areas fused and formed myofibers (*B*, arrows). Furthermore, we observed more Lac-Z-positive myofibers in the MMP-1-treated group rather than in the nontreated muscle tissues (*C*), $P < 0.01$.
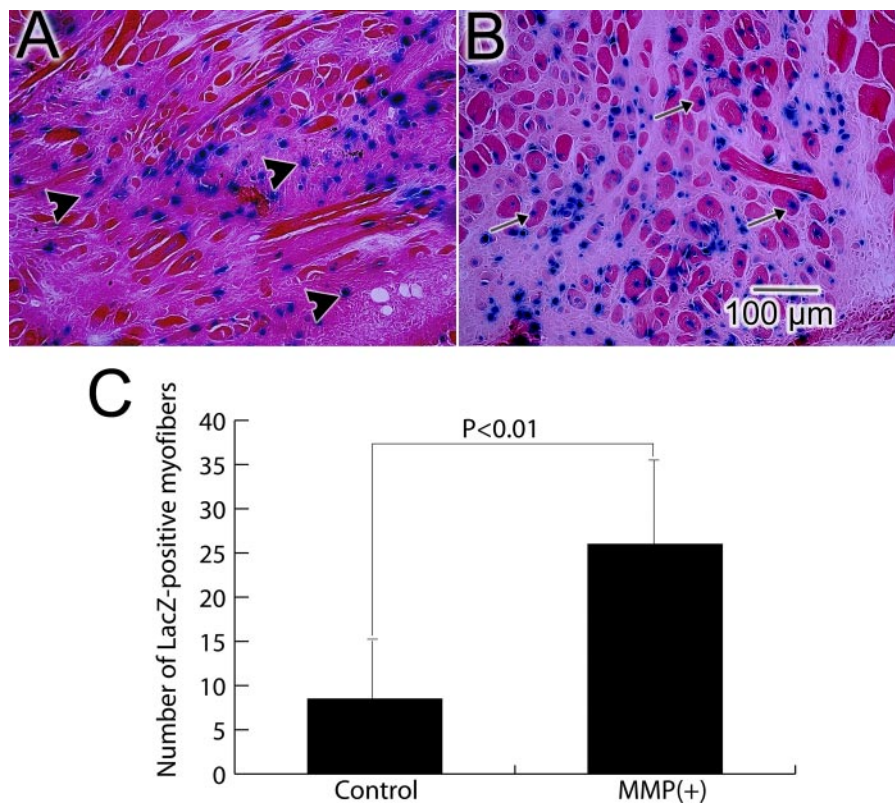
normal tissue architecture and function (11, 22). The application of this idea to skeletal muscle has not been investigated to the best of our knowledge. Satellite cells, muscle precursors that reside in the basement membrane, become activated after injury and are known to produce MMP-2 and -9 to aid in cell migration across the predominantly collagen IV-rich basement membrane (14). The repair process of injured muscle is a balance between the regeneration of myofibers and the depo-

Fig. 4. Effect of MMP-1 on skeletal muscle fibrosis after injury. Two weeks after therapy, the MMP-1 treatment group had significantly less fibrosis ($24 \pm 11\%$ fibrosis; *A*) compared with the control group ($35 \pm 15\%$ fibrosis; $P < 0.01$; *B*). A single injection of MMP-1 directly into the site of fibrous tissue formation is able to digest overgrown elements of the ECM (*C*).
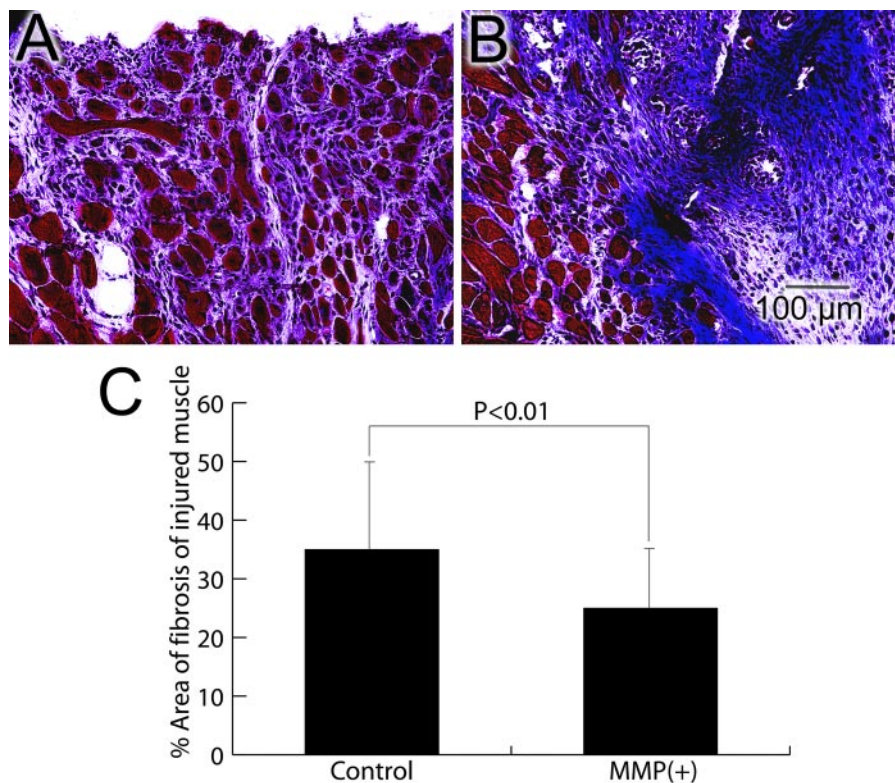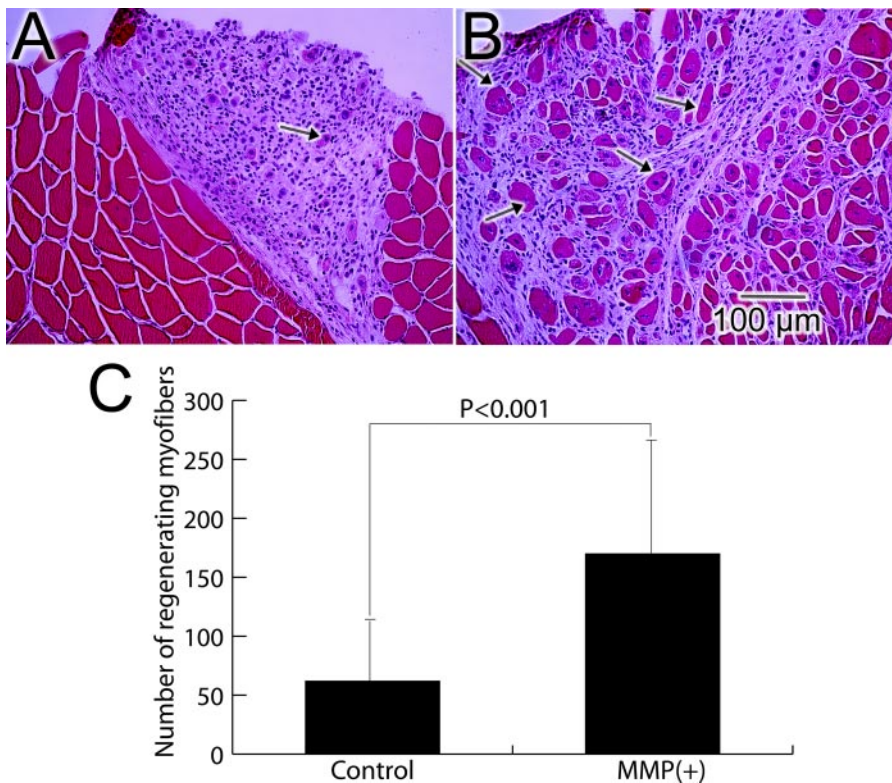
Fig. 5. Enhanced muscle regeneration with MMP-1 therapy. Our results showed more regenerating myofibers in the MMP-1-treated scarred areas than in the control scarred areas 2 wk after injection (*A*, *B*; arrows). Observing the centronuclear myofibers within the zone of injury (*C*), we found that MMP-1 therapy significantly enhanced the number of regenerating myofibers after injury. MMP-1 therapy group: 170 ± 96 myofibers vs. control group: 62 ± 51 myofibers ($P < 0.001$).

sition of connective tissue that supports these myofibers. After skeletal muscle injury, the deposition of connective tissue predominates while the regeneration of myofibers is limited. The predominant components of the ECM connective and fibrous tissue are collagen types I and III (2). MMP-2 and -9 have minimal effect on these types of collagen. The introduction of MMP-1 (collagenase), which specifically targets collagen I and III, may aid regeneration by removing this blockade. We postulated that the removal of this barrier will reestablish an environment conducive to muscle regeneration. Myoblasts
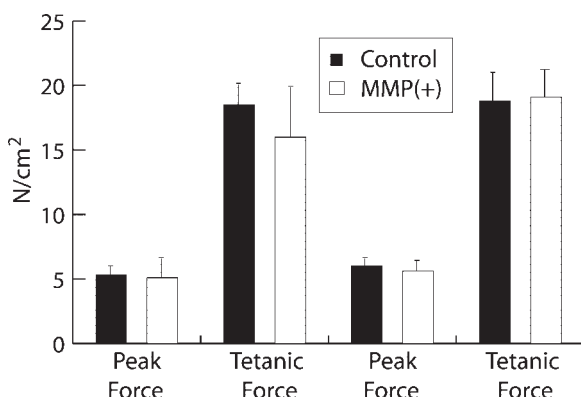

Fig. 6. Muscle physiology test. The specific peak and tetanic forces of the treated and nontreated tibialis anterior muscles were measured 6 days (the first set of bars showing peak and tetonic forces) and 21 days (the second set of bars showing peak and tetanic force) following treatment. The specific peak forces for the MMP-1-treated and the control groups were 5.2 ± 1.7 and 5.4 ± 0.7 N/cm^2, respectively, at 6 days after MMP-1 therapy and 5.8 ± 0.8 and 6.0 ± 0.8 N/cm^2 21 days after therapy. The specific tetanic forces for the MMP-1-treated and control groups were 16 ± 4 and 18 ± 2 N/cm^2 at 6 days and 19 ± 4 and 19 ± 4 N/cm^2 at 21 days, respectively.

require MMPs for migration, and it is known that satellite cells express gelatinases to cross the basement membrane (7, 15). Since satellite cells are capable of producing MMPs that are relatively ineffective against scar tissue, it would be reasonable to hypothesize that these precursors would be prevented from migrating, fusing, and contributing to the reparative process. Thus it is possible that the elimination of this barrier would aid in repair through either the digestion of scar tissues or the activation of muscle cell migration and invasion.

The first portion of this study was to assess the affect of MMP-1 delivery on normal muscle tissue by injecting a broad range of doses, ranging from 10 to 400 ng, into normal skeletal muscle. Even in the highest concentrations, MMP-1 did not show any negative effect to either muscle or to the structural integrity of the ECM that surrounds normal muscle fibers. These data are corroborated by the lack of effect demonstrated by MMP-1 on the proliferation of myoblasts and fibroblasts in culture.

The technique of intramuscular injection of MMP-1 directly into the zone of injury as performed in this model is technically challenging. The simultaneous intramuscular injection of C2C12 myoblasts transduced with the Lac-Z reporter gene and the MMP-1 or the injection of our placebo (MMP-1 and PBS control) into each limb served as a biologically observable confirmation that the MMP-1 reached its intended target. Only those samples containing cells that stained positively for Lac-Z in the zone of injury (nearly 80%) were analyzed. This eliminated the inclusion of samples in which the MMP-1 may have been erroneously targeted.

In testing the main hypothesis of this study, we demonstrated that the use of a single dose of 100 ng of MMP-1 delivered directly into the fibrous tissue produced a significant

reduction of residual collagen in the zone of injury. This, in turn, appears to have led to a significant improvement in the number of regenerating myofibers. Thus MMP-1 delivered into the area of fibrosis that develops following skeletal muscle injury results in the dual therapeutic effect of decreasing residual fibrous tissue while simultaneously enhancing the process of repair.

While the presumed biological half-life of MMP-1 in vivo is no longer than a few hours, our results indicated a remarkable outcome after a relatively short exposure to MMP-1. This may be related to the dose of MMP-1, the timing of therapy, or the timing of exposure. Similarly, it may also be related to the choice of reagent of the MMP-1 mixture rather than fully activated MMP-1. The activity of the MMP-1 preparation, supplied and administered as a mixture of active and pro-enzyme, was determined to be a ratio of ~1:3. While the true enzyme kinetics of our dose delivery was not specifically measured, one may speculate that the activated portion may have initiated the granulation tissue remodeling cascade, whereas the bulk of the enzyme, in its latent form, may have allowed for a slow and sustained release in vivo through the plasminogen/urokinase system (4).

The injection of MMP-1 3 wk after a laceration, while empirically selected, represents the time point at which the regenerative phase has declined substantially and the deposition of fibrous tissue appears to be at its peak. This may represent the time of highest potential for improved regeneration and the formation and degradation of the different elements of the ECM as they are in a dynamic state. Various biological factors such as growth factors and satellite cells are still active; the tissue is still poised for regeneration and its plasticity can be manipulated more easily. Although beyond the scope of this study, the release of intrinsic growth factors within the ECM might aid initially in the regenerative process. Other authors observed the relationship between MMP and the local release of various growth factors (21).

The histological response to MMP-1 injection into fibrous skeletal muscle demonstrates promising results; however, the goal of this therapeutic intervention is to also restore the functional status of the tissue. There was no difference demonstrated in regard to peak forces generated by control and experimental groups at either time point. As for the measured tetanic force produced by the muscles, we observed no change in the control group between 6 and 21 days after PBS injection. This suggests that there is little improvement in the functional status of untreated injured muscle between 4 and 6 wk after a laceration injury. One might speculate that any functional recovery regained after injury is obtained by 4 wk after healing has begun and will remain unchanged, mirroring the end point of the regenerative phase observed during histology. Although there were no statistically significant differences between the control and MMP-1-treated groups, interesting trends were observed. Six days following MMP-1 therapy, there was a reduction in the tetanic force produced in the treated group compared with the control group. This may be a result of the active degradation and subsequent remodeling initiated by MMP-1. At this early time point, the tissue has most likely lost tensile properties in the area of previous fibrous tissue, which is mirrored as reduced force production. Three weeks after treatment, as the tissue matures and the zone of injury is populated by regenerating myofibers (as observed histologi-

cally), the force produced in the MMP-1-treated group improves from that measured at 1 wk and returns to the level of the control group. This improvement most likely represents a delay in the correlation of histological findings and functional findings, a phenomenon commonly seen in skeletal muscle injury studies. As the regenerating muscle continues to regenerate and mature, the force produced may eventually exceed that of the control group; however, this is speculative and requires future study.

Skeletal muscle fibrosis following an injury represents a difficult therapeutic dilemma. Traditional therapies have proven ineffective and experimental therapies thus far have focused on prophylactic treatment of injuries to prevent fibrosis. Our work with MMP therapy might represent an initial stage in addressing this problem. This study demonstrated that a single dose of MMP-1 delivered intramuscularly into the site of fibrosis effectively reduces residual fibrosis and enhances muscle regeneration. Continued work on this topic may yield more strategies to optimize dose, delivery, and timing, which might eventually lead to an improvement in functional status.

REFERENCES

1. **Almekinders LC.** Anti-inflammatory treatment of muscular injuries in sports. *Sports Med* 15: 139–145, 1993.
2. **Best TM, Hunter KD.** Muscle injury and repair. *Phys Med Rehabil Clin N Am* 11: 251–266, 2000.
3. **Best TM, Shehadeh SE, Leverson G, Michel JT, Corr DT, Aeschlimann D.** Analysis of changes in mRNA levels of myoblast- and fibroblast-derived gene products in healing skeletal muscle using quantitative reverse transcription-polymerase chain reaction. *J Orthop Res* 19: 565–572, 2001.
4. **Brinckerhoff CE, Matrisian LM.** Matrix metalloproteinases: a tail of a frog that became a prince. *Nat Rev Mol Cell Biol* 3: 207–214, 2002.
5. **Chan YS, Li Y, Foster W, Horaguchi T, Somogyi G, Fu FH, Huard J.** Antifibrotic effects of suramin in injured skeletal muscle after laceration. *J Appl Physiol* 95: 771–780, 2003.
6. **Dioszegi M, Cannon P, Van Wart HE.** Vertebrate collagenases. *Methods Enzymol* 248: 413–431, 1995.
7. **El Fahime E, Torrente Y, Caron NJ, Bresolin MD, Tremblay JP.** In vivo migration of transplanted myoblasts requires matrix metalloproteinase activity. *Exp Cell Res* 258: 279–287, 2000.
8. **Foster W, Li Y, Usas A, Somogyi G, Huard J.** Gamma interferon as an antifibrosis agent in skeletal muscle. *J Orthop Res* 21: 798–804, 2003.
9. **Fukushima K, Badlani N, Usas A, Riano F, Fu F, Huard J.** The use of an antifibrosis agent to improve muscle recovery after laceration. *Am J Sports Med* 29: 394–402, 2001.
10. **Hurme T, Kalimo H, Lehto M, Jarvinen M.** Healing of skeletal muscle injury: an ultrastructural and immunohistochemical study. *Med Sci Sports Exerc* 23: 801–810, 1991.
11. **Iimuro Y, Nishio T, Morimoto T, Nitta T, Stefanovic B, Choi SK, Brenner DA, Yamaoka Y.** Delivery of matrix metalloproteinase-1 attenuates established liver fibrosis in the rat. *Gastroenterology* 124: 445–458, 2003.

12. **Jarvinen MJ, Lehto MU.** The effects of early mobilisation and immobilisation on the healing process following muscle injuries. *Sports Med* 15: 78–89, 1993.

13. **Kalimo H, Rantanen J, Järvinen M.** Muscle injuries in sports. *Baillieres Clin Orthop* 2: 1–24, 1997.

14. **Kherif S, Lafuma C, Dehaupas M, Lachkar S, Fournier JG, Verdiere-Sahuque M, Fardeau M, Alameddine HS.** Expression of matrix metalloproteinases 2 and 9 in regenerating skeletal muscle: a study in experimentally injured and mdx muscles. *Dev Biol* 205: 158–170, 1999.

15. **Lewis MP, Tippett HL, Sinanan AC, Morgan MJ, Hunt NP.** Gelatinase-B (matrix metalloproteinase-9; MMP-9) secretion is involved in the migratory phase of human and murine muscle cell cultures. *J Muscle Res Cell Motil* 21: 223–233, 2000.

16. **Li Y, Foster W, Deasy BM, Chan Y, Prisk V, Tang Y, Cummins J, Huard J.** Transforming growth factor-beta1 induces the differentiation of myogenic cells into fibrotic cells in injured skeletal muscle: a key event in muscle fibrogenesis. *Am J Pathol* 164: 1007–1019, 2004.

17. **Li Y, Huard J.** Differentiation of muscle-derived cells into myofibroblasts in injured skeletal muscle. *Am J Pathol* 161: 895–907, 2002.

18. **Negishi S, Li Y, Usas A, Fu FH, Huard J.** The effect of relaxin treatment on skeletal muscle injuries. *Am J Sports Med* 33: 1816–1824, 2005.

19. **Okamoto T, Akaike T, Suga M, Tanase S, Horie H, Miyajima S, Ando M, Ichinose Y, Maeda H.** Activation of human matrix metalloproteinases by various bacterial proteinases. *J Biol Chem* 272: 6059–6066, 1997.

20. **Orchard JW, Seward HG.** AFL injury report 2003. *J Sci Med Sport* 7: 264–265, 2004.

21. **Sanderson MP, Dempsey PJ, Dunbar AJ.** Control of ErbB signaling through metalloprotease mediated ectodomain shedding of EGF-like factors. *Growth Factors* 24: 121–136, 2006.

22. **Siller-Lopez F, Sandoval A, Salgado S, Salazar A, Bueno M, Garcia J, Vera J, Galvez J, Hernandez I, Ramos M, Aguilar-Cordova E, Armendariz-Borunda J.** Treatment with human metalloproteinase-8 gene delivery ameliorates experimental rat liver cirrhosis. *Gastroenterology* 126: 1122–1133; discussion 1949, 2004.

23. **Stricklin GP, Jeffrey JJ, Roswit WT, Eisen AZ.** Human skin fibroblast procollagenase: mechanisms of activation by organomercurials and trypsin. *Biochemistry* 22: 61–68, 1983.

24. **Visse R, Nagase H.** Matrix metalloproteinases and tissue inhibitors of metalloproteinases: structure, function, and biochemistry. *Circ Res* 92: 827–839, 2003.

25. **Woods C, Hawkins RD, Maltby S, Hulse M, Thomas A, Hodson A.** The Football Association Medical Research Programme: an audit of injuries in professional football—analysis of hamstring injuries. *Br J Sports Med* 38: 36–41, 2004.

26. **Worrell TW.** Factors associated with hamstring injuries. An approach to treatment and preventative measures. *Sports Med* 17: 338–345, 1994.

27. **Zhang Y, Gray RD.** Characterization of folded, intermediate, and unfolded states of recombinant human interstitial collagenase. *J Biol Chem* 271: 8015–8021, 1996.

MMP-1 enhances muscle cell migration and differentiation

William Wang [1,2], Haiying Pan [2], Bahiyyah S. Jefferson [2], Yong Li [2,3,4]

1. University of Pittsburgh, School of Medicine, 2. The Laboratory Molecular Pathology,

Stem Cell Research Center (SCRC), Children's Hospital of UPMC. 3. Department of

Orthopaedic Surgery, 4. Department of Pathology, University of Pittsburgh.

*Correspondence should be addressed to:

Yong Li, MD., Ph.D.

Director, The Laboratory Molecular Pathology,

Stem Cell Research Center (SCRC),

3312 Rangos Research Center

3460 Fifth Avenue

Pittsburgh, PA 15213-2583

Phone: 412-692-5794, Fax: 412-692-7095

E-mail: yongli@pitt.edu

1

Abstract:

Injured skeletal muscle has an enormous capacity to regenerate itself through a highly coordinated sequence of events involving myoblast migration and differentiation into myotubes and myofibers. Fibrosis may impede muscle regeneration by posing as a mechanical barrier to cell migration and fusion, providing inappropriate signals for cell differentiation, and limiting vascular perfusion of the injury site, leading to incomplete functional recovery. Our previous study has demonstrated Matrix Metalloproteinase-1 (MMP-1) could digest fibrous scar tissue and improve muscle healing after injuries. The goal of this study is to investigate if MMP1 could further enhance muscle regeneration by improving myoblast migration and differentiation capability. *In vitro* wound healing assays and Western blot analysis both demonstrated that MMP-1 enhances myoblast migration. We also discovered that MMP-1 enhances myoblast differentiation, which is a critical step in the sequence of muscle regeneration. Western blot analysis also demonstrated the up-regulation of key myogenic factor, myogenin after MMP-1 treating. *In vivo,* we detected C2C12 (myoblasts) transplantation was greatly improved following MMP1 treatment within these dystrophic skeletal muscles of MDX mice model. Thus, MMP-1 may be able to improve the recovery of muscle function after injury or diseased by increasing the number of myofibers generated by activated myoblasts in addition to increasing the myoblast coverage area by promoting migration, thus fostering a greater degree of grafting.

Key Words: MMP-1, Migration, Differentiation, Muscle injury, Fibrosis, Regeneration.

2

Introduction

Muscle injuries are among the most common injuries seen in orthopaedic clinics and present a challenging problem in traumatology. Fibrosis is a consequence of the local overgrowth of extracellular matrix (ECM) at the site of injury, and poses a significant barrier preventing complete muscle regeneration and leading to incomplete recovery, pain, and functional deficits. Accelerated ECM deposition may impede muscle regeneration by creating mechanical barriers against cell migration and fusion, providing inappropriate signals for cell differentiation, and limiting vascular perfusion of the injury site, leading to incomplete functional recovery and a propensity for re-injury.[1-3]

Experimental studies have demonstrated the efficacy of preventing fibrosis after muscle injury by blocking key steps in the fibrotic cascade, such as Transforming Growth Factor β (TGF-β).[4-8] However, treating patients before the onset of fibrosis is often unlikely; most persons with muscle injuries seek treatment only after the onset of fibrosis and the concomitant pain and functional deficits it produces. Additionally, pervasive skeletal muscle fibrosis can be caused by neuromuscular dysfunction and various musculoskeletal diseases.

Duchenne Muscular Dystrophy (DMD) is an X-linked muscle disorder characterized by progressive muscle weakness caused by a lack of dystrophin expression in the sarcolemma of muscle fibers. Patients diagnosed with Duchenne Muscular Dystrophy begin to experience fibrous scar tissue formation in their muscles during their teenage years.[9, 10] This anomalous generation of matrix protein is thought to be driven by the

3

repeated degeneration, inflammation, and regeneration of muscle in DMD patients.[11, 12] Fibrous scar tissue continues to impede muscle cell migration, fusion and muscle regeneration even when myogenic cells are transplanted into the region. Poor cell survival and low dispersion of grafted cells outside of the injection site following transplantation have hindered the overall success of this technology.[13] Significant improvements in cell survival have been obtained following immunosuppresive therapy[14, 15], but few studies have been centered on muscle cell migration, especially after myogenic cell transplantation.

We believe that it is this secondary pathological process of DMD, namely fibrous scar tissue formation, which poses the most significant obstacle to myogenic cell migration, fusion, and regeneration. Digesting fibrous scar tissue could remodel the microenvironment to make it more hospitable to fusion, migration, and myogenic cell regeneration, subsequently enhancing the myogenic transplantation process and improving muscle healing, not only in injured skeletal muscle, but also in patients suffering from DMD.

Matrix Metalloproteinases (MMPs) are a family of zinc-dependent proteolytic enzymes with the ability to digest specific components of the extracellular matrix.[16] They present a promising approach to treat fibrosis following skeletal muscle injury or as a consequence of neuromuscular disease. MMP-1, in particular, has the ability to digest the main constitutive proteins in fibrous scar tissue, native fibrillar collagens type I and III, while sparing collagen type IV, which is a component of the basement membrane.[17-19] MMP-1

may also play important roles in ECM remodeling and cell signaling with its ability to act on cell surface, matrix, and non-matrix substrates such as insulin-growth factor binding proteins, L-selectin, and tumor necrosis factor-α.[20, 21]

Previous work in our laboratory has indicated that MMP-1 can help remove the fibrous blockade to enhance muscle healing.[22] We hypothesize that MMP-1 can further enhance muscle regeneration by directly improving myoblast migration as well as differentiation capability. This may ultimately enhance muscle regeneration by improving the myoblast's ability to increase the number of regenerating myofibers within an area of injury as well as increase the effective range that myoblasts-enhanced muscle regeneration can occur. We tested this hypothesis by studying the effects of MMP-1 on myoblasts *in vitro* as well as studying myoblast transplantation *in vivo*.

Materials and Methods

In vitro

1. Cell Differentiation Assay

C2C12 cells were purchased from the American Type Culture Collection (Rockville, MD). The cells were cultured complete medium containing Dulbecco's Modified Eagle's Medium (DMEM; Invitrogen, Carlsbad, CA) supplemented with 10% fetal bovine serum, 10% horse serum, 0.5% chicken embryo extract, and 1% penicillin/streptomycin (P/S) at 37°C in a 5% CO_2 atmosphere in 12 well plates until 75% confluent. Cells were subsequently incubated in differentiation media containing serum-free DMEM supplemented with 1% penicillin/streptomycin and treated with 0, 1.0, 10, or 100ng/mL of MMP-1 (Sigma, M1802) for 3, 5, and 7 days. Cells were fixed in cold methanol for 1 minute and washed with phosphate buffered saline (PBS). The fixed cells were immunostained for Myosin Heaven Chain (MyHC, Sigma, St. Louis, MO) and 4',6-Diamidino-2-phenylindole (DAPI, Sigma, St. Louis, MO) to visualize mature myotubes. The differentiation was quantified by averaging the number of myotubes counted in 5 high power fields.

2. *In Vitro* Wound Healing Assay

C2C12 cells were cultured in 12 well plates (described above) to 70% confluency. Cells were then placed in serum-free DMEM supplemented with 1% P/S and treated with 0, 1.0, 10, or 100 ng/mL of MMP-1. An artificial wound was created by disrupting the monolayer with a sterile plastic pipette tip. Cells were incubated for 1, 4, 6, and 12 hours to allow for migration back into the wound area. Cells were then fixed in cold methanol,

washed with PBS, and then stained with DAPI to help visualize migration. Northern Eclipse Software (Empix Imaging Inc, Mississauga, ON, Canada) was used to quantify the average migration distance C2C12 cells traveled past the original wound demarcation.

3. Flow Cytometry

C2C12 cells were cultured in complete media (described above). Cells were then placed in serum-free DMEM supplemented with 1% P/S and treated with 0, 1.0, 10, or 100 ng/mL of MMP-1 for 18 hours. Cells were incubated with either polyclonal n-cadherin (sc-31031; Santa Cruz Biotechnology, Santa Cruz, CA) or β-catenin (sc-1496; Santa Cruz Biotechnology, Santa Cruz, CA) primary antibodies and subsequently with a PE-conjugated secondary antibody. Marked cell samples were analyzed with a FACS Caliber flow cytometer (BD Biosciences, Sparks, MD) and CellQuest software (BD Biosciences, Sparks, MD).

4. Western Blot Analysis

C2C12 cells were harvested after 48 hours incubation with or without MMP-1 (0, 1.0, 10, 100 ng/mL) in serum-free DMEM. After lysing, the samples were separated by 12% sodium dodecyl-sulfate-polyacrylamide electrophoresis gel and transferred to nitrocellulose membranes. Anti-PreMMP2 antibodies (Sigma, St. Louis, MO), anti-TIMP-1 (sc-5538, Santa Cruz Biotechnology, Santa Cruz, CA) and anti-Myogenin (Sigma, St. Louis, MO) were used as primary antibodies. Mouse Glyceraldehyde 3-phosphate dehydrogenase (GAPDH, Sigma, St. Louis, MO) was used for protein quantification.

In vivo

1. Myoblast transplantation in Dystrophic Skeletal Muscle

9 week old MDX/SCID mice (C57BL/10ScSn-Dmd[mdx] crossed with C57BL/6J-Prkdc[scid]/SzJ) were injected with C2C12 cells with MMP-1 (M-1609, Sigma, St. Louis, MO). 1×10^5 LacZ positive C2C12 cells were mixed with 200 ng of MMP-1 in a volume of 5 µL PBS containing fluorescence beads (1 µg/mL, Molecular Probes, Eugene, Oregon), which was then injected into the left GMs of MDX/SCID mice. The same number of LacZ positive C2C12 diluted with 5 µL of PBS with fluorescence beads was injected into the right GMs of the mouse to serve as a control. Muscle tissues were harvested for histological analysis at 2 weeks after transplantation. GMs were isolated, mounted, and frozen in 2-methylbutane cooled in liquid nitrogen. Each muscle specimen was cryostat sectioned at 10µm for histological analysis. LacZ staining with Eosin and immunohistochemistry for dystrophin (Sigma, St. Louis, MO) were performed [6,7]. Myoblast migration distances from the initial site of injection were quantified using Northern Eclipse Software (Empix Imaging Inc, Mississauga, ON, Canada).

Statistics

Statistical significance was assessed by a Student's t-test; $P < 0.05$ was considered significant.

Results

MMP-1 Stimulated Myoblast Migration *In Vitro*

Our laboratory has previously shown that MMP-1 can improve migration of transplanted myoblasts (C2C12) in scarred muscle. However, we did not have direct evidence that MMP-1 actually stimulated C2C12 migration directly. We utilized an *in vitro* wound healing assay, flow cytometry, and Western Blot analysis to determine whether MMP-1 could alter C2C12 migration. After culturing C2C12 cells to 70% confluence, we created artificial wounds as described previously, and measured migration distances of C2C12 cells back into the wound area. Our results indicate that MMP-1 can enhance C2C12 migration. We observed a significant difference in migration distance for C2C12 cells treated with 10 ng/mL of MMP-1 at 4 and 6 hours after injury when compared to the control group (Fig. 1). N-cadherin and β-catenin are two proteins expressed with myoblast migration,[23, 24] and were used as markers for C2C12 cell migration analyzed by flow cytometry. Flow cytometry results demonstrated that MMP-1 promoted the upregulation of both N-cadherin and β-catenin in C2C12 cells in a dose-dependent manner when treated with 0.1, 1, 10, and 100 ng/mL of MMP-1 (Fig. 2). Western Blot analysis further demonstrates that MMP-1 treatment enhances myoblast migration. It has been reported in the literature that PreMMP2 and TIMP are upregulated with myoblast migration.[14, 25-29] Expression of PreMMP2 increased in a dose dependent manner when treated with 0.1, 1, 10, and 100 ng/mL of MMP-1 (Fig. 3). Expression of TIMP was upregulated in a dose-dependent manner when treated with 0.1, 10, and 100 ng/mL of MMP-1 (Fig. 3).

MMP-1 Stimulated C2C12 Differentiation *In Vitro*

C2C12 cells proliferate when maintained in growth media containing serum, but differentiate into multinucleated myotubes when grown in serum-free media. This progression of differentiation is similar to that observed for myogenesis in vivo.[30] We investigated whether MMP-1 could enhance C2C12 differentiation *in vitro* using a differentiation assay as well as Western Blot analysis. When cultured in differentiation media, C2C12 cells displayed a dose-dependent increase in differentiation capacity when treated with 10, and 100 ng/mL of MMP-1 compared to control groups (Fig. 4 A-C). Treatment with 10 and 100 ng/mL of MMP-1 produced significantly more myotubes compared to the control group at days 3 and 5 (Fig. 4). To further demonstrate that MMP-1 enhances cell differentiation, we used Western Blot analysis of myogenin, which has previously been shown to be a protein controlling myofiber formation.[26] When cultured in differentiation media, C2C12 cells displayed a dose-dependent increase in the expression of myogenin when treated with 0.1, 1, 10, and 100 ng/mL of MMP-1.

MMP-1 Enhances Myoblast Migration and Differentiation *In Vivo*

We elected to test the effects of MMP-1 on myoblast migration and differentiation by transplanting C2C12 cells in *mdx* mice. The *mdx* mouse contains a nonsense mutation in the dystrophin gene, which leads to the absence of full-length dystrophin protein in skeletal muscle, thus providing a suitable model for human DMD.[9, 31] By transplanting C2C12 cells into the GM of MDX/SCID mice, we were able to assess whether MMP-1 was able to enhance myoblast migration based upon migration distance from the initial injection area through histological analysis. The original injection area was able to be

visualized by injecting fluorescent beads along with C2C12 cells. Concomitant injection of MMP-1 along with C2C12 cells significantly increased the migration area covered by the C2C12 cells (Fig. 5). We were also able to assess the effects of MMP-1 on myoblast differentiation and fusion with host myofibers using immunohistochemical analysis. Since MDX/SCID mice are deficient in dystrophin, dystrophin positive myofibers represent transplanted C2C12 cells that have differentiated and fused with host myofibers. When C2C12 cells were injected with MMP-1, significantly more dystrophin-positive myofibers were visualized compared to control injections (Fig. 5).

Discussion

Injured skeletal muscle has an enormous capacity to heal itself in a process that is dependent on the activation and differentiation of myoblasts.[2, 32-34] Disruption of the basal lamina and plasma membrane of skeletal muscle cells leads to the release of satellite cells, which follow a highly coordinated sequence of steps in which they migrate towards injured muscle and subsequently differentiate and fuse together to form myoblasts, multinucleated myotubes, and ultimately, mature muscle fibers.[2, 34] Unfortunately, excess deposition of the ECM in the form of fibrotic scar tissue often leads to incomplete recovery. A persistent imbalance between collagen biosynthesis and degradation contributes to scar formation and fibrosis in tissues; high levels of collagens have been detected in injured skeletal muscle[4, 8, 35] and inhibition of collagen deposition has been able to reduce scar tissue formation in injured skeletal muscle.[36] Additionally, muscle injuries usually result in hematomas that are gradually replaced by granulation tissue that fosters fibrosis. [1-3, 34, 37]

The clinical applications of anti-fibrotic therapies such as suramin and decorin are limited in scope because most persons with muscle injuries seek treatment for muscle injuries only after the onset of fibrosis. Furthermore, large quantities of fibrotic tissue are already present in the skeletal muscles of patients who suffer from neuromuscular disorders like DMD. Previous studies have demonstrated that MMP collagenases such as MMP-1 are capable of removing fibrotic tissue within skeletal muscle,[22] are essential for myoblast migration *in vivo*,[38-40] and also appear to be involved in satellite cell activation, which

function as myoblast precursors capable of differentiating and fusing with muscle fibers to repair damage.[41]

We have previously demonstrated that MMP-1 can help remove the fibrous blockade against migrating myoblasts, thereby improving myoblast migration *in vivo*.[22] We were able to replicate these results in dystrophin-deficient MDX/SCID mice by demonstrating that transplanted myoblasts covered a significantly larger area from the initial injection site. Our results demonstrate the MMP-1 not only removes fibrous scar tissue from skeletal muscle, but can also activate myoblast migration. We observed this directly by examining MMP-1's effects on C2C12 cell migration into artificial wounds *in vitro*. This was further supported by the upregulation of 4 migration-related proteins (n-cadherin, β-catenin, preMMP-2, and TIMP-1) after treatment with MMP-1. We had previously hypothesized that MMP-1 may be liberating growth factors and cell signaling molecules or acting on cell adhesion sites located within the ECM. Given our *in vitro* experiments in the absence of ECM, MMP-1 may also be acting on binding proteins present on the myoblast cell surface to directly promote migration or may be involved in a more complex signaling cascade.

Myoblasts differentiate into multinucleated myotubes, which eventually fuse with mature muscle fibers to regenerate muscle.[2, 34] Our results indicate that MMP-1 can promote C2C12 myoblast differentiation *in vitro* as well as *in vivo*. C2C12 cells treated with MMP-1 produce significantly more myotubes when cultured *in vitro*. Myoblasts transplanted into fibrotic skeletal muscles of MDX/SCID mice showed significantly

increased numbers of regenerating myofibers when treated with MMP-1. We were also able to support these results on a molecular level; C2C12 cells treated with MMP-1 upregulated their expression of myogenin, which is a checkpoint protein involved in myofiber formation. Because myoblast differentiation is a critical step in the process of muscle regeneration, MMP-1 may improve the recovery of muscle function after injury by increasing the number of myofibers generated by activated myoblasts.

For patients suffering from DMD, increases in myoblast migration and fusion with host fibers after muscle cell transplantation would greatly improve the success of myoblast transplantation. To date, limited myoblast migration distances from the sites of transplantation have complicated therapy.[13] As a result of this limited migration, repeated injections are required in order to obtain sustainable engraftment. Unfortunately, repeated injections not only cause pain and discomfort for patients, but also foster additional fibrosis via direct trauma to the skeletal muscle. Treatment with MMP-1 may augment the success of muscle cell transplantation by improving the efficacy of transplanted cells as well as reducing the number of injections required to sustain engraftment.

Acknowledgments

References:

1.   Garrett WE, Jr.: Muscle strain injuries: clinical and basic aspects, Med Sci Sports Exerc 1990, 22:436-443
2.   Li Y, Cummins, J., Huard, J.: Muscle Injury and Repair, Current Opinion in Orthopaedics 2001, 12:409-415
3.   Lehto MU, Jarvinen MJ: Muscle injuries, their healing process and treatment, Ann Chir Gynaecol 1991, 80:102-108
4.   Chan YS, Li Y, Foster W, Horaguchi T, Somogyi G, Fu FH, Huard J: Antifibrotic effects of suramin in injured skeletal muscle after laceration, J Appl Physiol 2003, 95:771-780
5.   Fukushima K, Badlani N, Usas A, Riano F, Fu F, Huard J: The use of an antifibrosis agent to improve muscle recovery after laceration, Am J Sports Med 2001, 29:394-402
6.   Li Y, Huard J: Differentiation of muscle-derived cells into myofibroblasts in injured skeletal muscle, Am J Pathol 2002, 161:895-907
7.   Li Y, Foster W, Deasy BM, Chan Y, Prisk V, Tang Y, Cummins J, Huard J: Transforming growth factor-beta1 induces the differentiation of myogenic cells into fibrotic cells in injured skeletal muscle: a key event in muscle fibrogenesis, Am J Pathol 2004, 164:1007-1019
8.   Sato K, Li Y, Foster W, Fukushima K, Badlani N, Adachi N, Usas A, Fu FH, Huard J: Improvement of muscle healing through enhancement of muscle regeneration and prevention of fibrosis, Muscle Nerve 2003, 28:365-372
9.   Hoffman EP, Brown RH, Jr., Kunkel LM: Dystrophin: the protein product of the Duchenne muscular dystrophy locus, Cell 1987, 51:919-928
10.   Partridge TA: Invited review: myoblast transfer: a possible therapy for inherited myopathies?, Muscle Nerve 1991, 14:197-212
11.   Iimuro Y, Nishio T, Morimoto T, Nitta T, Stefanovic B, Choi SK, Brenner DA, Yamaoka Y: Delivery of matrix metalloproteinase-1 attenuates established liver fibrosis in the rat, Gastroenterology 2003, 124:445-458
12.   Karpati G, Holland P, Worton RG: Myoblast transfer in DMD: problems in the interpretation of efficiency, Muscle Nerve 1992, 15:1209-1210
13.   Skuk D: Myoblast transplantation for inherited myopathies: a clinical approach, Expert Opin Biol Ther 2004, 4:1871-1885
14.   Sato H, Okada Y, Seiki M: Membrane-type matrix metalloproteinases (MT-MMPs) in cell invasion, Thromb Haemost 1997, 78:497-500
15.   Werb Z, Chin JR: Extracellular matrix remodeling during morphogenesis, Ann N Y Acad Sci 1998, 857:110-118
16.   Brinckerhoff CE, Matrisian LM: Matrix metalloproteinases: a tail of a frog that became a prince, Nat Rev Mol Cell Biol 2002, 3:207-214
17.   Sakaida I, Hironaka K, Kimura T, Terai S, Yamasaki T, Okita K: Herbal medicine Sho-saiko-to (TJ-9) increases expression matrix metalloproteinases (MMPs) with reduced expression of tissue inhibitor of metalloproteinases (TIMPs) in rat stellate cell, Life Sci 2004, 74:2251-2263

18.	Roach DM, Fitridge RA, Laws PE, Millard SH, Varelias A, Cowled PA: Up-regulation of MMP-2 and MMP-9 leads to degradation of type IV collagen during skeletal muscle reperfusion injury; protection by the MMP inhibitor, doxycycline, Eur J Vasc Endovasc Surg 2002, 23:260-269

19.	Vincenti MP, Brinckerhoff CE: Transcriptional regulation of collagenase (MMP-1, MMP-13) genes in arthritis: integration of complex signaling pathways for the recruitment of gene-specific transcription factors, Arthritis Res 2002, 4:157-164

20.	McCawley LJ, Matrisian LM: Matrix metalloproteinases: they're not just for matrix anymore!, Curr Opin Cell Biol 2001, 13:534-540

21.	Pardo A, Selman M: MMP-1: the elder of the family, Int J Biochem Cell Biol 2005, 37:283-288

22.	Bedair H, Liu TT, Kaar JL, Badlani S, Russell AJ, Li Y, Huard J: Matrix metalloproteinase-1 therapy improves muscle healing, J Appl Physiol 2007, 102:2338-2345

23.	Brand-Saberi B, Gamel AJ, Krenn V, Muller TS, Wilting J, Christ B: N-cadherin is involved in myoblast migration and muscle differentiation in the avian limb bud, Dev Biol 1996, 178:160-173

24.	Woodfield RJ, Hodgkin MN, Akhtar N, Morse MA, Fuller KJ, Saqib K, Thompson NT, Wakelam MJ: The p85 subunit of phosphoinositide 3-kinase is associated with beta-catenin in the cadherin-based adhesion complex, Biochem J 2001, 360:335-344

25.	Takino T, Watanabe Y, Matsui M, Miyamori H, Kudo T, Seiki M, Sato H: Membrane-type 1 matrix metalloproteinase modulates focal adhesion stability and cell migration, Exp Cell Res 2006, 312:1381-1389

26.	Ohtake Y, Tojo H, Seiki M: Multifunctional roles of MT1-MMP in myofiber formation and morphostatic maintenance of skeletal muscle, J Cell Sci 2006, 119:3822-3832

27.	Mendes O, Kim HT, Lungu G, Stoica G: MMP2 role in breast cancer brain metastasis development and its regulation by TIMP2 and ERK1/2, Clin Exp Metastasis 2007, 24:341-351

28.	Gong YL, Xu GM, Huang WD, Chen LB: Expression of matrix metalloproteinases and the tissue inhibitors of metalloproteinases and their local invasiveness and metastasis in Chinese human pancreatic cancer, J Surg Oncol 2000, 73:95-99

29.	Kim HJ, Park CI, Park BW, Lee HD, Jung WH: Expression of MT-1 MMP, MMP2, MMP9 and TIMP2 mRNAs in ductal carcinoma in situ and invasive ductal carcinoma of the breast, Yonsei Med J 2006, 47:333-342

30.	Lluri G, Jaworski DM: Regulation of TIMP-2, MT1-MMP, and MMP-2 expression during C2C12 differentiation, Muscle Nerve 2005, 32:492-499

31.	Sicinski P, Geng Y, Ryder-Cook AS, Barnard EA, Darlison MG, Barnard PJ: The molecular basis of muscular dystrophy in the mdx mouse: a point mutation, Science 1989, 244:1578-1580

32.	Abe R, Donnelly SC, Peng T, Bucala R, Metz CN: Peripheral blood fibrocytes: differentiation pathway and migration to wound sites, J Immunol 2001, 166:7556-7562

33.	Crisco JJ, Jokl P, Heinen GT, Connell MD, Panjabi MM: A muscle contusion injury model. Biomechanics, physiology, and histology, Am J Sports Med 1994, 22:702-710

34.   Huard J, Li Y, Fu FH: Muscle injuries and repair: current trends in research, J Bone Joint Surg Am 2002, 84-A:822-832

35.   Foster W, Li Y, Usas A, Somogyi G, Huard J: Gamma interferon as an antifibrosis agent in skeletal muscle, J Orthop Res 2003, 21:798-804

36.   Velleman SG: The role of the extracellular matrix in skeletal muscle development, Poult Sci 1999, 78:778-784

37.   Menetrey J, Kasemkijwattana C, Fu FH, Moreland MS, Huard J: Suturing versus immobilization of a muscle laceration. A morphological and functional study in a mouse model, Am J Sports Med 1999, 27:222-229

38.   Carmeli E, Moas M, Reznick AZ, Coleman R: Matrix metalloproteinases and skeletal muscle: a brief review, Muscle Nerve 2004, 29:191-197

39.   Rivilis I, Milkiewicz M, Boyd P, Goldstein J, Brown MD, Egginton S, Hansen FM, Hudlicka O, Haas TL: Differential involvement of MMP-2 and VEGF during muscle stretch- versus shear stress-induced angiogenesis, Am J Physiol Heart Circ Physiol 2002, 283:H1430-1438

40.   El Fahime E, Torrente Y, Caron NJ, Bresolin MD, Tremblay JP: In vivo migration of transplanted myoblasts requires matrix metalloproteinase activity, Exp Cell Res 2000, 258:279-287

41.   Yamada M, Tatsumi R, Kikuiri T, Okamoto S, Nonoshita S, Mizunoya W, Ikeuchi Y, Shimokawa H, Sunagawa K, Allen RE: Matrix metalloproteinases are involved in mechanical stretch-induced activation of skeletal muscle satellite cells, Muscle Nerve 2006, 34:313-319

42.   Peault B, Rudnicki M, Torrente Y, Cossu G, Tremblay JP, Partridge T, Gussoni E, Kunkel LM, Huard J: Stem and progenitor cells in skeletal muscle development, maintenance, and therapy, Mol Ther 2007, 15:867-877

Figure legends:

Figure 1: Myoblasts (C2C12) were grown to confluence and artificially wounded by disrupting the monolayer with a sterile pipette. C2C12 (white arrowheads) show an enhanced ability to migrate into the wound area after 4 and 6 hours of treatment with MMP-1 (10ng/mL). Red lines represent original line demarcating the wound area. Green lines represent the approximate migration area.
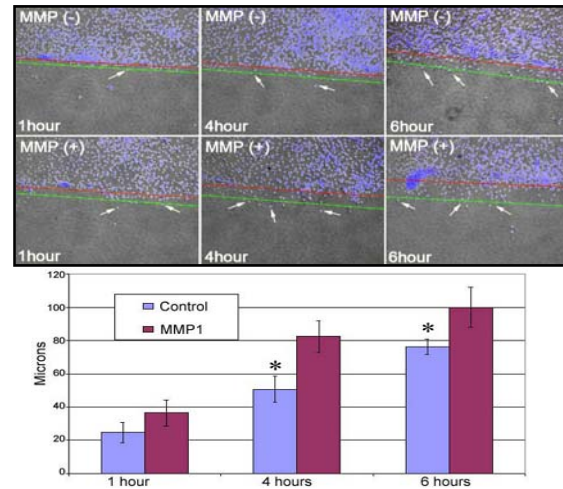
Figure 1

Figure 2

Figure 2: Myoblasts (C2C12) treated with MMP-1 for 18 hours display a dose-dependent upregulation of 2 migration-related proteins: n-cadherin (top row) and β-catenin (bottom row). Flow cytometry results for 0.1, 1.0, 10, and 100 ng/mL MMP-1 treated cells.
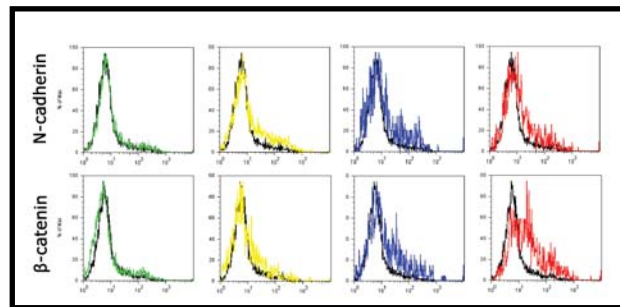

Figure 3

Figure 3: Myoblasts (C2C12) were treated with either 0, 1.0, 10, or 100 ng/mL of MMP-1 for 7 hours. Western blot analysis showed a dose-dependent increase in the expression of migration related proteins Pre-MMP2 and TIMP as well as a myogenic protein, Myogenin. GAPDH staining served as the control.
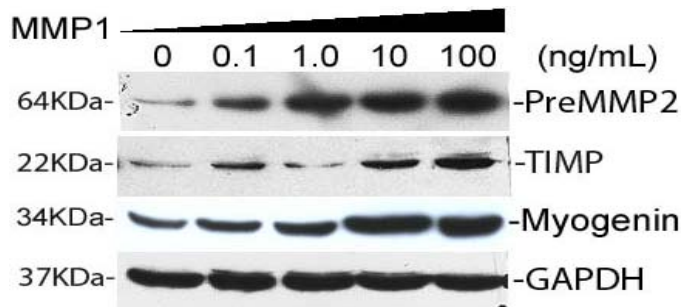

19

Figure 4: C2C12 were cultured until 75% confluent. They were subsequently treated with either 0, 1.0, 10, or 100 ng/mL of MMP-1 in differentiation medium for 3, 5, and 7 days (day 3 shown). Myotubes were immunostained with MyHC (red) and nuclei were stained with DAPI (blue). The number of myotubes were quantified by averaging the count from 5 high powered fields using a fluorescent microscope. C2C12 displayed a dose-dependent increase in ability to differentiate into myotubes at 10 and 100 ng compared to control. * $p < 0.05$
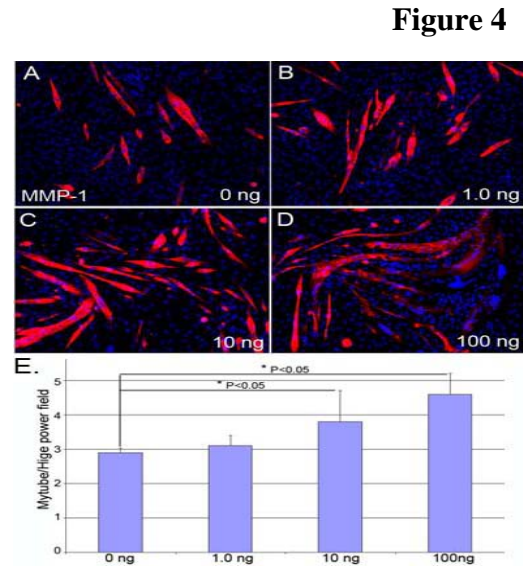

Figure 4

Figure 5: 1x105 LacZ positive C2C12 and fluorescent beads were injected into the gastrocnemius muscles (GM) of MDX/SCID mice along with 200ng of MMP-1 in the left GM and PBS in the right GM. GMs were harvested at different time points. LacZ staining with eosin along with immunohistochemistry for dystrophin were performed. MMP-1 treated cells fused to a greater degree (4A) compared to control cells (4C) at 2 weeks post transplant. Using immunohistochemistry, higher numbers of positive myofibers were detected within MMP-1 treated muscle (4B) compared to control (4D) at 2 weeks. MMP-1 treated C2C12 migrated at increased distances from the original injection site (Fig 4E). Red: dystrophin, Green: beads, Blue: nuclei, White asterisks: dystrophin positive myofibers. * $p < 0.05$.
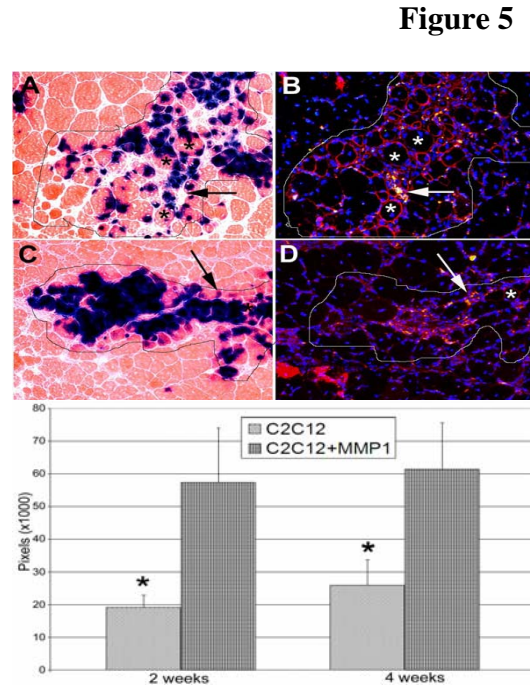
Figure 5

Matrix Metalloproteinase-1 enhances muscle cell migration and dedifferentiaiton

William Wang [1,2], Haiying Pan [1], Bahiyyah Jefferson [1], Yong Li [1,3] *

1. Stem Cell Research Center (SCRC), Children's Hospital of Pittsburgh; 2. University Pittsburgh, School of Medicine; 3. Department of Orthopaedic Surgery and Department of Pathology, University of Pittsburgh.

Abstract

Muscle injuries are among the most common injuries seen in orthopaedic clinics today and present a challenging problem in everyday life. Damaged muscle fibers undergo extensive regeneration; however, muscle cell migration is limited by the presence fibrous scar tissue, which precludes the complete recovery of muscle function. We hypothesize that Matrix Metalloproteinase-1 (MMP-1), a proteolytic enzyme, may be useful for scar digestion, which would consequently create inroads for myoblast migration after muscle injuries. We have previously determined that MMP-1 could improve muscle healing by digesting fibrous scar tissue. In this experiment, our objective was to observe whether MMP-1 could increase muscle cell migration and differentiation. Our results indicate that C2C12 (myoblast) cells treated with MMP-1 resulted in an increased differentiation and migration capacity *in vitro*. We also found that C2C12's expression of migration-related proteins, n-cadherin and β-catenin, was increased after MMP1 treatment. Additionally, MMP-1 appears to enhance myoblast migration and regeneration *in vivo*. Using a mouse muscle injury model, we injected Lac-Z-labeled C2C12 cells directly into fibrous scar tissue along with MMP-1. Our results indicated an increase in the ability of the C2C12 cells to differentiate and fuse with host myofibers as determined by histological analysis. We have determined that MMP1 can digest fibrous scar tissue and act on the extracellular matrix (ECM) to release growth factors to produce a microenvironment more suitable for muscle cell regeneration in injured muscle. Based on the preliminary results from this study, we have determined that MMP-1 improves muscle healing after injury by remodeling the ECM, but that it may also directly act upon myoblasts to enhance migration and regenerative ability.

Key words: MMP1, muscle injury, fibrous scar tissue, myoblast, migration, differentiation.

Cellular caspase-8-like inhibitory protein (cFLIP) prevents inhibition of muscle cell differentiation induced by cancer cells

Zhilong Jiang* and Paula R. Clemens*,†,1

*Department of Neurology, School of Medicine, University of Pittsburgh, Pennsylvania, USA; and †Neurology Service, Department of Veterans Affairs Medical Center, Pittsburgh, Pennsylvania, USA

ABSTRACT   Cachexia is a frequent complication of cancer or other chronic diseases. To investigate the pathophysiology of cancer cachexia and pursue treatment options, we developed an *in vitro* assay of the effects of cancer cell-produced cytokines on primary muscle cells derived from murine skeletal muscle. These studies led to the novel observation that factors secreted by cell lines from prostate cancer and melanoma significantly inhibit differentiation of primary mouse muscle cells. The expression of interleukin (IL) -1β, TNF-α, and proteolysis-inducing factor (PIF) by cancer cells used in this study suggested their role in preventing myogenic differentiation. Both NF-κB binding and transcriptional activity were enhanced in muscle cells treated with conditioned media from cancer cells or with proinflammatory cytokines. Stable expression of IKBSR, a known repressor of NF-κB activation, and cellular caspase-8-like inhibitory protein (cFLIP) inhibited activation of NF-κB in cancer cell media-treated muscle cells with an accompanying enhancement of myogenic protein expression and differentiation. In contrast, overexpression of antiapoptotic protein Bcl-xL did not protect myoblast cells exposed to the same treatment. Instead, we observed enhanced activation of NF-κB in Bcl-xL overexpressing cells. These studies show that the *in vitro* system recapitulates some of the molecular events causing muscle cachexia and provides the basis for new treatment approaches.—Jiang, Z., Clemens, P. R. Cellular caspase-8-like inhibitory protein (cFLIP) prevents inhibition of muscle cell differentiation induced by cancer cells. *FASEB J.* 20, E1979–E1989 (2006)

Key Words: cachexia · NF-κB · apoptosis

CACHEXIA OR MUSCLE wasting is a common syndrome in patients with malignant cancer (1, 2) and other chronic diseases such as rheumatoid arthritis (3) and chronic heart failure (4). A full understanding of the underlying mechanism of cachexia is an important step in finding novel therapeutic targets for treatment of this clinical condition. Previous studies showed that higher levels of some proinflammatory cytokines contribute to the development of cachexia (5, 6). For example, serum TNF-α and interleukin (IL) -1α levels are markedly increased in patients with rheumatoid arthritis and cancer (3, 7). Chronic administration of exogenous TNF-α to an animal model generated cachexia (8). In addition to TNF-α, other cytokines such as IL-6, IL-1β, IL-1α, and proteolysis-inducing factor (PIF) have been reported to contribute to the development of muscle wasting (5, 6, 9).

Further studies *in vitro* and *in vivo* have provided evidence that a principal mechanism by which TNF-α and IL-1α lead to progressive muscle wasting is through the activation of transcription factor NF-κB (10–12). Activated NF-κB translocates to the nucleus and inhibits expression or stabilization of myogenic regulatory factors such as MyoD (10, 13). MyoD is a muscle-specific basic helix-loop-helix transcription factor whose expression and binding to promoter elements result in the expression of genes in the muscle differentiation program such as myogenin and cyclin-dependent kinase (Cdk) inhibitor p21 (10). Failure of this myogenic program results in muscle wasting.

Because phosphorylation and degradation of IκB inhibitory protein (IκBα) results in activation of NF-κB, the introduction of a phosphorylation-defective mutant of IκBα, IκB super repressor (IKBSR), can prevent NF-κB activation. Studies have shown that overexpression of IKBSR prevents NF-κB activation and ameliorates the inhibitory effect of TNF-α or IL-1 on expression and stability of MyoD in muscle cells (10, 13).

Cellular caspase-8-like inhibitory protein (cFLIP) is an antiapoptotic protein responsible for cell survival and cell resistance to apoptosis by inhibition of pro-caspase-8 processing at the death-inducing signaling complex (DISC) (14–18). Bcl-xL is another antiapoptotic protein and is localized to the endoplasmic reticulum so as to prevent cytochrome *c* release from mitochondria (19). Recent studies showed that both cFLIP and Bcl-xL influenced NF-κB activation and cell survival in a variety of cell lines such as 293 cells, HeLa

cells, and PC12 cells, a differentiated neuronal cell line (20–22). However, whether cFLIP and Bcl-xL affect NF-κB activity and survival in muscle cells has not been previously studied.

In this study, we first determined the effect of secreted factors from different cancer cell lines on myoblast cell differentiation *in vitro*. We then investigated whether overexpression of IKBSR, cFLIP, or Bcl-xL is able to influence muscle cell differentiation *in vitro* and whether activation or suppression of the NF-κB signaling pathway is involved in this process.

MATERIALS AND METHODS

Cell lines and plasmids

Human embryonic kidney 293 cells [American Type Culture Collection (ATCC), Rockville, MD, USA] and human prostate cancer cell lines PC-3 and DU-145 (ATCC,), human melanoma cells Mel (Steven Rosenberg, National Cancer Institute, NIH, Bethesda, MD, USA) and murine colon cancer cells MC-38 (Steven Rosenberg, National Cancer Institute) were maintained in RPMI1640 supplemented with 10% heat-inactivated fetal calf serum, 20 mM L-glutamine, and 1% penicillin-streptomycin. Conditioned media were collected 48 h after cells were seeded in fresh RPMI1640 medium. Cell culture reagents were purchased from Invitrogen (Carlsbad, CA, USA).

A mutant IκBα cDNA IKBSR (1.1 kb) containing an N-terminal hemagglutinin tag was subcloned into pRc/CMV2 with cytomegalovirus (CMV) promoter replaced by the chicken β-actin promoter (Joseph DiDonato, Department of Cancer Biology, Lerner Research Institute, Cleveland Clinic Foundation, Cleveland, OH, USA). A 1.4 kb cFLIP$_L$ cDNA (Steven Graham, Department of Neurology, University of Pittsburgh, Pittsburgh, PA, USA) was subcloned into pCR3.V64-Met-Flag-stop driven by the CMV promoter (Invitrogen). A 0.6 kb rat Bcl-xL cDNA (Jun Chen, Department of Neurology, University of Pittsburgh) was subcloned into pcDNA3.1 driven by the CMV promoter (Invitrogen). For some experiments, a GFP expression vector pN1-GFP (Clontech, Palo Alto, CA, USA) was used.

Primary myoblast cells and generation of cell lines

Primary myoblast cells were prepared from the hind limb muscles of 3-wk-old C57BL/10 (C57) mice (23). Briefly, the muscle mass was minced into a coarse slurry using razor blades. Cells were enzymatically dissociated by adding 1% collagenase D (Boehringer Mannhein, Mannheim, Germany) for 2 h at 37°C. The single cell suspension was filtered through an 85 μm nytex filter and preplated in a collagen-coated dish in myoblast growth media. After 2 h, the supernatant was withdrawn from the dish and replated in a fresh collagen-coated dish. After 4–5 serial passages, the culture was enriched with small, round myoblast cells. Cells were assayed for desmin expression and the ability to differentiate when cultured in fusion medium (DMEM with 2% horse serum) to assure that >85% of the cells in the culture were myogenic.

Stable expression of IKBSR, cFLIP, and Bcl-xL cDNAs in primary C57 myoblasts was obtained by transfection of C57 myoblast cells with each expression plasmid or an empty control vector pcDNA3.1 by Lipofectamine 2000 (LF 2000)

(Invitrogen). At 48 h after transfection, cells were passaged at 1:50 of their density in the presence 0.4 mg/ml G418 (Sigma, St. Louis, MO, USA). Antibiotic resistant clones were expanded and tested for expression of the transgene by immunochemistry and Western blot analysis.

NF-κB activity assay

Collagen-coated 24-well culture plates were seeded with C57 myoblast cells (0.5×10^5 cells) 1 day before transfection with the NF-κB-driven GFP reporter plasmid pNF-κB-hrGFP (200 ng/well) (Stratagene, La Jolla, CA, USA) using Lipofectamine 2000. To normalize for transfection efficiency, the β-galactosidase plasmid pCMV-β (100 ng/well, Clontech, Mountain View, CA, USA) was added to all transfections. At 6 h after transfection, the DNA-LP 2000 complex was removed and replaced with conditioned media (1:2 dilution) or F12 media containing cytokines TNF-α, IFN-γ, IL-1β, and IL-6 (PharMingen, Rockville, MD, USA). GFP-positive and β-galactosidase-positive cells were counted 24 h after transfection. The β-galactosidase-expressing cells were detected by X-gal staining reagent (5 mM $FeK_3(CN)_6$, 5 mM $K_4Fe(CN)_6 3H_2O$, 1 μg/μl X-gal, and 2 mM $MgCl_2$) at 37°C for 2 h. At least 8 fields per well were counted at 100× magnification. NF-κB activity assay was presented as the ratio of GFP-positive to β-galactosidase-positive cells.

Gel shift assay

For gel shift analysis, a nuclear extract of each sample was prepared from 3×10^6 cells treated or untreated with indicated cytokines or tumor cell conditioned media, using NE-PER nuclear and cytoplasmic extraction reagents (Pierce, Rockford, IL, USA). The protein concentration of each nuclear extract was measured by the bicinchoninic acid (BCA) assay (Pierce). NF-κB oligonucleotides (2 μl, 1.75 pmol/μl, oligonucleotide sequence 5′-AGTTGA GGG GAC TTT CCC AGG C-3′, 3′-TCA ACT CCC CTG AAAGGG TCC G-5′) (Promega, Madison, WI, USA) were ^{32}P-labeled with 1 μl 10 μCi [γ^{32}] ATP (Amersham Biosciences, Piscataway, NJ, USA) by using the DNA 5′-end labeling system kit (Promega) in a volume of 20 μl at 37°C for 1 h. The reaction was stopped by addition of 2 μl 0.5 mol/L EDTA and 88 μl TE buffer. The binding reaction mixture (20 μl), which contained 35 fmol ^{32}P-labeled NF-κB oligonucleotides, 10 μg nuclear extracts, 1 μg poly (dI:dC), was incubated at room temperature for 1–2 h in 1× binding buffer (Pierce). Unlabeled NF-κB oligonucleotides (1.75 pmol) were added in the binding reaction mixture as a competitor. DNA-protein complexes were resolved by electrophoresis through 5% polyacrylamide gels in 0.5× TBE buffer at 100 V for 1 h. The gel was subsequently dried and autoradiographed with intensifying screens at −80°C. Gel supershift assays were performed by addition of 2 μl of antibodies, antip65 and antip50 (200 μg/0.1 ml) (Santa Cruz Biotechnology, Inc. Santa Cruz, CA, USA) to the reaction mixture and incubation for 45 min at room temperature.

Immunocytochemical staining for myogenic proteins

We assessed the extent of myogenic differentiation morphologically by determining the myogenic index, which is defined as the fraction of nuclei residing in multinucleated myotube cells expressing myosin, myoD, or myogenin. Briefly, C57 myoblast cells were treated with 50% conditioned media or the indicated cytokines. After 48 h, treated C57 myoblast cells were cultured in DMEM medium supplied with 2% heat-inactivated horse serum, 20 mM L-glutamine, and 1% penicillin-streptomycin (myoblast fusion medium) for

4–5 days to promote differentiation into multinucleated myotubes. Cells were washed with PBS and fixed with 4% paraformaldehyde and 0.1% Triton X-100 for 10 min, followed by washing and incubation with PBS containing 10% goat serum for 30 min. Fixed cells were incubated with rabbit antimyosin (1:300 dilution) (M-7523, Sigma) antibody (Ab) for 2 h, followed by incubation with Cy3-conjugated anti-rabbit or Cy3-conjugated anti-mouse Ab (1:300 dilution) (Jackson ImmunoResearch Laboratory, Inc., West Grove, PA, USA) for 1 h. Cell nuclei were stained with Hoechst for 5 min. Myosin, myoD, or myogenin-positive cells and cell nuclei were visualized using fluorescence microscopy. The differentiation of myoblast cells into myotubes was scored by the ratio of nuclei in myosin-positive cells to total nuclei in one field. At least 8 fields per sample were counted at 200× magnification.

Western blot analysis for myogenic proteins

Treated C57 myoblast cells were cultured in DMEM supplied with 2% heat-inactivated horse serum, 20 mM L-glutamine, and 1% penicillin-streptomycin antibiotics for 4 days to differentiate into myotubes. Cells were washed, harvested, and lysed with cell culture lysis reagent buffer (Promega) (40 mM Tris-HCl, [pH 7.8], 300 mM NaCl, 2% (v/v) Nonidet P-40, 1% triton X-100, 1 mM DTT, 1 mM $NaVO_4$, and complete protease inhibitor cocktail) for 30 min on ice. Cell lysates were obtained by centrifugation (10,000 g, 20 min). Protein concentrations were determined by BCA protein assay (Pierce). Cell lysates (30 µg/lane) were separated by 7.5% sodium dodecyl sulfate-PAGE and transferred to Hybond-enhanced chemiluminescence (ECL) nitrocellulose membrane (Amersham Pharmacia Biotech, UK). Membranes were incubated with TBST (12.5 mM Tris-HCl pH 7.5, 68.5 mM NaCl, 0.1% Tween 20) supplied with 5% goat serum, 5% skim milk overnight at 4°C. Then membranes were incubated with primary Ab mouse antimyosin or antimyoD (Sigma) for 1–2 h, followed by incubation with horseradish peroxidase (HRP) -conjugated anti-mouse immunoglobulin (Ig) (Amersham Biosciences). The blots were developed with ECL substrate solution (Amersham Biosciences), and exposed to Kodak X-Omat Blue film (NEN Life Sciences, Inc. Boston, MA, USA).

Lactate dehydrogenase activity assay

Lactate dehydrogenase (LDH) activity was assessed by colorimetric assay according to the manufacturer's instructions (Promega). Briefly, 50 µl cell culture media was removed from cells after treatment and mixed with 50 µl substrate diluted in assay buffer. The mixture was incubated at room temperature in the dark for 15 min, followed by the addition of 50 µl stop solution. Absorbance was read at 492 nm. A cytotoxicity index was calculated according to the manufacturer's instructions and expressed as a fold change from the results observed when control 293 cell conditioned media was applied to muscle cells in parallel experiments.

Caspase-3 activity and cleavage analysis

Caspase-3 activity was assessed using a colorimetric caspase-3 assay kit (Sigma). Briefly, myoblast cells were harvested by centrifugation at 1400 rpm 24 h after treatment. Supernatants were removed and discarded. Cells were lysed in cold lysis buffer (50 mM HEPES, pH 7.4, 5 mM CHAPS, 5 mM DTT) for 20 min, followed by centrifugation for 20 min at 4°C. The protein content of cell lysates was determined by BCA assay. Proteins (100–200 µg) were added to the final volume of 100 µl reaction buffer in the presence of DTT and caspase-3

specific substrate. Caspase-3 inhibitor was added as a control in each reaction to confirm the specific cleavage of caspase-3 in this assay according to the manufacturer's guidelines. Samples were incubated at 37°C overnight and analyzed at 405 nm. Caspase-3 activity was expressed as µmol pNA/h/ml.

Cleaved caspase-3 fragments were further analyzed by Western blot analysis. Cellular extracts (20 µg) were electrophoresed on a 12% sodium dodecyl sulfate-polyacrylamide gel and transferred to Hybond-ECL nitrocellulose membrane. Membranes were incubated with primary Ab rabbit anticaspase-3 (Cell Signaling Technology, Beverly, MA, USA) overnight at 4°C, followed by incubation with horseradish peroxidase-conjugated anti-rabbit secondary Ab (Jackson ImmunoResearch Lab, Inc). The blots were washed three times and incubated with ECL substrate solution (Amersham Biosciences) for 1 min according to the manufacturer's instructions and visualized with X-ray film.

RT-polymerase chain reaction (RT-PCR) for cytokine transcripts

Total cellular RNA was extracted from cells using TRIzol reagent (Invitrogen), according to the manufacturer's instruction. Single-stranded cDNA was generated at 42°C for 1 h in a 50 µl reverse transcriptase (RT) reaction containing 100 ng of total RNA as template, 0.5 µg oligo $(dT)_{12–18}$ random primers, 1 µl 10 mM dNTP mix, 1 µl 0.1 M DTT, 1 µl 25 mM $MgCl_2$ and 1 µl SuperScript II Rnase H⁻ reverse transcriptase (Invitrogen). Total RNA and oligo $(dT)_{12–18}$ random primers were heated at 68°C for 2 min, then incubated on ice for 5 min prior to being mixed with other reagents in the RT reaction. RT products (5 µl) were used for polymerase chain reaction (PCR) amplification in a 25 µl reaction using SuperMix (Invitrogen). Primer sequences for cytokines and β-actin were designed on the basis of published sequences in GENBANK spanning exon-exon boundaries as listed in **Table 1**. These primers are cDNA-specific and do not produce PCR products with genomic DNA as a template. Amplification was carried out for 35 cycles consisting of 94°C, 45 s; 55°C, 45 s; 72°C, 1 min 30 s. PCR products were separated on a 2% agarose gel that was stained with ethidium bromide. RNA extracted from healthy donor PBMCs stimulated with 5 µg/ml PHA for 24 h was used as a positive control of some cytokine transcripts. RT reaction without reverse transcriptase was a negative control for each sample. Simultaneously, β-actin transcripts were detected in each sample as an internal control.

Statistical analysis

All values were presented as mean ± SEM in one independent experiment. Statistical significance was determined with 2-way and unpaired Student's t test. Differences were considered statistically significant at a value of $P < 0.05$.

RESULTS

Conditioned media from human prostate cancer (PC-3) and human melanoma (Mel) cell lines inhibits myogenic differentiation *in vitro*

Primary myoblast cultures were derived from C57 mouse hind limb muscle tissue. Exposure to conditioned media from human prostate cancer (PC-3) or human melanoma (Mel) cells inhibited differentiation

TABLE 1. *Primers used to detect cytokine transcripts by polymerase chain reaction*[a]

TNF-α (24)	444 bp	5′-GAGTGACAAGCCTGTAGCCCATGTTGTAGCA-3′
		5′-GCAATGATCCCAAAGTAGACCTGCCCAGACT-3′
IFN-γ (25)	493 bp	5′-ATGAAATATACAAGTTATATCTTGGCTTT-3′
		5′-GATGCTCTTCGACCTCGAAACAGCAT-3′
IL-1β (25)	248 bp	5′-GACACATGGGATAACGAGGC-3′
		5′-ACGCAGGACAGGTACAGATT-3′
IL-6 (25)	189 bp	5′-ATGTAGCCGCCCCACACAGA-3′
		5′-CATCCATCTTTTTCAGCCAT-3′
PIF (2)	361 bp	5′-ACTCTCCTCTTCCTGACAGCTCTGG-3′
		5′-CTGCTGCTCCTGGGTATCATTTCTC-3′
β-Actin (24)	636 bp	5′-TTCTACAATGAGCTGCGTGT-3′
		5′-GCCAGACAGCACTGTGTTGG-3′

[a] TNF-α: tumor necrosis factor-alpha; IL: interleukin; IFN-γ: interferon-gamma; PIF: proteolysis-inducing factor. Reference numbers appear in parentheses.

as assessed by myotube formation and the quantity of myosin expression (**Fig. 1***A*). Exposure to conditioned media from another human prostate cancer cell line, DU-145, resulted in a lesser effect on differentiation. In contrast, a murine colon cancer cell line, MC-38, showed no inhibition of muscle cell culture differentiation. Muscle cells exposed to conditioned media from normal human 293 cells (negative control) differentiated normally with an appearance similar to muscle cells exposed to differentiation media alone. Quantitative analysis of muscle cell differentiation, assessed by the ratio of nuclei in myosin-expressing myotubes to total nuclei in randomly selected fields, showed that conditioned media from PC-3, DU-145 and Mel cells significantly inhibited the formation of myotubes from myoblasts compared with conditioned media from 293 control cells (Fig. 1*B*). We further showed that the inhibitory effect of conditioned media from PC-3 cells on muscle cell differentiation *in vitro* was dose dependent (Fig. 1*C*). Although myoblasts exposed to cancer cell conditioned media remained viable and attached to the collagen-coated dish, we wondered whether a component of the effect on differentiation could be cytotoxicity. To assess this, we measured LDH release into the culture media. Higher levels of LDH release, expressed as a fold change from LDH release due to exposure to conditioned media from 293 cells, were observed after exposure to conditioned media from PC-3 and Mel cells (Fig. 1*D*). These results demonstrated an *in vitro* cell culture system reflecting elements of cancer cachexia that could be further exploited to understand the molecular mechanisms of cachexia and to develop treatment strategies.

IL-1β, TNF-α, and PIF are expressed by PC-3 cells

To explore the mechanism of the inhibitory effect on muscle cell differentiation, cytokine transcripts were amplified by RT-PCR of total RNA from each tumor cell line. Primer sequences for cytokines (TNF-α, IFN-γ, IL-1β, IL-6, PIF) and internal control gene β-actin were designed to exon sequences that span introns to avoid genomic DNA amplification. We detected production of IL-1β transcripts from both PC-3 and Mel cells, but

not from other cells used in this study (**Fig. 2***A*). Detectable levels of TNF-α and PIF transcripts were detected from PC-3 and Mel cells but not from other cells. IFN-γ and IL-6 transcripts were not detected from any of the cell lines. These data suggested that PC-3 and Mel cells produced cytokines (interleukin-1β, TNF-α, and PIF) that may play critical roles in the inhibitory effect on muscle cell differentiation and viability. Supporting this hypothesis, preincubating PC-3 media with different concentrations of neutralizing antibodies against human IL-1β or TNF-α alone, or both together, effectively decreased LDH release (Fig. 2*B*) and enhanced expression of myoD, myosin, and myogenin (data not shown) from muscle cells compared with exposure to untreated conditioned media from PC-3 cells.

To provide further evidence that cytokines were mediators of the effects observed with exposure to cancer cell conditioned media, muscle cells were treated with cytokines TNF-α, IFN-γ, IL-1β, or IL-6 at a dose of 20 ng/ml to directly determine whether these cytokines could inhibit muscle cell differentiation. Exposure to IFN-γ, IL-1β, and IL-6, either alone or in combination, impaired muscle cell differentiation (**Fig. 3***A*) but had only a small effect on LDH release (Fig. 3*B*). Exposure to TNF-α alone or combined with the other cytokines for 48 h *in vitro* resulted in a cytotoxic effect demonstrated by increased LDH release (Fig. 3*B*).

Stable expression of cFLIP, but not Bcl-xL, by muscle cells partially reverses the inhibition of muscle cell differentiation induced by exposure to conditioned media from tumor cells

Muscle cells were stably transduced with the IκBα super repressor, IKBSR, a mutated form of IκBα that prevents the activation of NF-κB. Primary muscle cells were also stably transduced with cFLIP, Bcl-xL, an empty control vector pcDNA3.1, or a GFP expression vector pN1-GFP, as confirmed by immunohistochemistry and Western blot after 2 wk of antibiotic selection in culture (data not shown). Muscle cell differentiation, as assessed by the expression of myosin, was partially preserved after
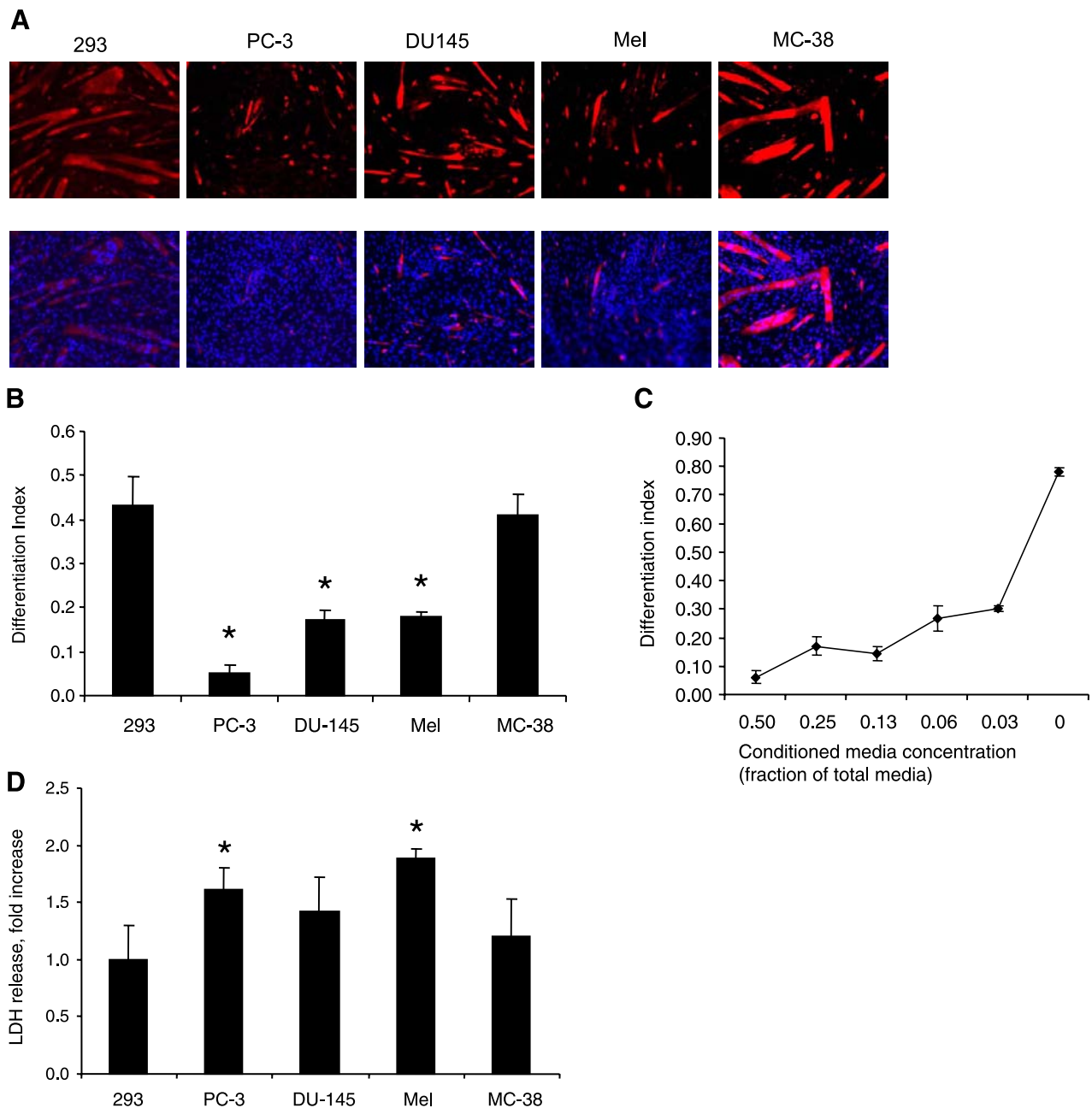
Figure 1. Conditioned tumor media from prostate cancer cell lines (PC-3 and DU-145) and a melanoma cell line (Mel) inhibit myogenic differentiation and increase LDH release. A) Primary myoblast cells were cultured in growth media in the presence of conditioned media (293 (noncancer cell control), PC-3, DU145, Mel, MC-38) (1:2 dilution) for 48 h and induced to differentiate in differentiation media for 4 days. Myosin protein expression was visualized by immunohistochemistry (red) and cell nuclei were stained using Hoechst (blue). B) Quantitative analysis of myoblast cell differentiation. The total number of nuclei and those in myosin-positive myotubes were scored. At least 8 fields at 200× magnification were counted for each sample. Myogenic differentiation was assessed by the ratio of nuclei in myosin-positive myotubes to total nuclei and expressed as the mean differentiation index ± SEM ($n=8$, *$P<0.05$) vs. 293 conditioned media-treated cells. C) PC-3 media inhibits myogenic differentiation in a dose-dependent manner. Cells were cultured in growth media in the presence of PC-3 media for 48 h, then induced to differentiate by culturing in differentiation media for 4 days. Myogenic differentiation index (expressed as mean± SEM, $n=4$) was quantitatively analyzed after detection of myosin by immunohistochemistry and nuclei by Hoechst staining. D) Analysis of lactate dehydrogenase (LDH) activity. LDH release was analyzed 48 h after myoblast cells were maintained in tumor cell conditioned media (1:2 dilution). Results are expressed as mean fold increase ± SEM ($n=4$, *$P<0.05$) vs. 293 conditioned media treated cells. Results shown are representative of at least 4 independent experiments.

exposure to PC-3, Mel, and DU-145 conditioned media by stable expression of cFLIP and IKBSR (**Fig. 4A**). Quantitation of muscle cell differentiation (Fig. 4B) and Western blot analysis for myosin and MyoD protein

expression (Fig. 4C) confirmed these results. In contrast, Bcl-xL overexpression did not protect against inhibition of muscle cell differentiation induced by exposure to PC-3, Mel, or DU-145 cell conditioned
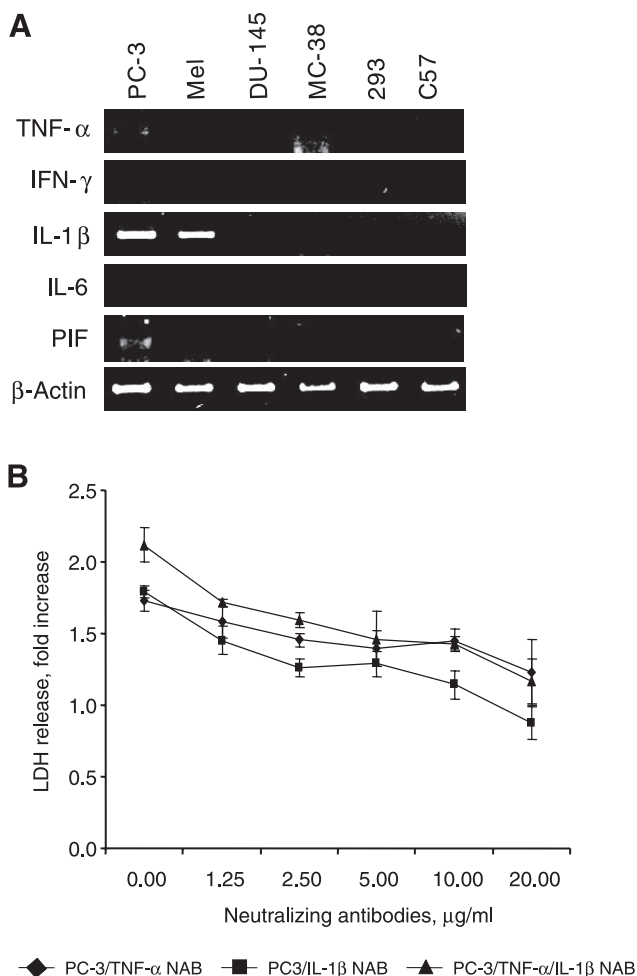
A

	PC-3	Mel	DU-145	MC-38	293	C57
TNF-α						
IFN-γ						
IL-1β						
IL-6						
PIF						
β-Actin						

B

◆ PC-3/TNF-α NAB ■ PC3/IL-1β NAB ▲ PC-3/TNF-α/IL-1β NAB

Figure 2. TNF-α, IL-1β, and PIF are mediators in failure of myogenic differentiation and LDH release due to PC-3 media exposure. *A)* RT-PCR analysis of TNF-α, IFN-γ, IL-1β, IL-6, and PIF transcripts expressed by tumor cells. Transcripts of β-actin were analyzed as a loading control. *B)* Addition of anti-TNF-α or anti-interleukin-1β neutralizing Ab (NAB) to PC-3 cell conditioned media decreased myoblast LDH release after exposure to PC-3 cell media. LDH release from myoblast cells was measured 48 h after cells were cultured with PC-3 conditioned media (1:2 dilution) preincubated with increasing concentrations of neutralizing antibodies for 1 h at 37°C. LDH release from negative control myoblasts was measured 48 h after the cells were cultured with 293 conditioned media (1:2 dilution) without preincubation with NAB. Results are expressed as mean fold increase ± SEM LDH release *vs.* 293 conditioned media-treated cells that have not been treated with NAB (*n*=3).

media (Fig. 4*A*). LDH release from stably transduced muscle cells was measured after exposure to conditioned media from tumor cell lines for 48 h prior to differentiation media for 4 days (Fig. 4*D*). Cells overexpressing either a negative control plasmid or IKBSR had increased levels of LDH release induced by exposure to conditioned media from PC-3 or DU-145 cells. However, cells overexpressing cFLIP or Bcl-xL were protected from the cytotoxicity induced by these cell supernatants. cFLIP protected against cytotoxicity induced by conditioned media from Mel cells, but Bcl-xL or IKBSR did not.

Stable expression of cFLIP, but not Bcl-xL, by muscle cells inhibits the activation of NF-κB

We observed NF-κB activation by gel shift analysis in nuclear extracts of differentiating muscle cells when exposed to cytokine IL-1β or conditioned media from PC-3 cells at a higher level than when exposed to conditioned media from normal control 293 cells (**Fig. 5*A***). Stable expression of cFLIP protected muscle cells from NF-κB activation upon exposure to IL-1β or conditioned media from PC-3 cells, similar to the protection seen with stable expression of IKBSR. However, stable expression of Bcl-xL in muscle cells resulted in higher levels of NF-κB activation with exposure to conditioned media from 293 cells, and an even higher
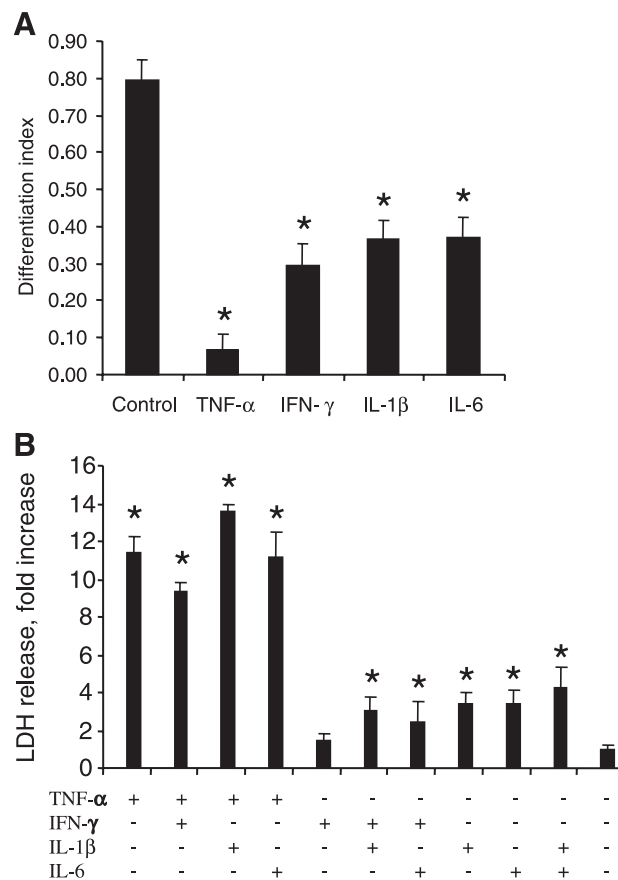
A

B

TNF-α	+	+	+	+	-	-	-	-	-	-
IFN-γ	-	+	-	-	+	+	+	-	-	-
IL-1β	-	-	+	-	-	+	-	+	-	+	-
IL-6	-	-	-	+	-	-	+	-	+	+	-

Figure 3. TNF-α, IFN-γ, IL-1β, and IL-6 inhibit myogenic differentiation and induce LDH release by myoblast cells. *A)* Myogenic differentiation was inhibited by TNF-α, IFN-γ, IL-1β, and IL-6. Myoblast cells were treated with TNF-α, IFN-γ, IL-1β, and IL-6 alone, each at a concentration of 20 ng/ml, and maintained in differentiation media for 4 days. Control cells were not exposed to a cytokine. Myogenic differentiation was quantitatively analyzed after detection of myosin by immunohistochemistry and nuclei by Hoechst staining and expressed as the mean differentiation index ± SEM (*n*=4, **P*<0.05). *B)* LDH release by myoblast cells treated with TNFα, IFN-γ, IL-1β, and IL-6 alone or in combination with the concentration of each cytokine at 20 ng/ml for 2 days. LDH release is expressed as mean fold increase ± SEM *vs.* untreated media cells (*n*=3, **P*<0.05).
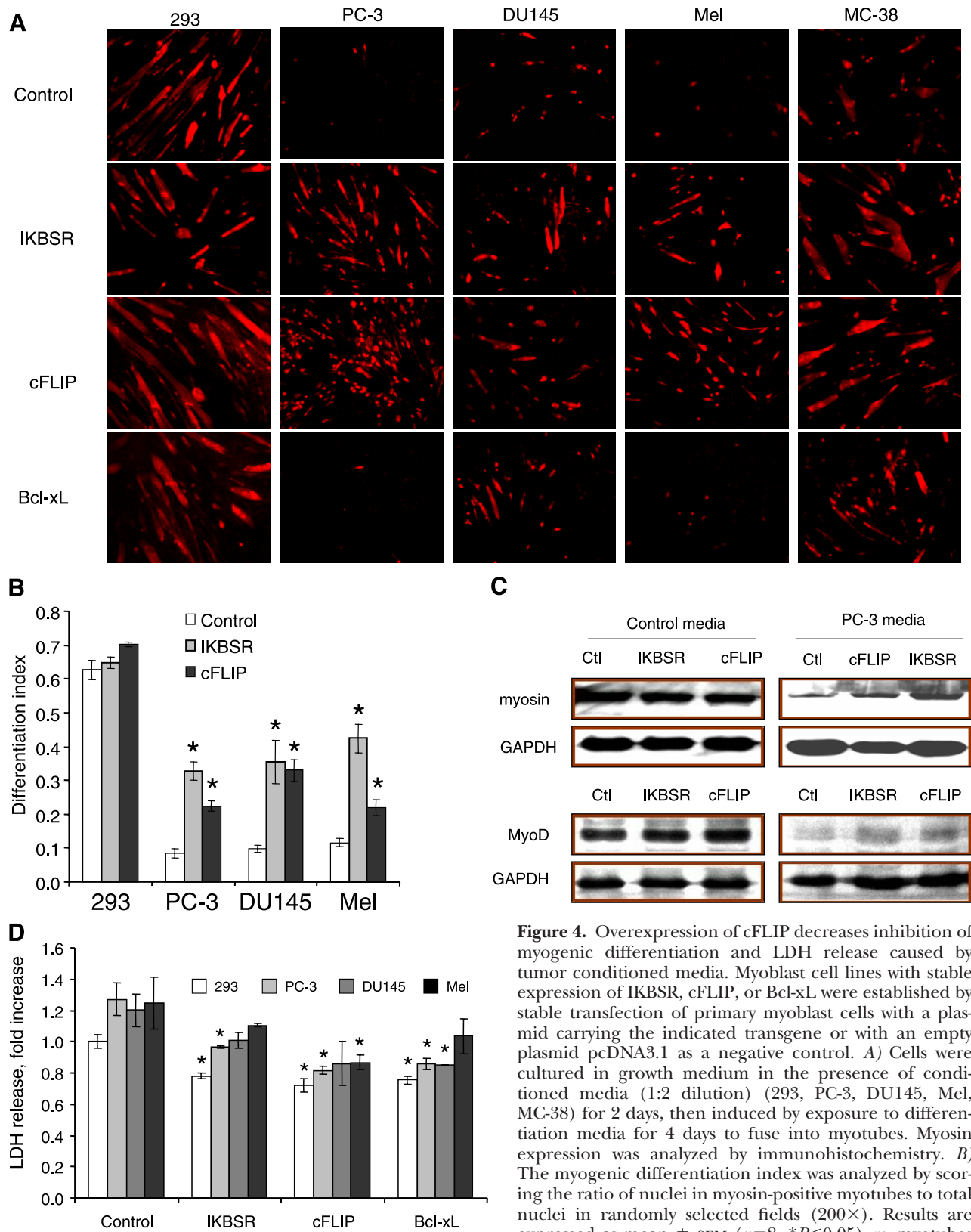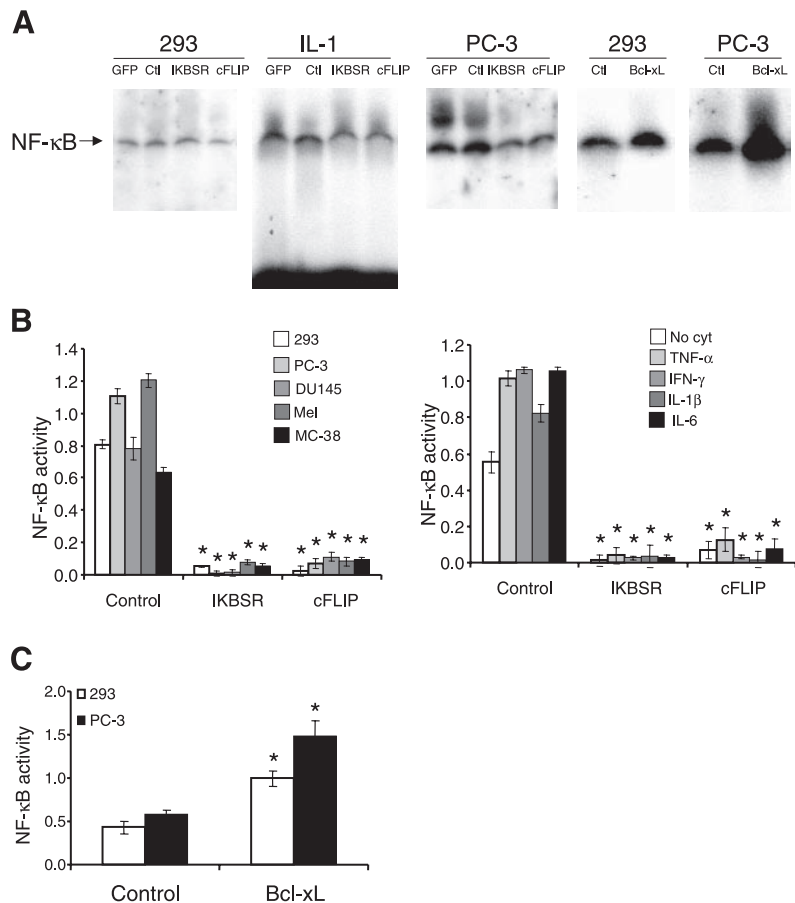
Figure 4. Overexpression of cFLIP decreases inhibition of myogenic differentiation and LDH release caused by tumor conditioned media. Myoblast cell lines with stable expression of IKBSR, cFLIP, or Bcl-xL were established by stable transfection of primary myoblast cells with a plasmid carrying the indicated transgene or with an empty plasmid pcDNA3.1 as a negative control. *A)* Cells were cultured in growth medium in the presence of conditioned media (1:2 dilution) (293, PC-3, DU145, Mel, MC-38) for 2 days, then induced by exposure to differentiation media for 4 days to fuse into myotubes. Myosin expression was analyzed by immunohistochemistry. *B)* The myogenic differentiation index was analyzed by scoring the ratio of nuclei in myosin-positive myotubes to total nuclei in randomly selected fields (200×). Results are expressed as mean ± SEM (*n*=8, *P<0.05) *vs.* myotubes transfected with empty expression vector (control). *C)* Western blot analysis of myosin and myoD expression in myotubes treated with 293 or PC-3 media (1:2 dilution) and cultured in differentiation media for 4 days. Whole cell extracts were prepared and 30 µg total protein was used in Western blot analysis to detect myosin and myoD protein expression. Glyceraldehyde-3-phosphate dehydrogenase (GAPDH) expression was used as a loading control. *D)* LDH release was assayed from cells cultured in conditioned media (1:2 dilution) for 2 days. LDH release is expressed as mean fold increase ± SEM *vs.* control cells (*n*=3, *P<0.05).

Figure 5. Overexpression of cFLIP and Bcl-xL suppressed NF-κB activity in myoblasts. *A)* Analysis of NF-κB binding activity to a consensus NF-κB oligonucleotide. Myoblast cells were cultured for 60 min in the presence of 20 ng/ml IL-1β or 24 h in the presence of 293 or PC-3 media (1:2 dilution). Nuclear extracts were prepared and assessed for DNA binding activity to a consensus NF-κB oligonucleotide by electromobility shift assay (EMSA). Lane markers indicate cells with stable expression of IKBSR, cFLIP, or Bcl-xL, GFP from a GFP expression plasmid or untransduced (Ctl). *B)* Analysis of NF-κB transcriptional activity. Myoblast cells with stable expression of IKBSR or cFLIP (Control cells are untransduced) were cotransfected with pNF-κB-hrGFP (200 ng/well) and pCMV-β (100 ng/well). 6 h after transfection, cells were cultured in the presence or absence of conditioned media (1:2 dilution) (left panel) or cytokines (no cytokine (no cyt) or 20 ng/ml TNF-α, IFN-γ, IL-1β, or IL-6) alone (right panel). GFP-positive and β-galactosidase-positive cells were counted 24 h after treatment. At least 8 randomly selected fields per well were counted (magnification 100×). NF-κB activity is presented as a ratio of GFP-positive to β-galactosidase-positive cells, expressed as mean ± SEM *vs.* control myoblast cells. One of at least four independent experiments is shown ($n=8$, $P<0.05$). *C)* Analysis of NF-κB transcriptional activity in myoblast cells with stable expression of Bcl-xL cotransfected with pNF-κB-hrGFP (200 ng/well) and pCMV-β (100 ng/well). 6 h after transfection, cells were cultured in the presence of 293 or PC-3 cell conditioned

media (1:2 dilution). The GFP-positive and β-galactosidase-positive cells were counted 24 h after treatment. At least 8 randomly selected fields per well were counted (magnification 100×). NF-κB activity is presented as a ratio of GFP-positive to β-galactosidase-positive cells, expressed as mean ± SEM *vs.* control myoblast cells. One of at least 4 independent experiments is shown ($n=8$, $P<0.05$).

level of NF-κB activation with exposure to conditioned media from PC-3 cells.

NF-κB activation was also analyzed in a transcriptional assay using a transiently transfected reporter plasmid that expresses enhanced GFP (EGFP) from a promoter element that must be activated by binding of nuclear NF-κB (Fig. 5*B*). Increased NF-κB-induced transcriptional activation was observed in muscle cells when exposed to conditioned media from PC-3 or Mel cells or to inflammatory cytokines (TNF-α, IFN-γ, IL-1β, or IL-6). Stable overexpression of IKBSR or cFLIP prevented NF-κB-induced transcriptional activation induced by tumor cell conditioned media or inflammatory cytokines. Further confirmation that cFLIP prevented NF-κB activation was obtained by showing that inhibition of NF-κB activation was reversed by treatment of the cells stably overexpressing cFLIP with a small interference RNA (siRNA) to cFLIP (data not shown). Consistent with gel shift analysis of NF-κB activation, stable overexpression of Bcl-xL enhanced NF-κB-induced transcriptional activation in this assay in the setting of exposure to PC-3 cell conditioned media (Fig. 5*C*).

Stable expression of cFLIP or Bcl-xL by muscle cells inhibits the activation of caspase-3

Caspase-3 activity was enhanced in muscle cells exposed to conditioned media from PC-3 or Mel cells compared with muscle cells exposed to conditioned media from normal control 293 cells (**Fig. 6**). Stable overexpression of cFLIP or Bcl-xL inhibited the PC-3 or Mel cell conditioned media-induced increase of caspase-3 activity (Fig. 6*A*) and caspase-3 cleavage as demonstrated by Western blot analysis (Fig. 6*B*). Stable expression of IKBSR in muscle cells did not appear to inhibit the increase in caspase-3 activity induced in muscle cells by exposure to conditioned media from PC-3 or Mel cells.

DISCUSSION

We report here a new *in vitro* cell culture assay to study the effects of cancer cell cytokines on muscle cell differentiation and use this assay to test novel gene transfer approaches for the treatment of cancer cachexia. Exposure to conditioned media from selected
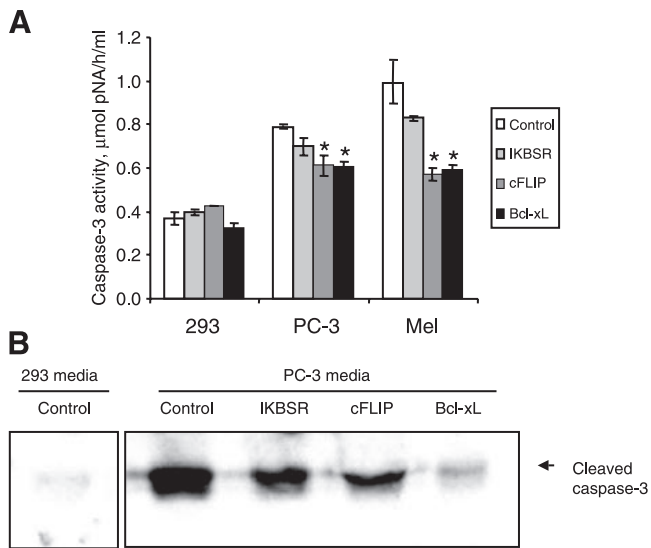
A

B

Figure 6. Overexpression of cFLIP and Bcl-xL inhibit caspase-3 activation. Myoblast cells with stable expression of IKBSR, cFLIP, Bcl-xL, or empty vector (control) plasmid were cultured with 1:2 dilution of conditioned media from the indicated cell line (293, PC-3, or Mel) for 24 h. A) Cell extracts (100–200 µg/well) were assayed for caspase-3 specific activity, expressed as µmol pNA/h/ml. Data are presented as mean ± SEM (n=3, P<0.05) vs. control myoblast cells and represent one of three independent experiments. B) Cell extracts were assayed by Western blot for caspase-3 cleavage. After cells were maintained in conditioned media (1:2 dilution) for 24 h, total cell extracts were prepared and 20 µg of each cell extract was used for detection of cleaved caspase-3 fragments.

human cancer cell lines resulted in failure of muscle cell differentiation. A known intracellular mechanism of NF-κB activation as a cause of cancer cachexia was recapitulated in this *in vitro* system. Consistent with previous reports *in vivo*, we demonstrated that human prostate cancer PC-3 cells express PIF as well as TNF-α and IL-1β transcripts (2). We observed a direct correlation between inhibition of myogenic differentiation in the *in vitro* assay and the expression of IL-1β transcripts by specific human cancer cell lines tested. Furthermore, we observed a direct correlation between NF-κB activation and inhibition of myogenic differentiation in the *in vitro* assay. Exposure to inflammatory cytokines and to conditioned media from human cancer cells each resulted in NF-κB activation within primary muscle cells. Failure of myogenic differentiation and the associated activation of NF-κB were prevented by stable expression of either IKBSR or cFLIP, but not by Bcl-xL.

The underlying mechanism of the cachexia-inducing effects of proinflammatory cytokines (TNF-α, IL-1β, or PIF) has been extensively studied recently. Activation of NF-κB participates in a key signaling pathway resulting in the inhibition of myogenic differentiation (10, 11). Consistent with previous studies, in this study we found that exposure to secreted factors from PC-3 and Mel cancer cell lines resulted in activation of NF-κB in treated myoblast cells, as demonstrated by higher bind-

ing activity of nuclear NF-κB to consensus NF-κB oligonucleotides and higher levels of NF-κB transcriptional activity. Results demonstrating NF-κB activation in cancer cytokine-treated muscle cells suggest that IL-1β, TNF-α, or PIF produced from PC-3 or Mel cells activate NF-κB by phosphorylation and degradation of IκBα, thus facilitating the translocation of NF-κB to the nucleus. Shown in previous studies and confirmed in our study, expression of myoD was decreased in cancer cytokine-treated muscle cells. Other studies demonstrate that TNF-α exposure resulted in decreased myoD expression that is due to stimulatory effects on myoD protein degradation and inhibitory effects on its transcription by activated NF-κB, ultimately leading to a failure of initiation of the muscle differentiation process (13).

Recent reports suggest that certain molecules involved in signaling pathways that result in apoptosis can promote or inhibit NF-κB activation in particular cell lines. Caspase-8, Fas-associated death domain (FADD), FLIP, TRAIL-R, TNF-R1, and procaspase-8 activate NF-κB in a variety of cells, using a TRAF2/NIK/IKKs-dependent pathway (20, 26–30) that can be blocked by their inhibitors or dominant-negative mutants (22, 28, 31). cFLIP and Bcl-xL are both important antiapoptotic molecules. cFLIP is a caspase-8 homologue devoid of protease activity and contains two death effector domains and a catalytically inactive caspase-like domain. cFLIP inhibits procaspase-8 processing at the DISC in most cells, thus inhibiting the extrinsic apoptotic signal pathway (14–16, 28). Bcl-xL is localized to the endoplasmic reticulum to prevent cytochrome *c* release from mitochondria, and thus inhibits the intrinsic apoptotic signal pathway (19). Previous studies demonstrated the cell-specific effects of cFLIP and Bcl-xL on NF-κB activity in other cell lines (20, 22, 26, 27, 32–34). We speculated that cFLIP and Bcl-xL could promote muscle cell differentiation by effects on NF-κB activation and apoptosis. Therefore, in this study we investigated whether cFLIP and Bcl-xL influenced NF-κB activity, apoptosis, and myogenic differentiation in primary cells derived from skeletal muscle.

We observed that cFLIP overexpression inhibited IL-1β or PC-3 or Mel media-induced NF-κB activation in myoblast cells, thus promoting myogenic differentiation of treated myoblast cells, as demonstrated by enhanced myotube formation and muscle-specific protein expression. Stable expression of cFLIP yielded similar results to stable expression of IKBSR. Both IKBSR and cFLIP inhibited NF-κB activation, as determined by levels of nuclear NF-κB binding activity and nuclear NF-κB-mediated transcription.

In contrast, overexpression of Bcl-xL enhanced NF-κB activation in myoblast cells, with further increases upon exposure to conditioned media from PC-3 cells. The contrasting results with cFLIP and Bcl-xL suggest differential effects on NF-κB activation by these molecules in muscle cells. Further studies are required to understand the intricacies of signaling cascades that underpin this result. However, it is interesting to spec-

ulate that although the antiapoptotic properties of Bcl-xL may have promoted muscle cell differentiation, its ability to increase activation of NF-κB may have counteracted this beneficial effect, resulting in a net failure of protection from the detrimental effects of cancer cell cytokines on muscle cell differentiation.

We considered whether the inhibition of muscle cell differentiation induced by exposure to certain cancer cell cytokines might be in part a cytotoxic effect. Although high doses of inflammatory cytokines, such as TNF-α, result in severe cytotoxicity with loss of cell attachment (data not shown), such effects were not observed under conditions used for the studies reported here. By measuring LDH release, however, we demonstrated more subtle cytotoxicity in inflammatory cytokine or cancer cell-derived cytokine-treated muscle cells, as expressed as a fold change in LDH release compared with untreated or 293 cell conditioned media-treated cells. Furthermore, PC-3 cell media significantly increased caspase-3 activity and cleavage in muscle cells. However, overexpression of cFLIP and Bcl-xL, important antiapoptotic proteins, but not IKBSR, provided protection from cytotoxicity and this protection was accompanied by a reduction in caspase-3 activation, suggesting that activation of the apoptosis pathway was involved in the cytotoxic effect of tumor media.

Taken together, this study provides an *in vitro* assay that demonstrates secretion of cachexia-inducing factors by certain cancer cell lines causing inhibition of myogenic differentiation by activation of NF-κB and apoptosis. Overexpression of cFLIP in muscle cells inhibits both NF-κB-mediated and apoptotic pathways, thereby preventing tumor media-induced inhibition of myogenic differentiation and cytotoxicity. These findings point to the potential to design novel molecular therapeutics for the treatment of cancer-induced muscle wasting. FJ

REFERENCES

1. Tisdale, M. J. (2002) Cachexia in cancer patients. *Nat. Rev. Cancer* **2**, 862–871
2. Wang, Z., Corey, E., Hass, G. M., Higano, C. S., True, L. D., Wallace, D., Jr., Tisdale, M. J., and Vessella, R. L. (2003) Expression of the human cachexia-associated protein (HCAP) in prostate cancer and in a prostate cancer animal model of cachexia. *Int. J. Cancer* **105**, 123–129
3. Vreugdenhil, G., Lowenberg, B., Van Eijk, H. G., and Swaak, A. J. (1992) Tumor necrosis factor alpha is associated with disease activity and the degree of anemia in patients with rheumatoid arthritis. *Eur. J. Clin. Invest.* **22**, 488–493
4. Anker, S. D., and Rauchhaus, M. (1999) Insights into the pathogenesis of chronic heart failure: immune activation and cachexia. *Curr. Opin. Cardiol.* **14**, 211–216
5. Espat, N. J., Copeland, E. M., and Moldawer, L. L. (1994) Tumor necrosis factor and cachexia: a current perspective. *Surg. Oncol.* **3**, 255–262
6. Tisdale, M. J. (1997) Biology of cachexia. *J. Natl. Cancer Inst.* **89**, 1763–1773
7. Nakashima, J., Tachibana, M., Ueno, M., Baba, S., and Tazaki, H. (1995) Tumor necrosis factor and coagulopathy in patients with prostate cancer. *Cancer Res.* **55**, 4881–4885
8. Fong, Y., Moldawer, L. L., Marano, M., Wei, H., Barber, A., Manogue, K., Tracey, K. J., Kuo, G., Fischman, D. A., and Cerami, A. (1989) Cachectin/TNF or IL-1 alpha induces cachexia with redistribution of body proteins. *Am. J. Physiol.* **256**, R659–R665
9. Pfitzenmaier, J., Vessella, R., Higano, C. S., Noteboom, J. L., Wallace, D., Jr., and Corey, E. (2003) Elevation of cytokine levels in cachectic patients with prostate carcinoma. *Cancer* **97**, 1211–1216
10. Guttridge, D. C., Mayo, M. W., Madrid, L. V., Wang, C. Y., and Baldwin, A. S., Jr. (2000) NF-kappaB-induced loss of MyoD messenger RNA: possible role in muscle decay and cachexia. *Science* **289**, 2363–2366
11. Langen, R. C., Schols, A. M., Kelders, M. C., Wouters, E. F., and Janssen-Heininger, Y. M. (2001) Inflammatory cytokines inhibit myogenic differentiation through activation of nuclear factor-kappaB. *FASEB J.* **15**, 1169–1180
12. Li, Y. P., and Reid, M. B. (2000) NF-kappaB mediates the protein loss induced by TNF-alpha in differentiated skeletal muscle myotubes. *Am. J. Physiol.* **279**, R1165–R1170
13. Langen, R. C., Van, D., V, Schols, A. M., Kelders, M. C., Wouters, E. F., and Janssen-Heininger, Y. M. (2004) Tumor necrosis factor-alpha inhibits myogenic differentiation through MyoD protein destabilization. *FASEB J.* **18**, 227–237
14. Goltsev, Y. V., Kovalenko, A. V., Arnold, E., Varfolomeev, E. E., Brodianskii, V. M., and Wallach, D. (1997) CASH, a novel caspase homologue with death effector domains. *J. Biol. Chem.* **272**, 19641–19644
15. Hu, S., Vincenz, C., Ni, J., Gentz, R., and Dixit, V. M. (1997) I-FLICE, a novel inhibitor of tumor necrosis factor receptor-1- and CD-95-induced apoptosis. *J. Biol. Chem.* **272**, 17255–17257
16. Irmler, M., Thome, M., Hahne, M., Schneider, P., Hofmann, K., Steiner, V., Bodmer, J. L., Schroter, M., Burns, K., Mattmann, C., et al. (1997) Inhibition of death receptor signals by cellular FLIP. *Nature* **388**, 190–195
17. Okano, H., Shiraki, K., Inoue, H., Kawakita, T., Yamanaka, T., Deguchi, M., Sugimoto, K., Sakai, T., Ohmori, S., Fujikawa, K., et al. (2003) Cellular FLICE/caspase-8-inhibitory protein as a principal regulator of cell death and survival in human hepatocellular carcinoma. *Lab. Invest.* **83**, 1033–1043
18. Willems, F., Amraoui, Z., Vanderheyde, N., Verhasselt, V., Aksoy, E., Scaffidi, C., Peter, M. E., Krammer, P. H., and Goldman, M. (2000) Expression of c-FLIP(L) and resistance to CD95-mediated apoptosis of monocyte-derived dendritic cells: inhibition by bisindolylmaleimide. *Blood* **95**, 3478–3482
19. Danial, N. N., and Korsmeyer, S. J. (2004) Cell death: critical control points. *Cell* **116**, 205–219
20. Kataoka, T., Budd, R. C., Holler, N., Thome, M., Martinon, F., Irmler, M., Burns, K., Hahne, M., Kennedy, N., Kovacsovics, M., and Tschopp, J. (2000) The caspase-8 inhibitor FLIP promotes activation of NF-kappaB and Erk signaling pathways. *Curr. Biol.* **10**, 640–648
21. Song, Y. S., Park, H. J., Kim, S. Y., Lee, S. H., Yoo, H. S., Lee, H. S., Lee, M. K., Oh, K. W., Kang, S. K., Lee, S. E., and Hong, J. T. (2004) Protective role of Bcl-2 on beta-amyloid-induced cell death of differentiated PC12 cells: reduction of NF-kappaB and p38 MAP kinase activation. *Neurosci. Res.* **49**, 69–80
22. Wajant, H., Haas, E., Schwenzer, R., Muhlenbeck, F., Kreuz, S., Schubert, G., Grell, M., Smith, C., and Scheurich, P. (2000) Inhibition of death receptor-mediated gene induction by a cycloheximide-sensitive factor occurs at the level of or upstream of Fas-associated death domain protein (FADD). *J. Biol. Chem.* **275**, 24357–24366
23. Rando, T. A., and Blau, H. M. (1994) Primary mouse myoblast purification, characterization, and transplantation for cell-mediated gene therapy. *J. Cell Biol.* **125**, 1275–1287
24. Huang, Y. T., Sheen, T. S., Chen, C. L., Lu, J., Chang, Y., Chen, J. Y., and Tsai, C. H. (1999) Profile of cytokine expression in nasopharyngeal carcinomas: a distinct expression of interleukin 1 in tumor and CD4+ T cells. *Cancer Res.* **59**, 1599–1605
25. Jeong, C. W., Ahn, K. S., Rho, N. K., Park, Y. D., Lee, D. Y., Lee, J. H., Lee, E. S., and Yang, J. M. (2003) Differential in vivo cytokine mRNA expression in lesional skin of intrinsic vs. extrinsic atopic dermatitis patients using semiquantitative RT-PCR. *Clin. Exp. Allergy* **33**, 1717–1724

26. Chaudhary, P. M., Eby, M. T., Jasmin, A., Kumar, A., Liu, L., and Hood, L. (2000) Activation of the NF-kappaB pathway by caspase 8 and its homologs. *Oncogene* **19,** 4451–4460

27. Kataoka, T., and Tschopp, J. (2004) N-terminal fragment of c-FLIP(L) processed by caspase 8 specifically interacts with TRAF2 and induces activation of the NF-kappaB signaling pathway. *Mol. Cell. Biol.* **24,** 2627–2636

28. Micheau, O., Lens, S., Gaide, O., Alevizopoulos, K., and Tschopp, J. (2001) NF-kappaB signals induce the expression of c-FLIP. *Mol. Cell. Biol.* **21,** 5299–5305

29. Qin, Z., Wang, Y., and Chasea, T. N. (2000) A caspase-3-like protease is involved in NF-kappaB activation induced by stimulation of N-methyl-D-aspartate receptors in rat striatum. *Brain Res. Mol.* **80,** 111–122

30. Yeh, W. C., Shahinian, A., Speiser, D., Kraunus, J., Billia, F., Wakeham, A., de la Pompa, J. L., Ferrick, D., Hum, B., Iscove, N., *et al.* (1997) Early lethality, functional NF-kappaB activation, and increased sensitivity to TNF-induced cell death in TRAF2-deficient mice. *Immunity* **7,** 715–725

31. Todorov, P. T., McDevitt, T. M., Cariuk, P., Coles, B., Deacon, M., and Tisdale, M. J. (1996) Induction of muscle protein degradation and weight loss by a tumor product. *Cancer Res.* **56,** 1256–1261

32. Bannerman, D. D., Eiting, K. T., Winn, R. K., and Harlan, J. M. (2004) FLICE-like inhibitory protein (FLIP) protects against apoptosis and suppresses NF-kappaB activation induced by bacterial lipopolysaccharide. *Am. J. Pathol.* **165,** 1423–1431

33. Chen, G. G., Liang, N. C., Lee, J. F., Chan, U. P., Wang, S. H., Leung, B. C., and Leung, K. L. (2004) Over-expression of Bcl-2 against Pteris semipinnata L-induced apoptosis of human colon cancer cells via a NF-kappa B-related pathway. *Apoptosis* **9,** 619–627

34. Crawford, M. J., Krishnamoorthy, R. R., Rudick, V. L., Collier, R. J., Kapin, M., Aggarwal, B. B., Al-Ubaidi, M. R., and Agarwal, N. (2001) Bcl-2 overexpression protects photooxidative stress-induced apoptosis of photoreceptor cells via NF-kappaB preservation. *Biochem. Biophys. Res. Commun.* **281,** 1304–1312

Cellular caspase-8-like inhibitory protein (cFLIP) prevents inhibition of muscle cell differentiation induced by cancer cells

Zhilong Jiang* and Paula R. Clemens*,†,1

*Department of Neurology, School of Medicine, University of Pittsburgh, Pennsylvania, USA; and †Neurology Service, Department of Veterans Affairs Medical Center, Pittsburgh, Pennsylvania, USA

To read the full text of this article, go to http://www.fasebj.org/cgi/doi/10.1096/fj.06-6347fje

SPECIFIC AIMS

Cachexia is a frequent complication of cancer or other chronic diseases. To investigate the pathophysiology of cancer cachexia and pursue treatment options, we developed an *in vitro* assay of the effects of cancer cell-produced cytokines on primary muscle cells derived from murine skeletal muscle. In this study we first determined the effect of secreted factors from different cancer cell lines on myoblast cell differentiation *in vitro*. We then investigated whether overexpression of IKBSR, cFLIP, or Bcl-xL is able to influence muscle cell differentiation *in vitro* and whether activation or suppression of the NF-κB signaling pathway is involved in this process.

PRINCIPAL FINDINGS

1. Conditioned media from human prostate cancer (PC-3) and human melanoma (Mel) cell lines inhibits myogenic differentiation *in vitro*

Primary myoblast cultures were derived from mouse hind limb muscle tissue. Exposure to conditioned media from human prostate cancer, PC-3, or human melanoma (Mel) cells diluted 1:1 with growth media prior to differentiation inhibited differentiation, as assessed by myotube formation and myosin expression. Exposure to conditioned media from another human prostate cancer cell line, DU-145, had less effect on differentiation. In contrast, a murine colon cancer cell line, MC-38, showed no inhibition of muscle cell culture differentiation. Muscle cells exposed to conditioned media from normal human 293 cells (negative control) differentiated normally, with an appearance similar to muscle cells exposed only to growth media prior to differentiation. Quantitative analysis of muscle cell differentiation assessed by the ratio of nuclei in myosin-expressing myotubes to total nuclei in randomly selected fields showed that conditioned media from PC-3, DU-145, and Mel cells significantly inhibited formation of myotubes from myoblasts compared with

conditioned media from 293 control cells. We showed that the inhibitory effect of conditioned media from PC-3 cells on muscle cell differentiation *in vitro* was dose dependent. We wondered whether a component of the effect on differentiation could be cytotoxicity. We measured LDH release into the culture media. Higher levels of LDH release, expressed as a fold change from LDH release due to exposure to conditioned media from 293 cells, were observed after exposure to conditioned media from PC-3 and Mel cells. These results demonstrated an *in vitro* cell culture system reflecting elements of cancer cachexia that could be exploited in order to understand the molecular mechanisms of cachexia and to develop treatment strategies.

2. Interleukin 1β (IL-1β), TNF-α, and proteolysis-inducing factor (PIF) are expressed by PC-3 cells

As assessed by RT-PCR of the tumor cell lines, PC-3 cells expressed IL-1β, TNF-α, and PIF transcripts, suggesting these cytokines may play critical roles in the inhibitory effect on muscle cell differentiation and viability. Supporting this hypothesis, preincubating PC-3 media with different concentrations of neutralizing antibodies against human IL-1β or TNF-α, alone or both together, decreased LDH release and enhanced expression of myosin, myoD, and myogenin from muscle cells compared with exposure to untreated conditioned media from PC-3 cells.

3. Stable expression of cFLIP, but not Bcl-xL, by muscle cells partially reverses the inhibition of muscle cell differentiation induced by exposure to conditioned media from tumor cells

Muscle cells were stably transduced with IκBα super repressor, IKBSR, a mutated form of IκBα that prevents

activation of NF-κB and promotes muscle cell differentiation. With IKBSR as positive control, we tested whether cFLIP or Bcl-xL would promote muscle cell differentiation. Muscle cell differentiation assessed by myosin expression was partially preserved after exposure to PC-3, Mel, and DU-145 conditioned media by stable expression of cFLIP and IKBSR. In contrast, Bcl-xL overexpression did not protect against inhibition of muscle cell differentiation induced by exposure to PC-3, Mel, or DU-145 cell conditioned media. To assess the effect of IKBSR, cFLIP, and Bcl-xL on cytotoxicity, LDH release from stably transduced muscle cells was measured after exposure to conditioned media from tumor cell lines. Cells overexpressing either a negative control plasmid or IKBSR had increased levels of LDH release induced by exposure to conditioned media from PC-3 cells, but cells overexpressing cFLIP or Bcl-xL were protected from cytotoxicity induced by the PC-3 cell supernatant.

4. Stable expression of cFLIP, but not Bcl-xL, by muscle cells inhibits activation of NF-κB

We observed NF-κB activation by gel shift analysis in nuclear extracts of differentiating muscle cells when exposed to cytokine IL-1β or conditioned media from PC-3 cells at a higher level than when exposed to conditioned media from normal control 293 cells (**Fig. 1A**). Stable expression of cFLIP protected muscle cells from NF-κB activation upon exposure to IL-1β or conditioned media from PC-3 cells, similar to the protection seen with stable expression of IKBSR. However, stable expression of Bcl-xL in muscle cells resulted in higher levels of NF-κB activation with exposure to conditioned media from 293 cells and an even higher level of NF-κB activation with exposure to conditioned media from PC-3 cells.

NF-κB activation was also analyzed in a transcriptional assay using a transiently transfected reporter plasmid that expresses enhanced GFP (EGFP) from a promoter element that must be activated by binding of nuclear NF-κB (Fig. 1B). Increased NF-κB-induced transcriptional activation was observed in muscle cells when exposed to conditioned media from PC-3 or Mel cells or to inflammatory cytokines (TNF-α, IFN-γ, IL-1β, or IL-6). Stable overexpression of IKBSR or cFLIP prevented NF-κB-induced transcriptional activation induced by tumor cell conditioned media or inflammatory cytokines. Consistent with gel shift analysis of NF-κB activation, stable overexpression of Bcl-xL en-
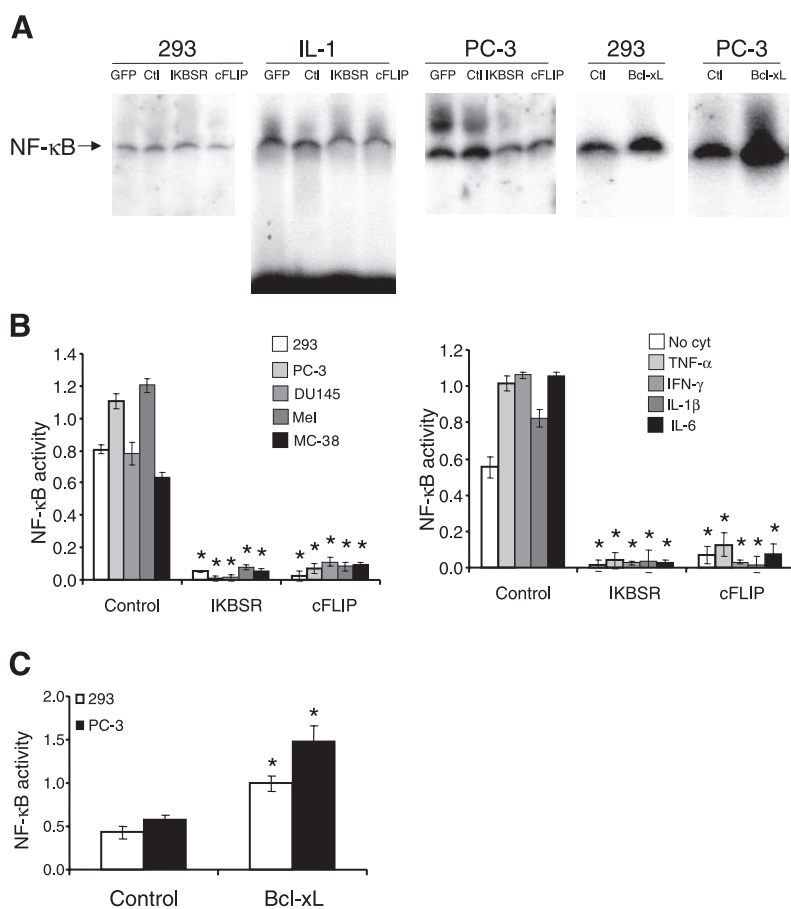

Figure 1. Overexpression of cFLIP and Bcl-xL suppressed NF-κB activity in myoblasts. *A)* Analysis of NF-κB binding activity to a consensus NF-κB oligonucleotide. Myoblast cells were cultured for 60 min in the presence of 20 ng/ml IL-1β or for 24 h in the presence of 293 or PC-3 media (1:2 dilution). Nuclear extracts were prepared and assessed for DNA binding activity to a consensus NF-κB oligonucleotide by EMSA. Lane markers indicate cells with stable expression of IKBSR, cFLIP, or Bcl-xL, GFP from a GFP expression plasmid or untransduced (Ctl). *B)* Analysis of NF-κB transcriptional activity. Myoblast cells with stable expression of IKBSR or cFLIP (control cells are untransduced) were cotransfected with pNF-κB-hrGFP (200 ng/well) and pCMV-β (100 ng/well). 6 h after transfection, cells were cultured in the presence or absence of conditioned media (1:2 dilution) (left panel) or cytokines [no cytokine (no cyt) or 20 ng/ml TNF-α, IFN-γ, IL-1β, or IL-6] alone (right panel). GFP-positive and β-galactosidase-positive cells were counted 24 h after treatment. At least 8 randomly selected fields/well were counted (100×). NF-κB activity is presented as a ratio of GFP-positive to β-galactosidase-positive cells expressed as mean ± SEM *vs.* control myoblast cells. One of at least 4 independent experiments is shown (*n*=8, *P*<0.05). *C)* Analysis of NF-κB transcriptional activity in myoblast cells with stable expression of Bcl-xL cotransfected with pNF-κB-hrGFP (200 ng/well) and pCMV-β (100 ng/well). 6 h after transfection cells were cultured in the presence of 293 or PC-3 cell conditioned media (1:2 dilution). GFP-positive and β-galactosidase-positive cells were counted 24 h after treatment. At least 8 randomly selected fields/well were counted (100×). NF-κB activity is presented as a ratio of GFP-positive to β-galactosidase-positive cells expressed as mean ± SEM *vs.* control myoblast cells. One of at least 4 independent experiments is shown (*n*=8, *P*<0.05).

hanced NF-κB-induced transcriptional activation in this assay in the setting of exposure to PC-3 cell conditioned media (Fig. 1*C*).

5. Stable expression of cFLIP or Bcl-xL by muscle cells inhibits activation of caspase-3

Caspase-3 activity was enhanced in muscle cells exposed to conditioned media from PC-3 or Mel cells compared with muscle cells exposed to conditioned media from normal control 293 cells. Stable overexpression of cFLIP or Bcl-xL inhibited the PC-3 or Mel cell conditioned media-induced increase of caspase-3 activity and caspase-3 cleavage as demonstrated by Western blot analysis. Stable expression of IKBSR in muscle cells did not appear to inhibit the increase in caspase-3 activity induced in muscle cells by exposure to conditioned media from PC-3 or Mel cells.

CONCLUSIONS AND SIGNIFICANCE

We report here a new *in vitro* cell culture assay to study the effects of cancer cell cytokines on muscle cell differentiation and use this assay to test novel gene transfer approaches for treatment of cancer cachexia. Exposure to conditioned media from selected human cancer cell lines resulted in failure of muscle cell differentiation. A known intracellular mechanism of NF-κB activation as a cause of cancer cachexia was recapitulated in this *in vitro* system. Consistent with previous reports *in vivo*, we demonstrated that human prostate cancer PC-3 cells express PIF as well as TNF-α and IL-1β transcripts. We observed a direct correlation between the inhibition of myogenic differentiation in the *in vitro* assay and expression of IL-1β transcripts by specific human cancer cell lines tested. We also observed a direct correlation between NF-κB activation and inhibition of myogenic differentiation in the *in vitro* assay. Exposure to inflammatory cytokines and to conditioned media from human cancer cells each resulted in NF-κB activation within primary muscle cells. Failure of myogenic differentiation and the associated activation of NF-κB were prevented by stable expression of either IKBSR or cFLIP, but not by Bcl-xL (**Fig. 2**).

Earlier studies demonstrate that activation of NF-κB plays a key role in cancer-induced cachexia. Consistent with previous studies, we found that exposure to secreted factors from PC-3 and Mel cancer cell lines resulted in activation of NF-κB in treated myoblast cells, as demonstrated by higher binding activity of nuclear NF-κB to consensus NF-κB oligonucleotides and higher levels of NF-κB transcriptional activity.

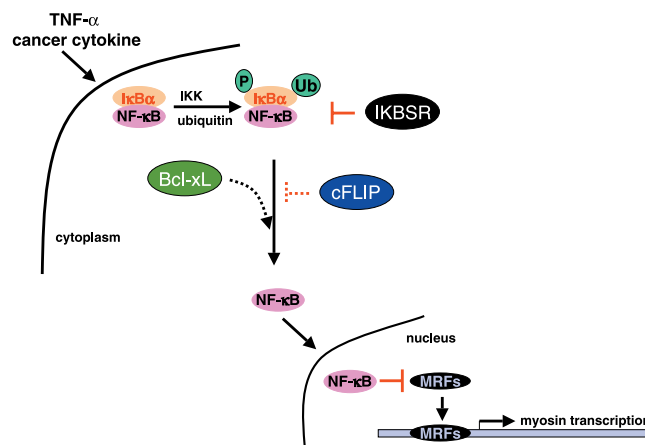cFLIP and Bcl-xL are important antiapoptotic mole-

Figure 2. Schematic diagram of proposed effect of cFLIP and Bcl-xL on NF-κB activation and muscle differentiation. cFLIP inhibits and Bcl-xL enhances NF-κB activation in muscle cells when stimulated with cancer cytokines *in vitro*. The lower level of NF-κB activation induced by expression of cFLIP was associated with rescue from failure of muscle cell differentiation. The higher level of NF-κB activation induced by expression of Bcl-xL was associated with exacerbation of the failure of muscle cell differentiation. Dotted lines indicate that the mechanism by which cFLIP and Bcl-xL expression inhibits and enhances NF-κB activation, respectively, is unknown. MRF, myosin regulatory factor.

cules. We investigated whether cFLIP and Bcl-xL influenced NF-κB activity and myogenic differentiation in primary cells derived from skeletal muscle. We noted that cFLIP overexpression inhibited IL-1β or PC-3 or Mel media-induced NF-κB activation in myoblast cells, thus promoting myogenic differentiation of treated myoblast cells as shown by enhanced myotube formation and muscle-specific protein expression. Stable expression of cFLIP yielded results similar to stable expression of IKBSR. Both IKBSR and cFLIP inhibited NF-κB activation as determined by levels of nuclear NF-κB binding activity and nuclear NF-κB-mediated transcription. In contrast, overexpression of Bcl-xL enhanced NF-κB activation in myoblast cells, with more increases upon exposure to conditioned media from PC-3 cells. Further studies are required to understand the intricacies of signaling cascades that underpin the contrasting results with cFLIP and Bcl-xL.

This study provides an *in vitro* assay that demonstrates secretion of cachexia-inducing factors by certain cancer cell lines that result in inhibition of myogenic differentiation by activation of NF-κB. Overexpression of cFLIP in muscle cells inhibits NF-κB-mediated and apoptotic pathways, preventing tumor media-induced inhibition of myogenic differentiation and cytotoxicity. These findings point to the potential to design novel molecular therapeutic treatments of cancer-induced muscle wasting. FJ